frontiers | Research Topics

Advances in the treatment of hormonal receptor positive (HR+) breast cancer

Edited by
Deniz Can Guven and Arunasalam Dharmarajan

Coordinated by
Wala Ben Kridis

Published in
Frontiers in Oncology

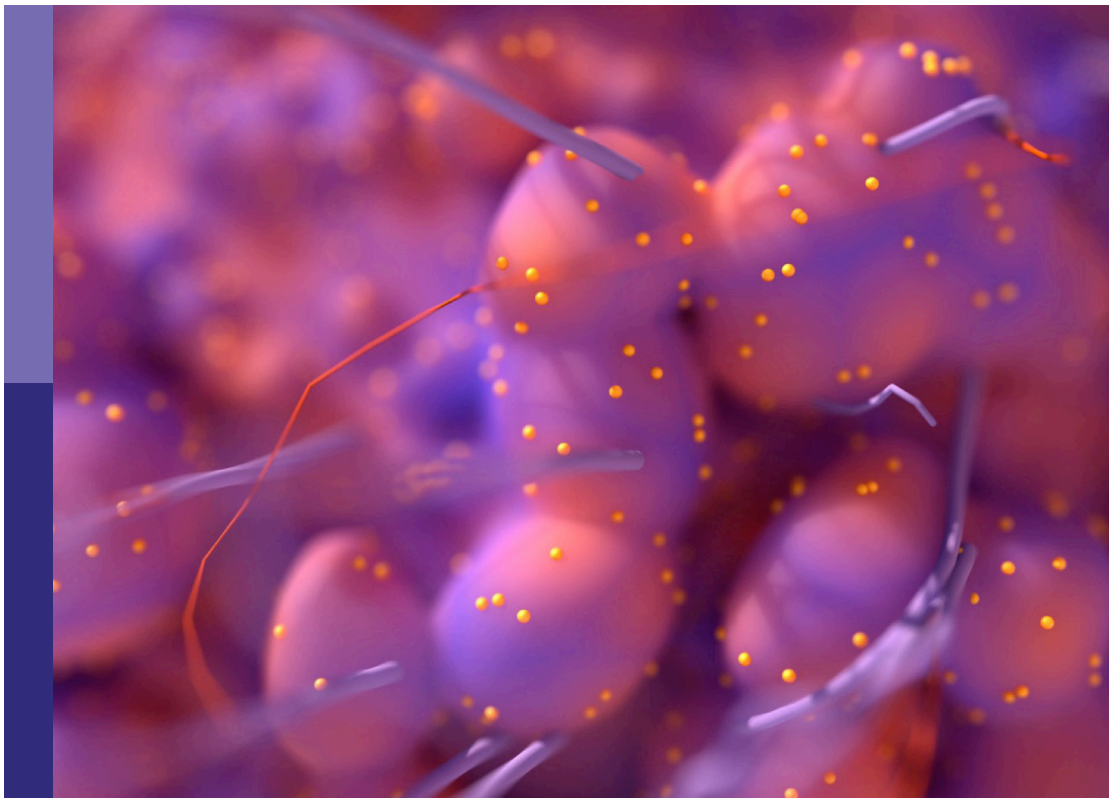

ISSN 1664-8714
ISBN 978-2-8325-5535-4
DOI 10.3389/978-2-8325-5535-4

About Frontiers

Frontiers is more than just an open access publisher of scholarly articles: it is a pioneering approach to the world of academia, radically improving the way scholarly research is managed. The grand vision of Frontiers is a world where all people have an equal opportunity to seek, share and generate knowledge. Frontiers provides immediate and permanent online open access to all its publications, but this alone is not enough to realize our grand goals.

Frontiers journal series

The Frontiers journal series is a multi-tier and interdisciplinary set of open-access, online journals, promising a paradigm shift from the current review, selection and dissemination processes in academic publishing. All Frontiers journals are driven by researchers for researchers; therefore, they constitute a service to the scholarly community. At the same time, the *Frontiers journal series* operates on a revolutionary invention, the tiered publishing system, initially addressing specific communities of scholars, and gradually climbing up to broader public understanding, thus serving the interests of the lay society, too.

Dedication to quality

Each Frontiers article is a landmark of the highest quality, thanks to genuinely collaborative interactions between authors and review editors, who include some of the world's best academicians. Research must be certified by peers before entering a stream of knowledge that may eventually reach the public - and shape society; therefore, Frontiers only applies the most rigorous and unbiased reviews. Frontiers revolutionizes research publishing by freely delivering the most outstanding research, evaluated with no bias from both the academic and social point of view. By applying the most advanced information technologies, Frontiers is catapulting scholarly publishing into a new generation.

What are Frontiers Research Topics?

Frontiers Research Topics are very popular trademarks of the *Frontiers journals series*: they are collections of at least ten articles, all centered on a particular subject. With their unique mix of varied contributions from Original Research to Review Articles, Frontiers Research Topics unify the most influential researchers, the latest key findings and historical advances in a hot research area.

Find out more on how to host your own Frontiers Research Topic or contribute to one as an author by contacting the Frontiers editorial office: frontiersin.org/about/contact

Advances in the treatment of hormonal receptor positive (HR+) breast cancer

Topic editors
Deniz Can Guven — Hacettepe University, Türkiye
Arunasalam Dharmarajan — Medical Centre, Sri Ramachandra Institute of Higher Education and Research, India

Topic coordinator
Wala Ben Kridis — Habib Bourguiba University Hospital, Tunisia

Citation
Guven, D. C., Dharmarajan, A., Ben Kridis, W., eds. (2024). *Advances in the treatment of hormonal receptor positive (HR+) breast cancer*. Lausanne: Frontiers Media SA. doi: 10.3389/978-2-8325-5535-4

Table of contents

frontiers | Frontiers in Oncology

TYPE Editorial
PUBLISHED 25 September 2024
DOI 10.3389/fonc.2024.1449566

OPEN ACCESS

EDITED AND REVIEWED BY
Kara Britt,
Peter MacCallum Cancer Centre, Australia

*CORRESPONDENCE
Wala Ben Kridis
walabenkridis@yahoo.fr

RECEIVED 15 June 2024
ACCEPTED 06 September 2024
PUBLISHED 25 September 2024

CITATION
Ben Kridis W, Wang Z, Guven DC and Dharmarajan A (2024) Editorial: Advances in the treatment of hormonal receptor positive (HR+) breast cancer.
Front. Oncol. 14:1449566.
doi: 10.3389/fonc.2024.1449566

Editorial: Advances in the treatment of hormonal receptor positive (HR+) breast cancer

Wala Ben Kridis[1]*, Zheng Wang[2], Deniz Can Guven[3] and Arunasalam Dharmarajan[4]

[1]Habib Bourguiba University Hospital, University of Sfax, Sfax, Tunisia, [2]Ruijin Hospital, School of Medicine, Shanghai Jiao Tong University, Shanghai, China, [3]Cancer Institute, Hacettepe University, Ankara, Türkiye, [4]Medical Centre, Sri Ramachandra Institute of Higher Education and Research, Chennai, India

KEYWORDS

breast cancer, CDK 4/6 inhibitors, PIK3CA, genetics, aromatase inhibiters, toxicity

Editorial on the Research Topic
Advances in the treatment of hormonal receptor positive (HR+) breast cancer

Breast cancer is the most common cancer in women. Breast cancer subtypes are classified according to histologic features, including morphology and receptor status. Information on the expression of estrogen receptor (ER), progesterone receptor, and human epidermal growth factor receptor 2 (HER2), as well as the proliferation index Ki67 (in early-stage disease), are relevant for clinical decisions. Molecular tests are now available to further classify the disease into subgroups, stratify risk or estimate the benefit of interventions. Some examples of such tests include the Recurrence Score (OncotypeDX), PAM50 (Prosigna), Mammaprint, Blueprint, and Breast Cancer Index (BCI), among others.

In recent years, the treatment of HR+HER2- breast cancer has been revolutionized by the introduction of the CDK4/6 inhibitors (CDK4/6i) palbociclib, ribociclib, and abemaciclib, the PI3 kinase inhibitor alpelisib, the antibody drug conjugates trastuzumab-deruxtecan and sacituzumab govitecan, the PARP inhibitor olaparib (when a germline BRCA 1 or 2 mutation is present) as well as the oral selective ER degrader elacestrant for patients with ESR1 mutations.

This Research Topic aims to widen the understanding of the advances in treatment for localized and metastatic HR+HER2- breast cancer to help improve the outcomes for patients. 11 articles were accepted. Starting with aromatase inhibitor and its toxicities. Aromatase inhibitors (AIs) are a cornerstone adjuvant treatment of many hormone receptor-positive breast cancers, and nearly half of women taking aromatase inhibitors suffer from AI-induced arthralgia (AIA), also known as AI associated musculoskeletal syndrome (AIMSS), for which there are limited evidence-based treatments. Pharmacologic management and complementary methods including supplements, exercise, physical therapy, yoga, acupuncture, and massage have all shown mixed results. Comprehensive diet and lifestyle strategies are understudied in AIA/AIMSS despite their disease-modifying effects across many chronic conditions. Wilson et al. reported a case of a woman with stage 2 estrogen and progesterone receptor-positive invasive ductal carcinoma on adjuvant anastrozole whose AI-induced arthralgia was durably controlled through a Mediterranean

plant-forward diet and daily physical activity guided by continuous glucose monitoring. They posit that diet and a lifestyle inclusive of daily physical activity constitute a low-cost, low-risk, and potentially high-reward strategy for controlling common AI-induced musculoskeletal symptoms and that more investigation in this arena, including well-designed randomized trials, is warranted. Chu et al. aimed to establish a high-risk prediction model for aromatase inhibitor associated bone loss (AIBL) in patients with hormone receptor-positive.

The identified risk factors were used to construct a prediction model using the eXtreme gradient boosting (XGBoost) machine learning method. Logistic regression and least absolute shrinkage and selection operator (LASSO) regression methods were used for comparison. A total of 113 subjects were included in the study. Time from diagnosis of breast cancer, duration of aromatase inhibitor therapy, hip fracture index, major osteoporotic fracture index, prolactin (PRL), and osteocalcin (OC) were found to be independent risk factors for AIBL ($p < 0.05$). The XGBoost model had a higher AUC compared to the logistic model and LASSO model (0.761 vs. 0.716, 0.691). Consequently, authors concluded that the XGBoost model outperformed the logistic and LASSO models in predicting the occurrence of AIBL in patients with hormone receptor-positive breast cancer receiving aromatase inhibitors.

Previous studies have shown that osteoporosis is a side effects of the breast cancer hormone therapy, although the exact mechanisms remain mostly unclear. Current clinical treatments, such as bisphosphonates, cause side effects and may impact the therapeutic response to endocrine drugs.

According to Xu et al. traditional Chinese medicine has great potential in the prevention and treatment of osteoporosis caused by endocrine therapy in breast cancer. For instance, isosinensetin, a flavonoid present in citrus fruits with antioxidant properties, has been shown to reduce bone loss in OVX mice and alleviate estrogen deficiency-induced osteoporosis in mice. Obacunone, a small molecule with a wide range of biological activities, can inhibit the formation and absorption function of OCs *in vitro* by targeting inhibitory factor of macrophage migration inhibitory factor (MIF). Thus, it is expected to be an effective drug for relieving osteoporosis caused by estrogen deficiency. It is necessary to explore their relationship with osteoporosis to provide new treatment strategies. The relationship between bone lymphatics and osteoporosis remains to be further explored. Additionally, the pathogenesis of breast cancer is not yet fully understood, and there is a need for more effective therapeutic drugs to reduce the occurrence of adverse reactions related to endocrine therapy.

In recent years, significant strides have been made in the management of HR+/HER2- breast cancer through the introduction of CDK4/6 inhibitors, such as palbociclib, ribociclib, and abemaciclib, thereby improving outcomes for adjuvant, advanced and/or metastatic settings. CDK4/6 inhibitors can block retinoblastoma protein hyperphosphorylation, inducing G1 arrest and curtailing proliferation.

Rodrigues Alves et al. reported the first case of a patient presenting with bilateral orbital metastases from bilateral lobular breast cancer, showing an impressive and sustained response to a first-line treatment regimen combining abemaciclib and letrozole. Orbital metastases represent 1-13% of all orbital neoplasm and affecting around 2-5% of patients with cancer. They are typically unilateral. Bilateral orbital metastases are reported in 4%. They are often identified after the primary tumor. However, in the case of Rodrigues Alves et al. they revealed the diagnosis of bilateral breast cancer without any other metastatic site. Furthermore, this is the first case of bilateral orbital metastases from bilateral breast cancer treated by abemaciclib and letrozole with complete response in both breasts and significant improvement on orbital imaging with good visual acuity. In case of progression after hormone therapy with CDK4/6 inhibitors, Elascestrant is indicated in case of ESR1 mutation. Zeng et al. evaluated the cost-effectiveness of elacestrant (ELA) and standard-of-care (SOC) as second-/third-line treatment for pretreated estrogen receptor (ER)– positive/human epidermal growth factor receptor 2 (HER2)– negative advanced or metastatic breast cancer (A/MBC) in the US. They concluded that ELA was not cost-effective for the second-/third-line treatment of patients with ER+/HER2–A/MBC compared with SOC in the US. In fact, ELA led to an incremental cost-effectiveness ratio (ICER) of $8,672,360/quality-adjusted life year (QALY) gained compared with SOC in the overall population and $2,900,560/QALY gained compared with fulvestrant (FUL) in the ESR1(estrogen receptor 1) mutation subgroup.

Consistent with previous studies, Chao et al. identified a high prevalence of PIK3CA mutations in 38% of the Taiwanese patients with breast cancer. The lower prevalence in premenopausal patients and patients with triple-negative breast cancer warrants further studies. Most of the mutations were in exon 9 and exon 20, with H1047R, E545K, and E542K being the hotspots. A longer time to treatment failure in wild-type PIK3CA cohorts treated with CDK4/6 inhibitors was reported, which demonstrated the better efficacy of CDK4/6 inhibitors in wild-type PIK3CA cohorts than that in the PIK3CA-mutant cohort. Everolimus, an mTOR inhibitor, reported a longer time to treatment failure in the PIK3CA-mutant cohort and demonstrated better efficacy.

Concerning the place of genetics in the diagnosis of breast cancer, AGR2 is a secreted protein widely existing in breast. Its endoplasmic reticulum retention sequence, protein disulfide isomerase active site and multiple protein binding sequences endow AGR2 with diverse functions inside and outside breast cancer cells. Zhang et al. concluded in their review that diagnostic tools such as microfluidic detection devices or biosensors can be developed to detect AGR2 specifically and sensitively. Combining AGR2 with other tumor markers can improve the sensitivity of breast cancer diagnosis, which is one of the hot spots that clinicians need to pay attention to in the future. So far, therapeutic strategies targeting AGR2 have shown promising results. For example, by constructing the bispecific antibodies of AGR2 antibody and immune checkpoint proteins, it can play its role in tumor tissue with maximum target concentration, which is a clinical transformation direction to improve the efficacy and reduce side effects.

Cancer-associated fibroblasts (CAFs) play a pivotal role in cancer progression and are known to mediate endocrine and chemotherapy resistance through paracrine signaling. Additionally, they directly influence the expression and growth dependence of ER in Luminal

breast cancer (LBC). Xu et al. aimed to investigate stromal CAF-related factors and develop a CAF-related classifier to predict the prognosis and therapeutic outcomes in LBC. They constructed a 5-gene prognostic model consisting of RIN2, THBS1, IL1R1, RAB31, and COL11A1 for CAF. Gene set enrichment analysis (GSEA) identified significant enrichment of ECM receptor interaction, regulation of actin cytoskeleton, epithelial-mesenchymal transition (EMT), and TGF-b signaling pathway gene sets in the high-CAF-risk group patients. Then, they concluded that the five-gene prognostic CAF signature presented in this study was not only reliable for predicting prognosis in LBC patients, but it was also effective in estimating clinical immunotherapy response. These findings have significant clinical implications, as the signature may guide tailored anti-CAF therapy in combination with immunotherapy for LBC patients.

Endeavors in the molecular characterization of breast cancer opened the doors to endocrine therapies in ER+/HER2- breast cancer, increasing response rates substantially. Despite that, taxane-based neoadjuvant chemotherapy is still a cornerstone for achieving breast-conserving surgery and complete tumor resection in locally advanced cancers with high recurrence risk.

Nonetheless, the rate of chemoresistance is high, and deselecting patients who will not benefit from chemotherapy is a significant task to prevent futile toxicities. Several multigene assays are being used to guide decisions on chemotherapy. However, their development as prognostic assays but not predictive assays limits predictive strength, leading to discordant results. Moreover, high costs impediment their use in developing countries. For global health equity, robust predictors that can be cost-effectively incorporated into routine clinical management are essential. Protein patched homolog 1 (PTCH1) is a member of the patched gene family and is the receptor for sonic hedgehog, a secreted molecule implicated in the formation of embryonic structures and in tumorigenesis. This gene functions as a tumor suppressor. β-Catenin (CTNNB1) is a dual function protein, involved in regulation and coordination of cell–cell adhesion and gene transcription. Ozcan suggests that PTCH1 and CTNNB1 can be used as robust and cost-effective predictors in developing countries to guide decisions on chemotherapy in ER +/HER2- breast cancer patients with a high risk of recurrence. The dual function of PTCH1 as a multidrug efflux pump and a hedgehog receptor, and the active involvement of CTNNB1 in breast cancer strongly indicate that PTCH1 and CTNNB1 can be potential drug targets to overcome chemoresistance in ER +/HER2- breast cancer patients.

The lethal-7 (Let-7i) family is an important microRNA (miRNA) group that usually exerts functions as a tumor suppressor. According to Zhou et al. Let-7i regulates tumors primarily by binding to the 3′ untranslated region (3′ UTR) of mRNA, which indirectly regulates post-transcriptional gene expression. Let-7i also has an epigenetic function via modulating DNA methylation to directly regulate gene expression. Let-7i performs a dual role by inducing both the promotion and inhibition of various malignancies, depending on its target. The mechanism of Let-7i action involves cancer cell proliferation, migration, invasion, apoptosis, epithelial-mesenchymal transition, EV transmission, angiogenesis, autophagy, and drug resistance sensitization. Let-7i is closely related to cancer, and hence, is a potential biomarker for the diagnosis and prognosis of various cancers. Therapeutically, it can be used to promote an anti-cancer immune response by modifying exosomes, thus exerting a tumor-suppressive effect.

We can conclude in this Research Topic that diet and a lifestyle inclusive of daily physical activity constitute a low-cost, low-risk, and potentially high-reward strategy for controlling common AI-induced symptoms. Furthermore, traditional Chinese medicine has great potential in the prevention and treatment of osteoporosis caused by endocrine therapy in breast cancer. XGBoost model outperformed the logistic and LASSO models in predicting the occurrence of AIBL in patients with hormone receptor-positive breast cancer receiving aromatase inhibitors. Therapically, elacestrant was not cost-effective for the second-/third-line treatment of patients with ER+/HER2–A/MBC compared with SOC in the US. Concerning patients with PIK3CA-mutation, Everolimus reported a longer time to treatment failure and demonstrated better efficacy. Regarding the place of genetics in the diagnosis of breast cancer, combining AGR2 with other tumor markers can improve the sensitivity of breast cancer diagnosis. Also, RIN2, THBS1, IL1R1, RAB31, and COL11A1 for CAF were not only reliable for predicting prognosis in LBC patients, but they were also effective in estimating clinical immunotherapy response. Finally, Let-7i can be used to promote an anti-cancer immune response by modifying exosomes, thus exerting a tumor-suppressive effect.

Author contributions

WB: Writing – original draft. ZW: Writing – review & editing. DG: Writing – review & editing. AD: Writing – review & editing.

Conflict of interest

The authors declare that the research was conducted in the absence of any commercial or financial relationships that could be construed as a potential conflict of interest.

Publisher's note

frontiers | Frontiers in Oncology

TYPE Original Research
PUBLISHED 27 April 2023
DOI 10.3389/fonc.2023.1182792

OPEN ACCESS

EDITED BY
Zheng Wang,
Shanghai Jiao Tong University, China

REVIEWED BY
Hangcheng Fu,
University of Louisville, United States
Xinyuan Ding,
Suzhou Municipal Hospital, China

*CORRESPONDENCE
Jingjing Wu
jswjj520@163.com
Meina Ye
yepangmi@163.com

†These authors have contributed equally to this work

RECEIVED 09 March 2023
ACCEPTED 11 April 2023
PUBLISHED 27 April 2023

CITATION
Chu M, Zhou Y, Yin Y, Jin L, Chen H, Meng T, He B, Wu J and Ye M (2023) Construction and validation of a risk prediction model for aromatase inhibitor-associated bone loss. *Front. Oncol.* 13:1182792. doi: 10.3389/fonc.2023.1182792

Construction and validation of a risk prediction model for aromatase inhibitor-associated bone loss

Meiling Chu†, Yue Zhou†, Yulian Yin†, Lan Jin, Hongfeng Chen, Tian Meng, Binjun He, Jingjing Wu* and Meina Ye*

Department of Breast Surgery, Longhua Hospital Shanghai University of Traditional Chinese Medicine, Shanghai, China

Purpose: To establish a high-risk prediction model for aromatase inhibitor-associated bone loss (AIBL) in patients with hormone receptor-positive breast cancer.

Methods: The study included breast cancer patients who received aromatase inhibitor (AI) treatment. Univariate analysis was performed to identify risk factors associated with AIBL. The dataset was randomly divided into a training set (70%) and a test set (30%). The identified risk factors were used to construct a prediction model using the eXtreme gradient boosting (XGBoost) machine learning method. Logistic regression and least absolute shrinkage and selection operator (LASSO) regression methods were used for comparison. The area under the receiver operating characteristic curve (AUC) was used to evaluate the performance of the model in the test dataset.

Results: A total of 113 subjects were included in the study. Duration of breast cancer, duration of aromatase inhibitor therapy, hip fracture index, major osteoporotic fracture index, prolactin (PRL), and osteocalcin (OC) were found to be independent risk factors for AIBL ($p < 0.05$). The XGBoost model had a higher AUC compared to the logistic model and LASSO model (0.761 *vs.* 0.716, 0.691).

Conclusion: The XGBoost model outperformed the logistic and LASSO models in predicting the occurrence of AIBL in patients with hormone receptor-positive breast cancer receiving aromatase inhibitors.

KEYWORDS

aromatase inhibitors, breast cancer, bone loss, risk prediction model, XGBoost, logistic regression, LASSO regression

Introduction

According to statistics from the International Agency for Research on Cancer, breast cancer is the most common malignant tumor worldwide, accounting for 11.7% of new cases in 2020 (1). Among breast cancer subtypes, hormone receptor-positive breast cancer represents approximately 70% (2). Endocrine therapy is an effective approach to reducing estrogen secretion, which can lower the risk of recurrence and metastasis by up to 50% (3). Aromatase inhibitors (AIs) are the primary drugs used for endocrine therapy in postmenopausal patients with hormone receptor-positive breast cancer. Ovarian function suppression (OFS) and AIs are also used in combination to treat premenopausal patients. AIs can improve the prognosis of hormone receptor-positive breast cancer (4), but the continuous reduction of estrogen levels can lead to aromatase inhibitor-associated bone loss (AIBL), which is associated with bone metabolic dysfunction, arthralgia, osteopenia, and osteoporosis (5). Logistic regression is a variant of the generalized linear model (GLM) commonly used for binary classification problems (6), while least absolute shrinkage and selection operator (LASSO) regression is used to select feature variables that are most useful for the model to avoid overfitting. Cross-validation is usually required to determine the best regularization parameters for LASSO regression (7). In contrast to traditional linear regression, eXtreme gradient boosting (XGBoost) is a machine learning algorithm that uses decision tree ensembles to build predictive models. It calculates the importance of features to eliminate unnecessary features and improve model performance and interpretability (8). The study established and verified XGBoost, LASSO regression, and logistic regression models to predict the incidence of AIBL. The prediction efficiency of the three models was compared, and the model with the best performance could provide valuable insights for AIBL treatment and prevention.

Study design

This study is a prospective interventional single-center study. The subjects of this study were breast cancer patients who were treated in the first department of the breast cancer clinic of Longhua Hospital affiliated with Shanghai University of Traditional Chinese Medicine from February 2022 to March 2023. A schematic diagram of the research flowchart is shown in Figure 1.

The Medical Ethics Committee of Longhua Hospital affiliated with the Shanghai University of Traditional Chinese Medicine approved this research. Written informed consent was obtained from all individual participants included in the study. The clinical trial registration number is ChiCTR2200057785.

Participant

Diagnostic criteria

The breast cancer diagnosis was based on the 2022 Guidelines for Diagnosis and Treatment of Breast Cancer by the Chinese Society of Clinical Oncology (CSCO), confirmed by basic and molecular pathology. Osteoporosis diagnosis was based on the bone mineral density measured by dual-energy X-ray absorptiometry (DXA) according to the World Health Organization (WHO) 1994 criteria (normal, T score ≥ −1.0; osteopenia, −2.5 < T score < −1.0; osteoporosis, T score ≤ −2.5) (9).

Inclusion criteria

1) Female patients diagnosed with breast cancer, with positive estrogen receptor (ER) and/or progesterone receptor (PR) by immunohistochemical examination of postoperative pathology; 2) age between 18 and 65 years; 3) patients who have undergone surgery, chemotherapy, radiotherapy, and/or targeted therapy; 4) patients who have received aromatase inhibitor treatment for at least 2 months; 5) patients who voluntarily underwent clinical investigation and related examinations and provided signed informed consent.

Exclusion criteria

1) Patients with concurrent diseases affecting bone metabolism (such as Cushing's syndrome, hyperthyroidism, rheumatism, or rheumatoid arthritis); 2) patients who have used hormone replacement therapy (such as glucocorticoids, parathyroid hormone, and estrogen) within 6 months; 3) patients with serious primary diseases of the cardiovascular, hepatic, renal, and hematopoietic systems; 4) patients with cognitive impairment and psychiatric disorders.

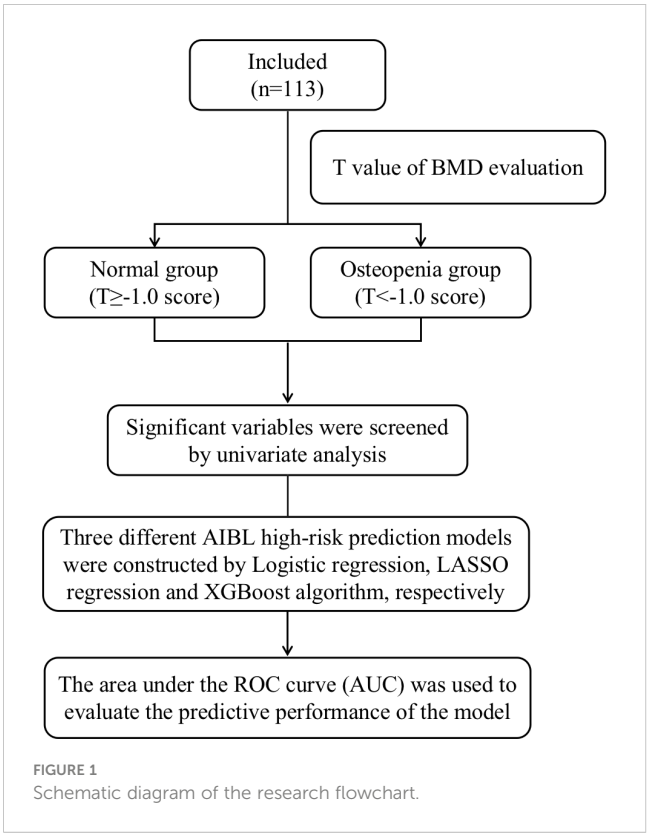

FIGURE 1
Schematic diagram of the research flowchart.

Materials and methods

Observation indexes

1) Bone mineral density (BMD) was measured by dual-energy X-ray absorptiometry (DXA).
2) Patient baseline characteristics, breast cancer diagnosis, and treatment information were collected as part of the study.
3) Three questionnaires were used in the study.

1) The Fracture Risk Assessment Tool (FRAX) measures the probability of major osteoporotic fracture and the 10-year probability of hip fracture due to osteoporosis. The FRAX scale was used to evaluate fracture risk in breast cancer patients receiving AI treatment, but BMD values were also included in the assessment to improve the accuracy of the algorithm (10). However, it has also been suggested that FRAX may underestimate the 10-year fracture risk in breast cancer patients (11).
2) The Western Ontario and McMaster Universities Osteoarthritis Index (WOMAC) is a commonly used scale to evaluate the severity of hip and knee arthritis, including pain, stiffness, and physical function (12).
3) Modified Score for the Assessment of Chronic Rheumatoid Affections of the Hands (M-SACRAH) is primarily used to assess functional status, stiffness, and pain in patients with hand osteoarthritis and rheumatoid arthritis (13). It has been widely used to assess the severity of osteoarticular side effects in patients undergoing AI treatment (14).
4) Examination indicators: the laboratory blood tests included routine biochemical tests and daily monitoring of endocrine therapy for breast cancer patients. Blood samples were collected from all subjects in the fasting state, and all subjects had completed surgery, chemotherapy, radiotherapy, and targeted therapy.

Data management

All data were collected using one-to-one questionnaires completed by the researcher and research subjects within 20 min to ensure accuracy. The collected data were then entered into an Excel sheet within 1 week of survey completion. Additionally, 20% of the data were manually checked for input errors and corrected accordingly.

Statistical methods

Descriptive statistics, including mean ± standard deviation for continuous variables and a number of cases and percentages for categorical variables, were used to describe the data. The independent sample *t*-test was used for comparing continuous variables with normal distribution between two groups, and the chi-square test was used for comparing categorical variables between groups. Statistical analyses were performed using SPSS 26.0 software.

Univariate analysis was performed to identify significant factors, followed by XGBoost machine learning, LASSO regression, and logistic regression analysis to build a prediction model to evaluate the association between the clinical characteristics of the study population, blood test indicators, and the incidence of AIBL. This analysis was conducted using R4.2.2, with statistical significance set at $p < 0.05$.

Results

Inclusion of patient

All eligible participants who voluntarily enrolled in the study completed the epidemiological questionnaire and underwent blood index detection and BMD examination. A total of 113 project volunteers were recruited from February 2022 to March 2023. Among them, 66 patients had osteopenia or osteoporosis, while the remainder had normal bone mass.

Univariate analysis

After normal distribution tests and intergroup comparison analyses were performed, the following screening indicators with significant differences between the osteopenia and normal bone mass groups were obtained: duration of breast cancer ($p = 0.001$), duration of aromatase inhibitor treatment ($p = 0.002$), major osteoporotic fracture index ($p < 0.001$), hip fracture index ($p < 0.001$), prolactin (PRL) ($p = 0.012$), and osteocalcin (OC) ($p = 0.025$). These findings are presented in Tables 1, 2.

Construction and validation of logistic regression prediction model for AIBL

Six significant risk factors were identified by univariate analysis, including duration of breast cancer, duration of aromatase inhibitor therapy, major osteoporotic fracture index, hip fracture index, PRL, and OC. Subsequently, the Akaike information criterion (AIC) method was used to select independent variables. Multivariate logistic regression analysis revealed that the three relevant variables included in the logistic model were the duration of breast cancer, hip fracture index, and PRL.

Among them, the duration of breast cancer and hip fracture index were independent risk factors for AIBL ($p < 0.05$) (Supplementary Table 1). The dataset was randomly split into a training set (70%) and a test set (30%). The logistic prediction model was constructed for these three variables in the training set (as shown in Table 3), and the corresponding nomogram was drawn (as shown in Figure 2A).

TABLE 1 Results of epidemiological univariate analysis in normal and osteopenia groups.

Variables		Osteopenia group (n = 66)	Normal group (n = 47)	*p*-Value (2-sided)
Age		48.61 ± 8.79	46.11 ± 7.50	0.113
BMI		22.87 ± 2.92	23.31 ± 2.70	0.418
Education	High school and below	19 (28.8%)	9 (19.1%)	0.242
	More than university	47 (71.2%)	38 (80.9%)	
Age at menarche		13.92 ± 1.13	13.60 ± 0.99	0.073
Menopause	No	40 (60.6%)	34 (72.3%)	0.265
	Less than 10 years	18 (27.3%)	11 (23.4%)	
	More than 10 years	8 (12.1%)	2 (4.3%)	
Number of pregnancies	No	1 (1.5%)	5 (10.6%)	0.153
	Once	24 (36.4%)	18 (38.3%)	
	Twice	22 (33.3%)	11 (23.4%)	
	More than three times	19 (28.8%)	13 (27.7%)	
Number of production times	No	3 (4.5%)	5 (10.6%)	0.391
	Once	48 (72.7%)	34 (72.3%)	
	Twice	15 (22.7%)	8 (17%)	
Family history of cancer		20 (30.3%)	15 (31.9%)	0.855
Duration of breast cancer (months)		27.08 ± 12.57	19.09 ± 10.74	0.001
Lymph node metastasis		27 (40.9%)	24 (51.1%)	0.285
Anthracycline-based chemotherapy		32 (68.1%)	15 (31.9%)	0.078
Targeted chemotherapy		11 (16.7%)	7 (14.9%)	0.800
Radiation therapy		47 (71.2%)	36 (76.6%)	0.523
Duration of aromatase inhibitor therapy (months)		19.92 ± 11.95	13.38 ± 9.25	0.002
Aromatase inhibitors	Exemestane	31 (47.0%)	32 (68.1%)	0.060
	Letrozole	14 (21.2%)	8 (17%)	
	Anastrozole	21 (31.8%)	7 (14.9%)	
Drink coffee		12 (18.2%)	12 (25.5%)	0.346
Smoking history		1 (1.5%)	0	0.397
Alcohol intake history		2 (3.0%)	1 (2.1%)	0.769
Exercise		27 (40.9%)	14 (29.8%)	0.226
History of fractures		8 (12.1%)	5 (10.6%)	0.808
History of fracture in parents		14 (21.2%)	6 (12.8%)	0.246
FRAX	Major osteoporotic fracture index	3.66 ± 3.39	2.11 ± 1.26	<0.001
	Hip fracture index	0.89 ± 1.76	0.17 ± 0.22	<0.001
WOMAC		34.09 ± 12.32	33 ± 10.36	0.960
M-SACRAH		15.05 ± 8.25	15.83 ± 11.89	0.676

BMI, body mass index; FRAX, Fracture Risk Assessment Tool; WOMAC, Western Ontario and McMaster Universities Osteoarthritis Index; M-SACRAH, Modified Score for the Assessment of Chronic Rheumatoid Affections of the Hands.

TABLE 2 Results of univariate analysis of blood indicators in normal and osteopenia groups.

Variables	Osteopenia group (n = 66)	Normal group (n = 47)	*p*-Value (2-sided)
*White blood cell count (10^9/L)	4.84 ± 1.00	5.10 ± 1.19	00.226
*Red blood cell count (10^{12}/L)	4.50 ± 0.34	4.47 ± 0.42	00.988
*Neutrophil count (10^9/L)	2.73 ± 0.76	3.02 ± 0.97	00.139
*Lymphocyte count (10^9/L)	2.17 ± 3.60	1.72 ± 0.50	00.668
*Hemoglobin (g/L)	135.18 ± 8.11	136.13 ± 9.99	00.399
*Platelet count (10^9/L)	201.02 ± 39.45	206.34 ± 46.72	00.514
#Alanine aminotransferase (U/L)	22.17 ± 15.62	20.85 ± 13.26	00.954
#Aspartate aminotransferase (U/L)	22.28 ± 7.14	21.73 ± 7.17	00.558
#γ-Glutamyl transpeptidase (U/L)	25.38 ± 17.42	27.72 ± 17.42	00.459
#Alkaline phosphatase (U/L)	86.27 ± 35.97	77.97 ± 23.90	00.377
#Total protein (g/L)	74.11 ± 3.88	73.58 ± 6.08	00.722
#Total bilirubin (μmol/L)	13.63 ± 7.57	12.56 ± 5.99	00.193
$Creatinine (μmol/L)	54.97 ± 10.47	53.56 ± 15.16	00.947
$Blood urea nitrogen (mmol/L)	4.84 ± 1.13	4.71 ± 1.13	00.584
$Calcium (mmol/L)	2.42 ± 0.10	2.42 ± 0.11	00.804
**Estradiol (pg/ml)	21.85 ± 92.80	24.05 ± 110.11	00.076
**Follicle-stimulating hormone (IU/L)	33.62 ± 33.31	30.06 ± 34.37	00.192
**Luteinizing hormone (IU/L)	12.07 ± 16.24	10.29 ± 15.27	00.781
**PRL (ng/ml)	172.56 ± 85.30	236.43 ± 122.33	00.012
**Progesterone (ng/ml)	0.82 ± 0.55	0.70 ± 0.32	00.589
**Testosterone (nmol/L)	1.36 ± 2.86	1.26 ± 1.38	00.586
##25-Hydroxyvitamin D (nmol/L)	73.21 ± 23.18	68.54 ± 22.43	00.286
##β-Isomerized C-telopeptide (pg/ml)	551.51 ± 283.52	641.77 ± 275.78	00.094
##Osteocalcin (ng/ml)	23.64 ± 9.56	27.65 ± 10.32	00.025
##Growth hormone (μg/L)	1.08 ± 1.39	0.98 ± 1.25	00.566

*represents blood routine test, #represents liver function test, $represents kidney function test, **represents sex hormone level test, and ##represents bone metabolism level test.
PRL, prolactin.

Assuming that the probability of AIBL in patients with hormone receptor-positive breast cancer treated with aromatase inhibitors is P, Logit(P) = −1.272 + 0.079 * (duration of breast cancer) + 3.673 * (hip fracture index) − 0.007 * (PRL). As shown in the table, a longer duration of breast cancer after diagnosis and a higher hip fracture index were associated with a higher incidence of osteopenia. However, patients with higher PRL levels had a lower incidence of osteopenia. The length of the line segment corresponding to each variable in the nomogram represented the degree of influence on the outcome variable (i.e., the occurrence of osteopenia). The corresponding score or category of the variable represents the probability of osteopenia.

TABLE 3 Multivariable logistic regression model with stepwise variable selection.

Variables	*β* coefficient	Z	*p*-Value
Constant	−1.272	−1.042	0.298
Duration of breast cancer	0.079	2.427	0.015
Hip fracture index	3.673	2.919	0.004
PRL	−0.007	−1.826	0.068

PRL, prolactin.

Calibration refers to the degree to which the predicted probability of an outcome is consistent with the observed probability. The calibration curve showed that the predicted probability of AIBL in the training set was close to the actual probability when the risk of AIBL was low, while there was an overestimation or underestimation when the actual probability was high (Figure 2B). The receiver operating characteristic (ROC) curve was used to reflect the sensitivity and specificity of the prediction model. The ROC curve's ordinate can measure the sensitivity of the model, and the value on the abscissa is the

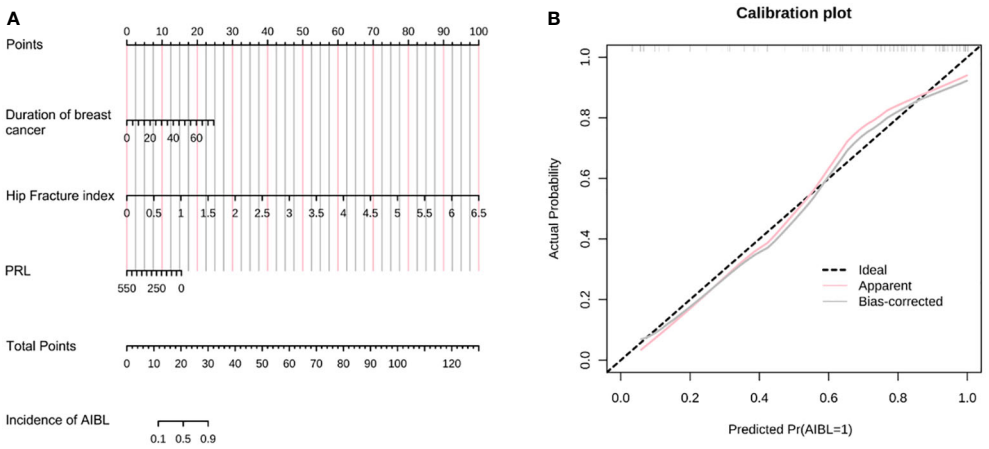

FIGURE 2
(A) The nomogram of AIBL incidence in hormone receptor-positive breast cancer patients using the logistic regression method. **(B)** The calibration curve of the nomogram. AIBL, aromatase inhibitor-associated bone loss.

inverse measure model's specificity (1 – specificity). The area under the ROC curve (AUC) is usually used as the model's performance measure. As shown in Figure 3, the AUC of the AIBL prediction model based on the logistic regression method was 0.874, the specificity was 0.918, the sensitivity was 0.733, and the cutoff value was 0.533. In the validation set, the corresponding values were 0.716 for AUC, 0.529 for specificity, and 0.882 for sensitivity, and the cutoff value was 0.703. Therefore, the logistic prediction model of AIBL was found to be deficient in terms of calibration and discrimination.

Construction and validation of the LASSO regression prediction model

The dependent variable in this study was the occurrence of osteopenia, while the six identified risk factors were considered independent variables in the LASSO regression model. The penalty term coefficient lambda was determined *via* fivefold cross-validation. The results showed that the AUC was maximal when the model was compressed to three variables (Figure 4A), and the corresponding lambda was 0.0817. The three variables selected were the duration of breast cancer, hip fracture index, and prolactin, which were consistent with the results of the logistic model. The model coefficients corresponding to the three variables are shown in Supplementary Table 2. The degree of compression of the six variables under different penalty parameter lambda is illustrated in Figure 4B. In classification models, the AUC value is commonly used as the evaluation index. The expression of the LASSO model on the test set was poor, with an AUC value of only 0.691 (Figure 4C).

Construction and validation of a prediction model using XGBoost machine learning algorithm

XGBoost was developed by Tianqi Chen in 2016 and is based on the idea of building a basic learner in the training set (8), adjusting

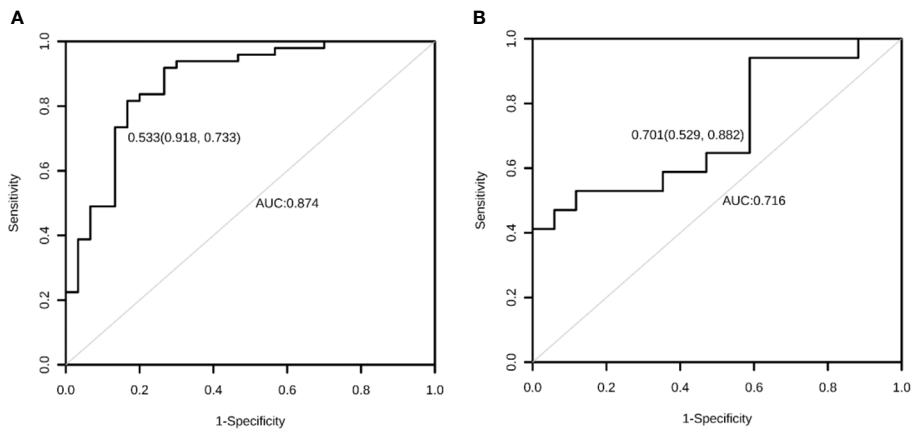

FIGURE 3
The ROC curve of the AIBL prediction model for the training set **(A)** and the test set **(B)** using the logistic regression method. ROC, receiver operating characteristic; AIBL, aromatase inhibitor-associated bone loss.

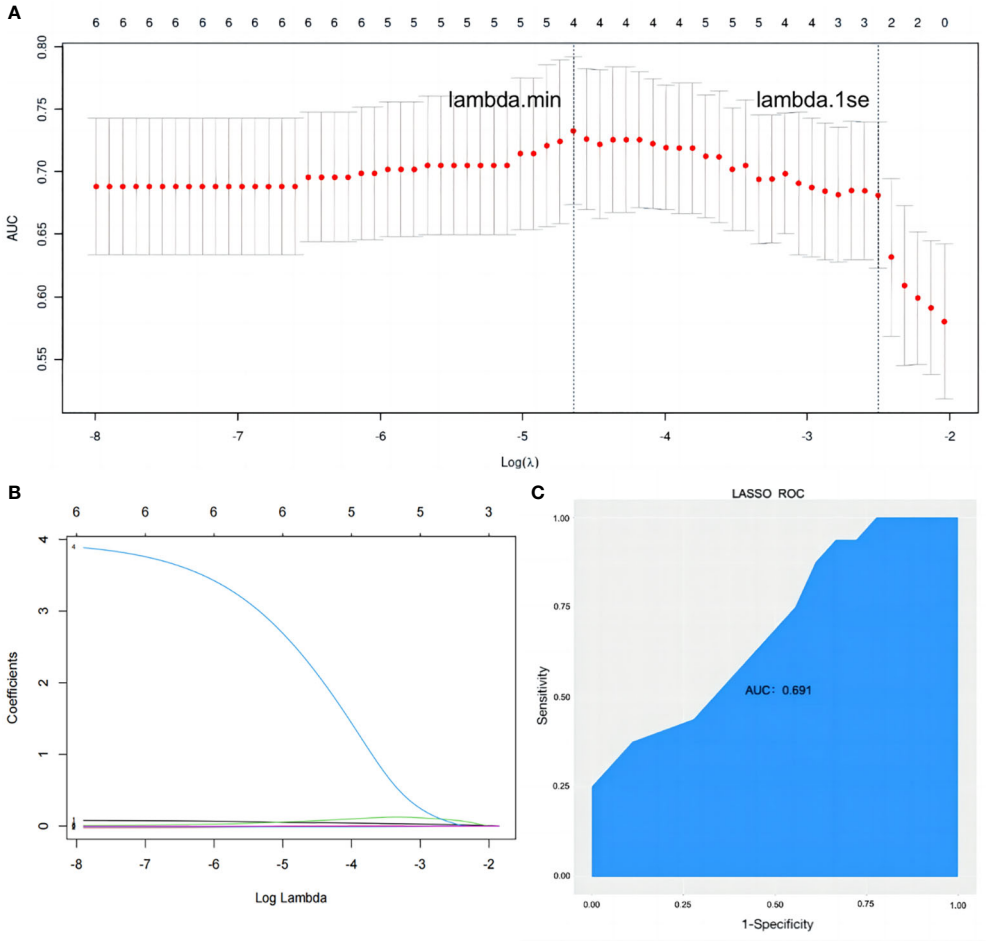

FIGURE 4
Establishment and validation of a binary outcome prediction model based on LASSO regression. **(A)** In the LASSO model, the optimal parameter (lambda) was selected using a fivefold cross-validation approach. The log(lambda) plot was used to identify lambda.1se, which was used to obtain the included feature factors. The relationship between AUC and log(lambda) was shown. **(B)** LASSO coefficient profiles of the six variables. **(C)** The ROC curve of prediction model. LASSO, least absolute shrinkage and selection operator; AUC, area under the receiver operating characteristic curve; ROC, receiver operating characteristic.

the sample distribution according to the results of the basic learner and repeating this process until the number of basic learners reaches the set value. The XGBoost algorithm has been widely used in disease risk prediction in medical research (15–17).

The dataset of 113 subjects was randomly divided into training and test sets in a 7:3 ratio. The XGBoost prediction model was constructed by adjusting each parameter, and the importance of the six variables included in the AIBL model was calculated and arranged (as shown in Table 4; Figure 5). Hip fracture index and prolactin were found to be the two most important factors, accounting for more than half of the proportion, followed by the duration of breast cancer and osteocalcin level, which accounted for one-third. Major osteoporotic fracture index and aromatase inhibitor treatment time accounted for more than 5%. The sum of the importance ratios of all features was 1.

In summary, the AIBL prediction model constructed by the XGBoost machine learning algorithm has demonstrated the importance of each characteristic variable, and no irrelevant information was included. The random split validation method was employed for internal validation of this part of the XGBoost machine learning prediction model. The test set data were incorporated into the XGBoost prediction model while adjusting the parameters: the maximum depth of the tree was set to 6, the learning rate to 0.5, and the maximum number of iterations to 25, and the other parameters were set to default. The ROC curve (Figure 6) was generated, and the AUC was found to be 0.761, with a specificity of 0.667, a sensitivity of 0.818, and a cutoff value of 0.491. These results indicate that the XGBoost model exhibits excellent predictive performance.

Summary

This study included a total of 113 eligible patients of whom 66 had osteopenia. A set of 48 candidate predictors, comprising

TABLE 4 The ranking table of the importance of the XGBoost algorithm for the six variables in the AIBL prediction model.

Variables	Gain	Cover	Frequency	Importance
Hip fracture index	0.30	0.20	0.13	0.30
PRL	0.26	0.22	0.25	0.26
Duration of breast cancer	0.15	0.14	0.12	0.15
OC	0.15	0.22	0.23	0.15
Major osteoporotic fracture index	0.09	0.16	0.19	0.09
Duration of aromatase inhibitor therapy	0.05	0.05	0.09	0.05

XGBoost, eXtreme gradient boosting; AIBL, aromatase inhibitor-associated bone loss; PRL, prolactin; OC, osteocalcin.

basic patient information, breast cancer diagnosis and treatment, and three scales of FRAX, WOMAC, and M-SACRAH, involving 23 variables, as well as 25 blood index tests were identified. With the use of logistic, LASSO, and XGBoost algorithms, three prediction models were constructed and validated to predict the incidence of AIBL in hormone receptor-positive breast cancer patients. The logistic and LASSO regression models included three predictive factors, namely, the duration of breast cancer, hip fracture index, and prolactin. The performance of the three models was evaluated using the area under the ROC curve, with the XGBoost model demonstrating superior performance.

Discussion

The mechanism of AIBL in hormone receptor-positive breast cancer patients is analogous to that of postmenopausal women with osteoporosis, where a significant decrease in estrogen levels leads to bone loss. However, AIBL patients are affected by various factors, such as OFS treatment, radiotherapy, and chemotherapy, in addition to AI treatment. The screening tools for osteoporosis, such as OSTA (18) and SCORE (19), which are applicable to all women, mainly consider recognized high-risk factors such as age, body mass index (BMI), and fracture history. These tools cannot comprehensively screen high-risk factors in the AIBL group. Therefore, the AIBL model constructed in this study serves as a supplement to current screening tools in the field of osteoporosis. The primary target of the prediction model is the high-risk factors of AIBL in hormone receptor-positive breast cancer patients. This model aims to provide technical support for early intervention and further refine screening for this high-risk group.

The hip fracture index is a significant high-risk factor for AIBL in both models and is consistent with previous research

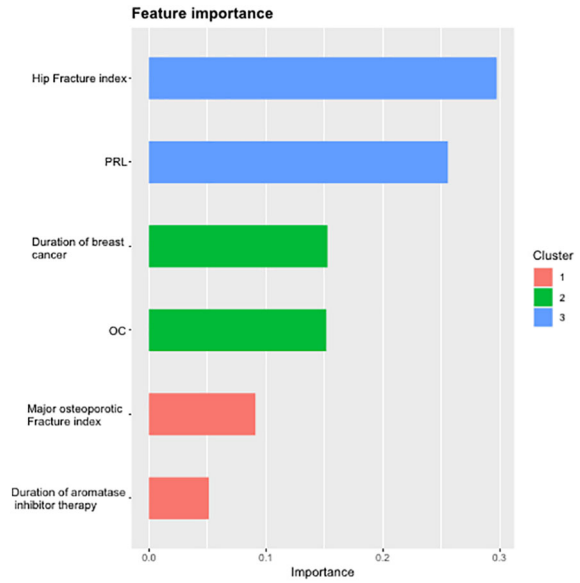

FIGURE 5
Importance ranking diagram of variables in AIBL prediction model. AIBL, aromatase inhibitor-associated bone loss.

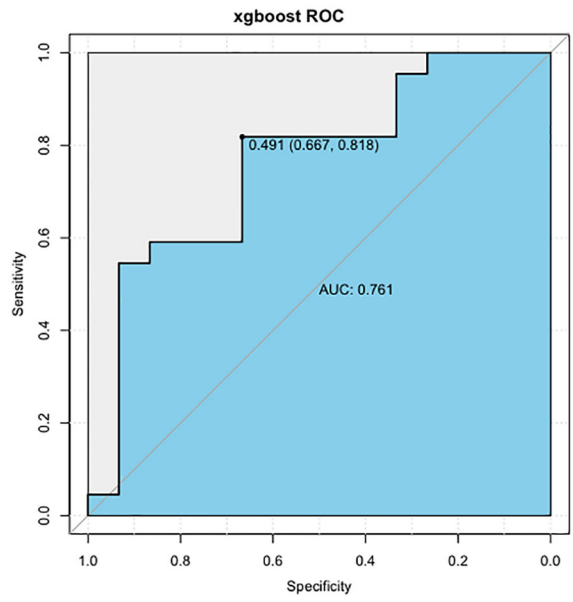

FIGURE 6
ROC curve of AIBL prediction model constructed by XGBoost algorithm. ROC, receiver operating characteristic; AIBL, aromatase inhibitor-associated bone loss; XGBoost, eXtreme gradient boosting.

(11). PRL is secreted by the anterior pituitary gland, and studies have shown that women with hyperprolactinemia and prolactinomas have a higher incidence of vertebral fractures when compared to the normal population (20). Another study suggests that an increase in normal PRL levels may have a positive effect on BMD in patients with type 2 diabetes mellitus (T2DM) rather than a significant increase in PRL (21). Our study indicates that higher levels of PRL are negatively associated with the development of AIBL and may serve as protective factors. However, the study sample size was inadequate to provide a specific numerical range for the protective effect of PRL. Furthermore, there is a lack of *in vivo* or *in vitro* animal experiments to further elucidate the underlying mechanisms.

A meta-analysis of screening tools for osteoporosis (22) highlighted a common issue that the sensitivity was usually close to or above 90% at a specific threshold, the specificity was often below 50%, and the AUC values were generally between 0.5 and 0.8. In contrast, the XGBoost model developed in this study achieved a sensitivity of 66.7% and a specificity of 81.8% at a threshold of 0.491, with an AUC of 0.761. The AIBL risk prediction model incorporates blood indicators, which may be more expensive than medical history collection but can avoid the bias of subjective reporting and provide more reliable information. Moreover, the blood indicators used in the model are common in China and are more accessible than BMD testing. Using the risk prediction model to screen patients who have recently undergone blood tests can prompt the diagnosis of osteopenia by BMD testing. The AIBL prediction model can also be used to screen patients with metal implants who cannot undergo BMD testing to reduce the rate of missed diagnosis. Although the three risk prediction models developed in this study may not be as simple and economical as the FARX screening tool, they can screen patients with a high risk of bone loss based on the existing blood test results without additional economic cost. Despite routine calcium supplementation during AI treatment, more than half of patients still develop osteopenia or osteoporosis, suggesting that calcium supplementation alone may not meet the body's needs. Increasing the dose of calcium supplementation, adding vitamin D, or even bisphosphonates may be necessary for high-risk AIBL patients. In conclusion, the risk prediction models developed in this study using traditional logistic regression, LASSO regression, and XGBoost algorithm have clinical significance and practical application value, with the XGBoost algorithm demonstrating better performance.

In recent years, machine learning has been increasingly applied in the medical field, including in the development of bone loss risk prediction models. This study utilized the XGBoost algorithm to construct an AIBL prediction model, which complements the traditional logistic and LASSO algorithms and provides a fine division of the applicable population for bone loss. XGBoost machine learning has demonstrated superior performance in dealing with multiple complex variables and non-linear problems compared to traditional logistic regression and LASSO machine learning algorithms (15). However, the small number of research subjects and screening variables in this study limits the prediction performance of XGBoost. Future studies should continue to collect patients who meet the criteria and expand the database to observe the powerful performance of the XGBoost algorithm in processing high-dimensional data in building a risk prediction model. The AIBL prediction model developed in this study involves the cost of blood index testing, which may make it difficult to obtain information and promote implementation. Additionally, the lack of external validation raises concerns about the model's suitability for large-scale use in the real world. Future research should focus on the derivation and improvement of the AIBL prediction model for early warning of osteoporosis, specifically screening patients with osteoporosis according to blood biochemical indicators ($T < -2.5$). This population is at higher risk of fracture and experiences more noticeable arthralgia. The warning tool can help diagnose patients in a timely manner, adopt corresponding treatment, improve compliance with AI endocrine drugs, and successfully complete the full course of breast cancer treatment, which is the main goal of this study.

Data availability statement

The original contributions presented in this study are included in the article/Supplementary Material. Further inquiries can be directed to the corresponding authors.

Ethics statement

The Medical Ethics Committee of Longhua Hospital affiliated with the Shanghai University of Traditional Chinese Medicine approved this research.

Author contributions

MC and YZ: conceptualization, formal analysis, data curation, and visualization. MC: writing—original draft. YZ and LJ: validation, visualization, and writing—review and editing. YY: methodology. HC, TM and BH: investigation, validation, and data curation. JW and MY: supervision, project administration, and funding acquisition. All authors contributed to the article and approved the submitted version.

Funding

This study was supported by Shanghai Science and Technology Innovation Action Plan (21Y11923000).

Conflict of interest

The authors declare that the research was conducted in the absence of any commercial or financial relationships that could be construed as a potential conflict of interest.

Publisher's note

All claims expressed in this article are solely those of the authors and do not necessarily represent those of their affiliated organizations, or those of the publisher, the editors and the reviewers. Any product that may be evaluated in this article, or claim that may be made by its manufacturer, is not guaranteed or endorsed by the publisher.

Supplementary material

The Supplementary Material for this article can be found online at: https://www.frontiersin.org/articles/10.3389/fonc.2023.1182792/full#supplementary-material

References

1. Sung H, Ferlay J, Siegel RL, Laversanne M, Soerjomataram I, Jemal A, et al. Global cancer statistics 2020: GLOBOCAN estimates of incidence and mortality worldwide for 36 cancers in 185 countries. *CA Cancer J Clin* (2021) 71:209–49. doi: 10.3322/caac.21660

2. Howlader N, Altekruse SF, Li CI, Chen VW, Clarke CA, Ries LA, et al. US Incidence of breast cancer subtypes defined by joint hormone receptor and HER2 status. *J Natl Cancer Inst* (2014) 106:8. doi: 10.1093/jnci/dju055

3. Waks AG, Winer EP. Breast cancer treatment: a review. *Jama* (2019) 321:288–300. doi: 10.1001/jama.2018.19323

4. Cuzick J, Sestak I, Forbes JF, Dowsett M, Cawthorn S, Mansel RE, et al. Use of anastrozole for breast cancer prevention (IBIS-II): long-term results of a randomised controlled trial. *Lancet* (2020) 395:117–22. doi: 10.1016/s0140-6736(19)32955-1

5. Condorelli R, Vaz-Luis I. Managing side effects in adjuvant endocrine therapy for breast cancer. *Expert Rev Anticancer Ther* (2018) 18:1101–12. doi: 10.1080/14737140.2018.1520096

6. Nick TG, Campbell KM. Logistic regression. *Methods Mol Biol* (2007) 404:273–301. doi: 10.1007/978-1-59745-530-5_14

7. Hu JY, Wang Y, Tong XM, Yang T. When to consider logistic LASSO regression in multivariate analysis? *Eur J Surg Oncol* (2021) 47:2206. doi: 10.1016/j.ejso.2021.04.011

8. Chen T, Guestrin C. XGBoost: a scalable tree boosting system. *ACM* (2016), 785–94. doi: 10.1145/2939672.2939785

9. Kanis JA, Melton LJ3rd, Christiansen C, Johnston CC, Khaltaev N. The diagnosis of osteoporosis. *J Bone Miner Res* (1994) 9:1137–41. doi: 10.1002/jbmr.5650090802

10. Leslie WD, Morin SN, Lix LM, Niraula S, McCloskey EV, Johansson H, et al. Performance of FRAX in women with breast cancer initiating aromatase inhibitor therapy: a registry-based cohort study. *J Bone Miner Res* (2019) 34:1428–35. doi: 10.1002/jbmr.3726

11. Hadji P, Aapro MS, Body JJ, Gnant M, Brandi ML, Reginster JY, et al. Management of aromatase inhibitor-associated bone loss (AIBL) in postmenopausal women with hormone sensitive breast cancer: joint position statement of the IOF, CABS, ECTS, IEG, ESCEO IMS, and SIOG. *J Bone Oncol* (2017) 7:1–12. doi: 10.1016/j.jbo.2017.03.001

12. Bellamy N, Buchanan WW, Goldsmith CH, Campbell J, Stitt LW. Validation study of WOMAC: a health status instrument for measuring clinically important patient relevant outcomes to antirheumatic drug therapy in patients with osteoarthritis of the hip or knee. *J Rheumatol* (1988) 15:1833–40.

13. Sautner J, Andel I, Rintelen B, Leeb BF. Development of the m-SACRAH, a modified, shortened version of SACRAH (Score for the assessment and quantification of chronic rheumatoid affections of the hands). *Rheumatology* (2004) 43:1409–13. doi: 10.1093/rheumatology/keh360

14. Martinez JA, Wertheim BC, Roe DJ, Chalasani P, Cohen J, Baer L, et al. Sulindac improves stiffness and quality of life in women taking aromatase inhibitors for breast cancer. *Breast Cancer Res Treat* (2022) 192:113–22. doi: 10.1007/s10549-021-06485-0

15. Hou N, Li M, He L, Xie B, Wang L, Zhang R, et al. Predicting 30-days mortality for MIMIC-III patients with sepsis-3: a machine learning approach using XGboost. *J Transl Med* (2020) 18:462. doi: 10.1186/s12967-020-02620-5\

16. Li Y, Xu Y, Ma Z, Ye Y, Gao L, Sun Y. An XGBoost-based model for assessment of aortic stiffness from wrist photoplethysmogram. *Comput Methods Programs BioMed* (2022) 226:107128. doi: 10.1016/j.cmpb.2022.107128

17. Song X, Zhu J, Tan X, Yu W, Wang Q, Shen D, et al. XGBoost-based feature learning method for mining COVID-19 novel diagnostic markers. *Front Public Health* (2022) 10:926069. doi: 10.3389/fpubh.2022.926069

18. Koh LK, Sedrine WB, Torralba TP, Kung A, Fujiwara S, Chan SP, et al. A simple tool to identify asian women at increased risk of osteoporosis. *Osteoporos Int* (2001) 12:699–705. doi: 10.1007/s001980170070

19. Lydick E, Cook K, Turpin J, Melton M, Stine R, Byrnes C. Development and validation of a simple questionnaire to facilitate identification of women likely to have low bone density. *Am J Manag Care* (1998) 4:37–48.

20. Mazziotti G, Mancini T, Mormando M, De Menis E, Bianchi A, Doga M, et al. High prevalence of radiological vertebral fractures in women with prolactin-secreting pituitary adenomas. *Pituitary* (2011) 14:299–306. doi: 10.1007/s11102-011-0293-4

21. Chen J, Liu G, Li Q, Deng W. Prolactin is associated with bone mineral density in subjects with type 2 diabetes mellitus. *Front In Endocrinol* (2022) 13:964808. doi: 10.3389/fendo.2022.964808

22. Nayak S, Edwards DL, Saleh AA, Greenspan SL. Systematic review and meta-analysis of the performance of clinical risk assessment instruments for screening for osteoporosis or low bone density. *Osteoporos Int* (2015) 26:1543–54. doi: 10.1007/s00198-015-3025-1

frontiers | Frontiers in Oncology

TYPE Review
PUBLISHED 01 May 2023
DOI 10.3389/fonc.2023.1195885

OPEN ACCESS

EDITED BY
Zheng Wang,
Shanghai Jiao Tong University, China

REVIEWED BY
Shun Gong,
Northern Theater General Hospital, China
Zheng He,
Qilu Hospital of Shandong University (Qingdao), China

*CORRESPONDENCE
Zhongzhao Wang
wangzhongzhao206@sina.com
Hu Chang
changhu2@163.com
Lixue Xuan
xuanlx@hotmail.com

RECEIVED 29 March 2023
ACCEPTED 19 April 2023
PUBLISHED 01 May 2023

CITATION
Zhang K, Li Y, Kong X, Lei C, Yang H, Wang N, Wang Z, Chang H and Xuan L (2023) AGR2: a secreted protein worthy of attention in diagnosis and treatment of breast cancer. *Front. Oncol.* 13:1195885. doi: 10.3389/fonc.2023.1195885

AGR2: a secreted protein worthy of attention in diagnosis and treatment of breast cancer

Ke Zhang[1], Yuan Li[1], Xiangyi Kong[1], Chuqi Lei[1], Huaiyu Yang[1], Nianchang Wang[2], Zhongzhao Wang[1]*, Hu Chang[3]* and Lixue Xuan[1]*

[1]Department of Breast Surgical Oncology, National Cancer Center/National Clinical Research Center for Cancer/Cancer Hospital, Chinese Academy of Medical Sciences and Peking Union Medical College, Beijing, China, [2]Department of Cancer Prevention, National Cancer Center/National Clinical Research Center for Cancer/Cancer Hospital, Chinese Academy of Medical Sciences and Peking Union Medical College, Beijing, China, [3]Administration Office, National Cancer Center/National Clinical Research Center for Cancer/Cancer Hospital, Chinese Academy of Medical Sciences and Peking Union Medical College, Beijing, China

AGR2 is a secreted protein widely existing in breast. In precancerous lesions, primary tumors and metastatic tumors, the expression of AGR2 is increased, which has aroused our interest. This review introduces the gene and protein structure of AGR2. Its endoplasmic reticulum retention sequence, protein disulfide isomerase active site and multiple protein binding sequences endow AGR2 with diverse functions inside and outside breast cancer cells. This review also enumerates the role of AGR2 in the progress and prognosis of breast cancer, and emphasizes that AGR2 can be a promising biomarker and a target for immunotherapy of breast cancer, providing new ideas for early diagnosis and treatment of breast cancer.

KEYWORDS

AGR2, breast cancer, protein disulfide isomerase, protein-protein interaction, protein secretion

Introduction

In 1998, Devon A.Thomson and Ronald J.Weigel of Stanford University in the United States used suppression subtractive hybridization (SSH) to screen the homologous gene with Xenopus anterior gradient-2 (XAG-2) from the cDNA library of estrogen receptor positive breast cancer cell line MCF7, named hAG-2, or anterior gradient-2 (AGR2) (1). AGR2 was only expressed in estrogen receptor positive breast cancer cell lines, but not in estrogen receptor negative breast cancer cell lines, which attracted great attention when it was found. Subsequently, a large number of studies showed that AGR2 was overexpressed in more than half of cases in breast cancer, prostate cancer, pancreatic cancer, esophageal cancer, which had a certain correlation with the development stage and pathological characteristics of the tumor, and might be involved in the process of tumor cell metastasis, survival, invasion and so on, indicating that AGR2 may be a new key gene related to cancer

regulation and biomarker. The regulatory effect and mechanism of AGR2 on tumor is an important hotspot in the field of tumor research. The correlation between AGR2 expression and ER positive rate of breast cancer cell lines and the ability of estradiol to induce its expression suggests that AGR2 may mediate the normal physiology and estrogen effect of breast cancer (2). This article focuses on the research progress of AGR2 and the occurrence, development and clinicopathological relationship of breast cancer.

AGR2 gene

A clone containing AGR2 gene was isolated from human genomic DNA library (3). The whole clone was labeled with biotin and used as a probe for FISH analysis. Highly specific signals were detected in chromosome region 7p21.3 of all metaphase cells, indicating that AGR2 gene is located in the region of human chromosome 7p21.3. The AGR2 gene spans a region of 50 kb in genomic DNA, containing 8 exons and 7 introns, and is mainly expressed in organs from endoderm (4). Hrstka et al. (5) carried out chromatin immunoprecipitation assay on AGR2 promoters. Compared with the control group, the amount of AGR2 promoter that coimmunoprecipitated with ERα antibody was approximately twofold increased, indicating that the transcription of AGR2 is estrogen responsive at the molecular level.

Structure of AGR2 protein

AGR2 protein, an endoplasmic reticulum resident protein mainly expressed in human epithelial cells, is composed of 175 amino acid sequences with a relative molecular weight of 20000 (6). It was assigned to the human protein disulfide isomerase (PDI) family later than all other members. Mainly located in the endoplasmic reticulum, PDI family proteins have 1-4 active motifs CXXC, which can catalyze the formation and isomerization of protein disulfide bonds, so as to stabilize proteins, and can also be used as molecular chaperone to inhibit protein aggregation (7). Park et al. (8) found that AGR2 is important for the production of intestinal mucin 2 (MUC2) *in vivo* by studying mouse intestinal epithelial cells. MUC2 is a cysteine-rich glycoprotein, which forms a protective mucus gel in the intestine. A cysteine residue in AGR2 thioredoxin-like domain forms mixed disulfide bonds with MUC2, which is a prerequisite for MUC2 secretion by intestinal epithelial cells. This indicates that AGR2 has two key properties of PDI: endoplasmic reticulum localization and functional thioredoxin-like domain (Figure 1).

Most protein-protein interactions in mammals are driven by linear peptide motifs. Similarly, three classical linear motifs in AGR2 define its core biochemical determinants (10). First, the N-terminal hydrophobic sequence (amino acids 1-20) directs AGR2 into the endoplasmic reticulum, which contains a secretory signal sequence that can be cutted, and the cutting site is located between Ala20 and Lys21. Secondly, the C-terminus includes another classical linear peptide motif, the endoplasmic reticulum retention motif containing the tetrapeptide sequence of lysine (K), threonine (T), glutamate (E), leucine (L), abbreviated as KTEL. This sequence is conserved in all vertebrates from Xenopus laevis to human (11). KTEL motif can bind to three known KDEL receptors, leading to ER localization (12). KTEL motif has specific functions. Gupta et al. (11) used two different cell lines, in which AGR2 induced the expression of EGF receptor ligand amphibian glycoprotein or transcription factor CDX2, and found that only the highly conserved wild-type carboxy terminal KTEL motifs could produce appropriate results. Deletion of KTEL motif will lead to AGR2

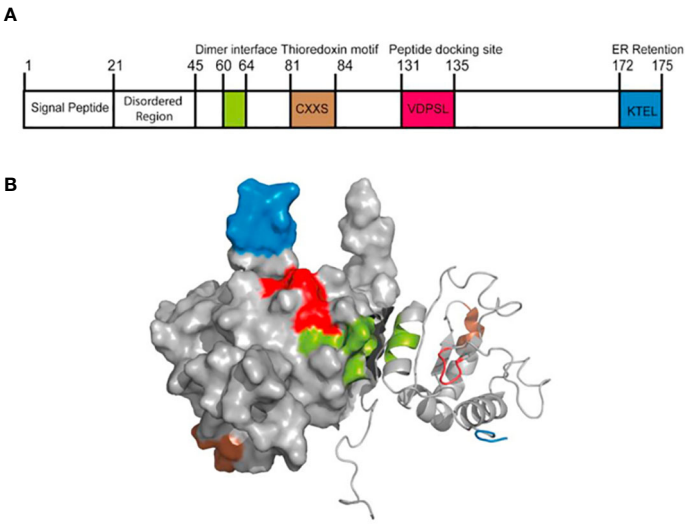

FIGURE 1
The structure of AGR2 protein. **(A)** The primary structure of AGR2 protein. The function of human AGR2 is highlighted; From left to right are signal peptide, N-terminal internal disordered region, dimerization motif (green), thioredoxin motif (brown), peptide docking site (red) and ER retention motif (blue). The structural domains of AGR2 determine its diverse functions. **(B)** Solution structure of dimer AGR2. The color coding of the functional pattern is based on **(A)**. Reprinted from (9). © 2020 The Author(s).

secretion and AGR2 loss of function. When the carboxyl terminal KDEL or KSEL is used instead of KTEL, the AGR2 function will also be lost. However, compared with the classical KDEL sequence, the affinity between KTEL motif and KDEL receptor is lower. This may have a significant impact on the transport of AGR2 protein to different compartments in cells and its corresponding functions. AGR2 can escape the ER localization mechanism and be secreted to play an autocrine/paracrine role (13). Dumartin et al. (14) found that AGR2 was also located on the outer surface of pancreatic cancer cells expressing AGR2. At the same time, AGR2 can also exist in the extracellular space, serum and urine (15, 16), which opens up other ways for its role in the tumor microenvironment. In order to explore the functional significance of KTEL motif on AGR2 secretion, Fessart et al. (17) used HEK-293T cells that did not secrete AGR2 and used different AGR2 mutation structures, in which KTEL motif was mutated into KDEL, K172D, K172A or stop was inserted before KTEL (ΔKTEL). The results showed that the level of extracellular AGR2 in mutant cells was at least equal to that observed in wild-type cells. This suggests that the secretion of AGR2 protein may be independent of its KTEL motif. In conclusion, KTEL motif is more likely to be necessary for intracellular AGR2 to function. In addition, the KTEL motif in AGR2 also plays a functional role in the metastasis pathway of cancer cells. Intracellular AGR2 can promote colorectal metastasis through KDEL-KDEL receptor-Gs-PKA axis (18).

The third key linear motif of AGR2 is CXXS motif. Classical thioredoxin has a conserved thioredoxin fold, which is composed of CXXC motif. CXXC motif mediates the formation of covalent bonds with downstream proteins containing cysteine, and then is resolved by oxidation-reduction (19). In contrast, AGR2 is part of the thioredoxin superfamily, which contains CXXS motif and lacks the ability of the dicysteine redox system to mediate the redox of downstream proteins (6). Therefore, it may block the antioxidant electron transfer system, thus creating a superoxide environment and enhancing the maintenance of cell damage during tumor formation (20). It contains a central and unique cysteine residue, through which, it is thought to mediate a non-redundant reaction when binding to the substrate (10). At the same time, this motif may form mixed disulfides with mucin (MUC1 (8), MUC2 (21) and MUC5AC (22)), contributing to their secretion. Nevertheless, the analytical nuclear magnetic resonance (NMR) of AGR2 structure shows that AGR2 can be stable in an antiparallel way through the Glu60-Lys64 interface and acts as a homodimer to catalyze the CXXS motif away from the interface (23). Therefore, compared with the typical thioredoxin motif, the dimer structure can be regarded as having the same stoichiometric redox capacity (9). Surprisingly, the deletion of 40 amino acids at the N-terminal of AGR2 could improve the stability of the dimer by three orders of magnitude (10). This suggests that the full-length AGR2 may tend to exist as a monomer rather than a complete dimer (24). The N-terminal plays a natural negative regulatory role to reduce the affinity of dimer. Therefore, pharmacological operation on the stability of AGR2 dimer is possible, because synthetic peptides from the N-terminal disordered region can reverse regulate the stability of AGR2 dimer, which suggests that we can develop a drug precursor that can change the stability of AGR2 dimer. Patel et al. (23) found that AGR221-175 with 20 amino acids removed from the N-terminal could significantly improve the adhesion rate of rat breast tumor cells. In contrast, AGR241-175 lacked the 21-40 region, which not only failed to improve the cell adhesion rate, but also showed a significantly reduced rate. The cell adhesion rates of monomer mutant protein E60A AGR221-175 and E60A AGR241-175 (48.3 ± 4.3%, 11.5 ± 0.3%) were not significantly different from the corresponding natural dimer protein AGR221-175 and AGR241-175 ($P = 0.58$, $P = 0.74$). This indicates that monomer and dimer forms have similar cell adhesion properties. Although the N-terminal 21-40 amino acids are disordered, they are specific in the role of cell adhesion. In addition to the dimer structure mediated by amino acids 60-64, AGR2 can also form disulfide bond via Cysteine-81 and reorient the dimer to different conformations (25). This homodimer triggers the activation of unfolded protein reaction (UPR) signaling pathway through the interaction with BiP/GRP78, and reduces ER stress-induced cell death.

AGR2 and interaction partners

Protein-protein interaction (PPI) is important for the correct structure and function of most protein complexes (26). Protein-protein interaction may significantly contribute to the regulation of key biological processes, such as cell growth, proliferation and cell homeostasis (27). Therefore, the identification and analysis of the physical interactions between various proteins is essential for revealing the functions of physiological proteins and understanding the molecular mechanisms leading to human diseases. Existing data show that AGR2 can bind to a variety of proteins, such as nuclear protein, cytoplasmic protein and plasma membrane protein (28), as described in Table 1.

Fletcher et al. (30) found two proteins interacting with AGR2 by yeast two-hybrid system, GPI anchored C4.4a protein and DAG-1 protein. Their expression in breast cancer samples was higher than that in adjacent normal tissues, and the protein expression in ER positive breast cancer was higher than that in ER negative breast cancer. C4.4a protein can bind to its ligand's laminin 1 and 5, and is associated with galectin 3 to promote cell metastasis (37). This associates AGR2 with GPI-anchored receptor proteins involved in hormone reactivity, cell adhesion, migration and metastasis. AGR2 may promote tumor metastasis through receptor adhesion and functional regulation. At the same time, the interaction with C4.4a and DAG-1 proteins may be a feasible target for the intervention of estrogen responsive breast cancer, which promotes researchers' interest in the research of proteins interacting with AGR2. Although C4.4a and DAG-1 proteins have not been biologically verified as real protein-protein interactions in human cells, Kumar et al. (38) found the interaction between newt extracellular receptor Prod1 and newt AGR2 using yeast two-hybrid system, and verified the direct signal transduction role of AGR2 in amphibian limb regeneration. Human CD59 protein and newt Prod1 protein have 23% homology, and both belong to Ly6 superfamily with the same core motif CCXXXXCN (39). Therefore, it is speculated that

TABLE 1 List of AGR2 interacting proteins validated by protein-protein interaction assays.

Protein Name	Method	Interacting Domain	Influence	Reference
Endoplasmic reticulum				
TMED2	Endoplasmic reticulum mammalian protein-protein interaction trap (ERMIT), coimmunoprecipitation	Amino acid K66 and amino acid Y111	Control AGR2 dimerization	(29)
KDELR	Bimolecular fluorescence completion	KTEL motif (Amino acid 172 - 175)	Identification of three human KDEL receptors with different specificities	(12)
Plasma membrane				
DAG1	The yeast two-hybrid system	–	Cancer metastasis	(30)
EGFR	Protein immunoblots	–	EGFR can be transported to the cell surface, thus affecting the cell signal transduction	(31)
LYPD3(C4.4A)	The yeast two-hybrid system	–	Cancer metastasis	(30, 32)
EpCAM	ELISA, colocalization, proximity ligation assay	The structural ring of amino acids 131 – 135 (VDPSL)	Use linear peptide motif as a tool for discovering new protein-protein interactions	(24)
MUC1	coimmunoprecipitation experiments	–	Initiation and progress of carcinogenesis	(21)
MUC2	coimmunoprecipitation experiments	CXXS motif	Without AGR2, mice could not produce intestinal mucin	(8)
Immature MUC5AC and MUC5B	coimmunoprecipitation experiments	–	excessive mucus production caused by allergic airway inflammation	(22)
Cathepsin B (CTSB) and D (CTSD)	Two-dimensional fluorescence difference gel electrophoresis (2D-DIGE)	–	Cancer metastasis	(14)
Cytoplasm				
Reptin	The yeast two-hybrid system	Amino acids 104 - 111	Cancer cell growth	(33)
TSG101	stable-isotope labelling by amino acids in cell culture (SILAC) analysis	–	P53 inhibitor, leading to tumor transformation	(34)
Ki67	SILAC analysis	–	Promote cell proliferation	(34)
TAK1/TAB1/2 complex	tandem affinity purification combined with liquid chromatography tandem mass spectrometry (TAP-LC-MS/MS)	–	Promote tumor metastasis	(35)
RASSF5/STK3/4	TAP-LC-MS/MS	–	Consolidate the ability to inhibit apoptosis	(35)
Mitochondria				
UNG1	Immunoprecipitation	–	Stabilize UNG1 and enhance its enzyme activity in DNA repair	(36)

CD59 may also be a binding target of AGR2 in human and needs to be validated in human cells in the future.

The most well characterized AGR2 binding protein is the AAA+ superfamily protein Reptin (33). AGR2 interacts with Reptin by forming a dispersed octapeptide loop domain through its 104-111 amino acid residues, which is a stable complex to regulate the ATPase activity and helicase function of Reptin. At the same time, this study showed that Reptin could be overexpressed in human breast cancer. Considering that the mutation of ATP binding site of Reptin will affect its oligomerization level, thermal stability and stability of binding with AGR2, the modification of ATP binding site is of great significance to explore the role of Reptin-AGR2 complex in the growth of breast cancer cells.

AGR2 protein can specifically bind to a specific peptide motif (TTIYY), thus driving the interaction with other proteins (40). This motif is rich in membrane associated protein, which indicates that AGR2 plays a role in this kind of protein. Mohtar et al. (24) located the dominant region of interaction with TTIYY peptide in AGR2 by hydrogen deuterium exchange mass spectrometry. It is in the structural ring of amino acids 131-135 (VDPSL). This intrinsic sequence specific peptide binding activity in AGR2 is important for

its carcinogenic function, which has been used to mine human protein databases to search for proteins with similar motif. If we can find a protein corresponding to the AGR2 specific peptide motif, which can compete with the client protein in the carcinogenic pathway to bind AGR2, it will help to weaken the role of AGR2 in cancer growth and metastasis.

In addition, under normal conditions, AGR2 has been shown to interact with subtype of uracil DNA glycosylase protein (UNG1), which plays a key role in base excision and repair of mitochondria (36). Guo et al. (41) observed that extracellular AGR2 directly interacted with vascular endothelial growth factor (VEGF) and fibroblast growth factor 2 (FGF2) and enhanced their effects, contributing to angiogenesis and tumor growth. In addition, AGR2 may also induce the expression of lactate dehydrogenase A (LDHA), phosphoglycerate kinase 1 (PGK1), kallikrein 2 (HK2) and enolase 1α (ENO1) through the MUC1/HIF-α pathway (42), thus induce glycolysis of cancer cells, promote cell proliferation, migration, invasion and tumor growth. AGR2 can target and regulate the coactivators of Hippo signaling pathway, YAP-1 and amphiregulin (AREG) (31). AREG may interact with epidermal growth factor receptor (EGFR) to promote the growth of cancer cells. In addition, AGR2 can also play a role as an inhibitor of p53 (20), making the p53-dependent cell proliferation checkpoint ineffective. AGR2 may inhibit the phosphorylation of p53 at Ser15 and Ser392 sites by targeting the plasma membrane, thereby preventing cell apoptosis. At the same time, AGR2 up-regulates dual specific phosphatase 10 (DUSP10) (43, 44), thereby inhibiting p38 mitogen activated protein kinase (p38 MAPK) and preventing the activation of p53. MAPK/ERK signaling pathway may also be involved in the role of AGR2 in tumor (45). Under physiological emergency conditions, AGR2 induced response in MDA-MB-231 cell line can be effectively blocked by PD98059, a specific inhibitor of ERK1/2. The purification of AGR2 binding protein by TAP also showed that the TAK1/TAB1/2 complex in MAPK signaling pathway might be involved in the process of AGR2 regulating tumorigenesis and metastasis (35). AGR2 also induces tumor metastasis by regulating mTOR complex 2 (mTORC2) pathway (46), promotes tumor cell dissemination through post transcriptional activation of cathepsin B (CTSB) and D (CTSD) (14), and prevents the activation of transforming growth factors β (TGF- β), which is involved in epithelial mesenchymal transition (EMT) during tumor invasion and metastasis, in order to maintain the epithelial phenotype (47). To summarize, intracellular and extracellular AGR2 can interact with other proteins through their intrinsic motifs and secretion functions, playing an essential role in tumor cell growth, angiogenesis, inhibition of apoptosis, and tissue metastasis.

Expression and regulation of AGR2

AGR2 can participate in a variety of biological effects through protein-protein interactions. Meanwhile, AGR2 activity can also be regulated in a variety of ways. In breast cancer, AGR2 co exists with estrogen receptor and is induced by estrogen (2). Li et al. (48) deciphered that insulin-like growth factor-1 (IGF-1) significantly induced AGR2 in MCF7 cell line through the estrogen response element (ERE) between -802 and -808 bp and the leucine zipper transcription factor binding site between -972 and -982 bp on the AGR2 promoter. Knockdown of AGR2 can reduce IGF-1-induced cell proliferation, migration and cell cycle progression, which indicates that AGR2 is a key regulator involved in the development of IGF-1-induced breast cancer. However, the expression of AGR2 is not entirely dependent on estrogen. Other factors can also induce its expression. A study (45) showed that under hypoxia or serum-free conditions, the expression of AGR2 in ER negative breast cancer cell line BT20 was 8 times higher than that in normal condition after 24 hours of culture. The expression of estrogen receptor in MDA-MB-231 cell line was analyzed in parallel with the induction level of AGR2. It was found that AGR2 was also expressed when estrogen receptor was not induced. The possible mechanism is endoplasmic reticulum stress in extreme environment. Cells activate a series of complementary adaptive mechanisms to respond to the increased demand for protein folding in. This adaptive mechanism is called unfolded protein response (UPR) (49). UPR may regulate AGR2 through IRE1α and ATF6, which indicates the functional role of AGR2 in endoplasmic reticulum protein balance (50). At the same time, Jung et al. (51) found that Twist1 directly stimulated the activity of AGR2 promoter, which was necessary to induce the expression of AGR2 under hypoxia, indicating that AGR2 was a downstream effector protein of Twist1 to induce the growth and metastasis of breast cancer. Independent of estrogen, Ondrouskova et al. (52) found that HER2 can also up-regulate AGR2 by activating the extracellular signal regulated kinase 1/2 (ERK1/2) - Akt pathway, leading to the proliferation of breast cancer cells, indicating that in estrogen receptor negative breast cancer, AGR2 expression level is significantly correlated with HER2 expression status. hnRNPL is a protein that increases in metastatic lesions in breast cancer cells. Xiu et al. (53) found that hnRNPL-LINC02273 complex can recruit to the AGR2 promoter region, and epigenetically up-regulate AGR2 by enhancing local H3K4me3 and H3K27ac levels, activating AGR2 transcription and promoting cancer metastasis. The expression of AGR2 is also regulated by a variety of miRNAs. For example, MiR-135b-5p enhances the sensitivity of breast cancer cells to adriamycin by targeting AGR2 (54). Circular RNA CircPVT1 mediates AGR2-HIF-1α axis through MiR-29a-3p, promoting the growth, invasion, migration and inhibiting apoptosis of breast cancer cells (55). LncRNA AFAP1-AS1 induces drug resistance via miR-653-5p/AGR2 axis (56). Therefore, clarifying the upstream and downstream proteins involved in AGR2 interactions and regulating the activity of AGR2 proteins by intervening in related molecular pathways is a strategy for inhibiting cancer growth and metastasis.

In conclusion, AGR2 has a unique primary protein structure, including secretory signal, endoplasmic reticulum retention sequence, as well as protein disulfide isomerase active site and a variety of protein binding sequences, which endows AGR2 with diverse roles in breast cancer cells. Intracellular AGR2 can promote the growth and survival of cancer cells, while extracellular AGR2 can be defined as a microenvironment regulator that makes cancer cells more aggressive (57).

Intracellular AGR2, as a protein disulfide isomerase, catalyzes the proper folding of multiple client proteins through PDI activity. For example, AGR2 can mediate the maturation of receptors including MUC5 and MUC2 by forming mixed disulfide bonds (8, 22). At the same time, AGR2 is very important in endoplasmic reticulum regulation and quality control. Overexpression of intracellular AGR2 may represent an intermediate entity between endoplasmic reticulum and tumor development (9). Endoplasmic reticulum stress and UPR activation can lead to the development of cancer (58). Under normal and basic condition, AGR2 mainly exists in homodimers. During endoplasmic reticulum stress, AGR2 dimers dissociate in a dose-dependent manner and form functional complexes with endoplasmic reticulum related degradation mechanism (ERAD) to isolate misfolded proteins from endoplasmic reticulum (29, 59). Conversely, if the balance between AGR2 dimer and monomer is broken, it will lead to the activation of pro-inflammatory response and the release of AGR2 into the extracellular environment (29), which indicates that the breaking of the relative balance between AGR2 dimer and monomer may be a sign of protein imbalance in endoplasmic reticulum (60). Although AGR2 usually exists in endoplasmic reticulum due to its protein folding and protein balance functions, AGR2 can escape the endoplasmic reticulum retrieval mechanism and locate in different cell compartments, such as cytoplasm, plasma membrane and extracellular environment, and affect downstream client proteins through protein-protein interaction. The secretion of extracellular AGR2 in cancer may be due to the saturation of endoplasmic reticulum receptor sites, because AGR2 is overexpressed in cancer cells (61). Clarke et al. (62) found that AGR2 is O-glycosylated when secreted from human and rat mammary epithelial cells, and the O-glycosylation of AGR2 may be important for AGR2-mediated cell adhesion. AGR2 in the extracellular environment may have a critical impact on the homeostasis of the tumor niche, which is a microenvironment conducive to tumor growth (28). Extracellular AGR2 can directly interact with vascular endothelial growth factor A through its thioredoxin motif, leading to enhanced VEGF/VEGFR2 signal transduction to promote vascular growth (63). Similarly, extracellular AGR2 can also directly promote the dimerization of VEGF and FGF2 and increase the concentration of active VEGF and FGF2 in the local environment of tumor, thus leading to the migration and aggregation of vascular endothelial cells and fibroblasts to the surrounding of tumor cells, and promoting angiogenesis, providing favorable conditions for the formation of tumor microenvironment (41). Meanwhile, AGR2 can be internalized into fibroblasts and cancer cells through endocytosis, then it will interact with β-catenin, resulting in β-catenin accumulation in the nucleus and regulating fibroblasts around tumor cells to affect tumor microenvironment (TME) (64, 65). Extracellular AGR2 and ER-α can interact to induce the expression of IGF-1, thereby promoting the proliferation, migration and epithelial-mesenchymal transition process in breast cancer cells and enhancing drug resistance (48). The existence of extracellular AGR2 can transform non tumor organs into tumor organs and enhance their growth by about 10 times, which is independent of its thioredoxin folding and endoplasmic reticulum retention motif (17). In this context, it is important to increase the understanding of the mechanisms and signals of AGR2 expression, localization and function. Similarly, future studies are needed to evaluate the complex coordination network of AGR2 cell function, because the change of AGR2 expression may affect the function of its interacting partners in different ways and damage the homeostasis and protein stability (Figure 2).

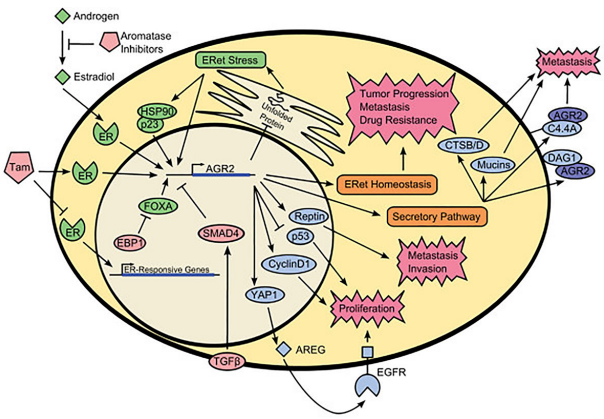

FIGURE 2
Schematic representation of AGR2 interactome. The green colored portion is the upstream activators of AGR2. The red colored portion is the upstream inhibitors of AGR2. The blue colored portion is proteins that interact with AGR2. AGR2 interacts with different proteins in the nucleus, cytoplasmic matrix, cell membrane, and outside of the cells to promote protein trafficking, protein homeostasis, cell signaling and proliferation, tumor progression and metastasis, drug resistance. Understanding the cancer promoting mechanism of AGR2 protein can help us better formulate cancer treatment strategies. Tam, tamoxifen; EBP1, ErbB3-binding protein 1; TGF-β, transforming growth factor β; ER, estrogen receptor; ERet, endoplasmic reticulum; FOXA, forkhead box family members A1 and A2; HSP90, heat-shock protein 90; YAP1, yes-associated protein 1; AREG, amphiregulin; CTSB/D, cathepsin B and cathepsin D; C4.4A, LY6/PLAUR domain containing 3; DAG1, dystroglycan 1; Reprinted from (2). Copyright © 2013 BioMed Central Ltd.

The clinical association between AGR2 and breast cancer

AGR2 was found by comparing the protein differences between ER positive and negative breast cancer cells (1). AGR2 only expressed in ER positive breast cancer cell lines, such as MCF7, T-47D, BT-474 and ZR-75, but not in ER negative breast cancer cell line MDA-MB-231 (66), which attracted a lot of attention once it was found, as described in Table 2. Later, experiments *in vivo* (75) and *in vitro* (5) confirmed that the expression of AGR2 protein was indeed regulated by estrogen. Fletcher et al. (30) used tissue microarray to show that AGR2 was expressed in 83% (n = 48) breast cancer cases, which was significantly correlated with ER expression (P = 0.01) and negatively correlated with EGFR expression (P = 0.009). Liu et al. (67) subsequently confirmed that the expression of AGR2 mRNA in MCF-7 breast cancer cells increased by 7.3 ± 0.2 times in the presence of estrogen. Immunohistochemical analysis of human breast tumors (n = 44) revealed that there was a significant correlation between ERα positive and AGR2 expression. Meanwhile, their research showed AGR2 could induce metastatic phenotype *in vivo*. The injection of AGR2 transfected rat mammary gland cells (Rama 37) into the mammary fat pad of homologous rats could induce a high incidence of lung metastasis, but the incidence of primary tumors in the rat model did not increase, which indicated that the expression of AGR2 may be related to metastasis. However, they did not analyze the correlation with patient survival. In addition, in a group of 225 ER positive breast cancer patients treated with tamoxifen, the survival rate of patients with AGR2 positive in breast cancer cells was lower than that of patients with AGR2 negative (68). In contrast, 126 patients with ER negative breast cancer did not show this relationship. Fritzsche et al. (69) studied the expression of AGR2 in 155 cases of breast cancer samples at the mRNA and protein levels, and confirmed that there was a significant correlation between the expression of AGR2 and ER status, but they also found that the expression of AGR2 was positively correlated with low cell proliferation rate, low-grade tumors and negative lymph nodes, indicating that AGR2 was associated with good prognosis of breast cancer. Compared with the above two different research results, the reason for the difference may be that the samples selected in the study are all tumors after endocrine therapy, and the prognosis of patients has a certain change. For example, the anti-estrogen effect of tamoxifen may affect the expression of AGR2 and bias the experimental results. Therefore, Barraclough et al. (70) performed only surgical treatment in 315 patients with operable breast cancer without adjuvant therapy including hormone therapy, and monitored the expression of AGR2 protein and the survival rate of patients. The results showed that after 20 years of follow-up, only 26% of patients with AGR2 positive cancer survived, while the survival rate of patients with AGR2 negative cancer was 96%, and the median survival time was significantly different, 68 months and more than 216 months respectively ($p<0.0001$), indicating that the presence of AGR2 in primary tumors is a possible prognostic indicator of poor prognosis in patients with breast cancer. Phoebe et al. (71) analyzed the main tumor mRNA data of women in the Molecular Taxonomy of Breast Cancer International Consortium (METABRIC) to determine AGR2 expression and disease-specific survival. The results showed that increased tumor AGR2 mRNA expression was associated with decreased disease specific survival (DSS) among 1341 women (P = 0.03). Vanderlaag et al. (76) knocked out AGR2 in breast cancer cell lines using siRNA

TABLE 2 Clinical research of AGR2 and breast cancer.

Researcher	Research Object	Research Type	Conclusion	Reference
Fletcher et al.	46 cDNA samples derived from breast tumor tissues	Retrospective study	Correlated with ER expression. Negatively correlated with EGFR expression.	(30)
Liu et al.	44 specimens from breast cancer patients	Retrospective study	Correlated with ER expression. Induced metastatic phenotype *in vivo*.	(67)
Innes et al.	225 patients with ER positive breast cancer treated with tamoxifen	Retrospective study	Associated with low survival rate in ER positive patients.	(68)
Fritzsche et al.	155 breast cancer patients	Retrospective study	Correlated with low cell proliferation rate, low grade tumor and negative lymph node.	(69)
Barraclough et al.	315 breast cancer patients who underwent surgery without adjuvant therapy	Longitudinal study	A possible prognostic indicator of poor prognosis in patients with breast cancer.	(70)
Phoebe et al.	Main tumor mRNA data of women in the Molecular Taxonomy of Breast Cancer International Consortium	Retrospective study	Correlated with low disease specific survival rate.	(71)
Kereh et al.	21 breast cancer patients	Cross-sectional observational study	Associated with breast cancer metastasis.	(72)
Maarouf et al.	118 breast cancer patients	Cross-sectional study	Promoted the metastasis and invasion of cancer cells. Correlated with the poor prognosis.	(73)
Lacambra et al.	504 breast cancer patients	Retrospective study	Significant difference of AGR2 expression rate in different molecular subtypes of breast cancer.	(74)

technology, which not only inhibited cell growth, but also led to cell death, and reduced the expression of survivin and c-Myc in ER positive cell lines. Survivin and c-Myc are related to the metastasis and invasion of breast cancer. Kereh et al. (72) compared the expression of AGR2 in metastatic patients and non-metastatic patients by counting the expression of AGR2 antibody on ELISA through cross-sectional observation study, and found that the average value of metastatic AGR2 was significantly higher than that of non-metastatic patients, 3.77 ng/dl and 1.76 ng/dl respectively (P <0.01), which also confirmed that AGR2 expression was associated with breast cancer metastasis. Maarouf et al. (73) also used ELISA method to evaluate the concentration of AGR2 in serum samples of breast cancer patients and healthy controls with or without metastasis. The results showed that the average value of AGR2 in healthy control group was 2.93 ± 0.42 ng/ml (n = 56), that in breast cancer group was 5.62 ± 0.87 ng/ml (n = 118), and that in breast cancer metastasis group was 13.7 ± 3.2 ng/ml (n = 23). AGR2 in patients with metastatic breast cancer was significantly higher than that in healthy controls (p<0.0001). These studies showed that in patients with ER positive breast cancer, AGR2 significantly promoted the metastasis and invasion of breast cancer cells, and was positively correlated with the poor prognosis of patients.

When considering molecular stratification, Lacambra et al. (74) retrospectively analyzed the immunohistochemical data of 504 breast cancer patients, and found that the expression rate of AGR2 in luminal A (n=226) was 50.4%, in luminal B (n=191) was 50.3%, in HER2-OE (n=40) was 35%, and in triple negative diseases was 4.3% (basal-like breast cancer, BLBC was 4.8%, unclassified was 3.8%). The positive rate of AGR2 in different molecular subtypes was significantly different (p<0.001). The expression of AGR2 was positively correlated with the expression of ER, PR and androgen receptor (AR), and negatively correlated with the expression of EGFR (p=0.002) and CK5/6 (p<0.001). These results further verified the data previously, showing that AGR2 was overexpressed in ER positive breast cancer. Interestingly, another research (77) revealed that the low expression of AGR2 is associated with the low overall survival of luminal A and the worst relapse free survival of basal-like breast cancer (BLBC). On the other hand, the high expression of AGR2 leads to worse overall survival and relapse free survival in luminal B patients and HER2 positive patients. A study (78) aimed to identify biomarkers of HER2 dependent breast cancer by proteomic methods found that AGR2 was overexpressed in more than 40% of HER2 positive breast cancer. The knockout of AGR2 resulted in enhanced invasion of MDA-MB435 cells. In the survival analysis of HER2 subgroup, it was found that in HER2 positive breast tumors, AGR2 expression was significantly increased at both mRNA and protein levels. In addition, in estrogen and progesterone receptor negative and HER2 positive cases, the increased expression of AGR2 was significantly correlated with the worse prognosis of patients (52, 79), indicating that AGR2 may be related to HER2 signal transduction.

So far, AGR2 participates in various tumor processes, such as differentiation, proliferation, migration, invasion and metastasis (80), and plays an important role in the progress and prognosis of breast cancer through its overexpression and non-canonical localizations. With the deepening of research, we found that the high expression of AGR2 marks the possible metastasis of breast cancer, which is one of the indicators of poor prognosis of breast cancer patients. However, its specific role in each molecular subtype of breast cancer has not yet been clarified. In different molecular subtypes, the level of AGR2 expression is related to the prognosis of patients, which should be further explored. Therefore, it is necessary to carry out more retrospective and prospective studies to clarify the molecular function and clinical role of AGR2, taking into account the heterogeneity and complexity of breast cancer molecules and the impact of breast cancer chemotherapy (Table 2).

AGR2 and biomarker

AGR2, as a promising biomarker, has aroused great interest because of its increased expression pattern in precancerous lesions, primary tumors and metastatic tumors, which is used to detect the most common cancers (81). As a secretory molecule, extracellular AGR2 can be detected in several biological fluid, including serum, plasma and urine, so it is a promising non-invasive biomarker. Meta analysis of 20 studies including 3285 patients showed that the increased expression of AGR2 was associated with poor overall survival in patients with solid tumors, especially breast cancer (82). Compared with primary breast tumors, the expression of a novel long non coding RNA called LINC02273 in metastatic lesions was significantly increased. When LINC02273 is combined with AGR2, it can be used as an independent prognostic factor to predict overall survival in patients with breast cancer (53). Maarouf et al. (73) confirmed that AGR2 could be detected in the serum of untreated breast cancer patients, and the level of AGR2 in patients was significantly higher than that in healthy individuals. In addition, the amount of AGR2 was significantly higher in patients with metastasis. Interestingly, extracellular AGR2 is not only clinically relevant in human tumors, but also significantly correlated with malignant mammary tumor (MMT) progression (P = 0.0007), distant tumor metastasis (P = 0.002) and poor overall survival (P = 0.0158) in dogs (83). In conclusion, we emphasize that AGR2 can be found in the body fluid of cancer patients, and its expression level can be distinguished from that of normal patients, which means that AGR2 may be used as a cancer marker for diagnosis or prognosis. It has certain reference value to infer whether the patient has a primary tumor and whether the tumor has metastasized based on the expression level of AGR2. At the same time, the combination of AGR2 and other biomarkers may be a promising strategy to improve the accuracy of early breast cancer detection (84). However, since AGR2 is not specific to breast, it cannot be used alone for early cancer detection as a serum biomarker, and needs to be integrated into the diagnostic score. So far, the detection of AGR2 protein level by enzyme-linked immunosorbent assay (ELISA) and the detection of AGR2 mRNA level by RT-PCR have extensive practical basis in the clinical detection of AGR2 (15, 85). However, these methods have expensive and complex equipment, so we are looking forward to developing simple, efficient and sensitive methods for detecting AGR2. Aptamers are small fragments of nucleotides or protein

peptides that are designed to bind to target molecules with specificity and high affinity (40). Multiple peptide aptamers are screened out by using the combined phage peptide library, which can recognize some epitopes of AGR2. The microarray composed of these peptide aptamers can be used to quantify AGR2 in clinical samples, providing a new and effective method for the determination of clinical markers. Hu et al. (86) showed a simple optical aptamer sensor for detecting AGR2 protein based on gold nanoparticles (AuNPs) and magnetic separation. The designed aptamer sensor is effective, sensitive and has low detection limit, which was successfully completed by using ultraviolet-visible molecular absorption spectrometry (UV-Vis). Lan et al. (87) used AGR aptamer coupled with a cytosine base sequence as Ag cluster template (MA@AgNCs) for targeting intracellular AGR. MA@AgNCs shows the maximum fluorescence peak at 565 and has excellent quantum yield (QY= 87.43%), small size, good biocompatibility, low toxicity and good stability. In addition, synthetic MA@AgNCs shows a high specificity in recognizing breast cancer cells. Graham et al. (88) designed a porous silicon based (PSi) aptamer that detected AGR2 by real-time monitoring the reflectivity changes of PSi nanostructures, with high selectivity and sufficient sensitivity. The emergence of aptamers provides a new research platform for efficient and rapid identification of AGR2, showing a good application prospect.

AGR2-related drug resistance in breast cancer

The incidence of ER positive breast cancer is the highest, accounting for about 75% of all cases of breast cancer (89). ER positive breast cancer usually responds well to endocrine therapy (ET). Endocrine therapy inhibits estrogen signal transduction in cancer cells, prevents their proliferation (cell inhibitory effect) and induces cell apoptosis (cell killing effect) (90). Although most ER positive breast cancer patients initially respond well to endocrine therapy, drug resistance will develop over time (acquired resistance), or some patients will not respond to endocrine therapy from the beginning (new resistance) (91). Therefore, ET resistance is an important clinical challenge in the treatment of breast cancer. Clinical studies (5, 92) had shown that the increased expression of AGR2 could mediate the resistance of tamoxifen as an estrogen agonist. Therefore, AGR2 level can be used to predict the resistance to tamoxifen and poor treatment response. Hrstka et al. (93) made tumor cells sensitive to tamoxifen by inhibiting the PDPK1-AKT pathway, which helped to exhaust the level of AGR2 protein, confirming the above view. Zamzam et al. (94) divided 224 ER positive breast cancer patients into three groups. Group 1 was sensitive to tamoxifen. Group 2 and group 3 were resistant to tamoxifen, and the level of AGR2 protein in all patients was mainly detected by ELISA. After 5 years of follow-up, they found that compared with group 1, the serum AGR2 level in group 2 and group 3 was significantly increased. This indicated that although ER expression itself was the main predictor of endocrine therapy response, the expression of AGR2 was closely related to the resistance of ER positive breast cancer patients to endocrine drugs (95), and serum AGR2 has potential availability as a biomarker for noninvasive early detection of tamoxifen resistance by ELISA. In addition to tamoxifen, Li et al. (48) found that the level of endogenous AGR2 was positively correlated with the resistance to fulvestrant in MCF-7 and T47D cells. The knockdown of AGR2 in MCF-7 cells strongly enhanced the G1 phase arrest and accelerated the degradation of ERα induced by fulvestrant. They also found that fulvestrant not only induced ER to enter the nucleus, but also caused AGR2 to relocate to the outer edge of the cell. This might be due to the conformational changes induced by fulvestrant and the subsequent phosphorylation of endoplasmic reticulum releasing AGR2 bound to ER. After treatment with fulvestrant, most of the ER entered the nucleus and released the bound AGR2. In addition, AGR2 can also communicate with HIF-1α, leading to hypoxia induced adriamycin resistance (96). The knockdown of AGR2 in MCF-7 cells led to the inhibition of adriamycin resistance induced by HIF-1α, while the increase of AGR2 level in MDA-MB-231 cells could enhance adriamycin resistance. A methyltransferase METTL3 may modify MALAT1 protein through N6 methyladenosine (m6A), recruit E2F1 and activate the expression of downstream AGR2, thus promoting the adriamycin resistance in breast cancer (97). Maarouf et al. (73) observed that the expression of AGR2 in tumor was negatively correlated with the aging marker p16. AGR2 induced the reproliferation of aging cells by activating AKT and mTORC2 signal transduction, leading to chemotherapy resistance. Whether it is by stabilizing HIF-1α to mediate the multiple drug resistance of breast cancer cells (96), or by promoting the localization of EGFR in the cell membrane, enhancing the EGFR signal to cause cancer cell proliferation (31), or by inhibiting the cell survival p38 MAPK pathway, inhibiting the activation of p53 transcription, and increasing the drug resistance of tumor cells to DNA damage drugs (43), it shows that the overexpression of AGR2 plays an important role in the treatment of breast cancer resistance.

Potential therapeutic targets in breast cancer

With the gradual deepening of research, the key regulation of AGR2 in cancer is gradually clear. It can be used as a cytoplasmic protein or through secretory form, mediate inflammatory response and external stimuli, regulate endoplasmic reticulum stress, affect the activity of p53, so as to regulate the survival, adhesion and metastasis of tumor cells, enhance the malignant transformation of tumor and promote the resistance of cancer cells to drugs. Therefore, AGR2 is an important target for cancer treatment.

The first antibody developed against AGR2 is a mouse monoclonal antibody, called 18A4, which has been proved to inhibit the growth of breast cancer cells *in vitro* (98). Subsequent studies produced a humanized version of this antibody, 18A4Hu I, and reported that it inhibited the growth of AGR2 positive ovarian cancer xenografts (99). The AGR2 monoclonal antibody aims to specifically target the extracellular AGR2, without affecting the intracellular AGR2 retention protein associated with endoplasmic

reticulum (100). Recently, in a preclinical mouse model of lung cancer, 18A4 antibody has been shown to improve survival and prevent AGR2 induced tumor progression by regulating p53 and MAPK pathways, without any toxic effect on major organs (101, 102). A study by Cocce et al. (103) based on the transcription factor FOXA1, membrane receptor LYPD3 and its ligand AGR2, identified a new target pathway for endocrine therapy of drug-resistant breast cancer. They showed that inhibiting the activity of this pathway with blocking antibodies against LYPD3 or AGR2 inhibited the growth of endocrine therapy resistant breast cancer in the preclinical model, and again provided the basis for the development of humanized antibodies against AGR2. Jung et al. (51) found that Twist1 is a new transcription factor that controls the expression of AGR2, and AGR2 is a key factor in Twist1 mediated breast cancer cell proliferation and migration. Therefore, targeting ER and Twist1 pathway at the same time may be enough to inhibit AGR2 and improve the survival rate of breast cancer patients. Considering the difference of AGR2 expression levels in different breast cancer patients, Zhang et al. (104) divided samples from patients with breast cancer into the high and low AGR2 expression subgroups. They found that patients with relatively AGR2 low expression exhibited immune "hot" tumors and immunosuppressive phenotype with high abundance of tumor immune cell infiltration, while patients with AGR2 high expression displayed opposite immunological characteristics, lacking immune cell infiltration. The outcome suggests that breast cancer patients with relatively AGR2 low expression may be more suitable for the treatment of immunotherapy, while the AGR2 high expression subgroup can firstly inhibit the expression of AGR2 by monoclonal antibody and transform poor immunogenic (cold) tumors into highly immunogenic and well-infiltrated (hot) tumors, which provides a personalized immunotherapy strategy for breast cancer based on AGR2. At the same time, bispecific antibodies (BsAb) have gradually become popular. In breast cancer, although PD-1/PD-L1 inhibitors have been proved to be more effective and less toxic than chemotherapy, immune related adverse events (irAE) have been observed, and in some cases, they may be related to irreversible organ damage or death (105). If AGR2 antibody and PD-1/PD-L1 inhibitors are combined to form a bispecific antibody, taking advantage of the increased expression of AGR2 in tumor cells, AGR2 antibody targets the tumor microenvironment and guides PD-1/PD-L1 inhibitors to enrich in the tumor bodies, thus reducing the non-specific over-activation of the immune system and maintaining the original or even additional tumor killing effect. Roy et al. (106) designed and synthesized BsAb AGR2xPD1, which showed higher anti-tumor response compared with the group of 18A4HU monoclonal antibody (mAb), the group of PD1 mAb and the combination treatment group of 18A4HU mAb and PD1 mAb. Wang et al. (107) focused their research on inhibiting AGR2 expression on proteasome inhibitors. They found that proteasome inhibitor MG132/bortezomib inhibited AGR2 expression at both mRNA and protein levels by activating autophagy. The combination of proteasome inhibitor and bevacizumab could enhance the anti-tumor efficiency of bevacizumab by decreasing the expression level of AGR2 and reducing its role in tumor cell angiogenesis. However, autophagy plays a dual role in tumor cell survival during chemotherapy and cancer gene targeting therapy, which means that cells can also recycle organelles to provide an energy supply by activating autophagy, leading to drug resistance (108). Therefore, more studies are needed in the future to prove the potential inhibitory effect of proteasome inhibitors alone or in combination with targeted drugs on the growth and metastasis of breast cancer and the benefits of clinical transformation. In addition to ER positive breast cancer, in HER2 positive breast cancer, ER signal transduction may also act as an escape pathway (109), leading to resistance to HER2 therapy. Therefore, blocking AGR2 directly may be an option for patients with HER2 positive breast tumors (52). The development and application of AGR2 targeted monoclonal antibodies, selective peptides and microRNAs can inhibit the growth and migration of breast cancer cells and enhance drug sensitivity (110). Zhang et al. (111) designed a hexapeptide based on the combination of AGR2 with the largest subunit of RNA Polymerase II (RNAPII) in a peptide motif dependent manner, which interfered with RNAPII by competitively destroying the AGR2-RNAPII complex, leading to RNAPII dysfunction and accompanied by the activation of DNA damage response in early tumor lesions, and proved to be effective in the treatment of breast cancer. It is worth mentioning that because the key linear motif of AGR2 protein exists in CXXS motif rather than in CXXC motif, AGR2 protein is more likely to form a homodimer to attain the same redox capacity. The stability of the dimer can be changed by studying a drug precursor to mediate the disorder region at the N-terminal of the protein, thus affecting the function of AGR2 in breast cancer. In the near future, it has a good prospect to test and apply AGR2 antibody in clinical trials and clinical patients.

Conclusion

In the past few years, AGR2 protein has aroused great interest in oncology. Its various carcinogenic properties and pathological effects mainly depend on the specificity of its cellular or extracellular localization. Intracellular AGR2 is a catalyst for the protein balance of endoplasmic reticulum to meet the secretory needs of cancer cells, while extracellular AGR2 is involved in the pro cancer signal transduction of epithelial tumorigenesis, ECM remodeling, inflammatory response and angiogenesis. In addition, this secreted AGR2 can be found in the body fluid of cancer patients, and the expression level can be distinguished from normal patients, which indicates that AGR2 can be used as a marker for diagnosis, prognosis and drug resistance. Diagnostic tools such as microfluidic detection devices or biosensors can be developed to detect AGR2 specifically and sensitively. Combining AGR2 with other tumor markers can improve the sensitivity of breast cancer diagnosis, which is one of the hot spots that clinicians need to pay attention to in the future. So far, therapeutic strategies targeting AGR2 have shown promising results. For example, by constructing the bispecific antibodies of AGR2 antibody and immune checkpoint proteins, it can play its role in tumor tissue with maximum target concentration, which is a clinical transformation direction to improve the efficacy and reduce side

effects. However, we also need to study the changes of key genes in AGR2 related signaling pathways, and better understand the upstream and downstream molecular mechanisms of AGR2. The in-depth understanding of the mechanism of AGR2 is of great significance for the study of the mechanism of tumor occurrence and development, as well as the early diagnosis, treatment and prognosis of AGR2 as a molecular target in clinic.

Author contributions

KZ: investigation, data curation, visualization, methodology, and writing-original draft. YL: investigation, visualization, writing-original draft, and funding acquisition. XK: methodology, writing-original draft, and writing-review and editing. CL: writing-original draft, and funding acquisition. HY: writing-original draft, and funding acquisition. NW: data curation and writing-original draft. ZW: conceptualization, supervision, validation, and project administration. HC: validation, supervision, and writing-review and editing. LX: conceptualization, resources, supervision, and funding acquisition. All authors contributed to the article and approved the submitted version.

Funding

This work was supported by the Chinese Academy of Medical Sciences Clinical and Translational Medicine Research Fund Project (No. 2019XK320067), the Natural Science Foundation of China (No. 82103047), the CAMS Innovation Fund for Medical Sciences (CIFMS) (No. 2022-I2M-C&T-B-087), the Non-profit Central Research Institute Fund of Chinese Academy of Medical Sciences (No. 2022-JKCS-04), the Beijing Association for Science and Technology's "Golden-Bridge Seed Funding Program" (No. ZZ22027), the Beijing Hope Run Special Fund of Cancer Foundation of China (No. LC2020L01), the Beijing Hope Run Special Fund of Cancer Foundation of China (No. LC2019L07), the Beijing Hope Run Special Fund of Cancer Foundation of China (No. LC2022A19), the Chinese Young Breast Experts Research project (No. CYBER-2021-005), the XianSheng Clinical Research Special Fund of China International Medical Foundation (No. Z-2014-06-2103), the Beijing Xisike Clinical Oncology Research Foundation (No. Y-Young2021-0017), and the Beijing Xisike Clinical Oncology Research Foundation (No. Y-NESTLE2022QN-0018).

Conflict of interest

The authors declare that the research was conducted in the absence of any commercial or financial relationships that could be construed as a potential conflict of interest.

Publisher's note

References

1. Thompson DA, Weigel RJ. Hag-2, the human homologue of the xenopus laevis cement gland gene xag-2, is coexpressed with estrogen receptor in breast cancer cell lines. *Biochem Biophys Res Commun* (1998) 251(1):111–6. doi: 10.1006/bbrc.1998.9440

2. Salmans ML, Zhao F, Andersen B. The estrogen-regulated anterior gradient 2 (Agr2) protein in breast cancer: a potential drug target and biomarker. *Breast Cancer Res* (2013) 15(2):204. doi: 10.1186/bcr3408

3. Petek E, Windpassinger C, Egger H, Kroisel PM, Wagner K. Localization of the human anterior gradient-2 gene (Agr2) to chromosome band 7p21.3 by radiation hybrid mapping and fluorescencein situ hybridisation. *Cytogenet Cell Genet* (2000) 89 (3-4):141–2. doi: 10.1159/000015594

4. Shih LJ, Lu YF, Chen YH, Lin CC, Chen JA, Hwang SP. Characterization of the Agr2 gene, a homologue of X. *Laevis Anterior Gradient 2 Zebrafish Danio Rerio. Gene Expr Patterns* (2007) 7(4):452–60. doi: 10.1016/j.modgep.2006.11.003

5. Hrstka R, Nenutil R, Fourtouna A, Maslon MM, Naughton C, Langdon S, et al. The pro-metastatic protein anterior gradient-2 predicts poor prognosis in tamoxifen-treated breast cancers. *Oncogene* (2010) 29(34):4838–47. doi: 10.1038/onc.2010.228

6. Persson S, Rosenquist M, Knoblach B, Khosravi-Far R, Sommarin M, Michalak M. Diversity of the protein disulfide isomerase family: identification of breast tumor induced Hag2 and Hag3 as novel members of the protein family. *Mol Phylogenet Evol* (2005) 36(3):734–40. doi: 10.1016/j.ympev.2005.04.002

7. Shishkin SS, Eremina LS, Kovalev LI, Kovaleva MA. Agr2, Erp57/Grp58, and some other human protein disulfide isomerases. *Biochem (Mosc)* (2013) 78(13):1415–30. doi: 10.1134/S000629791313004X

8. Park SW, Zhen G, Verhaeghe C, Nakagami Y, Nguyenvu LT, Barczak AJ, et al. The protein disulfide isomerase Agr2 is essential for production of intestinal mucus. *Proc Natl Acad Sci U.S.A.* (2009) 106(17):6950–5. doi: 10.1073/pnas.0808722106

9. Moidu NA, AR NS, Syafruddin SE, Low TY, Mohtar MA. Secretion of pro-oncogenic Agr2 protein in cancer. *Heliyon* (2020) 6(9):e05000. doi: 10.1016/j.heliyon.2020.e05000

10. Brychtova V, Mohtar A, Vojtesek B, Hupp TR. Mechanisms of anterior gradient-2 regulation and function in cancer. *Semin Cancer Biol* (2015) 33:16–24. doi: 10.1016/j.semcancer.2015.04.005

11. Gupta A, Dong A, Lowe AW. Agr2 gene function requires a unique endoplasmic reticulum localization motif. *J Biol Chem* (2012) 287(7):4773–82. doi: 10.1074/jbc.M111.301531

12. Raykhel I, Alanen H, Salo K, Jurvansuu J, Nguyen VD, Latva-Ranta M, et al. A molecular specificity code for the three mammalian kdel receptors. *J Cell Biol* (2007) 179(6):1193–204. doi: 10.1083/jcb.200705180

13. Chevet E, Fessart D, Delom F, Mulot A, Vojtesek B, Hrstka R, et al. Emerging roles for the pro-oncogenic anterior gradient-2 in cancer development. *Oncogene* (2013) 32(20):2499–509. doi: 10.1038/onc.2012.346

14. Dumartin L, Whiteman HJ, Weeks ME, Hariharan D, Dmitrovic B, Iacobuzio-Donahue CA, et al. Agr2 is a novel surface antigen that promotes the dissemination of pancreatic cancer cells through regulation of cathepsins b and d. *Cancer Res* (2011) 71(22):7091–102. doi: 10.1158/0008-5472.CAN-11-1367

15. Shi T, Gao Y, Quek SI, Fillmore TL, Nicora CD, Su D, et al. A highly sensitive targeted mass spectrometric assay for quantification of Agr2 protein in human urine and serum. *J Proteome Res* (2014) 13(2):875–82. doi: 10.1021/pr400912c

16. Park K, Chung YJ, So H, Kim K, Park J, Oh M, et al. Agr2, a mucinous ovarian cancer marker, promotes cell proliferation and migration. *Exp Mol Med* (2011) 43 (2):91–100. doi: 10.3858/emm.2011.43.2.011

17. Fessart D, Domblides C, Avril T, Eriksson LA, Begueret H, Pineau R, et al. Secretion of protein disulphide isomerase Agr2 confers tumorigenic properties. *Elife* (2016) 5:e13887. doi: 10.7554/eLife.13887

18. Zhang H, Chi J, Hu J, Ji T, Luo Z, Zhou C, et al. Intracellular Agr2 transduces Pge2 stimuli to promote epithelial-mesenchymal transition and metastasis of colorectal cancer. *Cancer Lett* (2021) 518:180–95. doi: 10.1016/j.canlet.2021.06.025

19. Jessop CE, Watkins RH, Simmons JJ, Tasab M, Bulleid NJ. Protein disulphide isomerase family members show distinct substrate specificity: P5 is targeted to bip client proteins. *J Cell Sci* (2009) 122(Pt 23):4287–95. doi: 10.1242/jcs.059154

20. Pohler E, Craig AL, Cotton J, Lawrie L, Dillon JF, Ross P, et al. The barrett's antigen anterior gradient-2 silences the P53 transcriptional response to DNA damage. *Mol Cell Proteomics* (2004) 3(6):534–47. doi: 10.1074/mcp.M300089-MCP200

21. Norris AM, Gore A, Balboni A, Young A, Longnecker DS, Korc M. Agr2 is a Smad4-suppressible gene that modulates Muc1 levels and promotes the initiation and progression of pancreatic intraepithelial neoplasia. *Oncogene* (2013) 32(33):3867–76. doi: 10.1038/onc.2012.394

22. Schroeder BW, Verhaeghe C, Park SW, Nguyenvu LT, Huang X, Zhen G, et al. Agr2 is induced in asthma and promotes allergen-induced mucin overproduction. *Am J Respir Cell Mol Biol* (2012) 47(2):178–85. doi: 10.1165/rcmb.2011-0421OC

23. Patel P, Clarke C, Barraclough DL, Jowitt TA, Rudland PS, Barraclough R, et al. Metastasis-promoting anterior gradient 2 protein has a dimeric thioredoxin fold structure and a role in cell adhesion. *J Mol Biol* (2013) 425(5):929–43. doi: 10.1016/j.jmb.2012.12.009

24. Mohtar MA, Hernychova L, O'Neill JR, Lawrence ML, Murray E, Vojtesek B, et al. The sequence-specific peptide-binding activity of the protein sulfide isomerase Agr2 directs its stable binding to the oncogenic receptor epcam. *Mol Cell Proteomics* (2018) 17(4):737–63. doi: 10.1074/mcp.RA118.000573

25. Ryu J, Park SG, Lee PY, Cho S, Lee DH, Kim GH, et al. Dimerization of pro-oncogenic protein anterior gradient 2 is required for the interaction with Bip/Grp78. *Biochem Biophys Res Commun* (2013) 430(2):610–5. doi: 10.1016/j.bbrc.2012.11.105

26. Bouchalova P, Sommerova L, Potesil D, Martisova A, Lapcik P, Koci V, et al. Characterization of the Agr2 interactome uncovers new players of protein disulfide isomerase network in cancer cells. *Mol Cell Proteomics* (2022) 21(2):100188. doi: 10.1016/j.mcpro.2021.100188

27. Ryan DP, Matthews JM. Protein-protein interactions in human disease. *Curr Opin Struct Biol* (2005) 15(4):441–6. doi: 10.1016/j.sbi.2005.06.001

28. Delom F, Mohtar MA, Hupp T, Fessart D. The anterior gradient-2 interactome. *Am J Physiol Cell Physiol* (2020) 318(1):C40–C7. doi: 10.1152/ajpcell.00532.2018

29. Maurel M, Obacz J, Avril T, Ding YP, Papadodima O, Treton X, et al. Control of anterior gradient 2 (Agr2) dimerization links endoplasmic reticulum proteostasis to inflammation. *EMBO Mol Med* (2019) 11(6):e10120. doi: 10.15252/emmm.201810120

30. Fletcher GC, Patel S, Tyson K, Adam PJ, Schenker M, Loader JA, et al. Hag-2 and hag-3, human homologues of genes involved in differentiation, are associated with oestrogen receptor-positive breast tumours and interact with metastasis gene C4.4a and dystroglycan. *Br J Cancer* (2003) 88(4):579–85. doi: 10.1038/sj.bjc.6600740

31. Dong A, Wodziak D, Lowe AW. Epidermal growth factor receptor (Egfr) signaling requires a specific endoplasmic reticulum thioredoxin for the post-translational control of receptor presentation to the cell surface. *J Biol Chem* (2015) 290(13):8016–27. doi: 10.1074/jbc.M114.623207

32. Arumugam T, Deng D, Bover L, Wang H, Logsdon CD, Ramachandran V. New blocking antibodies against novel Agr2-C4.4a pathway reduce growth and metastasis of pancreatic tumors and increase survival in mice. *Mol Cancer Ther* (2015) 14(4):941–51. doi: 10.1158/1535-7163.MCT-14-0470

33. Maslon MM, Hrstka R, Vojtesek B, Hupp TR. A divergent substrate-binding loop within the pro-oncogenic protein anterior gradient-2 forms a docking site for reptin. *J Mol Biol* (2010) 404(3):418–38. doi: 10.1016/j.jmb.2010.09.035

34. Gray TA, Alsamman K, Murray E, Sims AH, Hupp TR. Engineering a synthetic cell panel to identify signalling components reprogrammed by the cell growth regulator anterior gradient-2. *Mol Biosyst* (2014) 10(6):1409–25. doi: 10.1039/c4mb00113c

35. Yu H, Zhao J, Lin L, Zhang Y, Zhong F, Liu Y, et al. Proteomic study explores Agr2 as pro-metastatic protein in hcc. *Mol Biosyst* (2012) 8(10):2710–8. doi: 10.1039/c2mb25160d

36. Liu Z, Hu Y, Gong Y, Zhang W, Liu C, Wang Q, et al. Hydrogen peroxide mediated mitochondrial Ung1-Prdx3 interaction and Ung1 degradation. *Free Radic Biol Med* (2016) 99:54–62. doi: 10.1016/j.freeradbiomed.2016.07.030

37. Paret C, Bourouba M, Beer A, Miyazaki K, Schnolzer M, Fiedler S, et al. Ly6 family member C4.4a binds laminins 1 and 5, associates with galectin-3 and supports cell migration. *Int J Cancer* (2005) 115(5):724–33. doi: 10.1002/ijc.20977

38. Kumar A, Godwin JW, Gates PB, Garza-Garcia AA, Brockes JP. Molecular basis for the nerve dependence of limb regeneration in an adult vertebrate. *Science* (2007) 318 (5851):772–7. doi: 10.1126/science.1147710

39. Garza-Garcia A, Harris R, Esposito D, Gates PB, Driscoll PC. Solution structure and phylogenetics of Prod1, a member of the three-finger protein superfamily implicated in salamander limb regeneration. *PloS One* (2009) 4(9):e7123. doi: 10.1371/journal.pone.0007123

40. Murray E, McKenna EO, Burch LR, Dillon J, Langridge-Smith P, Kolch W, et al. Microarray-formatted clinical biomarker assay development using peptide aptamers to anterior gradient-2. *Biochemistry* (2007) 46(48):13742–51. doi: 10.1021/bi7008739

41. Guo H, Zhu Q, Yu X, Merugu SB, Mangukiya HB, Smith N, et al. Tumor-secreted anterior gradient-2 binds to vegf and Fgf2 and enhances their activities by promoting their homodimerization. *Oncogene* (2017) 36(36):5098–109. doi: 10.1038/onc.2017.132

42. Gong W, Ekmu B, Wang X, Lu Y, Wan L. Agr2-induced glucose metabolism facilitated the progression of endometrial carcinoma Via enhancing the Muc1/Hif-1alpha pathway. *Hum Cell* (2020) 33(3):790–800. doi: 10.1007/s13577-020-00356-4

43. Hrstka R, Bouchalova P, Michalova E, Matoulkova E, Muller P, Coates PJ, et al. Agr2 oncoprotein inhibits P38 mapk and P53 activation through a Dusp10-mediated regulatory pathway. *Mol Oncol* (2016) 10(5):652–62. doi: 10.1016/j.molonc.2015.12.003

44. Zhou X, Zhang W, Dou M, Li Z, Liu Z, Li J, et al. (125)I seeds inhibit proliferation and promote apoptosis in cholangiocarcinoma cells by regulating the Agr2-mediated P38 mapk pathway. *Cancer Lett* (2022) 524:29–41. doi: 10.1016/j.canlet.2021.10.014

45. Zweitzig DR, Smirnov DA, Connelly MC, Terstappen LW, O'Hara SM, Moran E. Physiological stress induces the metastasis marker Agr2 in breast cancer cells. *Mol Cell Biochem* (2007) 306(1-2):255–60. doi: 10.1007/s11010-007-9562-y

46. Tiemann K, Garri C, Lee SB, Malihi PD, Park M, Alvarez RM, et al. Loss of er retention motif of Agr2 can impact mtorc signaling and promote cancer metastasis. *Oncogene* (2019) 38(16):3003–18. doi: 10.1038/s41388-018-0638-9

47. Sommerova L, Ondrouskova E, Vojtesek B, Hrstka R. Suppression of Agr2 in a tgf-Beta-Induced smad regulatory pathway mediates epithelial-mesenchymal transition. *BMC Cancer* (2017) 17(1):546. doi: 10.1186/s12885-017-3537-5

48. Li Z, Wu Z, Chen H, Zhu Q, Gao G, Hu L, et al. Induction of anterior gradient 2 (Agr2) plays a key role in insulin-like growth factor-1 (Igf-1)-Induced breast cancer cell proliferation and migration. *Med Oncol* (2015) 32(6):577. doi: 10.1007/s12032-015-0577-z

49. Hetz C. The unfolded protein response: controlling cell fate decisions under er stress and beyond. *Nat Rev Mol Cell Biol* (2012) 13(2):89–102. doi: 10.1038/nrm3270

50. Dumartin L, Alrawashdeh W, Trabulo SM, Radon TP, Steiger K, Feakins RM, et al. Er stress protein Agr2 precedes and is involved in the regulation of pancreatic cancer initiation. *Oncogene* (2017) 36(22):3094–103. doi: 10.1038/onc.2016.459

51. Jung SY, Yun J, Kim SJ, Kang S, Kim DY, Kim YJ, et al. Basic helix-Loop-Helix transcription factor Twist1 is a novel regulator of anterior gradient protein 2 homolog (Agr2) in breast cancer. *Biochem Biophys Res Commun* (2019) 516(1):149–56. doi: 10.1016/j.bbrc.2019.05.191

52. Ondrouskova E, Sommerova L, Nenutil R, Coufal O, Bouchal P, Vojtesek B, et al. Agr2 associates with Her2 expression predicting poor outcome in subset of estrogen receptor negative breast cancer patients. *Exp Mol Pathol* (2017) 102(2):280–3. doi: 10.1016/j.yexmp.2017.02.016

53. Xiu B, Chi Y, Liu L, Chi W, Zhang Q, Chen J, et al. Linc02273 drives breast cancer metastasis by epigenetically increasing Agr2 transcription. *Mol Cancer* (2019) 18 (1):187. doi: 10.1186/s12943-019-1115-y

54. Zhang Y, Xia F, Zhang F, Cui Y, Wang Q, Liu H, et al. Mir-135b-5p enhances doxorubicin-sensitivity of breast cancer cells through targeting anterior gradient 2. *J Exp Clin Cancer Res* (2019) 38(1):26. doi: 10.1186/s13046-019-1024-3

55. Wang J, Huang K, Shi L, Zhang Q, Zhang S. Circpvt1 promoted the progression of breast cancer by regulating mir-29a-3p-Mediated Agr2-Hif-1alpha pathway. *Cancer Manag Res* (2020) 12:11477–90. doi: 10.2147/CMAR.S265579

56. Zuo T, Jiang P, Fu J, Zhang Y. Lncrna Afap1-As1 induces gefitinib resistance of lung adenocarcinoma through the mir-653-5p/Agr2 axis. *Ther Clin Risk Manag* (2023) 19:1–13. doi: 10.2147/TCRM.S374162

57. Tsai HW, Chen YL, Wang CI, Hsieh CC, Lin YH, Chu PM, et al. Anterior gradient 2 induces resistance to sorafenib Via endoplasmic reticulum stress regulation in hepatocellular carcinoma. *Cancer Cell Int* (2023) 23(1):42. doi: 10.1186/s12935-023-02879-w

58. Alasiri G, Fan LY, Zona S, Goldsbrough IG, Ke HL, Auner HW, et al. Er stress and cancer: the foxo forkhead transcription factor link. *Mol Cell Endocrinol* (2018) 462 (Pt B):67–81. doi: 10.1016/j.mce.2017.05.027

59. Higa A, Mulot A, Delom F, Bouchecareilh M, Nguyen DT, Boismenu D, et al. Role of pro-oncogenic protein disulfide isomerase (Pdi) family member anterior gradient 2 (Agr2) in the control of endoplasmic reticulum homeostasis. *J Biol Chem* (2011) 286(52):44855–68. doi: 10.1074/jbc.M111.275529

60. Martisova A, Sommerova L, Krejci A, Selingerova I, Kolarova T, Zavadil Kokas F, et al. Identification of Agr2 gene-specific expression patterns associated with epithelial-mesenchymal transition. *Int J Mol Sci* (2022) 23(18):10845. doi: 10.3390/ijms231810845

61. Vitello EA, Quek SI, Kincaid H, Fuchs T, Crichton DJ, Troisch P, et al. Cancer-secreted Agr2 induces programmed cell death in normal cells. *Oncotarget* (2016) 7 (31):49425–34. doi: 10.18632/oncotarget.9921

62. Clarke C, Rudland P, Barraclough R. The metastasis-inducing protein Agr2 is O-glycosylated upon secretion from mammary epithelial cells. *Mol Cell Biochem* (2015) 408(1-2):245–52. doi: 10.1007/s11010-015-2502-3

63. Jia M, Guo Y, Zhu D, Zhang N, Li L, Jiang J, et al. Pro-metastatic activity of Agr2 interrupts angiogenesis target bevacizumab efficiency via direct interaction with vegfa and activation of nf-kappab pathway. *Biochim Biophys Acta Mol Basis Dis* (2018) 1864 (5 Pt A):1622–33. doi: 10.1016/j.bbadis.2018.01.021

64. Merugu SB, Zhou B, Mangukiya HB, Negi H, Ghulam R, Roy D, et al. Extracellular Agr2 activates neighboring fibroblasts through endocytosis and direct binding to beta-catenin that requires Agr2 dimerization and adhesion domains. *Biochem Biophys Res Commun* (2021) 573:86–92. doi: 10.1016/j.bbrc.2021.08.028

65. Zhu Q, Mangukiya HB, Mashausi DS, Guo H, Negi H, Merugu SB, et al. Anterior gradient 2 is induced in cutaneous wound and promotes wound healing through its adhesion domain. *FEBS J* (2017) 284(17):2856–69. doi: 10.1111/febs.14155

66. Kurpinska A, Suraj-Prazmowska J, Stojak M, Jarosz J, Mateuszuk L, Niedzielska-Andres E, et al. Comparison of anti-cancer effects of novel protein disulphide isomerase (Pdi) inhibitors in breast cancer cells characterized by high and low Pdia17 expression. *Cancer Cell Int* (2022) 22(1):218. doi: 10.1186/s12935-022-02631-w

67. Liu D, Rudland PS, Sibson DR, Platt-Higgins A, Barraclough R. Human homologue of cement gland protein, a novel metastasis inducer associated with breast carcinomas. *Cancer Res* (2005) 65(9):3796–805. doi: 10.1158/0008-5472.CAN-04-3823

68. Innes HE, Liu D, Barraclough R, Davies MP, O'Neill PA, Platt-Higgins A, et al. Significance of the metastasis-inducing protein Agr2 for outcome in hormonally treated breast cancer patients. *Br J Cancer* (2006) 94(7):1057–65. doi: 10.1038/sj.bjc.6603065

69. Fritzsche FR, Dahl E, Pahl S, Burkhardt M, Luo J, Mayordomo E, et al. Prognostic relevance of Agr2 expression in breast cancer. *Clin Cancer Res* (2006) 12(6):1728–34. doi: 10.1158/1078-0432.CCR-05-2057

70. Barraclough DL, Platt-Higgins A, de Silva Rudland S, Barraclough R, Winstanley J, West CR, et al. The metastasis-associated anterior gradient 2 protein is correlated with poor survival of breast cancer patients. *Am J Pathol* (2009) 175(5):1848–57. doi: 10.2353/ajpath.2009.090246

71. Ann P, Seagle BL, Shilpi A, Kandpal M, Shahabi S. Association of increased primary breast tumor Agr2 with decreased disease-specific survival. *Oncotarget* (2018) 9(33):23114–25. doi: 10.18632/oncotarget.25225

72. Kereh DS, Pieter J, Hamdani W, Haryasena H, Sampepajung D, Prihantono P. Correlation of Agr2 expression with the incidence of metastasis in luminal breast cancer. *Breast Dis* (2021) 40(S1):S103–S7. doi: 10.3233/BD-219015

73. Maarouf A, Boissard A, Henry C, Leman G, Coqueret O, Guette C, et al. Anterior gradient protein 2 is a marker of tumor aggressiveness in breast cancer and favors Chemotherapy–Induced senescence escape. *Int J Oncol* (2022) 60(1):5. doi: 10.3892/ijo.2021.5295

74. Lacambra MD, Tsang JY, Ni YB, Chan SK, Tan PH, Tse GM. Anterior gradient 2 is a poor outcome indicator in luminal breast cancer. *Ann Surg Oncol* (2015) 22(11):3489–96. doi: 10.1245/s10434-015-4420-8

75. Wilson CL, Sims AH, Howell A, Miller CJ, Clarke RB. Effects of oestrogen on gene expression in epithelium and stroma of normal human breast tissue. *Endocr Relat Cancer* (2006) 13(2):617–28. doi: 10.1677/erc.1.01165

76. Vanderlaag KE, Hudak S, Bald L, Fayadat-Dilman L, Sathe M, Grein J, et al. Anterior gradient-2 plays a critical role in breast cancer cell growth and survival by modulating cyclin D1, estrogen receptor-alpha and survivin. *Breast Cancer Res* (2010) 12(3):R32. doi: 10.1186/bcr2586

77. de Moraes CL, Cruz EMN, Valoyes MAV, Naves do Amaral W. Agr2 and Agr3 play an important role in the clinical characterization and prognosis of basal like breast cancer. *Clin Breast Cancer* (2022) 22(2):e242–e52. doi: 10.1016/j.clbc.2021.07.008

78. Wang J, Xu B. Targeted therapeutic options and future perspectives for Her2-positive breast cancer. *Signal Transduct Target Ther* (2019) 4:34. doi: 10.1038/s41392-019-0069-2

79. Duran MC, Vega F, Moreno-Bueno G, Artiga MJ, Sanchez L, Palacios J, et al. Characterisation of tumoral markers correlated with Erbb2 (Her2/Neu) overexpression and metastasis in breast cancer. *Proteomics Clin Appl* (2008) 2(9):1313–26. doi: 10.1002/prca.200780020

80. Fessart D, Villamor I, Chevet E, Delom F, Robert J. Integrative analysis of genomic and transcriptomic alterations of Agr2 and Agr3 in cancer. *Open Biol* (2022) 12(7):220068. doi: 10.1098/rsob.220068

81. Jach D, Cheng Y, Prica F, Dumartin L, Crnogorac-Jurcevic T. From development to cancer - an ever-increasing role of Agr2. *Am J Cancer Res* (2021) 11(11):5249–62.

82. Tian SB, Tao KX, Hu J, Liu ZB, Ding XL, Chu YN, et al. The prognostic value of Agr2 expression in solid tumours: a systematic review and meta-analysis. *Sci Rep* (2017) 7(1):15500. doi: 10.1038/s41598-017-15757-z

83. Yuan SH, Chang SC, Huang Y, Liu HP. Serum level of tumor-overexpressed Agr2 is significantly associated with unfavorable prognosis of canine malignant mammary tumors. *Anim (Basel)* (2021) 11(10):2923. doi: 10.3390/ani11102923

84. Whitwell HJ, Worthington J, Blyuss O, Gentry-Maharaj A, Ryan A, Gunu R, et al. Improved early detection of ovarian cancer using longitudinal multimarker models. *Br J Cancer* (2020) 122(6):847–56. doi: 10.1038/s41416-019-0718-9

85. Wayner EA, Quek SI, Ahmad R, Ho ME, Loprieno MA, Zhou Y, et al. Development of an Elisa to detect the secreted prostate cancer biomarker Agr2 in voided urine. *Prostate* (2012) 72(9):1023–34. doi: 10.1002/pros.21508

86. Aydogdu Tig G, Pekyardimci S. An electrochemical sandwich-type aptasensor for determination of lipocalin-2 based on graphene Oxide/Polymer composite and gold nanoparticles. *Talanta* (2020) 210:120666. doi: 10.1016/j.talanta.2019.120666

87. Lan J, Wu X, Luo L, Liu J, Yang L, Wang F. Fluorescent Ag clusters conjugated with anterior gradient-2 antigen aptamer for specific detection of cancer cells. *Talanta* (2019) 197:86–91. doi: 10.1016/j.talanta.2018.12.089

88. Arshavsky-Graham S, Ward SJ, Massad-Ivanir N, Scheper T, Weiss SM, Segal E. Porous silicon-based aptasensors: toward cancer protein biomarker detection. *ACS Meas Sci Au* (2021) 1(2):82–94. doi: 10.1021/acsmeasuresciau.1c00019

89. DeSantis CE, Ma J, Gaudet MM, Newman LA, Miller KD, Goding Sauer A, et al. Breast cancer statistics, 2019. *CA Cancer J Clin* (2019) 69(6):438–51. doi: 10.3322/caac.21583

90. Coser KR, Wittner BS, Rosenthal NF, Collins SC, Melas A, Smith SL, et al. Antiestrogen-resistant subclones of mcf-7 human breast cancer cells are derived from a common monoclonal drug-resistant progenitor. *Proc Natl Acad Sci U.S.A.* (2009) 106(34):14536–41. doi: 10.1073/pnas.0907560106

91. Saatci O, Huynh-Dam KT, Sahin O. Endocrine resistance in breast cancer: from molecular mechanisms to therapeutic strategies. *J Mol Med (Berl)* (2021) 99(12):1691–710. doi: 10.1007/s00109-021-02136-5

92. Hengel SM, Murray E, Langdon S, Hayward L, O'Donoghue J, Panchaud A, et al. Data-independent proteomic screen identifies novel tamoxifen agonist that mediates drug resistance. *J Proteome Res* (2011) 10(10):4567–78. doi: 10.1021/pr2004117

93. Hrstka R, Murray E, Brychtova V, Fabian P, Hupp TR, Vojtesek B. Identification of an akt-dependent signalling pathway that mediates tamoxifen-dependent induction of the pro-metastatic protein anterior gradient-2. *Cancer Lett* (2013) 333(2):187–93. doi: 10.1016/j.canlet.2013.01.034

94. Zamzam Y, Abdelmonem Zamzam Y, Aboalsoud M, Harras H. The utility of Sox2 and Agr2 biomarkers as early predictors of tamoxifen resistance in er-positive breast cancer patients. *Int J Surg Oncol* (2021) 2021:9947540. doi: 10.1155/2021/9947540

95. Wright TM, Wardell SE, Jasper JS, Stice JP, Safi R, Nelson ER, et al. Delineation of a Foxa1/Eralpha/Agr2 regulatory loop that is dysregulated in endocrine therapy-resistant breast cancer. *Mol Cancer Res* (2014) 12(12):1829–39. doi: 10.1158/1541-7786.MCR-14-0195

96. Li Z, Zhu Q, Hu L, Chen H, Wu Z, Li D. Anterior gradient 2 is a binding stabilizer of hypoxia inducible factor-1alpha that enhances Cocl2 -induced doxorubicin resistance in breast cancer cells. *Cancer Sci* (2015) 106(8):1041–9. doi: 10.1111/cas.12714

97. Li S, Jiang F, Chen F, Deng Y, Pan X. Effect of M6a methyltransferase Mettl3 -mediated Malat1/E2f1/Agr2 axis on adriamycin resistance in breast cancer. *J Biochem Mol Toxicol* (2022) 36(1):e22922. doi: 10.1002/jbt.22922

98. Wu ZH, Zhu Q, Gao GW, Zhou CC, Li DW. [Preparation, characterization and potential application of monoclonal antibody 18a4 against Agr2]. *Xi Bao Yu Fen Zi Mian Yi Xue Za Zhi* (2010) 26(1):49–51.

99. Guo H, Chen H, Zhu Q, Yu X, Rong R, Merugu SB, et al. A humanized monoclonal antibody targeting secreted anterior gradient 2 effectively inhibits the xenograft tumor growth. *Biochem Biophys Res Commun* (2016) 475(1):57–63. doi: 10.1016/j.bbrc.2016.05.033

100. Boisteau E, Posseme C, Di Modugno F, Edeline J, Coulouarn C, Hrstka R, et al. Anterior gradient proteins in gastrointestinal cancers: from cell biology to pathophysiology. *Oncogene* (2022) 41(42):4673–85. doi: 10.1038/s41388-022-02452-1

101. Negi H, Merugu SB, Mangukiya HB, Li Z, Zhou B, Sehar Q, et al. Anterior gradient-2 monoclonal antibody inhibits lung cancer growth and metastasis by upregulating P53 pathway and without exerting any toxicological effects: a preclinical study. *Cancer Lett* (2019) 449:125–34. doi: 10.1016/j.canlet.2019.01.025

102. Liu AY, Kanan AD, Radon TP, Shah S, Weeks ME, Foster JM, et al. Agr2, a unique tumor-associated antigen, is a promising candidate for antibody targeting. *Oncotarget* (2019) 10(42):4276–89. doi: 10.18632/oncotarget.26945

103. Cocce KJ, Jasper JS, Desautels TK, Everett L, Wardell S, Westerling T, et al. The lineage determining factor Grhl2 collaborates with Foxa1 to establish a targetable pathway in endocrine therapy-resistant breast cancer. *Cell Rep* (2019) 29(4):889–903.e10. doi: 10.1016/j.celrep.2019.09.032

104. Zhang S, Liu Q, Wei Y, Xiong Y, Gu Y, Huang Y, et al. Anterior gradient-2 regulates cell communication by coordinating cytokine-chemokine signaling and immune infiltration in breast cancer. *Cancer Sci* (2023) 00:1–16. doi: 10.1111/cas.15775

105. Zhang K, Kong X, Li Y, Wang Z, Zhang L, Xuan L. Pd-1/Pd-L1 inhibitors in patients with preexisting autoimmune diseases. *Front Pharmacol* (2022) 13:854967. doi: 10.3389/fphar.2022.854967

106. Roy D, Liu GS, Zeling Wang A, Zhou B, Yunus FU, Raza G, et al. Construction and stable gene expression of Agr2xpd1 bi-specific antibody that enhances attachment between T-cells and lung tumor cells, suppress tumor cell migration and promoting Cd8 expression in cytotoxic T-cells. *Saudi Pharm J* (2023) 31(1):85–95. doi: 10.1016/j.jsps.2022.11.007

107. Wang D, Xu Q, Yuan Q, Jia M, Niu H, Liu X, et al. Proteasome inhibition boosts autophagic degradation of ubiquitinated-Agr2 and enhances the antitumor efficiency of bevacizumab. *Oncogene* (2019) 38(18):3458–74. doi: 10.1038/s41388-019-0675-z

108. Wang X, Yu J, Liu X, Luo D, Li Y, Song L, et al. Psmg2-controlled proteasome-autophagy balance mediates the tolerance for mek-targeted therapy in triple-negative breast cancer. *Cell Rep Med* (2022) 3(9):100741. doi: 10.1016/j.xcrm.2022.100741

109. Paplomata E, Nahta R, O'Regan RM. Systemic therapy for early-stage Her2-positive breast cancers: time for a less-Is-More approach? *Cancer* (2015) 121(4):517–26. doi: 10.1002/cncr.29060

110. Hong X, Li ZX, Hou J, Zhang HY, Zhang CY, Zhang J, et al. Effects of er-resident and secreted Agr2 on cell proliferation, migration, invasion, and survival in panc-1 pancreatic cancer cells. *BMC Cancer* (2021) 21(1):33. doi: 10.1186/s12885-020-07743-y

111. Zhang Z, Li H, Deng Y, Schuck K, Raulefs S, Maeritz N, et al. Agr2-dependent nuclear import of rna polymerase ii constitutes a specific target of pancreatic ductal adenocarcinoma in the context of wild-type P53. *Gastroenterology* (2021) 161(5):1601–14.e23. doi: 10.1053/j.gastro.2021.07.030

frontiers | Frontiers in Oncology

TYPE Original Research
PUBLISHED 03 May 2023
DOI 10.3389/fonc.2023.1191660

OPEN ACCESS

EDITED BY
Deniz Can Guven,
Hacettepe University, Türkiye

REVIEWED BY
Onur Baş,
Hacettepe University, Türkiye
Dingcheng Gao,
Cornell University, United States

*CORRESPONDENCE
De-Yuan Fu
fdy1003@163.com

†These authors have contributed equally to this work

RECEIVED 22 March 2023
ACCEPTED 24 April 2023
PUBLISHED 03 May 2023

CITATION
Xu A, Xu X-N, Luo Z, Huang X, Gong R-Q and Fu D-Y (2023) Identification of prognostic cancer-associated fibroblast markers in luminal breast cancer using weighted gene co-expression network analysis. *Front. Oncol.* 13:1191660. doi: 10.3389/fonc.2023.1191660

Identification of prognostic cancer-associated fibroblast markers in luminal breast cancer using weighted gene co-expression network analysis

An Xu[1†], Xiang-Nan Xu[2†], Zhou Luo[2], Xiao Huang[1], Rong-Quan Gong[1] and De-Yuan Fu[2*]

[1]Medical College of Yangzhou University, Yangzhou, Jiangsu, China, [2]Department of Thyroid and Breast Surgery, Northern Jiangsu People's Hospital, Yangzhou, Jiangsu, China

Background: Cancer-associated fibroblasts (CAFs) play a pivotal role in cancer progression and are known to mediate endocrine and chemotherapy resistance through paracrine signaling. Additionally, they directly influence the expression and growth dependence of ER in Luminal breast cancer (LBC). This study aims to investigate stromal CAF-related factors and develop a CAF-related classifier to predict the prognosis and therapeutic outcomes in LBC.

Methods: The Cancer Genome Atlas (TCGA) and Gene Expression Omnibus (GEO) databases were utilized to obtain mRNA expression and clinical information from 694 and 101 LBC samples, respectively. CAF infiltrations were determined by estimating the proportion of immune and cancer cells (EPIC) method, while stromal scores were calculated using the Estimation of STromal and Immune cells in MAlignant Tumors using Expression data (ESTIMATE) algorithm. Weighted gene co-expression network analysis (WGCNA) was used to identify stromal CAF-related genes. A CAF risk signature was developed through univariate and least absolute shrinkage and selection operator method (LASSO) Cox regression model. The Spearman test was used to evaluate the correlation between CAF risk score, CAF markers, and CAF infiltrations estimated through EPIC, xCell, microenvironment cell populations-counter (MCP-counter), and Tumor Immune Dysfunction and Exclusion (TIDE) algorithms. The TIDE algorithm was further utilized to assess the response to immunotherapy. Additionally, Gene set enrichment analysis (GSEA) was applied to elucidate the molecular mechanisms underlying the findings.

Results: We constructed a 5-gene prognostic model consisting of RIN2, THBS1, IL1R1, RAB31, and COL11A1 for CAF. Using the median CAF risk score as the cutoff, we classified LBC patients into high- and low-CAF-risk groups and found that those in the high-risk group had a significantly worse prognosis. Spearman correlation analyses demonstrated a strong positive correlation between the CAF risk score and stromal and CAF infiltrations, with the five model genes showing positive correlations with CAF markers. In addition, the TIDE analysis revealed that high-CAF-risk patients were less likely to respond to immunotherapy. Gene set

enrichment analysis (GSEA) identified significant enrichment of ECM receptor interaction, regulation of actin cytoskeleton, epithelial-mesenchymal transition (EMT), and TGF-β signaling pathway gene sets in the high-CAF-risk group patients.

Conclusion: The five-gene prognostic CAF signature presented in this study was not only reliable for predicting prognosis in LBC patients, but it was also effective in estimating clinical immunotherapy response. These findings have significant clinical implications, as the signature may guide tailored anti-CAF therapy in combination with immunotherapy for LBC patients.

KEYWORDS

luminal breast cancer (LBC), cancer-associated fibroblasts (CAFs), weighted gene co-expression network analysis (WGCNA), prognostic CAF markers, anti-CAF therapeutic approach

1 Introduction

Breast cancer (BC) is the most prevalent cancer among women worldwide and the second leading cause of cancer deaths (1, 2). While the current standard treatment for breast cancer has greatly improved survival, it remains a public health issue on a global scale (3). LBC is a subtype of breast cancer, including Luminal A and Luminal B, characterized by the presence of estrogen and/or progesterone receptors on the surface of cancer cells (4). Although LBC has the best prognosis among breast cancer subtypes, approximately 20-40% of LBCs eventually develop distant metastases, with half occurring 5 years or later after the diagnosis of the primary tumor (5). The tumor microenvironment (TME) in breast cancer comprises local factors, cancer cells, immune cells and stromal cells of the local and distant tissues (6, 7). Accumulating evidence indicated that the interaction between LBC cells and their microenvironment plays important roles in tumor proliferation, propagation and response to therapies (8–10).

CAFs are important components of the tumor microenvironment (TME) and are widely distributed in tumor stroma (11, 12). They play a crucial role in promoting tumor growth through direct effects on tumor cells and various interactions with receptors and ligands (13, 14). Moreover, they indirectly stimulate tumor growth and migration by releasing growth factors, cytokines, and exosomes, inducing metabolic reprogramming and anti-tumor resistance, and suppressing the immune system (15–17). Additionally, CAFs help to create a physical barrier through the deposition and reorganization of the extracellular matrix, which supports tumor cell invasion and restrains antitumor leukocyte infiltration, leading to tumor progression, immune evasion, and therapy resistance (18).

Studies have shown that CAFs can affect the response of LBC to hormone therapy, a common treatment, by altering the expression of estrogen receptors on cancer cells (19–21). Targeting CAFs can be achieved through various methods such as influencing secreted factors and signaling pathways, inducing a quiescent state in CAFs or targeting CAF-derived cells (18, 22). For example, losartan, an angiotensin receptor blocker, can convert myofibroblast CAFs into a quiescent state and enhance immune cell activity, thus improving the response of breast cancer cells to immune checkpoint blockers (23). In addition, blocking CD10 and GPR77 with neutralizing antibodies can decrease tumor growth and increase chemotherapy sensitivity in breast cancer models (24). Therefore, identifying common markers of CAFs can lead to the discovery of more specific markers and therapeutic targets for LBC.

Weighted gene co-expression network analysis (WGCNA) is a powerful bioinformatics algorithm that can identify highly and coordinately expressed genes and group them into gene modules to explore their relationships with a phenotype of interest (25). WGCNA has been previously used to identify cancer-associated fibroblast (CAF) markers (26–29). However, there has been no WGCNA analysis conducted on CAF and stromal infiltrations in LBC.

In this study, we employed WGCNA simultaneously on two transcriptome datasets from TCGA and GEO databases. We identified hub modules that were most correlated with stromal CAF infiltrations. Using univariate and Least Absolute Shrinkage and Selection Operator (LASSO) Cox regression analyses, we identified RIN2, THBS1, IL1R1, RAB31, and COL11A1 as prognostic CAF markers. We then constructed a five-gene CAF signature that could predict prognosis and therapeutic responses in LBC. Our findings suggest that the CAF model could be a promising anti-CAF therapeutic approach for LBC.

2 Materials and methods

2.1 The collection and preparation of data

The transcript per million (TPM) format RNA-seq data and clinical information relevant to Breast Invasive Carcinoma (TCGA-BRCA) samples were obtained from TCGA datasets (https://portal.gdc.cancer.gov/). The gene expression profiling dataset (GSE47994) was obtained from the Gene Expression Omnibus (https://www.ncbi.nlm.nih.gov/) database (30). We then screened

a total of 694 LBC patients from the TCGA-BRCA dataset and 101 LBC patients from the GSE47994 dataset who had prognostic data available, with follow-up times exceeding 365 days.

2.2 The estimation of CAF infiltration and the calculation of stromal score

Four methods were utilized to estimate the abundance of CAFs, including the Estimate the Proportion of Immune and Cancer cells (EPIC) algorithm based on cell-type deconvolution using constrained least square optimization (31), the xCell algorithm based on gene signature enrichment (32), the microenvironment cell populations-counter (MCP-counter) based on marker gene expressions (33), and the Tumor Immune Dysfunction and Exclusion (TIDE) algorithms, which also can predict anti-PD1 and anti-CTLA4 responses in tumor patients (34). The first three methods were executed *via* the deconvolute() function of the immunedeconv R package (version 2.0.3) (35), while the TIDE method was implemented through http://tide.dfci.harvard.edu/. Additionally, the Estimation of STromal and Immune cells in MAlignant Tumor tissues using Expression data (ESTIMATE) algorithm was utilized to calculate the stromal score, which indicates the level of stromal infiltration in each tumor sample, through the estimate R package (version 1.0.13) (36).

2.3 The creation of CAF and stromal co-expression networks

The WGCNA R package (version 1.72) was utilized to construct co-expression networks and identify hub genes that target cancer-associated fibroblast (CAF) infiltrations and stromal scores (25). The input genes for network construction were selected based on the median absolute deviation (MAD), with the top 5,000 genes selected for both the TCGA-BRCA and GSE47994 cohorts. The Pearson's correlation similarity matrix was calculated between each pair of genes (s_{ij}, where ij represents the gene pairs) and raised to a soft-thresholding power β (S_{ij}^{β}), based on the scale-free topology network criterion. The adjacency matrix was then clustered using the topological overlap measure (TOM) and dissimilarity (1-TOM) between genes, and a dynamic tree cut algorithm was applied to the dendrogram to identify gene modules with a minimum of 30 genes in each module. The first principal component of each module's expression was summarized as a module eigengene (ME), and the Pearson's correlations between MEs and EPIC-quantified CAF infiltrations, as well as the stromal score, were assessed to identify the most correlated module for further analysis. Hub genes were then identified by overlapping the most correlated module genes between the TCGA-BRCA and GSE47994 cohorts.

2.4 The analysis of gene ontology and the kyoto encyclopedia of genes and genomes

The clusterProfiler R package (version 3.14.3) was utilized to analyze the hub genes' biological functions, which included biological processes (BPs), molecular functions (MFs), and cellular components (CCs), as well as pathways according to GO and KEGG databases (37). $p < 0.05$ was considered statistically significant.

2.5 The creation and verification of a predictive algorithm

For CAF risk model construction, 694 LBC cases from TCGA-BRCA were selected based on their large sample size. The validation cohort consisted of 101 LBC cases from GSE47994 cohort. Univariate Cox regression analysis was performed to identify prognostic stromal CAF hub genes for overall survival (OS). Genes with $p < 0.05$ were selected for LASSO Cox regression analysis with 1,000 iterations using glmnet R package to reduce the number of genes (38). Then, the CAF risk model was constructed as follows: CAF risk score = $\sum (\beta_i * Exp_i)$, where β_i is the LASSO coefficient of *i*th gene and Exp_i is the expression value of *i*th gene. Using the median CAF risk score of the training cohort as the threshold, LBC patients from both cohorts were classified into high- and low-CAF-risk groups and the OS difference between the two groups was estimated using Kaplan–Meier curves and the log-rank test.

2.6 The collection of CAF markers and the analysis of their correlation

We collected CAF specific and nonspecific markers from published literature (39, 40). To verify the reliability of our CAF model markers in LBC, we examined the Spearman's correlations between the CAF risk score and the stromal score, as well as various CAF infiltration estimates (EPIC, xCell, MCP-counter, and TIDE). We also analyzed the correlations between CAF model genes and published CAF markers in both TCGA-BRCA and GSE47994 cohorts.

2.7 The prediction of chemotherapy and immunotherapy responses

Using the Genomics of Drug Sensitivity in Cancer [GDSC (https://www.cancerrxgene.org/)] database (41), half-maximal inhibitory concentration (IC50) values of common drugs (bleomycin, lapatinib, paclitaxel, camptothecin, cisplatin, docetaxel, methotrexate, and sunitinib) in each LBC sample were estimated based on the transcriptome data by ridge regression with ten-fold cross-validation in pRRophetic R package (version 0.5) (42). The TIDE (http://tide.dfci.harvard.edu/) online algorithm was then adopted for immune checkpoint blockade therapy response predictions (34). The chi-squared test was used to examine differences in response rates between high- and low-CAF-risk groups. The predictive efficacy of the CAF risk signature was evaluated by ROC curves and area under the curve (AUC) values.

2.8 Analysis of enrichment

To explore the enriched hallmark and KEGG pathway gene sets between high- and low-CAF-risk groups in GSE47994, gene set enrichment analysis (GSEA) was performed using the enrichplot and clusterProfiler R packages. The gene sets used were derived from the Molecular Signatures Database (MSigDB), specifically the "c2.cp.kegg.v7.4.symbols" and "h.all.v7.4.symbols" gene sets (43). Additionally, the enrichment scores of ECM receptor interaction, regulation of actin cytoskeleton, and TGF-β signaling pathway hallmark gene sets were calculated using ssGSEA (44). Finally, Spearman's correlation analysis was performed to assess the correlation between the CAF risk score and gene set enrichment scores.

2.9 The verification of results using the cancer cell line encyclopedia and human protein atlas databases

To validate the findings at the cellular level, mRNA expressions of the identified markers in 38 fibroblasts and 51 BC cell lines were downloaded from the Cancer Cell Line Encyclopedia [CCLE (https://portals.broadinstitute.org/ccle)] database (45). Expression patterns of these markers in fibroblasts and CRC cell lines were examined using heat maps and Wilcoxon tests. Additionally, immunohistochemical (IHC) staining images of these markers in LBC tissues were downloaded from the Human Protein Atlas [HPA (https://www.proteinatlas.org/)] online database (46).

2.10 Statistical analysis of the data

R software (version 4.2.2; https://www.r-project.org/) was used for all statistical analyses. The median CAF risk score was used as the cutoff value for each cohort to divide LBC patients into high- and low-CAF-risk subgroups. Pairwise comparisons were performed using the Wilcoxon test. Pearson correlation coefficient analysis was performed to evaluate the correlation between genes. Overall survival comparisons were made using the Kaplan-Meier curve with the log-rank test, which were adopted *via* the survival and survminer R packages. $p < 0.05$ was considered statistically significant.

3 Results

3.1 The prognostic value of CAF infiltrations and stromal scores in LBC patients

The flowchart of this research is displayed in Figure 1. CAF infiltrations were predicted by multiple methods, including EPIC, xCell, MCP-counter, and TIDE. The stromal score was calculated by the estimate algorithm. Their prognostic values on overall survival (OS) were evaluated *via* log-rank tests. Kaplan-Meier curves indicated that multiple higher CAF infiltrations and stromal scores were significantly associated with poorer OS in LBC patients. CAF_EPIC, CAF_TIDE, and stromal scores were significantly associated with poorer OS in TCGA-BRCA (Figures 2A–C), and CAF_EPIC, CAF_mcp-counter, and stromal scores were significantly associated with poorer OS in GSE47994 (Figures 2D–F), which highlights the importance of further studies exploring CAF and stromal-associated genes in LBC. In this study, the EPIC-estimated CAF abundances and stromal scores were summarized as phenotype data for subsequent analysis, and the data from the other three estimated CAF infiltrations were used for external validation of the identified CAF model.

3.2 Co-expression network analysis of CAF and stromal scores in two LBC datasets

WGCNA analysis was conducted on both TCGA-BRCA and GSE47994 datasets. To build a scale-free topology network, we estimated the soft threshold power (β) of 7 in TCGA-BRCA (scale-free R2 = 0.86) (Figure 3A) and 17 in GSE47994 (scale-free R2 = 0.86) (Figure 3B). In TCGA-BRCA, the hierarchical clustering tree identified 8 co-expression models (Figure 3C), and the magenta module exhibited the strongest positive correlation with the CAF proportion (Cor = 0.54, P = 7e-54) and stromal score (Cor = 0.78, P = 5e-144) (Figure 3E). In GSE47994, the dynamic hybrid cutting clustered 6 co-expression models (Figure 3D), with the brown module showing the strongest positive correlation with the CAF proportion (Cor = 0.88, P = 5e-25) and stromal score (Cor = 0.92, P = 2e-31) (Figure 3F). Therefore, we focused on these two modules for further investigations. A total of 1718 and 158 genes were included in the magenta and brown modules, respectively. In the magenta module, scatter plots indicated strong correlations between MM and GS for CAF (Cor = 0.64, p =1.3e-198) and stromal scores (Cor = 0.88, p < 1e-200) (Figure 3G). Similarly, in the brown module, strong correlations were observed between MM and GS for CAF (Cor = 0.64, P = 1.1e-19) and stromal scores (Cor = 0.82, p = 7e-40) (Figure 3H). Consequently, we selected 1718 genes from the TCGA-BRCA magenta module and 158 genes from the GSE47994 brown module as highly associated with CAF and stromal scores.

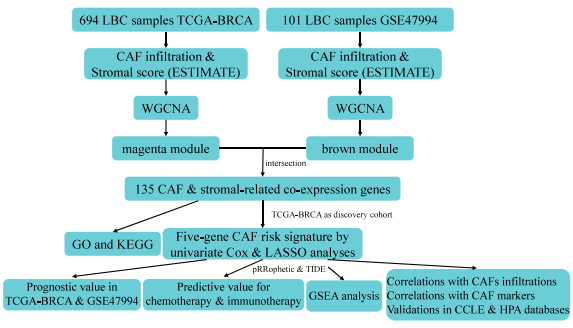

FIGURE 1
Work flow of this study.

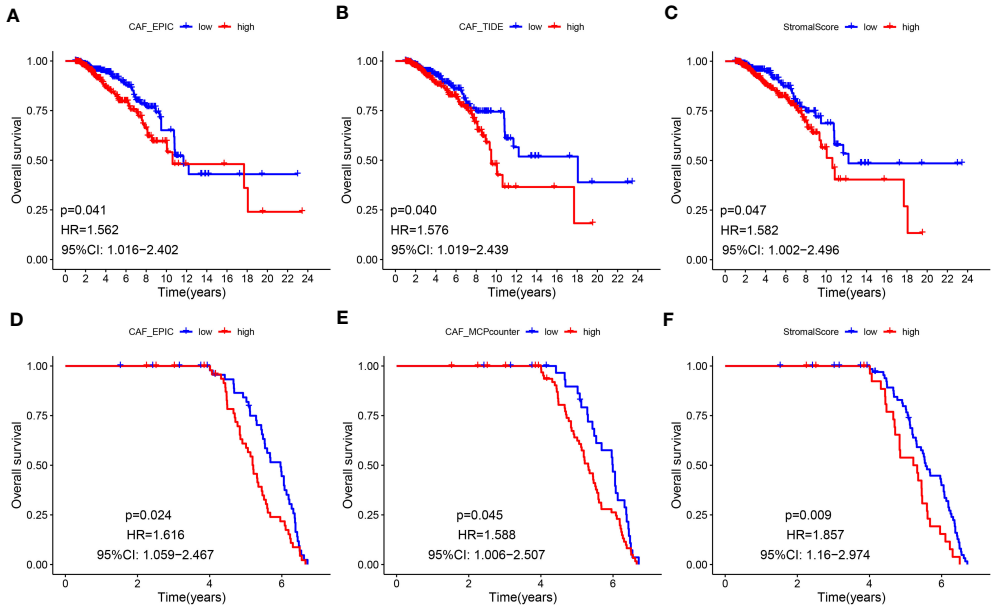

FIGURE 2
(A-F) Kaplan–Meier analyses of LBC patients. Multiple higher CAF infiltrations and stromal scores were significantly associated with worse overall survival in TCGA-BRCA **(A–C)** and GSE47994 **(D–F)**.

3.3 Functional analyses of CAF-related genes

The above CAF-related genes were overlapped and screened to 135 hub genes (Figure 4A). These genes were subjected to Gene Ontology (GO) and Kyoto Encyclopedia of Genes and Genomes (KEGG) analyses. The major enriched GO terms were related to extracellular matrix organization, extracellular structure organization, external encapsulating structure organization (BP), collagen-containing extracellular matrix and endoplasmic reticulum lumen (CC), and extracellular matrix structural constituents and collagen binding (MF) (Figure 4B). The main enriched KEGG pathways were human papillomavirus infection, the PI3K-Akt signaling pathway, and protein digestion and absorption (Figure 4C).

3.4 Construction a risk model based on stromal CAF

The 694 LBC samples from TCGA- BRCA were used as the training cohort owing to the larger sample size, and 101 GSE47994 samples were used as the validation group. By performing univariate Cox regression analysis of the 135 common hub genes, 20 OS-related genes with $p < 0.05$ were screened out and subjected to the following LASSO Cox regression analysis (Figures 4D, E). Five genes were finally identified for the CAF risk model construction: CAF risk score = expression of RIN2* 0.103 + expression of THBS1* 0.022 + expression of IL1R1* 0.068 + expression of RAB31* 0.055 + expression of COL11A1* 0.082 (Figure 4F). The median CAF risk score of the training cohort was 1.85, which was used as the cut-off value to classify LBC patients from each cohort into high- and low-CAF-risk groups. LBC patients in each cohort were divided into high– and low–CAF-risk groups with the median risk score as the cutoff value. Kaplan–Meier curves revealed that LBC patients in the high–CAF-risk group experienced worse OS than those in the low–CAF-risk group in both TCGA-BRCA (HR = 2.394, 95%CI: 1.531–3.745, log-rank $p < 0.001$) (Figure 4G) and GSE47994 (HR = 1.627, 95%CI: 1. 036–2.558, log-rank $p = 0.032$) (Figure 4H). These results indicated CAF and stromal-related signature genes were crucial prognostic markers in LBC.

3.5 Validation of the CAF risk score and the five-gene signature as indicators of CAF infiltrations

To evaluate the robustness of the CAF model as an indicator of CAF infiltrations, Spearman's correlation analyses were performed between the CAF risk score and stromal score as well as CAF abundances predicted by EPIC and three other methods: xCell, MCP-counter, and TIDE. The CAF risk score was strongly and positively correlated with multi-estimated CAF infiltrations and the stromal score in both TCGA-BRCA (Figure 5A) and GSE47994 (Figure 5B) cohorts. These results confirmed that the CAF risk score was a reliable predictor of CAF infiltrations. To further validate the correlation of the expression levels of the five genes with CAFs, their expression levels were compared with a set of collected CAF markers in both TCGA-BRCA (Figures 5C, E) and GSE47994 (Figures 5D, F) cohorts. A high and positive correlation was observed between the expression levels of the five genes and most

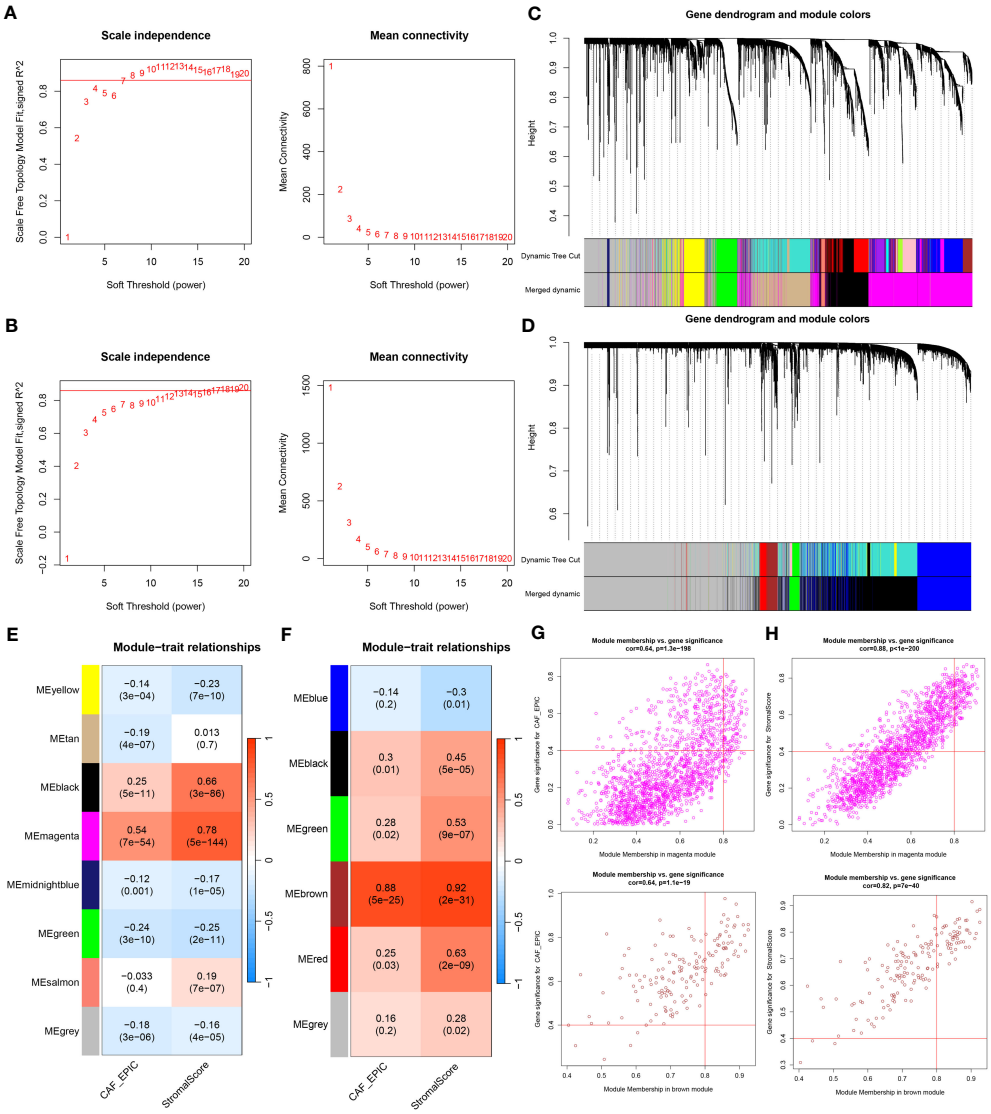

FIGURE 3
(A, B) Co-expression network constructed by WGCNA. The soft-thresholding power (β) of 7 and 17 was, respectively, selected based on the scale-free topology criterion in TCGA-BRCA **(A)** and GSE47994 **(B)**. **(C, D)**. Clustering dendrograms showing genes with similar expression patterns were clustered into co-expression modules in TCGA-BRCA **(C)** and GSE47994 **(D)**. The gray module indicates that genes were not assigned to any module. **(E, F)** Module-trait relationships revealing the correlations between each gene module eigengene and phenotype in TCGA-BRCA **(E)** and GSE47994 **(F)**. **(G, H)** Scatter plots of the module membership (MM) and gene significance (GS) of each gene in the magenta module of TCGA-BRCA **(G)** and the brown module of GSE47994 **(H)**. The horizontal axis is the correlation between the gene and co-expression module, and the vertical axis is the correlation between the gene and phenotype.

of the CAF markers in both cohorts. These results demonstrated that the five genes were representative of CAFs.

3.6 Chemotherapy and immunotherapy responses across CAF-risk groups

The standard treatment for LBC patients involves radical surgery followed by adjuvant chemotherapy and endocrine therapy (47). IC50 values for multiple anti-tumor drugs, including those used in breast cancer treatment, were estimated using the GDSC database for both the TCGA-BRCA (Figure 6A) and GSE47994 (Figure 6B) cohorts. Wilcoxon analyses indicated significant differences in IC50 values between high- and low-CAF-risk LBC patients. As for commonly used chemotherapy drugs for breast cancer, although not both datasets showed statistical significance, the results indicated that high-CAF-risk patients were sensitive to Alpelisib and Epirubicin, while low-CAF-risk patients were sensitive to Docetaxel, Fulvestrant, Lapatinib, Palbociclib, Ribociclib and Tamoxifen. However, Cyclophosphamide and Zoledronic acid exhibited different trends between the two datasets. In addition, the results from both datasets showed that high-CAF-risk patients were insensitive to several other drugs, including Axitinib, Dabrafenib, Irinotecan, Sorafenib, Topotecan, and Venetoclax. This suggests that higher CAF risk scores are more likely to induce resistance to these drugs in breast

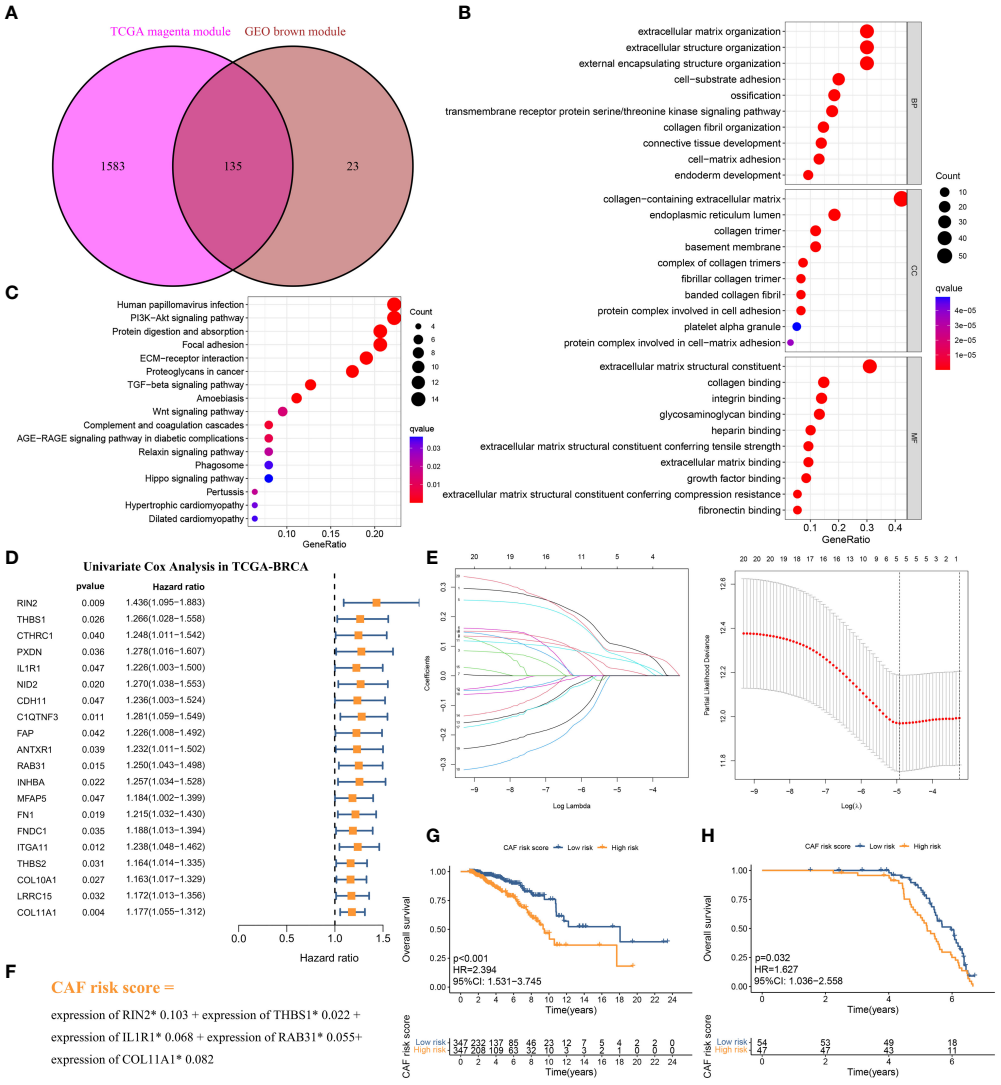

FIGURE 4
(A) The intersection of TCGA-BRCA magenta and GSE47994 brown module genes was presented in the Venn diagram. **(B, C)** GO analyses of the enriched biological process (BP), cellular component (CC), and molecular function (MF) terms **(B)** and KEGG pathway analysis **(C)** of the 135 genes. **(D)** Univariate Cox analysis for the screening of overall survival-associated genes in TCGA-BRCA. **(E)** Coefficient profiles of least absolute shrinkage and selection operator (LASSO) Cox regression analysis, and the adjustment parameter (lambda) was calculated based on the partial likelihood deviance with ten-fold cross validation. **(F)** Formulation of the CAF risk model. **(G, H)** Kaplan–Meier analyses identified gastric cancer patients in the high–CAF-risk group which exhibited worse overall survival in both TCGA-BRCA **(G)** and GSE47994 **(H)** cohorts.

cancer patients. Immunotherapy is among the most important advances in recent oncology, particularly for triple-negative and HER-2-positive breast cancer (48). Trials are also underway to assess the efficacy of immune checkpoint inhibitors such as pembrolizumab for Luminal breast cancer (49–51). To evaluate the CAF risk score as an immunotherapy predictor for LBC patients, the TIDE method was used. In TCGA-BRCA, the non-responder subgroup (n = 492) exhibited significantly higher CAF scores than the responder subgroup (n = 202) ($p < 2.2e-16$; Figure 6C). Low-CAF-risk patients (144/347) displayed higher immunotherapy sensitivity and lower TIDE scores than high-CAF-risk patients (58/347) ($p < 0.001$; Figures 6D, E). In GSE47994, the non-responder subgroup (n = 63) also had a significantly higher CAF score than the responder subgroup (n = 38) ($p = 1.9e-7$; Figure 6G). Low-CAF-risk patients (31/54) exhibited higher immunotherapy sensitivity and lower TIDE scores than high-CAF-risk patients (7/47) ($p < 0.001$; Figures 6H, I). The AUC values of 0.711 in TCGA-BRCA (Figure 6F) and 0.811 in GSE47994 (Figure 6J) indicate the excellent performance of the CAF model for predicting immunotherapy response.

3.7 GSEA of the five-gene CAF signature

To investigate the functional enrichment of the CAF signature, GSEA was conducted on the TCGA-BRCA dataset to compare the high- and low-CAF-risk groups. The analysis revealed significant enrichment in KEGG signaling pathways associated with ECM receptor interaction, focal adhesion, pathways in cancer, regulation of actin cytoskeleton, and tight junction in the high-

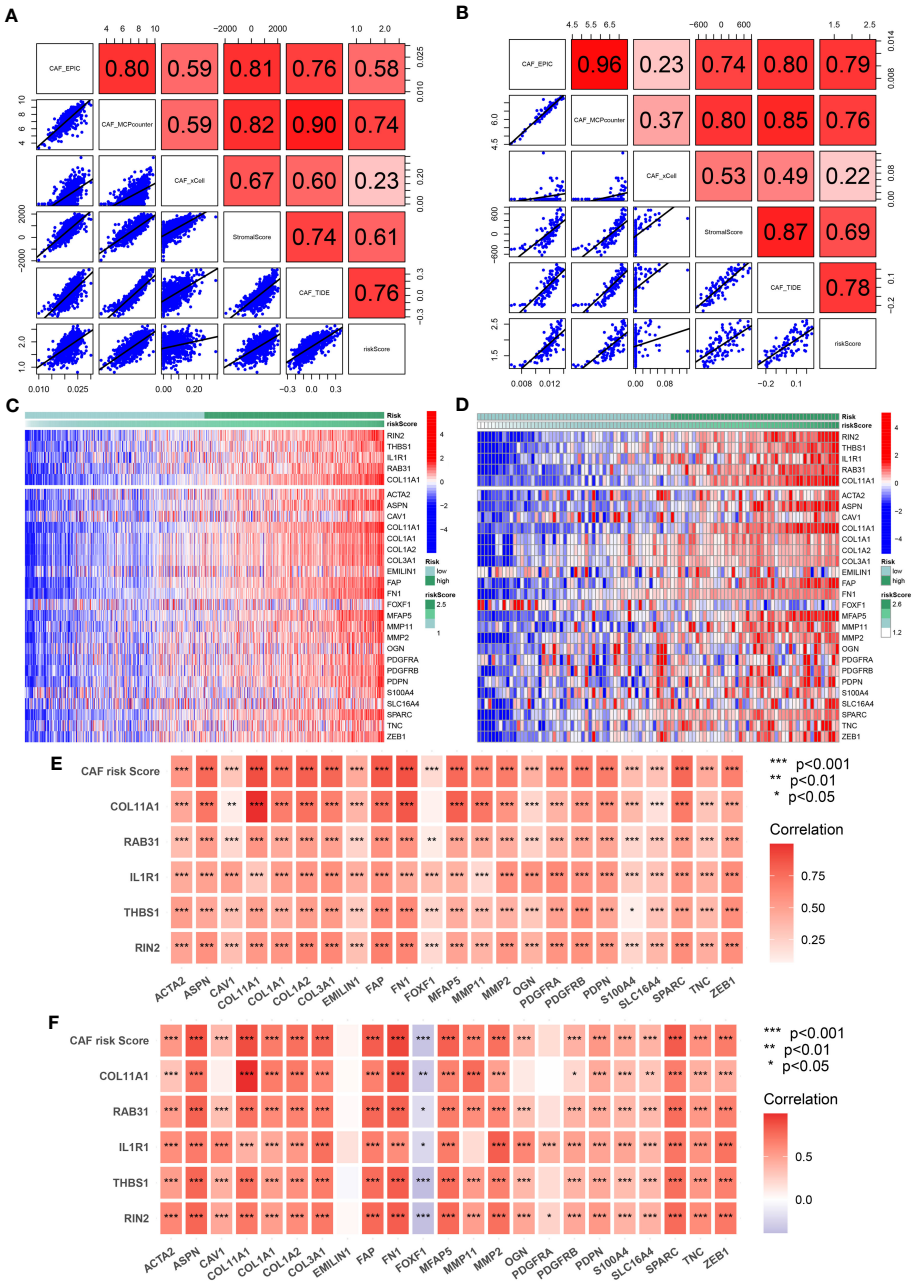

FIGURE 5
(A, B) Spearman's correlation analyses revealing the CAF risk score was strongly and positively correlated with stromal scores and multi-estimated CAF infiltrations in TCGA-BRCA **(A)** and GSE47994 **(B)** cohorts. **(C, D)** The heat map revealing the expression patterns of CAF markers identified five CAF genes with the CAF risk score in TCGA-BRCA **(C)** and GSE47994 **(D)** cohorts. **(E, F)** The CAF risk score and five signature genes were positively correlated with literature that reported CAF markers in TCGA-BRCA **(E)** and GSE47994 **(F)** cohorts.

CAF-risk group (Figure 7A). Moreover, the genes in the high-CAF-risk group were significantly enriched in Hallmarker gene sets related to angiogenesis, apical junction, coagulation, epithelial-mesenchymal transition (EMT), and inflammatory response (Figure 7B). Additionally, ssGSEA results indicated that the CAF risk score was positively correlated with enrichment scores for ECM receptor interaction, regulation of actin cytoskeleton, and TGF-β signaling pathway in both TCGA-BRCA (Figure 7C) and GSE47994 (Figure 7D).

3.8 Cross-dataset validation of important genes in CCLE and HPA

Based on the CCLE database, the mRNA expressions of the five hub genes (RIN2, THBS1, IL1R1, RAB31, COL11A1) were verified to be higher in fibroblast cell lines than those in BC cell lines (Wilcoxon test, all $p < 0.001$; Figures 8A, B). Additionally, to determine the protein expression characteristics of these CAF signature genes, the IHC images from the HPA database were

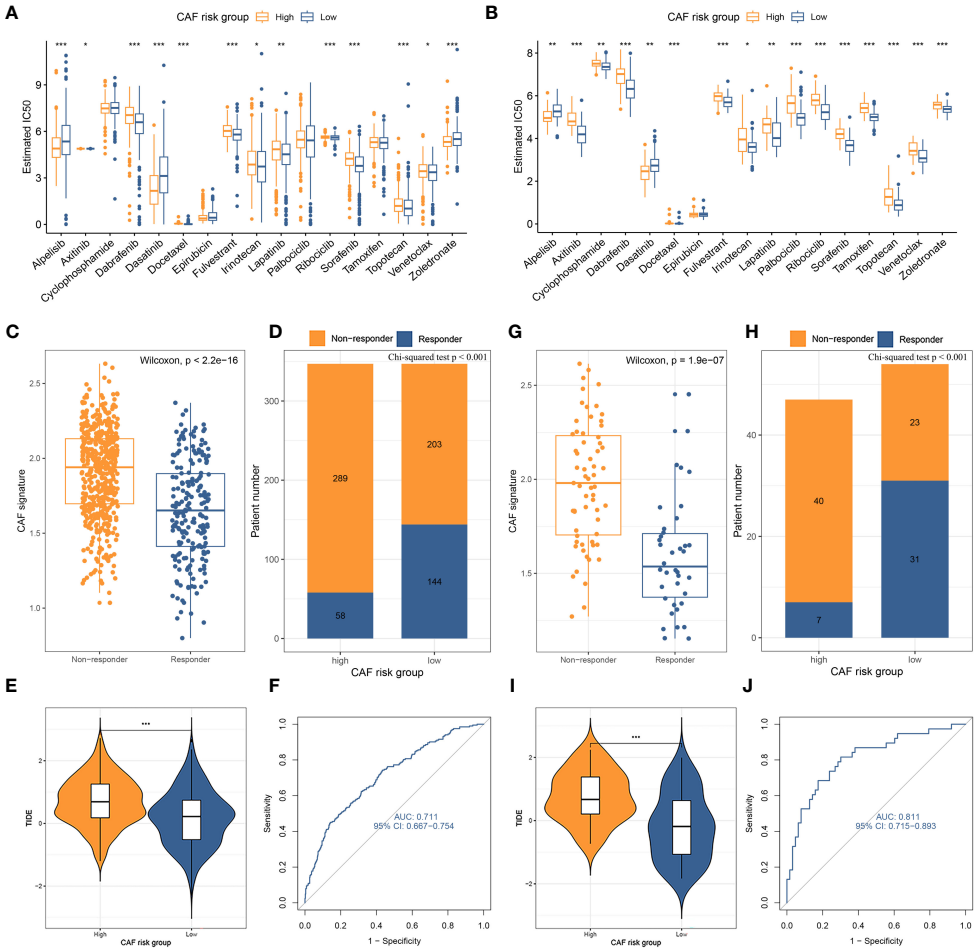

FIGURE 6
(A, B) Box plots comparing IC50 values of several chemotherapy drugs between high− and low−CAF-risk groups in TCGA-BRCA **(A)** and GSE47994 **(B)** cohorts. **(C–J)** TIDE immunotherapy prediction analyses. **(C, G)** The CAF risk score between TIDE-predicted immunotherapy-responders and non-responders in TCGA-BRCA **(C)** and GSE47994 **(G)**; **(D, H)** Distributions of responders and non-responders in high− and low− CAF-risk groups in TCGA-BRCA **(D)** and GSE47994 **(H)**; **(E, I)** Distributions of TIDE scores in high− and low− CAF-risk groups in TCGA-BRCA **(E)** and GSE47994 **(I)**; **(F, J)** ROC curves of the CAF risk score in predicting immunotherapy responses in TCGA-BRCA **(F)** and GSE47994 **(J)**. *p < 0.05, **p < 0.01, ***p < 0.001.

analyzed. The data demonstrated that these proteins (RIN2, THBS1, IL1R1 and RAB31) were deeply stained in BC stroma (Figure 8C). These verifications suggest that these genes might be CAF-specific markers.

3.9 Correlation between hub genes and HER2 in LBC

It is well known that the HER2 gene plays an important role in breast cancer, and overexpression or amplification of HER2 can lead to excess HER2 protein on the surface of breast cancer cells, leading to uncontrolled cell growth, tumor development and progression. To evaluate the correlation between the expression of the five hub genes (RIN2, THBS1, IL1R1, RAB31, COL11A1) and HER2 gene expression, we analyzed the gene expression data from TCGA-BRCA (Figure 8D) and GSE47994 (Figure 8E). Pearson correlation coefficient analysis revealed a significant positive correlation between the expression levels of these genes and HER2 gene expression ($p < 0.05$), with the exception of THBS1 and IL1R1 in GSE47994.

4 Discussion

Breast cancer is a complex and heterogeneous disease, consisting of multiple subtypes with distinct molecular and clinical characteristics (52). LBC is one of the most common subtypes, and some patients develop drug resistance and distant metastasis, and the prognosis of these patients is poor (4). While the molecular mechanisms underlying LBC development and progression have been extensively studied, the role of CAF in this subtype remains unclear. CAFs are a key component of the tumor microenvironment and have been shown to play a critical role in promoting tumor growth and progression, including in LBC (14, 19). Consistently, we observed that higher CAF and stromal scores were associated with worse OS after initial treatment in LBC. Therefore, identifying CAF-related factors and developing a CAF-related classifier for predicting

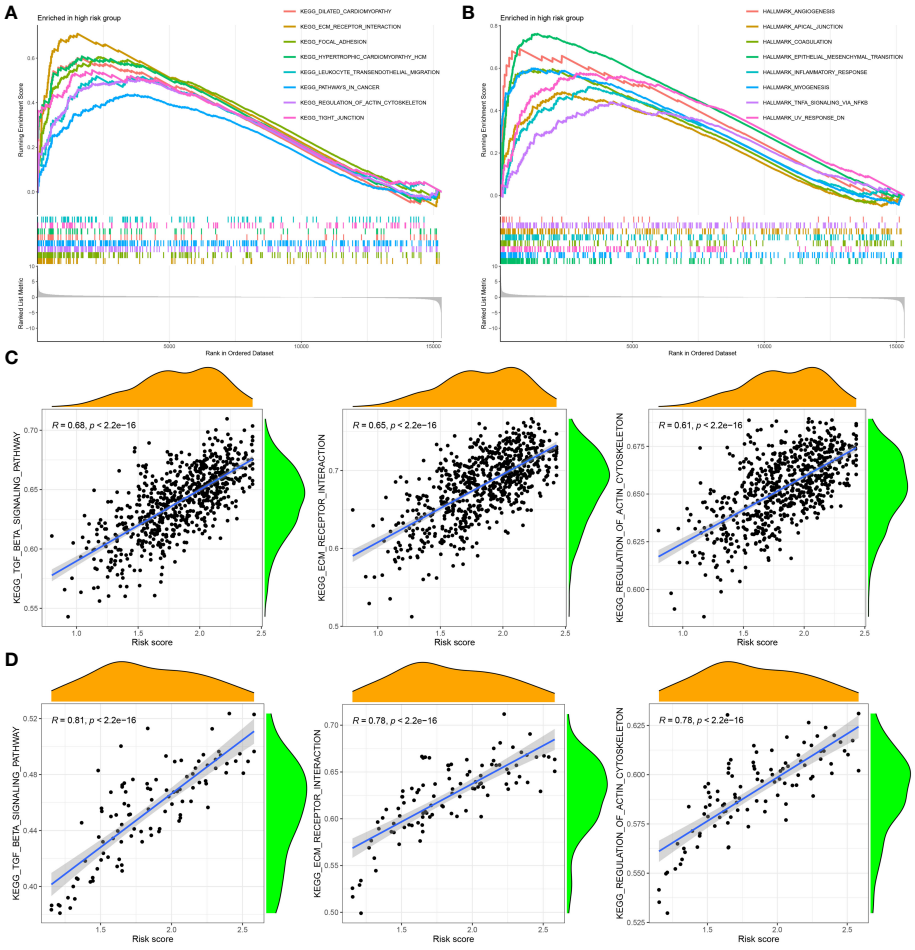

FIGURE 7
Gene set enrichment analysis (GSEA) of KEGG **(A)** and hallmark **(B)** gene sets between high-and low-CAF risk groups. **(C, D)** ssGSEA results showed CAF risk score was positively correlated with ECM receptor interaction, regulation of actin cytoskeleton, and TGF-β signaling pathway enrichment scores in both TCGA-BRCA **(C)** and GSE47994 **(D)**.

prognosis and therapeutic effects in LBC is of great significance. This is the first study utilizing WGCNA and multiple computational algorithms to uncover mutual co-expression networks between CAF and stromal components in two LBC cohorts: TCGA-BRCA and GSE47994. Through the application of univariate Cox and LASSO regression algorithms, a five-gene prognostic model for CAF (comprising RIN2, THBS1, IL1R1, RAB31, and COL11A1) was developed and subsequently validated. We found that LBC patients with a low CAF risk (using the median CAF risk score of 1.85 in the training set as a threshold) may benefit from a variety of antineoplastic agents, such as Axitinib, Docetaxel, Fulvestrant, Lapatinib, Palbociclib, Ribociclib, Tamoxifen, and others, indicating that high CAF infiltration may contribute to these drugs resistance. On the other hand, LBC patients with a high CAF risk may be more responsive to treatments such as Alpelisib, Epirubicin, and dasatinib. We also utilized the TIDE online algorithm and observed a strong correlation between lower CAF risk scores and improved immunotherapeutic response in LBC patients. However, Further experiments are required to elucidate the interplay between CAFs and Immunotherapy. It's worth noting that the TIDE algorithm primarily predicts the responses to anti-PD1 and anti-CTLA4 treatments in tumor patients, thus making pembrolizumab a more suitable candidate for follow-up studies.

To ensure the robustness of our model and avoid over-fitting, we employed four bioinformatics methods to quantify CAF infiltrations in LBC. We used the EPIC method for model construction and xCell, MCP-counter, and TIDE methods for correlation verification. Our results demonstrated a strong correlation between our model and CAF infiltrations, as well as CAF markers. Furthermore, based on analysis of the CCLE and HPA databases, we identified five genes as CAF-specific markers for LBC, with significantly higher expression observed in fibroblast cell lines and stromal parts of LBC. These findings further support the accuracy of our model in assessing CAF infiltration levels in LBC.

To investigate biological pathways associated with CAF risk in LBC, we performed GSEA analysis on TCGA-BRCA and GSE47994 dataset. GSEA revealed that ECM receptor interaction, focal adhesion, pathways in cancer, regulation of actin cytoskeleton and tight junction were highly and significantly enriched in the high–CAF-risk group; ssGSEA results also showed that the CAF risk score was positively correlated with ECM receptor interaction, regulation of actin cytoskeleton, and TGF-β signaling pathway enrichment scores

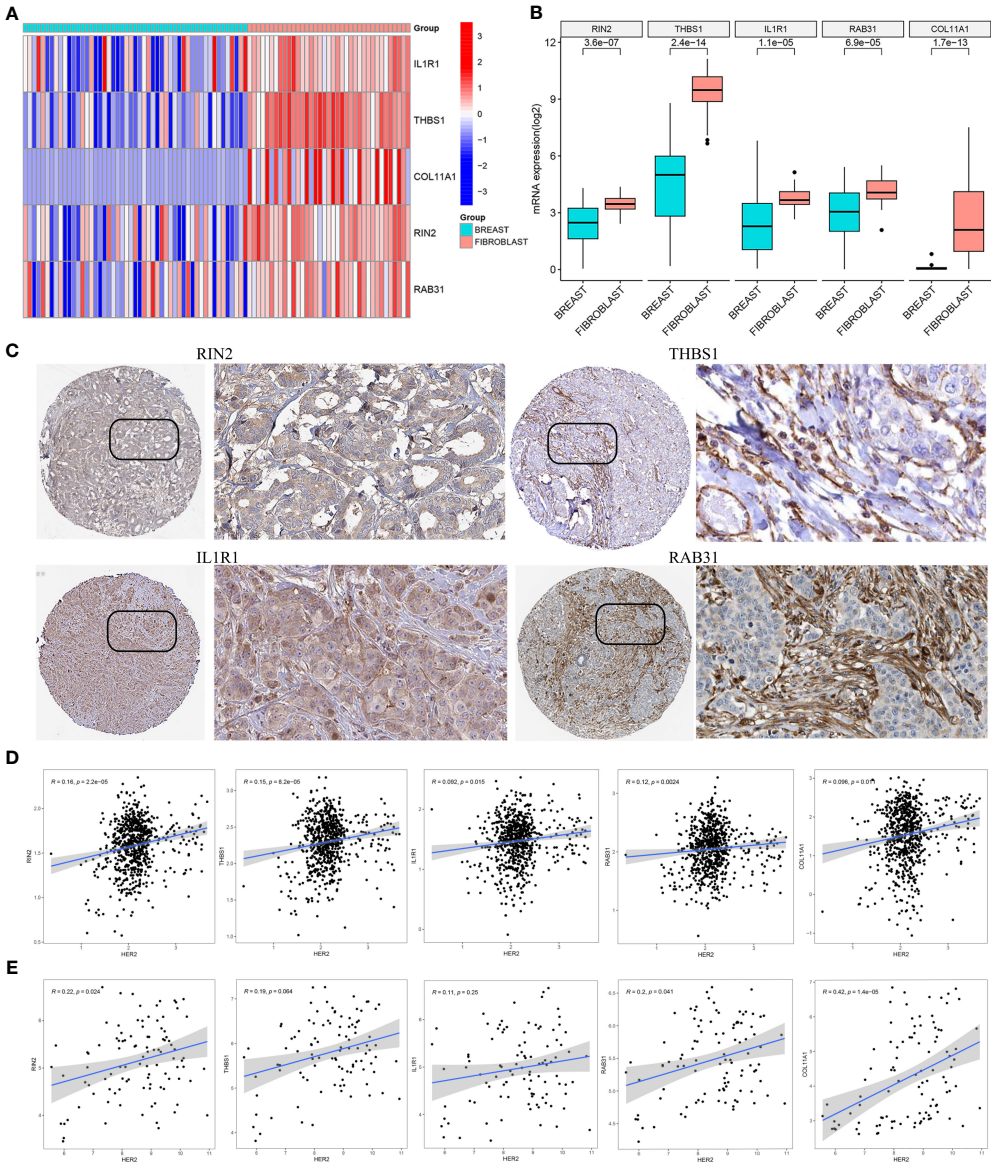

FIGURE 8
(A, B) The mRNA expression levels of the five CAF genes in the fibroblasts and breast cancer cell lines were illustrated in the heat map **(A)** and compared by Wilcoxon analysis **(B)**. **(C)** Protein expressions of RIN2, THBS1, IL1R1 and RAB31 in breast cancer specimens from the Human Protein Atlas database. Correlation between five hub genes and HER2 in TCGA-BRCA **(D)** and GSE47994 **(E)**.

in both two cohorts. CAFs play a crucial role in cancer progression by altering the extracellular matrix (ECM) composition and promoting cancer cell invasion and metastasis through the interaction of ECM proteins with specific receptors on the surface of cells (53–55). Furthermore, CAFs secrete fibronectin, which activates integrin receptors on cancer cells, triggering signaling pathways that enhance cancer cell proliferation, survival, and migration (56, 57). In addition, CAFs regulate the actin cytoskeleton of cancer cells, facilitating their ability to invade and migrate, by secreting growth factors such as TGF-β that promote the formation of stress fibers essential for cell migration and invasion (58, 59).

With respect to the five identified markers in the model, RIN2 is a gene that encodes a protein that interacts with Ras and Rab proteins, which are involved in cell signaling and membrane trafficking (60, 61). Biallelic defects in RIN2 are associated with MACS syndrome, a condition characterized by macrocephaly, alopecia, cutis laxa, and scoliosis, as well as with RIN2 syndrome, a related connective tissue disorder presenting similar symptoms (60, 62). Chiara Sandri et al. identified the Ras and Rab5 interacting protein RIN2 as a key effector in endothelial cells that interacts with R-Ras and mediates the pro-adhesion and tumor angiogenic activities of R-Ras (63). Furthermore, RIN2 has been identified as a signature gene that can be used to evaluate the clinical prognosis of patients with colorectal cancer, enabling more personalized diagnosis and treatment of the disease (64). THBS1 is a gene that encodes thrombospondin 1, a protein that is involved in cell adhesion, angiogenesis and inflammation (65). Previous studies have shown that THBS1 is highly expressed in gastric cancer (66), breast cancer (67), melanoma

(68) and oral squamous carcinoma (69), promoting tumor cell adhesion, proliferation, apoptosis, invasion and metastasis. THBS1 can modulate the invasion and migration of BC cells by affecting the TME, especially the CAFs (70). We observed that high-CAF-risk group LBC patients were less sensitive to several drugs, including docetaxel, which is consistent with the finding that up-regulation of THBS1 following neoadjuvant chemotherapy containing docetaxel was associated with docetaxel chemotherapy resistance in breast cancer patients (71). Additionally, THBS1 can protect MCF-7 cells from docetaxel-induced apoptosis by activating the integrin β1/mTOR pathway (71). IL1R1 is expressed in various types of cancer cells and CAF, which are stromal cells that support tumor growth and survival (72–74). IL1R1 signaling can modulate various aspects of tumor biology, such as angiogenesis, invasion, metastasis, immunity and drug resistance (75). Rosamaria et al. found that the expression of IL1R1 is regulated by hypoxia-inducible factor 1α (HIF-1α) and G-protein estrogen receptor (GPER) in breast cancer cells and CAFs (72). Puran Zhang et al. found that high expression of IL1R1 in gastric cancer is indicative of poor prognosis and a poorer response to 5-fluorouracil-based adjuvant chemotherapy and immune checkpoint blockade (74). In addition, IL1R1 has been found to be upregulated in ALDH+ cells and plays a crucial role in driving cancer stem cell (CSC) activity, which can lead to resistance to adjuvant endocrine therapies, including tamoxifen and fulvestrant, in breast cancer and promote bone metastasis (76, 77). RAB31, a protein secreted by CAF, is associated with malignant behavior in breast (78), hepatocellular (79), gastric (80), and colorectal cancers (81). Studies have shown the expression levels of RAB31 may serve as a crucial regulator of the transition between invasiveness and proliferation of breast cancer cells (78, 82). Recent research has shown that RAB31 is capable of inhibiting the TGF-β pathway by decreasing TGFB1 mRNA and antigen levels, thereby exerting an impact on the migration, invasion, and apoptosis of breast cancer cells (82). Additionally, Rab31 mediates cisplatin resistance and metastasis in stomach adenocarcinoma *via* epithelial-mesenchymal transition pathway (83). COL11A1 is a gene that encodes for collagen type XI alpha 1, a protein that is part of the extracellular matrix (ECM) (84). Studies have shown that COL11A1 can activate CAFs by stimulating the TGF-β signaling pathway that regulates cell proliferation and differentiation (85, 86). COL11A1 can also promotes cancer cell migration, metastasis, and therapy resistance by activating multiple signaling pathways (84, 87). Notably, COL11A1 has been shown to induce chemoresistance to cisplatin and paclitaxel in ovarian cancer cells through the AKT and Twist1 pathways (88, 89). Moreover, it may promote tumor immune infiltration and lead to a poor prognosis in breast cancer patients (90). However, there is not much functional validation of the five genes involved in risk signatures in the CAFs of LBC, which requires us to conduct further experiments on the five CAF markers in the future to evaluate the invasion and metastasis, drug resistance and immunosuppression of LBC.

It is worth mentioning that, in the initial analysis, we conducted the same analysis in the TCGA-BRCA database for different subtypes of breast cancer and found no significant difference in survival when analyzing CAF infiltration and stromal score in triple-negative breast cancer and HER2-positive breast cancer. However, Pearson correlation coefficient analysis revealed a significant positive correlation between the expression levels of these genes and HER2 gene expression in LBC. Meanwhile, targeted immunotherapy targeting cancer-associated fibroblasts has been reported to overcome drug resistance in HER2+ breast cancer treatment (91). Therefore, more analytical methods and experiments are needed to investigate the potential relationship between HER2 gene and CAF signature genes.

In conclusion, our study identified a five-gene CAF signature for predicting prognosis and therapeutic responses in LBC. Our findings provide important insights into the role of CAFs in promoting tumor growth and progression and highlight the importance of developing combination therapies that target both CAFs and the immune system. Our study has important clinical implications for guiding tailored anti-CAF therapy in combination with immunotherapy for LBC patients. There are also some limitations to our study. First, our study is retrospective, and therefore, our findings should be validated in a prospective study. Second, we did not perform functional experiments to validate the role of the identified CAF markers in promoting tumor growth and progression in LBC. Future studies should investigate the molecular mechanisms underlying the identified CAF markers and develop targeted therapies that can inhibit CAFs and promote anti-tumor immune responses.

Data availability statement

The original contributions presented in the study are included in the article/supplementary material. Further inquiries can be directed to the corresponding author.

Author contributions

AX and X-NX contributed to the conception and design. AX and ZL extracted the data from the databases. AX, X-NX, and XH contributed to the data analysis and interpretation. AX and X-NX drafted the manuscript. XH and D-YF revised the manuscript. D-YF supervised the entire study. All authors contributed to the article and approved the submitted version.

Funding

The National Natural Science Foundation of China (No.82072909).

Conflict of interest

The authors declare that the research was conducted in the absence of any commercial or financial relationships that could be construed as a potential conflict of interest.

Publisher's note

References

1. Giaquinto AN, Sung H, Miller KD, Kramer JL, Newman LA, Minihan A, et al. Breast cancer statistics, 2022. *CA Cancer J Clin* (2022) 72(6):524–41. doi: 10.3322/caac.21754

2. Siegel RL, Miller KD, Wagle NS, Jemal A. Cancer statistics, 2023. *CA Cancer J Clin* (2023) 73(1):17–48. doi: 10.3322/caac.21763

3. Wilkinson L, Gathani T. Understanding breast cancer as a global health concern. *Br J Radiol* (2022) 95(1130):20211033. doi: 10.1259/bjr.20211033

4. Pellegrino B, Hlavata Z, Migali C, De Silva P, Aiello M, Willard-Gallo K, et al. Luminal breast cancer: Risk of recurrence and tumor-associated immune suppression. *Mol Diagn Ther* (2021) 25(4):409–24. doi: 10.1007/s40291-021-00525-7

5. Pan H, Gray R, Braybrooke J, Davies C, Taylor C, McGale P, et al. 20-year risks of breast-cancer recurrence after stopping endocrine therapy at 5 years. *N Engl J Med* (2017) 377(19):1836–46. doi: 10.1056/NEJMoa1701830

6. Li JJ, Tsang JY, Tse GM. Tumor microenvironment in breast cancer-updates on therapeutic implications and pathologic assessment. *Cancers (Basel)* (2021) 13 (16):4233. doi: 10.3390/cancers13164233

7. Mittal S, Brown NJ, Holen I. The breast tumor microenvironment: Role in cancer development, progression and response to therapy. *Expert Rev Mol Diagn* (2018) 18 (3):227–43. doi: 10.1080/14737159.2018.1439382

8. Wang Y, Zhu M, Guo F, Song Y, Fan X, Qin G. Identification of tumor microenvironment-related prognostic biomarkers in luminal breast cancer. *Front Genet* (2020) 11:555865. doi: 10.3389/fgene.2020.555865

9. Zeppellini A, Galimberti S, Leone BE, Pacifico C, Riva F, Cicchiello F, et al. Comparison of tumor microenvironment in primary and paired metastatic Er+/Her2- breast cancers: Results of a pilot study. *BMC Cancer* (2021) 21(1):260. doi: 10.1186/s12885-021-07960-z

10. Lv J, Ren J, Zheng J, Zhang F, Han M. Prognosis of tumor microenvironment in luminal b-type breast cancer. *Dis Markers* (2022) 2022:5621441. doi: 10.1155/2022/5621441

11. Rimal R, Desai P, Daware R, Hosseinnejad A, Prakash J, Lammers T, et al. Cancer-associated fibroblasts: Origin, function, imaging, and therapeutic targeting. *Adv Drug Delivery Rev* (2022) 189:114504. doi: 10.1016/j.addr.2022.114504

12. Papait A, Romoli J, Stefani FR, Chiodelli P, Montresor MC, Agoni L, et al. Fight the cancer, hit the caf! *Cancers (Basel)* (2022) 14(15):3570. doi: 10.3390/cancers14153570

13. Wu F, Yang J, Liu J, Wang Y, Mu J, Zeng Q, et al. Signaling pathways in cancer-associated fibroblasts and targeted therapy for cancer. *Signal Transduct Target Ther* (2021) 6(1):218. doi: 10.1038/s41392-021-00641-0

14. Mao X, Xu J, Wang W, Liang C, Hua J, Liu J, et al. Crosstalk between cancer-associated fibroblasts and immune cells in the tumor microenvironment: New findings and future perspectives. *Mol Cancer* (2021) 20(1):131. doi: 10.1186/s12943-021-01428-1

15. Tan S, Yang Y, Yang W, Han Y, Huang L, Yang R, et al. Exosomal cargos-mediated metabolic reprogramming in tumor microenvironment. *J Exp Clin Cancer Res* (2023) 42(1):59. doi: 10.1186/s13046-023-02634-z

16. Hu JL, Wang W, Lan XL, Zeng ZC, Liang YS, Yan YR, et al. Cafs secreted exosomes promote metastasis and chemotherapy resistance by enhancing cell stemness and epithelial-mesenchymal transition in colorectal cancer. *Mol Cancer* (2019) 18 (1):91. doi: 10.1186/s12943-019-1019-x

17. Li Z, Sun C, Qin Z. Metabolic reprogramming of cancer-associated fibroblasts and its effect on cancer cell reprogramming. *Theranostics* (2021) 11(17):8322–36. doi: 10.7150/thno.62378

18. Barrett RL, Pure E. Cancer-associated fibroblasts and their influence on tumor immunity and immunotherapy. *Elife* (2020) 9:e57243. doi: 10.7554/eLife.57243

19. Brechbuhl HM, Finlay-Schultz J, Yamamoto TM, Gillen AE, Cittelly DM, Tan AC, et al. Fibroblast subtypes regulate responsiveness of luminal breast cancer to estrogen. *Clin Cancer Res* (2017) 23(7):1710–21. doi: 10.1158/1078-0432.CCR-15-2851

20. Louault K, Bonneaud TL, Seveno C, Gomez-Bougie P, Nguyen F, Gautier F, et al. Interactions between cancer-associated fibroblasts and tumor cells promote mcl-1 dependency in estrogen receptor-positive breast cancers. *Oncogene* (2019) 38 (17):3261–73. doi: 10.1038/s41388-018-0635-z

21. Sansone P, Berishaj M, Rajasekhar VK, Ceccarelli C, Chang Q, Strillacci A, et al. Evolution of cancer stem-like cells in endocrine-resistant metastatic breast cancers is mediated by stromal microvesicles. *Cancer Res* (2017) 77(8):1927–41. doi: 10.1158/0008-5472.CAN-16-2129

22. Glabman RA, Choyke PL, Sato N. Cancer-associated fibroblasts: Tumorigenicity and targeting for cancer therapy. *Cancers (Basel)* (2022) 14(16):3906. doi: 10.3390/cancers14163906

23. Chauhan VP, Chen IX, Tong R, Ng MR, Martin JD, Naxerova K, et al. Reprogramming the microenvironment with tumor-selective angiotensin blockers enhances cancer immunotherapy. *Proc Natl Acad Sci U.S.A.* (2019) 116(22):10674–80. doi: 10.1073/pnas.1819889116

24. Su S, Chen J, Yao H, Liu J, Yu S, Lao L, et al. Cd10(+)Gpr77(+) cancer-associated fibroblasts promote cancer formation and chemoresistance by sustaining cancer stemness. *Cell* (2018) 172(4):841–56 e16. doi: 10.1016/j.cell.2018.01.009

25. Langfelder P, Horvath S. Wgcna: An r package for weighted correlation network analysis. *BMC Bioinf* (2008) 9:559. doi: 10.1186/1471-2105-9-559

26. Feng S, Xu Y, Dai Z, Yin H, Zhang K, Shen Y. Integrative analysis from multicenter studies identifies a wgcna-derived cancer-associated fibroblast signature for ovarian cancer. *Front Immunol* (2022) 13:951582. doi: 10.3389/fimmu.2022.951582

27. Zheng H, Liu H, Li H, Dou W, Wang X. Weighted gene co-expression network analysis identifies a cancer-associated fibroblast signature for predicting prognosis and therapeutic responses in gastric cancer. *Front Mol Biosci* (2021) 8:744677. doi: 10.3389/fmolb.2021.744677

28. Liu B, Zhan Y, Chen X, Hu X, Wu B, Pan S. Weighted gene co-expression network analysis can sort cancer-associated fibroblast-specific markers promoting bladder cancer progression. *J Cell Physiol* (2021) 236(2):1321–31. doi: 10.1002/jcp.29939

29. Liu B, Chen X, Zhan Y, Wu B, Pan S. Identification of a gene signature for renal cell carcinoma-associated fibroblasts mediating cancer progression and affecting prognosis. *Front Cell Dev Biol* (2020) 8:604627. doi: 10.3389/fcell.2020.604627

30. Loi S, Michiels S, Salgado R, Sirtaine N, Jose V, Fumagalli D, et al. Tumor infiltrating lymphocytes are prognostic in triple negative breast cancer and predictive for trastuzumab benefit in early breast cancer: Results from the finher trial. *Ann Oncol* (2014) 25(8):1544–50. doi: 10.1093/annonc/mdu112

31. Racle J, de Jonge K, Baumgaertner P, Speiser DE, Gfeller D. Simultaneous enumeration of cancer and immune cell types from bulk tumor gene expression data. *Elife* (2017) 6:e26476. doi: 10.7554/eLife.26476

32. Aran D, Hu Z, Butte AJ. Xcell: Digitally portraying the tissue cellular heterogeneity landscape. *Genome Biol* (2017) 18(1):220. doi: 10.1186/s13059-017-1349-1

33. Becht E, Giraldo NA, Lacroix L, Buttard B, Elarouci N, Petitprez F, et al. Estimating the population abundance of tissue-infiltrating immune and stromal cell populations using gene expression. *Genome Biol* (2016) 17(1):218. doi: 10.1186/s13059-016-1070-5

34. Jiang P, Gu S, Pan D, Fu J, Sahu A, Hu X, et al. Signatures of t cell dysfunction and exclusion predict cancer immunotherapy response. *Nat Med* (2018) 24(10):1550–8. doi: 10.1038/s41591-018-0136-1

35. Sturm G, Finotello F, List M. Immunedeconv: An r package for unified access to computational methods for estimating immune cell fractions from bulk rna-sequencing data. *Methods Mol Biol* (2020) 2120:223–32. doi: 10.1007/978-1-0716-0327-7_16

36. Yoshihara K, Shahmoradgoli M, Martinez E, Vegesna R, Kim H, Torres-Garcia W, et al. Inferring tumour purity and stromal and immune cell admixture from expression data. *Nat Commun* (2013) 4:2612. doi: 10.1038/ncomms3612

37. Yu G, Wang LG, Han Y, He QY. Clusterprofiler: An r package for comparing biological themes among gene clusters. *OMICS* (2012) 16(5):284–7. doi: 10.1089/omi.2011.0118

38. Simon N, Friedman J, Hastie T, Tibshirani R. Regularization paths for cox's proportional hazards model *Via* coordinate descent. *J Stat Softw* (2011) 39(5):1–13. doi: 10.18637/jss.v039.i05

39. Han C, Liu T, Yin R. Biomarkers for cancer-associated fibroblasts. *biomark Res* (2020) 8(1):64. doi: 10.1186/s40364-020-00245-w

40. Nurmik M, Ullmann P, Rodriguez F, Haan S, Letellier E. In search of definitions: Cancer-associated fibroblasts and their markers. *Int J Cancer* (2020) 146(4):895–905. doi: 10.1002/ijc.32193

41. Yang W, Soares J, Greninger P, Edelman EJ, Lightfoot H, Forbes S, et al. Genomics of drug sensitivity in cancer (Gdsc): A resource for therapeutic biomarker discovery in cancer cells. *Nucleic Acids Res* (2013) 41(Database issue):D955–61. doi: 10.1093/nar/gks1111

42. Geeleher P, Cox N, Huang RS. Prrophetic: An r package for prediction of clinical chemotherapeutic response from tumor gene expression levels. *PloS One* (2014) 9(9): e107468. doi: 10.1371/journal.pone.0107468

43. Liberzon A, Birger C, Thorvaldsdottir H, Ghandi M, Mesirov JP, Tamayo P. The molecular signatures database (Msigdb) hallmark gene set collection. *Cell Syst* (2015) 1 (6):417–25. doi: 10.1016/j.cels.2015.12.004

44. Hanzelmann S, Castelo R, Guinney J. Gsva: Gene set variation analysis for microarray and rna-seq data. *BMC Bioinf* (2013) 14:7. doi: 10.1186/1471-2105-14-7

45. Ghandi M, Huang FW, Jane-Valbuena J, Kryukov GV, Lo CC, McDonald ER 3rd, et al. Next-generation characterization of the cancer cell line encyclopedia. *Nature* (2019) 569(7757):503–8. doi: 10.1038/s41586-019-1186-3

46. Uhlen M, Karlsson MJ, Zhong W, Tebani A, Pou C, Mikes J, et al. A genome-wide transcriptomic analysis of protein-coding genes in human blood cells. *Science* (2019) 366(6472):eaax9198. doi: 10.1126/science.aax9198

47. Goldner M, Pandolfi N, Maciel D, Lima J, Sanches S, Ponde N. Combined endocrine and targeted therapy in luminal breast cancer. *Expert Rev Anticancer Ther* (2021) 21(11):1237–51. doi: 10.1080/14737140.2021.1960160

48. Emens LA. Breast cancer immunotherapy: Facts and hopes. *Clin Cancer Res* (2018) 24(3):511–20. doi: 10.1158/1078-0432.CCR-16-3001

49. Rugo H, Delord J, Im S, Ott P, Piha-Paul S, Bedard P, et al. Abstract S5-07: Preliminary efficacy and safety of pembrolizumab (Mk-3475) in patients with Pd-L1–positive, estrogen receptor-positive (Er+)/Her2-negative advanced breast cancer enrolled in keynote-028. *Cancer Res* (2016) 76(4_Supplement):S5–07. doi: 10.1158/1538-7445.SABCS15-S5-07

50. Pusztai L, Han HS, Yau C, Wolf D, Wallace AM, Shatsky R, et al. Abstract Ct011: Evaluation of durvalumab in combination with olaparib and paclitaxel in high-risk Her2 negative stage Ii/Iii breast cancer: Results from the i-spy 2 trial. *Cancer Res* (2020) 80(16_Supplement):CT011–1. doi: 10.1158/1538-7445.AM2020-CT011

51. Tolaney SM, Barroso-Sousa R, Keenan T, Li T, Trippa L, Vaz-Luis I, et al. Effect of eribulin with or without pembrolizumab on progression-free survival for patients with hormone receptor-positive, Erbb2-negative metastatic breast cancer: A randomized clinical trial. *JAMA Oncol* (2020) 6(10):1598–605. doi: 10.1001/jamaoncol.2020.3524

52. Tsang JYS, Tse GM. Molecular classification of breast cancer. *Adv Anat Pathol* (2020) 27(1):27–35. doi: 10.1097/PAP.0000000000000232

53. Najafi M, Farhood B, Mortezaee K. Extracellular matrix (Ecm) stiffness and degradation as cancer drivers. *J Cell Biochem* (2019) 120(3):2782–90. doi: 10.1002/jcb.27681

54. Li C, Teixeira AF, Zhu HJ, Ten Dijke P. Cancer associated-Fibroblast-Derived exosomes in cancer progression. *Mol Cancer* (2021) 20(1):154. doi: 10.1186/s12943-021-01463-y

55. Winkler J, Abisoye-Ogunniyan A, Metcalf KJ, Werb Z. Concepts of extracellular matrix remodelling in tumour progression and metastasis. *Nat Commun* (2020) 11(1):5120. doi: 10.1038/s41467-020-18794-x

56. Wen S, Hou Y, Fu L, Xi L, Yang D, Zhao M, et al. Cancer-associated fibroblast (Caf)-derived Il32 promotes breast cancer cell invasion and metastasis *Via* integrin Beta3-P38 mapk signalling. *Cancer Lett* (2019) 442:320–32. doi: 10.1016/j.canlet.2018.10.015

57. Miyazaki K, Togo S, Okamoto R, Idiris A, Kumagai H, Miyagi Y. Collective cancer cell invasion in contact with fibroblasts through integrin-Alpha5beta1/Fibronectin interaction in collagen matrix. *Cancer Sci* (2020) 111(12):4381–92. doi: 10.1111/cas.14664

58. Chandra Jena B, Sarkar S, Rout L, Mandal M. The transformation of cancer-associated fibroblasts: Current perspectives on the role of tgf-beta in caf mediated tumor progression and therapeutic resistance. *Cancer Lett* (2021) 520:222–32. doi: 10.1016/j.canlet.2021.08.002

59. Kapoor M, Chinnathambi S. Tgf-Beta1 signalling in alzheimer's pathology and cytoskeletal reorganization: A specialized tau perspective. *J Neuroinflamm* (2023) 20(1):72. doi: 10.1186/s12974-023-02751-8

60. Rosato S, Syx D, Ivanovski I, Pollazzon M, Santodirocco D, De Marco L, et al. Rin2 syndrome: Expanding the clinical phenotype. *Am J Med Genet A* (2016) 170(9):2408–15. doi: 10.1002/ajmg.a.37789

61. Yuan W, Song C. The emerging role of Rab5 in membrane receptor trafficking and signaling pathways. *Biochem Res Int* (2020) 2020:4186308. doi: 10.1155/2020/4186308

62. Syx D, Malfait F, Van Laer L, Hellemans J, Hermanns-Le T, Willaert A, et al. The Rin2 syndrome: A new autosomal recessive connective tissue disorder caused by deficiency of ras and rab interactor 2 (Rin2). *Hum Genet* (2010) 128(1):79–88. doi: 10.1007/s00439-010-0829-0

63. Sandri C, Caccavari F, Valdembri D, Camillo C, Veltel S, Santambrogio M, et al. The r-Ras/Rin2/Rab5 complex controls endothelial cell adhesion and morphogenesis *Via* active integrin endocytosis and rac signaling. *Cell Res* (2012) 22(10):1479–501. doi: 10.1038/cr.2012.110

64. Wang XQ, Xu SW, Wang W, Piao SZ, Mao XL, Zhou XB, et al. Identification and validation of a novel DNA damage and DNA repair related genes based signature for colon cancer prognosis. *Front Genet* (2021) 12:635863. doi: 10.3389/fgene.2021.635863

65. Isenberg JS, Roberts DD. Thbs1 (Thrombospondin-1). *Atlas Genet Cytogenet Oncol Haematol* (2020) 24(8):291–9. doi: 10.4267/2042/70774

66. Zhang X, Huang T, Li Y, Qiu H. Upregulation of Thbs1 is related to immunity and chemotherapy resistance in gastric cancer. *Int J Gen Med* (2021) 14:4945–57. doi: 10.2147/IJGM.S329208

67. Shen J, Cao B, Wang Y, Ma C, Zeng Z, Liu L, et al. Hippo component yap promotes focal adhesion and tumour aggressiveness *Via* transcriptionally activating Thbs1/Fak signalling in breast cancer. *J Exp Clin Cancer Res* (2018) 37(1):175. doi: 10.1186/s13046-018-0850-z

68. Jayachandran A, Anaka M, Prithviraj P, Hudson C, McKeown SJ, Lo PH, et al. Thrombospondin 1 promotes an aggressive phenotype through epithelial-to-Mesenchymal transition in human melanoma. *Oncotarget* (2014) 5(14):5782–97. doi: 10.18632/oncotarget.2164

69. Pal SK, Nguyen CT, Morita KI, Miki Y, Kayamori K, Yamaguchi A, et al. Thbs1 is induced by Tgfb1 in the cancer stroma and promotes invasion of oral squamous cell carcinoma. *J Oral Pathol Med* (2016) 45(10):730–9. doi: 10.1111/jop.12430

70. Folgueira MA, Maistro S, Katayama ML, Roela RA, Mundim FG, Nanogaki S, et al. Markers of breast cancer stromal fibroblasts in the primary tumour site associated with lymph node metastasis: A systematic review including our case series. *Biosci Rep* (2013) 33(6):e00085. doi: 10.1042/BSR20130060

71. Wang T, Srivastava S, Hartman M, Buhari SA, Chan CW, Iau P, et al. High expression of intratumoral stromal proteins is associated with chemotherapy resistance in breast cancer. *Oncotarget* (2016) 7(34):55155–68. doi: 10.18632/oncotarget.10894

72. Lappano R, Talia M, Cirillo F, Rigiracciolo DC, Scordamaglia D, Guzzi R, et al. The Il1beta-Il1r signaling is involved in the stimulatory effects triggered by hypoxia in breast cancer cells and cancer-associated fibroblasts (Cafs). *J Exp Clin Cancer Res* (2020) 39(1):153. doi: 10.1186/s13046-020-01667-y

73. Sun R, Gao DS, Shoush J, Lu B. The il-1 family in tumorigenesis and antitumor immunity. *Semin Cancer Biol* (2022) 86(Pt 2):280–95. doi: 10.1016/j.semcancer.2022.05.002

74. Zhang P, Gu Y, Fang H, Cao Y, Wang J, Liu H, et al. Intratumoral il-1r1 expression delineates a distinctive molecular subset with therapeutic resistance in patients with gastric cancer. *J Immunother Cancer* (2022) 10(2):e004047. doi: 10.1136/jitc-2021-004047

75. De Francesco EM, Lappano R, Santolla MF, Marsico S, Caruso A, Maggiolini M. Hif-1alpha/Gper signaling mediates the expression of vegf induced by hypoxia in breast cancer associated fibroblasts (Cafs). *Breast Cancer Res* (2013) 15(4):R64. doi: 10.1186/bcr3458

76. Sarmiento-Castro A, Caamano-Gutierrez E, Sims AH, Hull NJ, James MI, Santiago-Gomez A, et al. Increased expression of interleukin-1 receptor characterizes anti-Estrogen-Resistant aldh(+) breast cancer stem cells. *Stem Cell Rep* (2020) 15(2):307–16. doi: 10.1016/j.stemcr.2020.06.020

77. Eyre R, Alferez DG, Santiago-Gomez A, Spence K, McConnell JC, Hart C, et al. Microenvironmental Il1beta promotes breast cancer metastatic colonisation in the bone *Via* activation of wnt signalling. *Nat Commun* (2019) 10(1):5016. doi: 10.1038/s41467-019-12807-0

78. Grismayer B, Solch S, Seubert B, Kirchner T, Schafer S, Baretton G, et al. Rab31 expression levels modulate tumor-relevant characteristics of breast cancer cells. *Mol Cancer* (2012) 11:62. doi: 10.1186/1476-4598-11-62

79. Sui Y, Zheng X, Zhao D. Rab31 promoted hepatocellular carcinoma (Hcc) progression *Via* inhibition of cell apoptosis induced by Pi3k/Akt/Bcl-2/Bax pathway. *Tumour Biol* (2015) 36(11):8661–70. doi: 10.1007/s13277-015-3626-5

80. Tang CT, Liang Q, Yang L, Lin XL, Wu S, Chen Y, et al. Rab31 targeted by mir-30c-2-3p regulates the Gli1 signaling pathway, affecting gastric cancer cell proliferation and apoptosis. *Front Oncol* (2018) 8:554. doi: 10.3389/fonc.2018.00554

81. Yang L, Tian X, Chen X, Lin X, Tang C, Gao Y, et al. Upregulation of Rab31 is associated with poor prognosis and promotes colorectal carcinoma proliferation *Via* the Mtor/P70s6k/Cyclin D1 signalling pathway. *Life Sci* (2020) 257:118126. doi: 10.1016/j.lfs.2020.118126

82. Soelch S, Beaufort N, Loessner D, Kotzsch M, Reuning U, Luther T, et al. Rab31-dependent regulation of transforming growth factor β expression in breast cancer cells. *Mol Med* (2021) 27(1):158. doi: 10.1186/s10020-021-00419-8

83. Chen K, Xu J, Tong YL, Yan JF, Pan Y, Wang WJ, et al. Rab31 promotes metastasis and cisplatin resistance in stomach adenocarcinoma through Twist1-mediated emt. *Cell Death Dis* (2023) 14(2):115. doi: 10.1038/s41419-023-05596-4

84. Nallanthighal S, Heiserman JP, Cheon DJ. Collagen type xi alpha 1 (Col11a1): A novel biomarker and a key player in cancer. *Cancers (Basel)* (2021) 13(5):935. doi: 10.3390/cancers13050935

85. Wu YH, Chang TH, Huang YF, Huang HD, Chou CY. Col11a1 promotes tumor progression and predicts poor clinical outcome in ovarian cancer. *Oncogene* (2014) 33(26):3432–40. doi: 10.1038/onc.2013.307

86. Wu YH, Huang YF, Chang TH, Chen CC, Wu PY, Huang SC, et al. Col11a1 activates cancer-associated fibroblasts by modulating tgf-Beta3 through the nf-Kappab/Igfbp2 axis in ovarian cancer cells. *Oncogene* (2021) 40(26):4503–19. doi: 10.1038/s41388-021-01865-8

87. Liu Z, Lai J, Jiang H, Ma C, Huang H. Collagen xi alpha 1 chain, a potential therapeutic target for cancer. *FASEB J* (2021) 35(6):e21603. doi: 10.1096/fj.202100054RR

88. Wu YH, Chang TH, Huang YF, Chen CC, Chou CY. Col11a1 confers chemoresistance on ovarian cancer cells through the activation of Akt/C/Ebpbeta pathway and Pdk1 stabilization. *Oncotarget* (2015) 6(27):23748–63. doi: 10.18632/oncotarget.4250

89. Wu YH, Huang YF, Chang TH, Chou CY. Activation of Twist1 by Col11a1 promotes chemoresistance and inhibits apoptosis in ovarian cancer cells by modulating nf-Kappab-Mediated ikkbeta expression. *Int J Cancer* (2017) 141(11):2305–17. doi: 10.1002/ijc.30932

90. Luo Q, Li J, Su X, Tan Q, Zhou F, Xie S. Col11a1 serves as a biomarker for poor prognosis and correlates with immune infiltration in breast cancer. *Front Genet* (2022) 13:935860. doi: 10.3389/fgene.2022.935860

91. Rivas EI, Linares J, Zwick M, Gomez-Llonin A, Guiu M, Labernadie A, et al. Targeted immunotherapy against distinct cancer-associated fibroblasts overcomes treatment resistance in refractory Her2+ breast tumors. *Nat Commun* (2022) 13(1):5310. doi: 10.1038/s41467-022-32782-3

frontiers | Frontiers in Oncology

TYPE Review
PUBLISHED 07 July 2023
DOI 10.3389/fonc.2023.1218206

OPEN ACCESS

EDITED BY
Deniz Can Guven,
Hacettepe University, Türkiye

REVIEWED BY
Sachin Chaugule,
University of Massachusetts Medical School, United States
Anjali P. Kusumbe,
University of Oxford, United Kingdom

*CORRESPONDENCE
Chunyu Li
chunyu_li@126.com
Guohui Li
lgh0603@cicams.ac.cn

†These authors have contributed equally to this work

RECEIVED 06 May 2023
ACCEPTED 23 June 2023
PUBLISHED 07 July 2023

CITATION
Xu J, Cao B, Li C and Li G (2023) The recent progress of endocrine therapy-induced osteoporosis in estrogen-positive breast cancer therapy.
Front. Oncol. 13:1218206.
doi: 10.3389/fonc.2023.1218206

The recent progress of endocrine therapy-induced osteoporosis in estrogen-positive breast cancer therapy

Jing Xu†, Bo Cao†, Chunyu Li* and Guohui Li*

National Cancer Center/National Clinical Research Center for Cancer/Cancer Hospital, Chinese Academy of Medical Sciences and Peking Union Medical College, Beijing, China

Breast cancer is a significant global health concern, and the discovery of endocrine therapy has played a crucial role in the treatment of estrogen-positive breast cancer. However, these therapies are often associated with osteoporosis-related adverse events, which increase the risk of fractures in breast cancer patients and can result in limited mobility and reduced quality of life. Previous studies have shown that osteoporosis is essential side effects of the breast cancer therapy, although the exact mechanisms remain mostly unclear. Current clinical treatments, such as bisphosphonates, cause side effects and may impact the therapeutic response to endocrine drugs. In this review, we explore the likelihood of endocrine therapy-induced osteoporosis in estrogen-positive breast cancer therapy and discuss the involved mechanisms as well as the therapeutic potential of drugs and drug combination strategies.

KEYWORDS

breast cancer, endocrine therapy, estrogen, osteoporosis, aromatase inhibitors

1 Introduction

Breast cancer is the most common cancer in women worldwide, accounting for 11.7% of total cases and 24.5% of cases in females according to the "Global Cancer Statistics 2020" (1) released by the International Agency for Research on Cancer (IARC) of the World Health Organization. It is also the leading cause of cancer deaths among women, accounting for 6.9% of total cancer deaths and 15.5% of female deaths. As of January 1, 2022, approximately 4.1 million women in the United States have a history of breast cancer (2). Current treatment options for breast cancer include surgery, radiotherapy, chemotherapy, endocrine therapy, targeted therapy, and traditional Chinese medicine (3). Surgery and radiotherapy are local treatments, and adjuvant systemic treatment is often required before or after surgery for non-metastatic breast cancer patients to reduce the recurrence rate. However, chemotherapy drugs can produce serious clinical side effects due to their high toxicity. Targeted drugs are only suitable for patients with positive human epidermal growth factor 2 (HER2). About 70% of patients with breast cancer are estrogen

receptor (ER) positive and/or progesterone receptor (PR) positive. Endocrine-assisted therapy has demonstrated good efficacy in this subtype of patients and is an important treatment option for them. However, long-term use of these medications may lead to osteoporosis, joint and muscle pain (4), endometrial thickening (5), hot flusher, sweating, irritability, fatigue, insomnia and other adverse reactions. Osteoporosis increases the risk of fractures in breast cancer patients, resulting in limited mobility and reduced quality of life. The probability of osteoporosis associated with endocrine therapy is related to the type of medication used by the patient. Although lifestyle interventions and bone density assessments are the primary preventive measures, they may not always solve this problem. Medication such as bisphosphonates may be necessary if severe osteoporosis occurs, but these drugs can lead to side effects that may impact the therapeutic response to endocrine drugs. It is unclear whether osteoporosis drugs interact with endocrine drugs or otherwise impact breast cancer treatment.

Osteoporosis caused by endocrine therapy is mainly related to a decrease of estrogen in patients. Estrogen plays an essential role in the development and structure of bones, and estrogen deficiency promotes bone resorption and loss (6). Specifically, estrogen inhibits bone renewal by reducing osteoclast (OC) -mediated bone resorption and enhancing osteoblast (OB) -mediated bone formation (7). Estrogen deficiency promotes OC differentiation and bone resorption leading to bone loss, but the exact mechanism is not yet clear. This review aims to provide an overview of endocrine therapy for breast cancer, explore the occurrence of osteoporosis caused by endocrine therapy and its possible mechanism, as well as examine the prevention and treatment of this type of osteoporosis. Our objective is to promote rational drug use and improve the quality of life of breast cancer patients.

2 Overview of osteoporosis associated with endocrine therapy in breast cancer

Breast cancer is a malignant tumor caused by uncontrolled proliferation of ductal epithelial cells of the breast, however its specific mechanisms are not fully understood. Research has revealed that the development of breast cancer is associated with various risk factors including genetic factors and unhealthy lifestyle choices (8, 9). Breast cancer can be categorized as luminal A (ER and PR positive, HER2 negative), luminal B (ER and PR positive, HER2 positive), HER2 positive, or triple negative based on molecular pathology. Both luminal A and B breast cancers can be treated with endocrine drugs or adjuvant therapy.

Osteoporosis is a disease characterized by a decrease in bone density and an increased risk of fracture. Osteoporosis is common in menopausal women, where it is associated with bone loss due to decreased estrogen levels, and the elderly population, in which it causes unbalanced bone resorption and formation. One meta-analysis showed that the global prevalence of osteoporosis in the elderly was as high as 21.7%, with the highest prevalence in the Asian population (24.3%) (10). The analysis estimated that in 2019, the prevalence of osteoporosis in Chinese men and women aged 50 + was 6.46% and 29.13%, respectively (11). This data suggests that elderly women have a higher incidence of osteoporosis.

The strategy of endocrine therapy is to reduce the production of estrogen or the binding level of estrogen to ERs in tumor cells, thereby inhibiting the growth and proliferation of tumor. Estrogen stimulates OBs and inhibits OCs, therefore the main cause of endocrine treatment-related osteoporosis in breast cancer is bone loss induced by estrogen depletion. Patients receiving this treatment often experience adverse effects such as estrogen deficiency-related osteoporosis-induced brittle fractures. The risk of osteoporosis in patients varies based on the targets of various endocrine drugs. The most accurate clinical indicator of osteoporosis is the measurement of bone mineral density (BMD) or bone mineral content (BMC) using dual-energy X-ray absorptiometry (12). BMD can predict bone fracture risk and is typically measured at the femoral neck, total hip, or lumbar spine. T-score is generally used to evaluate osteoporosis clinically. Patients with T-score lower than 2.5 can be preliminarily diagnosed as suffering from osteoporosis.

The main anti-estrogenic drugs commonly used in clinical practice are tamoxifen (TAM), toremifene, raloxifene, and fulvestrant. These drugs compete with estrogen in the body by binding ERs. TAM, despite being an ER agonist in the bone and uterus, acts as an antagonist in breast tissue and is considered a selective estrogen modulator (SERM) due to its tissue-specific effects (7, 13). Toremifene is a chlorinated derivative of TAM and is also used in breast cancer treatment. TAM is one of the most commonly used endocrine drugs in the treatment of breast cancer and has been used for around 50 years. A 2020 nationwide retrospective cohort study conducted by Lee Jihyound and other Korean researchers using data from the Health Insurance Review and Assessment Service (HIRA) concluded that TAM does not increase the risk of osteoporosis and osteoporotic fractures in breast cancer patients under 40 years of age and has a protective effect on bones in breast cancer patients aged 40 to 49 years (14). However, another research suggested that the 5-year rate of osteoporotic fracture for patients treated with tamoxifen was 6.9% (15). There was no significant difference (HR = 1.09; 95% CI = 0.96–1.23, p-value = 0.18) from the data of aromatase inhibitors (7.5%) mentioned in the paper. So more extensive real-world studies of TAM are needed to provide sufficient evidence of its association with osteoporosis in breast cancer patients who use the drug. Fluvestrant is a selective ER down-regulator (SERD) and induces the degradation of ERs by competitively binding with them. Although no studies have been conducted to correlate the use of fulvestrant with osteoporosis, there is a risk that the drug may cause osteoporosis based on its therapeutic mechanism. Thus, BMD is typically measured during the clinical use of fulvestrant to monitor the development of osteoporosis.

Aromatase inhibitors are often the first-choice treatment in postmenopausal women with breast cancer. When combined with aromatase, these drugs work by blocking the conversion of androgens into estrogen in the body, which reduces the estrogen levels and ultimately inhibits the growth of tumor cells. However, the use of aromatase inhibitors exacerbates the age-related reduction in BMD (16) due to the link between estrogen levels and bone health (Table 1) (20). Anastrozole, letrozole, and

exemestane are frequently used aromatase inhibitors, with the latter being a steroid. Exemestane is structurally similar to androstendione, the natural substrate of aromatase, and binds irreversibly to the aromatase to inactivate it. A randomized phase III trial showed no significant differences in efficacy or side effects among these three aromatase inhibitors (17). On the other hand, a meta-analysis revealed that all aromatase inhibitors had a higher incidence of osteoporosis compared to tamoxifen, but that the incidence of osteoporosis was lower in patients using exemestane than in those using anastrozole (OR: 0.8594, 95% CI: 0.5766-1.168) and letrozole (OR: 0.7358, 95% CI: 0.4301-1.307) (21). There may be differences between the two classes of aromatase inhibitors in terms of bone-related metabolism. Anastrozole use accelerates bone loss in patients with breast cancer, but the associated bone loss appears to be manageable and partially reversible with discontinuation of treatment, particularly in the lumbar spine (22–24). Irene E.G. van Hellemond et al. (18) concluded from a phase III DATA study that adjuvant use of anastrozole after 2-3 years of tamoxifen decreased BMD in postmenopausal breast cancer patients. In contrast, prolonged anastrozole treatment did not increase the incidence of osteoporosis. Similarly, patients treated with exemestane had a 2.6% decrease in spinal BMD from baseline at 6 months and only a 0.2% decrease from 6 months to 12 months (25).

LHRH analogues, such as goserelin, leuprorelin and triptorelin, are commonly used ovarian castrating drugs. This class of drug inhibits the secretion of luteinizing hormone and follicle-stimulating hormone in the anterior pituitary gland, resulting in significantly reduced estrogen in patients. Thus, these drugs are most suitable for premenopausal women. However, the use of these drugs can also results in decreased BMD, leading to osteopenia or osteoporosis (26). While these drugs have achieved some therapeutic success, their use is limited and there is a need for development of new breast cancer treatments.

Recently, CDK4/6 inhibitors have entered the clinic and have shown promise in treating ER-positive and HER2-negative advanced breast cancers. CDK4/6 inhibitors are cyclin-dependent kinase inhibitors that prevent tumor cells from entering the S phase from the G1 phase by acting on the cyclin-CDK4/6 complex, thereby inhibiting tumor growth. Palbociclib, ribociclib, abemaciclib, and trilaciclib are currently available CDK4/6 inhibitors. To date, there have been no reported cases of osteopenia or osteoporosis in breast cancer patients caused by CDK4/6 inhibitor use, although more research is required.

3 Mechanisms of endocrine drugs in breast cancer and drug-related osteoporosis

Several drugs have been studied that target ERs, which are activated by the female sex hormone estrogen. ERs are divided into two receptor subtypes, ERα and ERβ, which differ primarily in location (27). ERα is mainly found in breast cells and bone (28), making it a central target in the pathogenesis of breast cancer (29). There are two main estrogen synthesis pathways in humans: direct synthesis and secretion by the ovaries and synthesis from aromatase within the adrenal gland, fat, and other tissues. The former pathway is most prevalent in premenopausal women, while the latter is most common in postmenopausal women. Furthermore, there are three main types of estrogen in women: estrone (E1), estradiol (E2 or 17β-estradiol), and estradiol (E3). E2 is the most potent estrogen and is the main product of female premenopausal biosynthetic reactions (27).

PRs are typically co-expressed with ERs, but their role in the development of breast cancer is not fully understood. PR antagonists have not been clinically used due to serious side effects (30). The combination of estrogen and progesterone significantly affects metabolism, with estrogen tending to target tumor-promoting genes that alter glucose metabolism and progesterone targeting fat storage (31). Postmenopausal women who use estrogen and progesterone together have an increased risk of breast cancer (26%) (32) and increased breast cancer mortality (33). Additionally, a case cohort study of postmenopausal women demonstrated an increased risk of breast cancer with elevated circulating progesterone levels (16%) (34). Thus, PR plays an important role in the occurrence and progression of breast cancer. PR has two subtypes, PRA and PRB, and studies have found that a PR can bind to an ER after it is combined with its agonist, thus affecting ER-related behaviors (35). Both natural and synthetic progesterone antagonize the mitotic effect of estrogen

TABLE 1 Incidence of osteoporosis associated with aromatase inhibitors.

Trial(Ref)	Follow-up time	Enrolled patients	Design	Osteopenia	Osteoporosis
NCT00541086 (17)	60 months	3697	Anastrozole		21%
			Exemestane		22%
			Letrozole		22%
NCT00301457 (18)	7 years	1860	6 years anastrozole after 2 to 3 years of tamoxifen	46.9%	9.5%
			3 years anastrozole after 2 to 3 years of tamoxifen	42.8%	9.1%
NCIC CTG MA.27 (19)	4.1 years	7576	Exemestane		31%
			Anastrozole		35%

(36). PRB is activated by a ligand, and it then activates the transcription factor EB which induces autophagy in breast cancer cells (37). Moreover, PRs can interact with STAT1 to inhibit IFN-induced STAT1 phosphorylation, thereby inhibiting carcinoma development (38). Some evidence suggests that the role of progesterone in breast tumor promotion and growth may be mediated by a receptor activator of NF-κB ligand (RANKL)-dependent effect. RANKL inhibition does not directly interfere with progesterone and PR interaction (39).

Endocrine therapies for breast cancer can be divided into several categories based on the production pathway and role of the hormone receptors in the occurrence and progression of breast cancer (Table 2), including antiestrogen drugs (selective ER regulator, selective ER downregulation), aromatase inhibitors, luteinizing hormone releasing hormone analogues (LHRH analogues), progesterone drugs, and CDK4/6 inhibitors. The action and targets of these drugs are shown in Figures 1, 2 (produced by BioRender, and the website is https://www.biorender.com/).

Estrogen is an important hormone that helps regulate the metabolic process of bone by inhibiting OCs thereby preventing osteoporosis. Bone loss caused by endocrine therapy in patients with hormone receptor positive breast cancer is mainly due to estrogen deprivation (40). At the osteocyte level, estrogen inhibits OC differentiation which reduces the number of active remodeling units. The mechanism of osteoporosis associated with endocrine therapy in breast cancer is related to changes in cytokines, the RANK pathway, Wnt pathway, and MicroRNA after estrogen level reduction (Figure 3). However, the mechanism of its action in the skeleton caused by crosstalk between various pathways in skeletal cells has not been fully elucidated.

3.1 Cytokine

Previous studies have suggested that estrogen may exert bone-protective effects by inhibiting inflammatory cytokines, such as interleukin-1 (IL-1), IL-6, and tumor necrosis factor-α (TNF-α), that promote OC formation and bone resorption. Estrogen selectively regulates IL-1R isoforms in OC or OC-like cells thereby decreasing their IL-1 responsiveness and survival (41). Conversely, this IL-1 inhibition may be lost as estrogen levels decline, resulting in OC-mediated bone loss. Estrogen deficiency leads to increased secretion of IL-1 and TNF, increased macrophage colony-stimulating factor (M-CSF) (42), and increased osteoclasts. Animal studies have shown that IL-6-deficient ovariectomized (OVX) female mice do not experience significant changes in bone mass and are protected from bone loss caused by estrogen depletion (43).

3.2 RANK/RANKL/OPG pathway

Prior research has shown that the effect of estrogen on bone is related to the RANKL pathway, which promotes the transformation of osteoclast precursors (OCPs) into mature OCs. Activators of RANKL signaling include reactive oxygen species (ROS), the NF-κB pathway, and mitogen activated protein kinase (MAPK) (44).

The protein osteoprotegerin (OPG) can bind to RANKL within the bone remodeling environment to prevent excessive OC formation. Estrogen activates p38α (a p38MAPKs) to maintain OPG gene expression and production in bone marrow mesenchymal stem cells (BMSCs) to protect the bone (45, 46).

Reactive oxygen species (ROS), including superoxide ion (O^{2-}) and hydrogen peroxide (H_2O_2), are important components that regulate OC differentiation. The downstream target of ROS remains unclear, but increased oxidative stress may promote the cellular activity of OCs by triggering the NF-κB and MAPK signaling pathways (47). Under normal physiological conditions, ROS produced by OCs stimulate and promote bone tissue absorption (48). However, deficiency of the potent antioxidant estrogen leads to the accumulation of ROS in the body which in turn affects osteogenic differentiation of stem cells and the formation of osteoporosis (49).

Estrogen can inhibit RANKL expression in bone lining cells (50), and the reduced rate of RANKL formation subsequently reduces the differentiation of OCPs into OCs. Another mechanism by which E2 downregulates OC formation is by decreasing OCP reactivity to RANKL (51). E2 down-regulates the activation of Jun N-terminal kinase1 (JNK1). This decreased JNK1 activity leads to decreased nuclear levels and DNA binding of the key OC transcription factors c-Fos and c-Jun, which weakens the differentiation ability of OCPs. It was shown that when estrogen levels were reduced *in vivo*, RANKL expression was increased, the response of OCPs to free RANKL was enhanced, and bone resorption was increased.

E2 inhibits OC differentiation and stimulates mature apoptosis (52) by increasing the expression of transient receptor potential vanilloid 5 (TRPV5) channels (53). The specific mechanism is as follows: E2 enhances the expression of TRPV5 through the interaction of ERα with NF-κB, and NF-κB can directly bind to the TRPV5 promoter region from −286 nt ~−277 nt fragments. When estrogen is deficient, the expression of the TRPV5 channel weakens, OC differentiation enhances, and the risk of osteoporosis increases.

TABLE 2 Commonly used drugs and targets for endocrine therapy of breast cancer.

Type	Drugs	Target
Anti-estrogens	Tamoxifen, toremifene, raloxifene, fulvestrant	ER
Aromatase inhibitor	Anastrozole, letrozole, exemestane	Aromatase enzymes
LHRH analogues	Goserelin, leuprorelin, triptorelin	LHRH receptor
Progestogens	Megestrol	PR
CDK4/6 inhibitor	Palbociclib, ribociclib, abemaciclib, trilaciclib	CDK4、CDK6

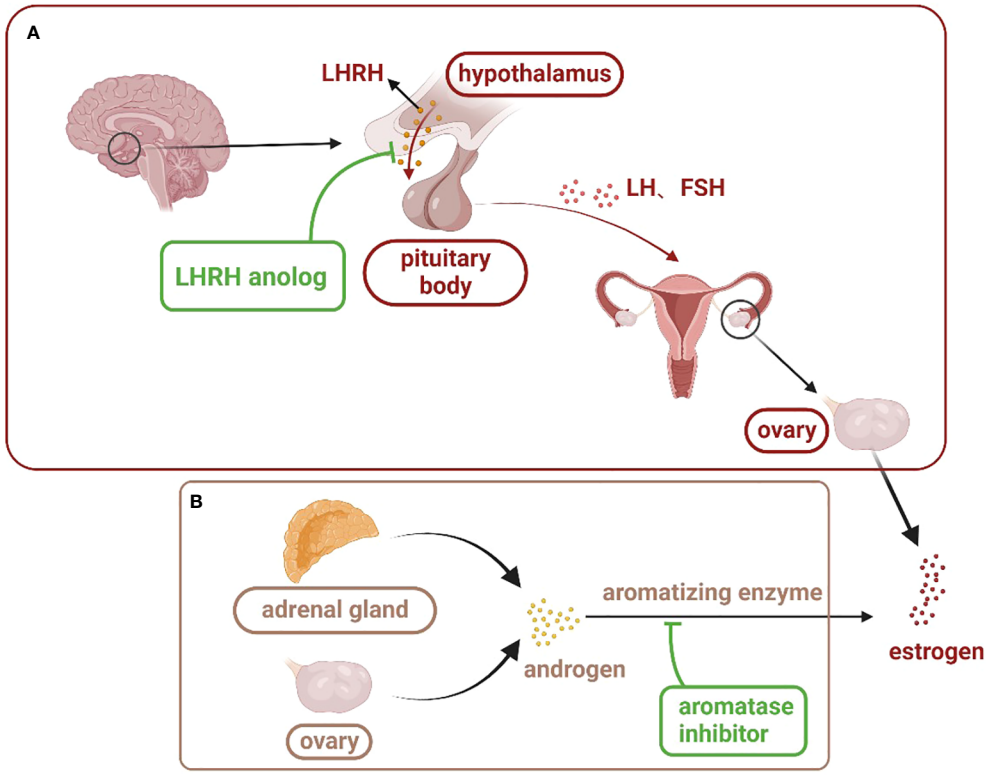

FIGURE 1
Estrogen production pathway in women: **(A)** is the main estrogen production pathway in premenopausal women. LHRH analogues inhibit the action of LHRH on the pituitary gland through competitive binding, thus inhibiting the secretion of estrogen in the ovary. **(B)** is the main estrogen production pathway in postmenopausal women. Aromatase inhibitors bind to androgens and prevent their conversion to estrogen. (LHRH, luteinizing hormone releasing hormone; LH, luteinizing hormone; FSH, follicle-stimulating hormone).

3.3 Wnt pathway

The Wnt pathway is highly conserved and present in both invertebrates and vertebrates. It plays a critical role in various physiological processes during early animal embryo development, including organ formation and tissue regeneration. The Wnt signaling pathway also regulates proliferation and differentiation of OBs by influencing gene transcription. Estrogen deficiency reduces GSK3β phosphorylation in OBs, leading to inhibition of the Wnt/β-catenin pathway and decreased OB proliferation (54). The Wnt agonist LiCl has been shown to induce the expression of the Fhl1 gene, which in turn promotes the expression of osteogenic markers such as Runt-associated transcription factor 2 (Runx2), osteocalcin (OCN), and osteopontin (OPN). This ultimately enhances OB differentiation significantly. Estrogen cannot directly act on OBs, but it can coordinate with LiCl to stimulate Fhl1 expression and promote OB differentiation (55).

3.4 MicroRNA

MicroRNA (miRNA) is a type of non-coding single-stranded RNA that plays a crucial role in the regulation of post-transcriptional gene expression and is essential for mammal bone development (56). Overexpression of miR-373 can promote the differentiation of BMSCs into OBs and reverse the decreased osteogenic differentiation ability of BMSCs caused by osteoporosis. Estrogen deficiency causes decreased miR-373 expression (57), significant enrichment of the miR-338 cluster (58), and elevated expression of miR-143/145 (59), leading to a decreased differentiation of BMSCs into OBs. Furthermore, estrogen can decrease the expression of miR-532-3p through up-regulation of long noncoding RNA H19 (lncRNA H19). LncRNA H19-mediated disruption of the miR-532-3p/SIRT1 axis has been shown to induce osteogenic differentiation of BMSCs which alleviated osteoporosis in OVX rats (60). However, osteogenic differentiation induced by this pathway is reduced if estrogen is deficient *in vivo*. Estrogen up-regulates miR-27a, which inhibits peroxisome proliferator-activated receptor gamma (PPARγ) in OCs and adenomatous polyposis coli (APC) expression, resulting in decreased OC production and reduced bone resorption (61). The estrogen-activated ERα pathway inhibits the production of miR-21 (62), which enhances Fasl protein to stimulate caspase-3 activity and induces the Fas/FasL system to regulate the lifespan of mature OCs (63), thereby inducing OC apoptosis. However, studies have also shown that estrogen deficiency-related decreased expression of miR-128 can lead to decreased OC production (64), thereby delaying or preventing the occurrence of osteoporosis. Overall, estrogen can inhibit the activity of OCs, reduce bone resorption, promote OB formation, and enhance bone formation by interacting with various miRNAs in OBs and OCs. Further research is required to uncover the

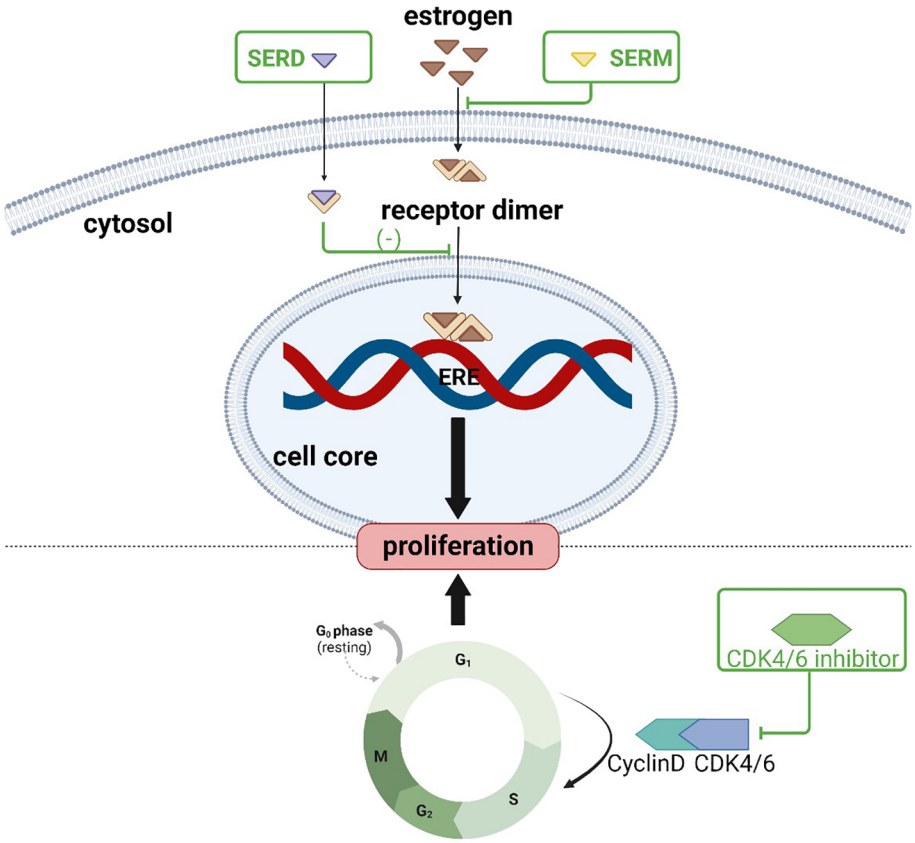

FIGURE 2
Action sites of anti-estrogen and CDK4/6 inhibitors: SERM and SERD bind to estrogen receptors, inhibiting downstream pathways and preventing tumor cell proliferation; CDK4/6 inhibitors prevent dividing tumor cells from the G1 phase into the S phase.

regulatory pathways of estrogen and miRNAs on bone remodeling in various bone cell types.

In addition, estrogen directly affects calcium absorption in the gut, and calcium plays an important role in bones (65). Therefore, low estrogen levels can lead to insufficient calcium intake in the body, which is a primary cause of osteoporosis.

These targets and pathways associated with osteoporosis are also present in other organs and tissues. Therefore, the design of drugs for the treatment of osteoporosis for these targets should also consider the side effects on organs and tissues. Specific targets of bone metabolism are necessary to explore for better treatment of bone-related diseases.

4 Strategies to prevent or treat osteoporosis caused by endocrine therapy for breast cancer

Although osteoporosis cannot be cured, it can be prevented, slowed down, or stopped through various means, including increasing bone formation and inhibiting bone resorption. Biochemical markers of bone turnover can indicate the events that occur during the bone remodeling cycle and are divided into bone formation and bone resorption markers (66). Clinical practices currently use serum osteocalcin, serum bone alkaline phosphatase (BAP), urinary N-terminal peptide of type 1 collagen (NTx), and urinary C-terminal peptide of type 1 collagen (CTx) to monitor bone turnover. Various guidelines (67–69) have recommended reducing the risk of fragility fractures through screening, life interventions, and pharmacological treatment as a primary goal of osteoporosis prevention and treatment. For breast cancer patients on endocrine medications, especially aromatase inhibitors, regular monitoring of BMD is paramount. Appropriate medications should be used to prevent the development of osteoporosis, and the patients who have been diagnosed with osteoporosis require medications to stop continued bone loss and prevent fractures. Anti-resorptive agents and anabolic agents are common medications used to prevent and treat osteoporosis (Table 3). Importantly, osteoporosis associated with breast cancer endocrine therapy differs from conventional osteoporosis management due to the need to balance the outcome and course of the cancer treatment. However, due to limited information on osteoporosis management in cancer patients, current clinical strategies for endocrine treatment-related osteoporosis in breast cancer reference normal osteoporosis (75).

4.1 Lifestyle intervention

In order to prevent or treat osteoporosis, breast cancer patients should quit using tobacco products and alcohol (76), take adequate

10.3389/fonc.2023.1218206

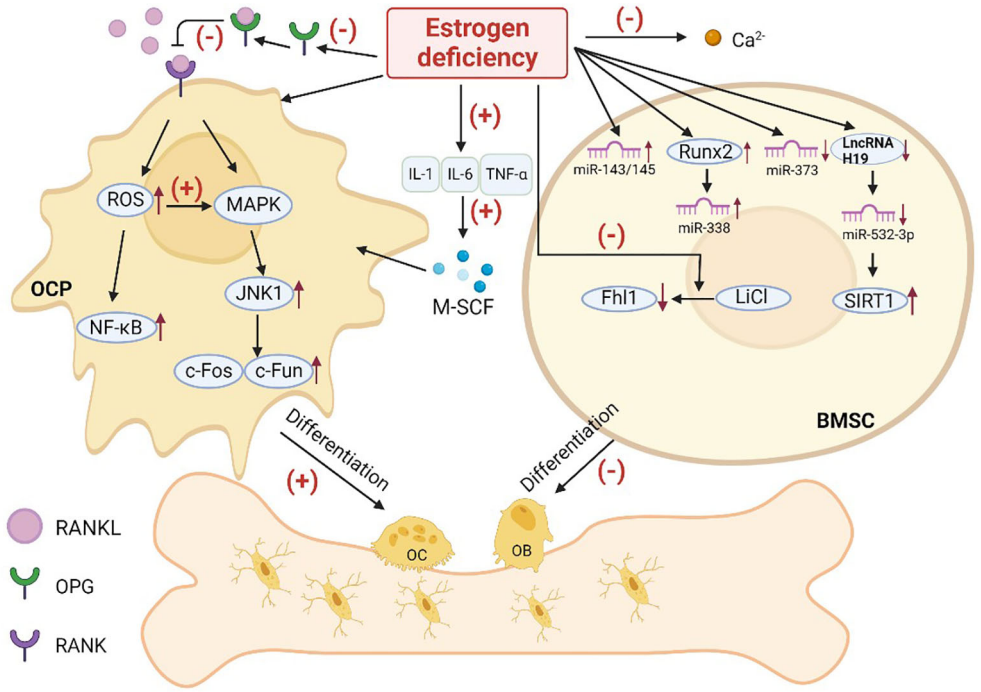

FIGURE 3
Possible pathways of osteoporosis caused by estrogen deficiency. (OC, osteoblast; OB, osteoblast; OCP, osteoclast precursor; BMSC, bone marrow mesenchymal stem cell; OPG, osteoprotegerin; RANKL, receptor activator of NF-κB ligand; RANK, receptor activator of NF-κB; IL-1, interleukin-1; IL-6, interleukin-6; TNF-α, tumor necrosis factor-α; M-SCF:; ROS, reactive oxygen species).

TABLE 3 Osteoporosis treatment drugs and targets.

Type	Category	Drug	Target spot
Antiresorptive agent	Bisphosphonates	Alendronate Ibandranate Risedronate Zoledronate	hydroxyapatite
	RANKL inhibitor	Denosumab	RANKL
	Calcitonin	Calcitonin	OB
	Hormone	Estrogen	ER
	SERMs	Raloxifene	ER
	Tissue-specific estrogen complex	Bazedoxifene	ER
Anabolic agent	Sclerostin inhibitor	Romosozumab-aqqg	Sclerostin
	Parathyroid hormone analogs	Teriparatide	OC
	Parathyroid hormone-associated protein analogues	Abaloparatide	OC
Potential drug	Active substance	Sirt3 inhibitor (70)	Sirt3
	Natural compound	Isosinensetin (71)	ROS
		Obacunone (44)	MIF
	Active ingredients of traditional Chinese medicine	Boldine (72)	ATF pathway
		Icariside I (73)	OC, OB
		Corylifol A (74)	ROS

calcium and vitamin D supplements (77), and exercise moderately. It may also be beneficial for patients to consume appropriate antioxidant functional foods. For example, one study reported that green tea consumption and exercise were negatively associated with osteoporosis (78). Additional studies have found that tea consumption reduces the risk of osteoporosis (79), and that weight-bearing and resistance exercise maintains BMD and improves the quality of life in postmenopausal women with low bone mass (80). However, there was not a strong BMD improvement in breast cancer patients.

4.2 Antiresorptive agent

Antiresorptive agents, including bisphosphonates, RANKL inhibitors, estrogens and SERMs, are the preferred drugs for the treatment of osteoporosis (81). Table 4 provides a list of clinical trials that have evaluated the use of antiresorptive agents. A recently published real-world study showed that early postmenopausal women with ER-positive breast cancer who were treated with aromatase inhibitors in combination with anti-bone resorptive therapy experienced a significant increase in both femur and lumbar BMD after 24 months (6.28%, 7.79%, respectively) (85). Anti-bone resorption therapy can significantly improve BMD in postmenopausal women with early breast cancer who are using aromatase inhibitors, thereby preventing bone loss. One study found that the combination of letrozole and zoledronic acid inhibited the growth of and induced apoptosis in MCF-7 and T-47D human breast cancer cell lines (86). As a bisphosphate, zoledronic acid can be used in the treatment and prevention of osteoporosis, though the clinical effect of the combined use of letrozole and zoledronic acid requires additional studies. A 24-month randomized controlled trial showed increased BMD and decreased bone resorption in total hip joint (+1.81%) and spine segments 1 to 4 (+2.85%) in subjects taking risedronate, calcium, and vitamin D without exercise (87). This indicates that bisphosphonates, calcium, and vitamin D are effective treatments for bone loss in postmenopausal breast cancer patients with hip and spine bone loss. However, oral bisphosphonates can have side effects that may cause patients to discontinue the drug midway through its use. For example, bisphosphates can cause irritation to the mucosa of the gastrointestinal tract, leading to esophagitis, dysphagia, and gastric ulcers (75). Additionally, some patients have experienced hypocalcemia (88). One study reported that approximately 20% of patients who received intravenous zoledronic acid experienced side effects including flu-like syndrome (69%), arthralgia (7.7%), and even renal failure (89).

Denosumab specifically targets RANKL, inhibits OC activation and progression caused by related pathways, reduces bone resorption, and increases BMD in the treatment of postmenopausal women with osteoporosis. The use of denosumab has been reported to increase BMD in the lumbar spine, hip, and femoral neck in breast cancer patients treated with aromatase inhibitors (90). Results from a randomized controlled trial exhibited that subcutaneous administration of denosumab every 6 months significantly reduced clinical fracture rates and significantly delayed time to first fracture in postmenopausal patients with hormone receptor-positive early-stage breast cancer treated with adjuvant aromatase inhibitors (91). However, denosumab does not specifically target bone (92), therefore it inhibits the RANKL pathway in other tissues. Its common side effects include hypocalcemia (93), nasopharyngitis, upper respiratory tract infections, urinary tract infections, arthralgia, headache, constipation, and skin rash (75).

Raloxifene, a selective hormone receptor modulator (SERM), is widely used for the prevention and treatment of postmenopausal osteoporosis (94). Results of a randomized clinical trial showed that 3 years of raloxifene treatment maintained BMD and reduced bone turnover. Moreover, raloxifene increased BMD in the spine and femoral neck and reduced the risk of vertebral fractures in postmenopausal women with osteoporosis (95). An animal trial also demonstrated that the osteoporosis drug lasoxifene has the potential to treat ER-positive patients who are resistant to aromatase inhibitors (96).

Hormone therapy is not a feasible treatment option for osteoporosis associated with endocrine therapy in breast cancer patients, as estrogen can promote the progression of breast tumors and affect the treatment of breast cancer.

TABLE 4 Clinical trials and efficacy of antiresorptive agents.

Trail(Ref)	Period	Enrolled patients	Design	BMD change		
				Total hip	Lumbar spine	Femoral neck
NCT02616744 (82)	2 years	171	Placebo 150mg monthly	-0.19 (-10.8%)	-0.09(-5.1%)	
			Ibandranate 150g monthly	+0.09 (+5.3%)	+0.28(+16.6%)	
Prospective randomized observational study (83)	24 months	84	Anastrozole		-4.8%	-3.5%
			Anastrozole plus risedronate		+6.86%	+2.8%
NCT00485953 (84)	24 months	109	Oral risedronate 35 mg once weekly	+0.6	+2.3	+0.4
			Oral placebo 35 mg once weekly	-2.7	-1.7	-2.1

4.3 Anabolic agent

Antiresorptive agents do not restore the bone mass and structure that is lost due to increased bone remodeling. On the other hand, anabolic agents increase the likelihood of new bone formation (97). In a randomized controlled trial, the most commonly used parathyroid hormone analog, Teriparatide, was found to be associated with a lower risk of new vertebral fractures (5.4%) at 24 months of use compared to risedronate (12.0%) in postmenopausal women with severe osteoporosis (98). However, some scientists argue that comparison between these two drugs is not clinically significant as they are administered in different ways (99). A recent meta-analysis revealed that teriparatide was linked to a reduced risk of vertebral fracture compared to bisphosphonate (RR= 0.57, 95% CI: 0.35-0.93, P = 0.024), and that the drug increased the mean percentage change in femoral neck BMD at 18 months ($P < 0.05$) (89). In conclusion, teriparatide is an effective drug for reducing the risk of vertebral fractures in postmenopausal women with osteoporosis, and it can increase the BMD of lumbar spine and femoral neck in the long term.

4.4 Potential drug development

Research on the mechanisms of osteoporosis caused by estrogen deficiency *in vivo* may lead to new breakthroughs in the development of osteoporosis drugs. Studies have shown that Connexin 43 half-channels (Cx43 HCs) demonstrate protective effects on bone cells and can inhibit bone loss in estrogen-deficient mice following ovariectomy (100). Another promising avenue of research is the mitochondrial protein deacetylase, Sirtuin-3 (Sirt3), which has a high mitochondrial content in OCs. Inhibition of this enzyme can damage mitochondria-related functions in OCs and reverse the increased bone resorption and bone mass loss caused by estrogen deficiency (70). Sirt3 inhibitors are promising for osteopenia caused by endocrine therapy in breast cancer.

Scientists are also investigating natural compounds and active ingredients in traditional Chinese medicine as potential drugs to treat osteoporosis. For instance, isosinensetin, a flavonoid present in citrus fruits with antioxidant properties, has been shown to reduce bone loss in OVX mice and alleviate estrogen deficiency-induced osteoporosis in mice (71). Obacunone, a small molecule with a wide range of biological activities, can inhibit the formation and absorption function of OCs *in vitro* by targeting inhibitory factor of macrophage migration inhibitory factor (MIF) (44). Thus, it is expected to be an effective drug for relieving osteoporosis caused by estrogen deficiency. Traditional Chinese medicine also shows promise in treating osteoporosis by invigorating the kidneys and spleen. One animal study showed that Bushen Jianpi Decoction improved bone loss without affecting estrogen levels in mice and may increase the sensitivity of breast tumor cells to endocrine drugs, thereby improving efficacy (101). Boldine, an alkaloid isolated from the Bordeaux tree, has a protective effect against bone loss in mice caused by estrogen deficiency (72) by inhibiting OC formation induced by activator of nuclear factor κB ligand receptor by impacting the AKT signaling pathway. Icariside I (GH01), a novel isopentenyl flavonoid isolated from epimedii, was shown to effectively ameliorate estrogen deficiency-induced osteoporosis and strengthen the trabecular and cortical bone in OVX mouse models by simultaneously regulating OB and OC differentiation (73). Eucommia ulmoides and psoralea were commonly used drugs (102). Corylifol A, an isoflavone isolated from psoralea fruit, inhibits OCs and absorption by inhibiting intracellular ROS levels to prevent bone loss caused by estrogen deficiency (74). Psoralen extracted from psoralen seed has been studied for its in anti-tumor effects, but it has also been shown to impact certain pathways that may result in anti-osteoporosis effects (103). Acid polysaccharide EuOCP3 extracted from Eucommia ulmoides skin can restore cortical bone thickness, increase mineralized bone area, increase the number of OBs, and reduce the number of OCs on the cortical bone surface in osteoporotic mice (104). The total flavones of Radix osteoblastum are widely used in the treatment of postmenopausal osteoporosis (105) are expected to emerge as a new treatment for breast cancer-related osteoporosis. There are also many effective Chinese medicine ingredients for osteoporosis, such as resveratrol, puerarin, astragaloside IV, and Danshensu (106).

5 Summery and prospects

Endocrine therapy for breast cancer can lead to osteoporosis, particularly in postmenopausal women who use aromatase inhibitors, which impacts patient quality of life. There are limited data on the management and prevention of cancer-related osteoporosis, with no drugs specifically targeted for these patients. More clinical studies are needed to provide more effective and safe treatment options. Traditional Chinese medicine has great potential in the prevention and treatment of osteoporosis caused by endocrine therapy in breast cancer. As the acquired and intrinsic resistance mechanisms of endocrine therapy drug and CDK4/6 inhibitors is gradually revealed, there is a need to develop novel endocrine drugs with higher efficacy and fewer side effects for breast cancer patients (107). Blood vessels and lymphatic vessels are important components of bone. Some studies have shown that the vascular system plays an important role in the process of bone metastasis (108). It is necessary to explore their relationship with osteoporosis to provide new treatment strategies. An animal study showed that Substance P(SP), an endogenous neuropeptide, blocked H-type vascular loss and sustained angiogenic factor enrichment in pretreated OVX mice. SP can mediate early vascular protection and inhibit bone density loss (109). The relationship between bone lymphatics and osteoporosis remains to be further explored. Additionally, the pathogenesis of breast cancer is not yet fully understood, and there is a need for more effective therapeutic drugs to reduce the occurrence of adverse reactions related to endocrine therapy.

Author contributions

JX collected the related paper, drafted, and revised the manuscript. BC participated in the design of the review, and helped to draft and revise the manuscript. CL and GL designed the review. All authors contributed to the article and approved the submitted version.

Funding

This work has been financially supported by CAMS Innovation Fund for Medical Sciences (CIFMS) (Grant no. 2021-I2M-1-014).

Conflict of interest

The authors declare that the research was conducted in the absence of any commercial or financial relationships that could be construed as a potential conflict of interest.

Publisher's note

References

1. Sung H, Ferlay J, Siegel RL, Laversanne M, Soerjomataram I, Jemal A, et al. Global cancer statistics 2020: GLOBOCAN estimates of incidence and mortality worldwide for 36 cancers in 185 countries. *CA: A Cancer J Clin* (2021) 71(3):209–49. doi: 10.3322/caac.21660

2. Giaquinto AN, Sung H, Miller KD, Kramer JL, Newman LA, Minihan A, et al. Breast cancer statistics, 2022. *CA: A Cancer J Clin* (2022) 72(6):524–41. doi: 10.3322/caac.21754

3. National Health Commission of the People's Republic of China. Guidelines for the diagnosis and treatment of breast cancer (2022 edition). *Chinese Journal of rational drug use* (2022) 19(10):1–26.

4. Hadji P, Kieback DG, Tams J, Hasenburg A, Ziller M. Correlation of treatment-emergent adverse events and clinical response to endocrine therapy in early breast cancer: a retrospective analysis of the German cohort of TEAM. *Ann Oncol* (2012) 23 (10):2566–72. doi: 10.1093/annonc/mds055

5. Lahti E, Blanco G, Kauppila A, Apaja-Sarkkinen M, Taskinen PJ, Laatikainen T. Endometrial changes in postmenopausal breast cancer patients receiving tamoxifen. *Obstet Gynecol* (1993) 81(5(5 (Pt 1):660–4.

6. Levin VA, Jiang X, Kagan R. Estrogen therapy for osteoporosis in the modern era. *Osteoporosis Int* (2018) 29(5):1049–55. doi: 10.1007/s00198-018-4414-z

7. Deroo BJ, Korach KS. Estrogen receptors and human disease. *J Clin Invest* (2006) 116(3):561–70. doi: 10.1172/JCI27987

8. Collaborative Group on Hormonal Factors in Breast C. Alcohol, tobacco and breast cancer – collaborative reanalysis of individual data from 53 epidemiological studies, including 58 515 women with breast cancer and 95 067 women without the disease. *Br J Cancer* (2002) 87(11):1234–45. doi: 10.1038/sj.bjc.6600596

9. Jung S, Wang M, Anderson K, Baglietto L, Bergkvist L, Bernstein L, et al. Alcohol consumption and breast cancer risk by estrogen receptor status: in a pooled analysis of 20 studies. *Int J Epidemiol* (2015) 45(3):916–28. doi: 10.1093/ije/dyv156

10. Salari N, Darvishi N, Bartina Y, Larti M, Kiaei A, Hemmati M, et al. Global prevalence of osteoporosis among the world older adults: a comprehensive systematic review and meta-analysis. *J Orthopaedic Surg Res* (2021) 16(1):669. doi: 10.1186/s13018-021-02821-8

11. Zeng Q, Li N, Wang Q, Feng J, Sun D, Zhang Q, et al. The prevalence of osteoporosis in China, a nationwide, multicenter DXA survey. *J Bone Mineral Res* (2019) 34(10):1789–97. doi: 10.1002/jbmr.3757

12. Marshall D, Johnell O, Wedel H. Meta-analysis of how well measures of bone mineral density predict occurrence of osteoporotic fractures. *BMJ* (1996) 312 (7041):1254–9. doi: 10.1136/bmj.312.7041.1254

13. Hayes DF, Rae JM. Pharmacogenomics and endocrine therapy in breast cancer. *J Clin Oncol* (2020) 38(6):525–8. doi: 10.1200/JCO.19.03119

14. Lee J, Alqudaihi HM, Kang MS, Kim J, Lee JW, Ko BS, et al. Effect of tamoxifen on the risk of osteoporosis and osteoporotic fracture in younger breast cancer survivors: a nationwide study. *Front Oncol* (2020) 10. doi: 10.3389/fonc.2020.00366

15. Blanchette PS, Lam M, Le B, Richard L, Shariff SZ, Ouédraogo AM, et al. The association between endocrine therapy use and osteoporotic fracture among post-menopausal women treated for early-stage breast cancer in Ontario, Canada. *Breast* (2021) 60:295–301. doi: 10.1016/j.breast.2021.09.010

16. Hamood R, Hamood H, Merhasin I, Keinan-Boker L. Hormone therapy and osteoporosis in breast cancer survivors: assessment of risk and adherence to screening recommendations. *Osteoporosis Int* (2019) 30(1):187–200. doi: 10.1007/s00198-018-4758-4

17. De Placido S, Gallo C, De Laurentiis M, Bisagni G, Arpino G, Sarobba MG, et al. Adjuvant anastrozole versus exemestane versus letrozole, upfront or after 2 years of tamoxifen, in endocrine-sensitive breast cancer (FATA-GIM3): a randomised, phase 3 trial. *Lancet Oncol* (2018) 19(4):474–85. doi: 10.1016/S1470-2045(18)30116-5

18. van Hellemond IEG, Smorenburg CH, Peer PGM, Swinkels ACP, Seynaeve CM, van der Sangen MJC, et al. Assessment and management of bone health in women with early breast cancer receiving endocrine treatment in the DATA study. *Int J Cancer* (2019) 145(5):1325–33. doi: 10.1002/ijc.32205

19. Goss PE, Ingle JN, Pritchard KI, Ellis MJ, Sledge GW, Budd GT, et al. Exemestane versus anastrozole in postmenopausal women with early breast cancer: NCIC CTG MA.27–a randomized controlled phase III trial. *J Clin Oncol* (2013) 31 (11):1398–404. doi: 10.1200/jco.2012.44.7805

20. Lee Y-K, Lee E-G, Kim HY, Lee Y, Lee S-M, Suh D-C, et al. Osteoporotic fractures of the spine, hip, and other locations after adjuvant endocrine therapy with aromatase inhibitors in breast cancer patients: a meta-analysis. *J Korean Med Sci* (2020) 35(46):e403. doi: 10.3346/jkms.2020.35.e403

21. Chen S, Lan B, Lv D, Ma F. Bone safety profile of steroidal aromatase inhibitor in comparison to non-steroidal aromatase inhibitors in postmenopausal women with breast cancer: a network meta-analysis. *J Clin Oncol* (2021) 39(15_suppl):527–. doi: 10.1200/JCO.2021.39.15_suppl.527

22. Eastell R, Hannon RA, Cuzick J, Dowsett M, Clack G, Adams JE. Effect of an aromatase inhibitor on BMD and bone turnover markers: 2-year results of the anastrozole, tamoxifen, alone or in combination (ATAC) trial (18233230). *J Bone Mineral Res* (2006) 21(8):1215–23. doi: 10.1359/jbmr.060508

23. Confavreux CB, Fontana A, Guastalla JP, Munoz F, Brun J, Delmas PD. Estrogen-dependent increase in bone turnover and bone loss in postmenopausal women with breast cancer treated with anastrozole. *Prev bisphosphonates Bone* (2007) 41(3):346–52. doi: 10.1016/j.bone.2007.06.004

24. Sestak I, Blake G, Patel R, Cuzick J, Howell A, Coleman R, et al. Off-treatment bone mineral density changes in postmenopausal women receiving anastrozole for 5 years: 7-year results from the IBIS-II prevention trial. *Br J Cancer* (2021) 124(8):1373–8. doi: 10.1038/s41416-020-01228-2

25. Hadji P, Ziller M, Kieback DG, Dornoff W, Tessen HW, Menschik T, et al. Effects of exemestane and tamoxifen on bone health within the tamoxifen exemestane adjuvant multicentre (TEAM) trial: results of a German, 12-month, prospective, randomised substudy. *Ann Oncol* (2009) 20(7):1203–9. doi: 10.1093/annonc/mdn762

26. Jonat W. Role of LHRH agonists in premenopausal women with oestrogen receptor-positive breast cancer: the ZEBRA experience. *Eur J Cancer* (2002) 38:39–40. doi: 10.1016/S0959-8049(02)00280-0

27. Saha T, Makar S, Swetha R, Gutti G, Singh SK. Estrogen signaling: an emanating therapeutic target for breast cancer treatment. *Eur J Medicinal Chem* (2019) 177:116–43. doi: 10.1016/j.ejmech.2019.05.023

28. Hewitt SC, Couse JF, Korach KS. Estrogen receptor transcription and transactivation estrogen receptor knockout mice: what their phenotypes reveal about mechanisms of estrogen action. *Breast Cancer Res* (2000) 2(5):345. doi: 10.1186/bcr79

29. Waks AG, Winer EP. Breast cancer treatment. *JAMA* (2019) 321(3):316–. doi: 10.1001/jama.2018.20751

30. Brisken C. Progesterone signalling in breast cancer: a neglected hormone coming into the limelight. *Nat Rev Cancer* (2013) 13(6):385–96. doi: 10.1038/nrc3518

31. Ward AV, Matthews SB, Fettig LM, Riley D, Finlay-Schultz J, Paul KV, et al. Estrogens and progestins cooperatively shift breast cancer cell metabolism. *Cancers* (2022) 14(7):1776. doi: 10.3390/cancers14071776

32. Investigators WGftWsHI. Risks and benefits of estrogen plus progestin in healthy postmenopausal WomenPrincipal results from the women's health initiative randomized controlled trial. *JAMA* (2002) 288(3):321–33. doi: 10.1001/jama.288.3.321

33. Chlebowski RT, Anderson GL, Gass M, Lane DS, Aragaki AK, Kuller LH, et al. Estrogen plus progestin and breast cancer incidence and mortality in postmenopausal women. *JAMA* (2010) 304(15):1684–92. doi: 10.1001/jama.2010.1500

34. Trabert B, Bauer DC, Buist DSM, Cauley JA, Falk RT, Geczik AM, et al. Association of circulating progesterone with breast cancer risk among postmenopausal women. *JAMA Network Open* (2020) 3(4):e203645–e. doi: 10.1001/jamanetworkopen.2020.3645

35. Mohammed H, Russell IA, Stark R, Rueda OM, Hickey TE, Tarulli GA, et al. Progesterone receptor modulates ERα action in breast cancer. *Nature* (2015) 523 (7560):313–7. doi: 10.1038/nature14583

36. Finlay-Schultz J, Gillen AE, Brechbuhl HM, Ivie JJ, Matthews SB, Jacobsen BM, et al. Breast cancer suppression by progesterone receptors is mediated by their modulation of estrogen receptors and RNA polymerase III. *Cancer Res* (2017) 77 (18):4934–46. doi: 10.1158/0008-5472.CAN-16-3541

37. Tan S, Bajalovic N, Wong ESP, Lin VCL. Ligand-activated progesterone receptor b activates transcription factor EB to promote autophagy in human breast cancer cells. *Exp Cell Res* (2019) 382(1):111433. doi: 10.1016/j.yexcr.2019.05.014

38. Goodman ML, Trinca GM, Walter KR, Papachristou EK, D'Santos CS, Li T, et al. Progesterone receptor attenuates STAT1-mediated IFN signaling in breast cancer. *J Immunol* (2019) 202(10):3076–86. doi: 10.4049/jimmunol.1801152

39. Gonzalez-Suarez E, Jacob AP, Jones J, Miller R, Roudier-Meyer MP, Erwert R, et al. RANK ligand mediates progestin-induced mammary epithelial proliferation and carcinogenesis. *Nature* (2010) 468(7320):103–7. doi: 10.1038/nature09495

40. Castañeda S, Casas A, González-del-Alba A, Martínez-Díaz-Guerra G, Nogués X, Ojeda Thies C, et al. Bone loss induced by cancer treatments in breast and prostate cancer patients. *Clin Trans Oncol* (2022) 24(11):2090–106. doi: 10.1007/s12094-022-02872-1

41. Sunyer T, Lewis J, Collin-Osdoby P, Osdoby P. Estrogen's bone-protective effects may involve differential IL-1 receptor regulation in human osteoclast-like cells. *J Clin Invest* (1999) 103(10):1409–18. doi: 10.1172/JCI4682

42. Kimble RB, Srivastava S, Ross FP, Matayoshi A, Pacifici R. Estrogen deficiency increases the ability of stromal cells to support murine osteoclastogenesis *via* an interleukin-1and tumor necrosis factor-mediated stimulation of macrophage colony-stimulating factor production*. *J Biol Chem* (1996) 271(46):28890–7. doi: 10.1074/jbc.271.46.28890

43. Poli V, Balena R, Fattori E, Markatos A, Yamamoto M, Tanaka H, et al. Interleukin-6 deficient mice are protected from bone loss caused by estrogen depletion. *EMBO J* (1994) 13(5):1189–96. doi: 10.1002/j.1460-2075.1994.tb06368.x

44. He J, Zheng L, Li X, Huang F, Hu S, Chen L, et al. Obacunone targets macrophage migration inhibitory factor (MIF) to impede osteoclastogenesis and alleviate ovariectomy-induced bone loss. *J Advanced Res* (2023) 1-14. doi: 10.1016/j.jare.2023.01.003

45. Cong Q, Jia H, Biswas S, Li P, Qiu S, Deng Q, et al. p38α MAPK regulates lineage commitment and OPG synthesis of bone marrow stromal cells to prevent bone loss under physiological and pathological conditions. *Stem Cell Rep* (2016) 6(4):566–78. doi: 10.1016/j.stemcr.2016.02.001

46. Hofbauer LC, Khosla S, Dunstan CR, Lacey DL, Spelsberg TC, Riggs BL. Estrogen stimulates gene expression and protein production of osteoprotegerin in human osteoblastic cells*. *Endocrinology* (1999) 140(9):4367–70. doi: 10.1210/endo.140.9.7131

47. Hong G, Chen Z, Han X, Zhou L, Pang F, Wu R, et al. A novel RANKL-targeted flavonoid glycoside prevents osteoporosis through inhibiting NFATc1 and reactive oxygen species. *Clin Trans Med* (2021) 11(5):e392. doi: 10.1002/ctm2.392

48. Agidigbi TS, Kim C. Reactive oxygen species in osteoclast differentiation and possible pharmaceutical targets of ROS-mediated osteoclast diseases. *Int J Mol Sci* (2019) 20(14):3576. doi: 10.3390/ijms20143576

49. Ding W, Zhou Q, Lu Y, Wei Q, Tang H, Zhang D, et al. ROS-scavenging hydrogel as protective carrier to regulate stem cells activity and promote osteointegration of 3D printed porous titanium prosthesis in osteoporosis. *Front Bioeng Biotechnol* (2023) 11:1103611. doi: 10.3389/fbioe.2023.1103611

50. Streicher C, Heyny A, Andrukhova O, Haigl B, Slavic S, Schüler C, et al. Estrogen regulates bone turnover by targeting RANKL expression in bone lining cells. *Sci Rep* (2017) 7(1):6460. doi: 10.1038/s41598-017-06614-0

51. Srivastava S, Toraldo G, Weitzmann MN, Cenci S, Ross FP, Pacifici R. Estrogen decreases osteoclast formation by down-regulating receptor activator of NF-κB ligand (RANKL)-induced JNK activation*. *J Biol Chem* (2001) 276(12):8836–40. doi: 10.1074/jbc.M010764200

52. Song T, Lin T, Ma J, Guo L, Zhang L, Zhou X, et al. Regulation of TRPV5 transcription and expression by E2/ERα signalling contributes to inhibition of osteoclastogenesis. *J Cell Mol Med* (2018) 22(10):4738–50. doi: 10.1111/jcmm.13718

53. Chen F, OuYang Y, Ye T, Ni B, Chen A. Estrogen inhibits RANKL-induced osteoclastic differentiation by increasing the expression of TRPV5 channel. *J Cell Biochem* (2014) 115(4):651–8. doi: 10.1002/jcb.24700

54. Song S, Guo Y, Yang Y, Fu D. Advances in pathogenesis and therapeutic strategies for osteoporosis. *Pharmacol Ther* (2022) 237:108168. doi: 10.1016/j.pharmthera.2022.108168

55. Wu S-M, Shih L-H, Lee J-Y, Shen Y-J, Lee H-H. Estrogen enhances activity of wnt signaling during osteogenesis by inducing Fhl1 expression. *J Cell Biochem* (2015) 116(7):1419–30. doi: 10.1002/jcb.25102

56. Ji X, Chen X, Yu X. MicroRNAs in osteoclastogenesis and function: potential therapeutic targets for osteoporosis. *Int J Mol Sci* (2016) 17(3):349. doi: 10.3390/ijms17030349

57. Li X-LW L-Y, Wang G-S, Zhao H-Y. MiR-373 promotes the osteogenic differentiation of BMSCs from the estrogen deficiency induced osteoporosis. *Eur Rev Med Pharmacol Sci* (2019) 23 - N. 17:7247–55. doi: 10.26355/eurrev_201909_18827

58. Lin C, Yu S, Jin R, Xiao Y, Pan M, Pei F, et al. Circulating miR-338 cluster activities on osteoblast differentiation: potential diagnostic and therapeutic targets for postmenopausal osteoporosis. *Theranostics* (2019) 9(13):3780–97. doi: 10.7150/thno.34493

59. Xu R, Shen X, Xie H, Zhang H, Liu D, Chen X, et al. Identification of the canonical and noncanonical role of miR-143/145 in estrogen-deficient bone loss. *Theranostics* (2021) 11(11):5491–510. doi: 10.7150/thno.55041

60. Li T, Jiang H, Li Y, Zhao X, Ding H. Estrogen promotes lncRNA H19 expression to regulate osteogenic differentiation of BMSCs and reduce osteoporosis *via* miR-532-3p/SIRT1 axis. *Mol Cell Endocrinol* (2021) 527:111171. doi: 10.1016/j.mce.2021.111171

61. Guo L, Chen K, Yuan J, Huang P, Xu X, Li C, et al. Estrogen inhibits osteoclasts formation and bone resorption *via* microRNA-27a targeting PPARγ and APC. *J Cell Physiol* (2019) 234(1):581–94. doi: 10.1002/jcp.26788

62. Sugatani T, Hruska KA. Down-regulation of miR-21 biogenesis by estrogen action contributes to osteoclastic apoptosis. *J Cell Biochem* (2013) 114(6):1217–22. doi: 10.1002/jcb.24471

63. Nakamura T, Imai Y, Matsumoto T, Sato S, Takeuchi K, Igarashi K, et al. Estrogen prevents bone loss *via* estrogen receptor α and induction of fas ligand in osteoclasts. *Cell* (2007) 130(5):811–23. doi: 10.1016/j.cell.2007.07.025

64. Shen G, Ren H, Shang Q, Zhang Z, Zhao W, Yu X, et al. miR-128 plays a critical role in murine osteoclastogenesis and estrogen deficiency-induced bone loss. *Theranostics* (2020) 10(10):4334–48. doi: 10.7150/thno.42982

65. Nie X, Jin H, Wen G, Xu J, An J, Liu X, et al. Estrogen regulates duodenal calcium absorption through differential role of estrogen receptor on calcium transport proteins. *Digestive Dis Sci* (2020) 65(12):3502–13. doi: 10.1007/s10620-020-06076-x

66. Hart SM, Eastell R. Biochemical markers of bone turnover. *Curr Opin Nephrol Hypertension* (1999) 8(4):421–7. doi: 10.1097/00041552-199907000-00005

67. Gregson CL, Armstrong DJ, Bowden J, Cooper C, Edwards J, Gittoes NJL, et al. UK Clinical guideline for the prevention and treatment of osteoporosis. *Arch Osteoporosis* (2022) 17(1):58. doi: 10.1007/s11657-022-01061-5

68. LeBoff MS, Greenspan SL, Insogna KL, Lewiecki EM, Saag KG, Singer AJ, et al. The clinician's guide to prevention and treatment of osteoporosis. *Osteoporosis Int* (2022) 33(10):2049–102. doi: 10.1007/s00198-021-05900-y

69. Belaya Z, Rozhinskaya L, Dedov I, Drapkina O, Fadeev V, Golounina O, et al. A summary of the Russian clinical guidelines on the diagnosis and treatment of osteoporosis. *Osteoporosis Int* (2023). 34, 429–447. doi: 10.1007/s00198-022-06667-6

70. Ling W, Krager K, Richardson KK, Warren AD, Ponte F, Aykin-Burns N, et al. Mitochondrial Sirt3 contributes to the bone loss caused by aging or estrogen deficiency. *JCI Insight* (2021) 6(10):e146728. doi: 10.1172/jci.insight.146728

71. Qin Y, Song D, Liao S, Chen J, Xu M, Su Y, et al. Isosinensetin alleviates estrogen deficiency-induced osteoporosis *via* suppressing ROS-mediated NF-κB/MAPK signaling pathways. *Biomedicine Pharmacother* (2023) 160:114347. doi: 10.1016/j.biopha.2023.114347

72. Chen K, Z-t Lv, Cheng P, Zhu W-t, Liang S, Yang Q, et al. Boldine ameliorates estrogen deficiency-induced bone loss *via* inhibiting bone resorption. *Front Pharmacol* (2018) 9. doi: 10.3389/fphar.2018.01046

73. Chen C, Wu M, Lei H, Cao Z, Wu F, Song Y, et al. A novel prenylflavonoid icariside I ameliorates estrogen deficiency-induced osteoporosis *via* simultaneous regulation of osteoblast and osteoclast differentiation. *ACS Pharmacol Trans Sci* (2023) 6(2):270–80. doi: 10.1021/acsptsci.2c00192

74. Xu Y, Song D, Lin X, Peng H, Su Y, Liang J, et al. Corylifol a protects against ovariectomized-induced bone loss and attenuates RANKL-induced osteoclastogenesis *via* ROS reduction, ERK inhibition, and NFATc1 activation. *Free Radical Biol Med* (2023) 196:121–32. doi: 10.1016/j.freeradbiomed.2023.01.017

75. Khan MI. Management of bone loss due to endocrine therapy during cancer treatment. *Osteoporosis Int* (2023) 34, 671-680, doi: 10.1007/s00198-023-06672-3

76. Shapiro CL, Poznak CV, Lacchetti C, Kirshner J, Eastell R, Gagel R, et al. Management of osteoporosis in survivors of adult cancers with nonmetastatic disease: ASCO clinical practice guideline. *J Clin Oncol* (2019) 37(31):2916–46. doi: 10.1200/JCO.19.01696

77. Antonini M, Salerno GR, Vieira ND, Cardoso MS, Solino M, Vasconcelos RNB, et al. Abstract P1-13-04: evaluation of the impact vitamin d and calcium supplementation on bone mineral density in breast cancer patients using or not taking aromatase inhibitors: 5-year follow-up. *Cancer Res* (2022) 82(4_Supplement): P1–13-04-P1-13-04. doi: 10.1158/1538-7445.SABCS21-P1-13-04

78. Wang Y, Ding H, Wang X, Wei Z, Feng S. Associated factors for osteoporosis and fracture in Chinese elderly. *Med Sci Monit* (2019) 25:5580–8. doi: 10.12659/MSM.914182

79. Sun K, Wang L, Ma Q, Cui Q, Lv Q, Zhang W, et al. Association between tea consumption and osteoporosis: a meta-analysis. *Medicine* (2017) 96(49):e9034. doi: 10.1097/MD.0000000000009034

80. Pasqualini L, Ministrini S, Lombardini R, Bagaglia F, Paltriccia R, Pippi R, et al. Effects of a 3-month weight-bearing and resistance exercise training on circulating osteogenic cells and bone formation markers in postmenopausal women with low bone mass. *Osteoporosis Int* (2019) 30(4):797–806. doi: 10.1007/s00198-019-04908-9

81. Chen L-R, Ko N-Y, Chen K-H. Medical treatment for osteoporosis: from molecular to clinical opinions. *Int J Mol Sci* (2019) 20(9):2213. doi: 10.3390/ijms20092213

82. Livi L, Scotti V, Desideri I, Saieva C, Cecchini S, Francolini G, et al. Phase 2 placebo-controlled, single-blind trial to evaluate the impact of oral ibandronate on bone mineral density in osteopenic breast cancer patients receiving adjuvant aromatase inhibitors: 5-year results of the single-centre BONADIUV trial. *Eur J Cancer* (2019) 108:100–10. doi: 10.1016/j.ejca.2018.12.005

83. Monda V, Lupoli GA, Messina G, Peluso R, Panico A, Villano I, et al. Improvement of bone physiology and life quality due to association of risedronate and anastrozole. *Front Pharmacol* (2017) 8. doi: 10.3389/fphar.2017.00632

84. Greenspan SL, Vujevich KT, Brufsky A, Lembersky BC, van Londen GJ, Jankowitz RC, et al. Prevention of bone loss with risedronate in breast cancer survivors: a randomized, controlled clinical trial. *Osteoporosis Int* (2015) 26(6):1857–64. doi: 10.1007/s00198-015-3100-7

85. Mugnier B, Goncalves A, Daumas A, Couderc A-L, Mezni E, Viret F, et al. Prevention of aromatase inhibitor–induced bone loss with anti-resorptive therapy in post-menopausal women with early-stage breast cancer. *Osteoporosis Int* (2023) 34, 703-711. doi: 10.1007/s00198-023-06683-0

86. Sheweita SA, Ammar RG, Sabra SA, Sultan AS. Letrozole and zoledronic acid changed signalling pathways involved in the apoptosis of breast cancer cells. *J Taibah Univ Med Sci* (2021) 16(1):112–20. doi: 10.1016/j.jtumed.2020.10.017

87. Waltman NL, Twiss JJ, Ott CD, Gross GJ, Lindsey AM, Moore TE, et al. The effect of weight training on bone mineral density and bone turnover in postmenopausal breast cancer survivors with bone loss: a 24-month randomized controlled trial. *Osteoporosis Int* (2010) 21(8):1361–9. doi: 10.1007/s00198-009-1083-y

88. Reid IR. Efficacy, effectiveness and side effects of medications used to prevent fractures. *J Internal Med* (2015) 277(6):690–706. doi: 10.1111/joim.12339

89. Yuan F, Peng W, Yang C, Zheng J. Teriparatide versus bisphosphonates for treatment of postmenopausal osteoporosis: a meta-analysis. *Int J Surg* (2019) 66:1–11. doi: 10.1016/j.ijsu.2019.03.004

90. Ellis GK, Bone HG, Chlebowski R, Paul D, Spadafora S, Smith J, et al. Randomized trial of denosumab in patients receiving adjuvant aromatase inhibitors for nonmetastatic breast cancer. *J Clin Oncol* (2008) 26(30):4875–82. doi: 10.1200/JCO.2008.16.3832

91. Gnant M, Pfeiler G, Dubsky PC, Hubalek M, Greil R, Jakesz R, et al. Adjuvant denosumab in breast cancer (ABCSG-18): a multicentre, randomised, double-blind, placebo-controlled trial. *Lancet* (2015) 386(9992):433–43. doi: 10.1016/S0140-6736(15)60995-3

92. Bundred N. Antiresorptive therapies in oncology and their effects on cancer progression. *Cancer Treat Rev* (2012) 38(6):776–86. doi: 10.1016/j.ctrv.2012.02.002

93. Dell'Aquila E, Armento G, Iuliani M, Simonetti S, D'Onofrio L, Zeppola T, et al. Denosumab for cancer-related bone loss. *Expert Opin Biol Ther* (2020) 20(11):1261–74. doi: 10.1080/14712598.2020.1814731

94. Kanis JA, Cooper C, Rizzoli R, Reginster JYon behalf of the Scientific Advisory Board of the European Society for C and Economic Aspects of O, et al. European Guidance for the diagnosis and management of osteoporosis in postmenopausal women. *Osteoporosis Int* (2019) 30(1):3–44. doi: 10.1007/s00198-018-4704-5

95. Ettinger B, Black DM, Mitlak BH, Knickerbocker RK, Nickelsen T, Genant HK, et al. Reduction of vertebral fracture risk in postmenopausal women with osteoporosis treated with RaloxifeneResults from a 3-year randomized clinical trial. *JAMA* (1999) 282(7):637–45. doi: 10.1001/jama.282.7.637

96. Lainé M, Fanning SW, Chang Y-F, Green B, Greene ME, Komm B, et al. Lasofoxifene as a potential treatment for therapy-resistant ER-positive metastatic breast cancer. *Breast Cancer Res* (2021) 23(1):54. doi: 10.1186/s13058-021-01431-w

97. Kraenzlin ME, Meier C. Parathyroid hormone analogues in the treatment of osteoporosis. *Nat Rev Endocrinol* (2011) 7(11):647–56. doi: 10.1038/nrendo.2011.108

98. Kendler DL, Marin F, Zerbini CAF, Russo LA, Greenspan SL, Zikan V, et al. Effects of teriparatide and risedronate on new fractures in post-menopausal women with severe osteoporosis (VERO): a multicentre, double-blind, double-dummy, randomised controlled trial. *Lancet* (2018) 391(10117):230–40. doi: 10.1016/S0140-6736(17)32137-2

99. Liel Y. Teriparatide vs risedronate for osteoporosis. *Lancet* (2018) 391 (10133):1895. doi: 10.1016/S0140-6736(18)30754-2

100. Ma L, Hua R, Tian Y, Cheng H, Fajardo RJ, Pearson JJ, et al. Connexin 43 hemichannels protect bone loss during estrogen deficiency. *Bone Res* (2019) 7(1):11. doi: 10.1038/s41413-019-0050-2

101. Huang X-H, Liang R-H, Su L, Guo W, Wang C-J. Mechanism of bushen jianpi decoction in preventing and treating osteoporosis caused by aromatase inhibitors in breast cancer treatment. *Cancer Biomarkers* (2017) 18:183–90. doi: 10.3233/CBM-160281

102. Jiayi L, Yuzhen P, Lijiang Z. Based on association rules and factor analysis to explore the rule of traditional Chinese medicine prescription for bone loss after endocrine therapy for breast cancer. *Clin J Traditional Chin Med* (2022) 34 (07):1274–80. doi: 10.16448/j.cjtcm.2022.0720

103. Xin Z, Wu X, Yu Z, Shang J, Xu B, Jiang S, et al. Mechanisms explaining the efficacy of psoralidin in cancer and osteoporosis, a review. *Pharmacol Res* (2019) 147:104334. doi: 10.1016/j.phrs.2019.104334

104. Song J, Zhang Y, Zhu Y, Jin X, Li L, Wang C, et al. Structural characterization and anti-osteoporosis effects of polysaccharide purified from eucommia ulmoides Oliver cortex based on its modulation on bone metabolism. *Carbohydr Polymers* (2023) 306:120601. doi: 10.1016/j.carbpol.2023.120601

105. Zhang F, Li Q, Wu J, Ruan H, Sun C, Zhu J, et al. Total flavonoids of drynariae rhizoma improve glucocorticoid-induced osteoporosis of rats: UHPLC-MS-Based qualitative analysis, network pharmacology strategy and pharmacodynamic validation. *Front Endocrinol* (2022) 13. doi: 10.3389/fendo.2022.920931

106. Jin-long Z, Ling-feng Z, Gui-hong L, He-tao H, Wei-yi Y, Ming-hui L, et al. Research progress on mechanism of active components of Chinese materiamedica in treatment of osteoporosis based on signaling pathway. *Chinese Traditional and Herbal Drugs* (2020) 51(23):6084-94.

107. Scheidemann ER, Shajahan-Haq AN. Resistance to CDK4/6 inhibitors in estrogen receptor-positive breast cancer. *Int J Mol Sci* (2021) 22(22):12292. doi: 10.3390/ijms222212292

108. Singh A, Veeriah V, Xi P, Labella R, Chen J, Romeo SG, et al. Angiocrine signals regulate quiescence and therapy resistance in bone metastasis. *JCI Insight* (2019) 4(13):e125679. doi: 10.1172/jci.insight.125679

109. Kim D, Piao J, Park JS, Lee D, Hwang DY, Hong HS. Substance p-mediated vascular protection ameliorates bone loss. *Oxid Med Cell Longev* (2023) 2023:9903336. doi: 10.1155/2023/9903336

frontiers | Frontiers in Oncology

TYPE Original Research
PUBLISHED 15 August 2023
DOI 10.3389/fonc.2023.1192946

OPEN ACCESS

EDITED BY
Deniz Can Guven,
Hacettepe University, Türkiye

REVIEWED BY
Baran Akagündüz,
Erzincan University, Türkiye
Wei-Pang Chung,
National Cheng Kung University Hospital, Taiwan

*CORRESPONDENCE
Chi-Cheng Huang
chishenh74@gmail.com
Ling-Ming Tseng
lmtseng@vghtpe.gov.tw

†These authors have contributed equally to this work

RECEIVED 24 March 2023
ACCEPTED 25 July 2023
PUBLISHED 15 August 2023

CITATION
Chao T-C, Tsai Y-F, Liu C-Y, Lien P-J, Lin Y-S, Feng C-J, Chen Y-J, Lai J-I, Hsu C-Y, Lynn JJ, Huang C-C and Tseng L-M (2023) Prevalence of *PIK3CA* mutations in Taiwanese patients with breast cancer: a retrospective next-generation sequencing database analysis. *Front. Oncol.* 13:1192946. doi: 10.3389/fonc.2023.1192946

Prevalence of *PIK3CA* mutations in Taiwanese patients with breast cancer: a retrospective next-generation sequencing database analysis

Ta-Chung Chao[1,2,3], Yi-Fang Tsai[1,2,4], Chun-Yu Liu[1,2,5], Pei-Ju Lien[1,4], Yen-Shu Lin[1,4], Chin-Jung Feng[1,4], Yen-Jen Chen[1,2,4], Jiun-I Lai[1,6,7], Chih-Yi Hsu[2,8], Jiun Jen Lynn[9], Chi-Cheng Huang[1,4,10*†] and Ling-Ming Tseng[1,2,4*†]

[1]Comprehensive Breast Health Center, Department of Surgery, Taipei Veterans General Hospital, Taipei, Taiwan, [2]School of Medicine, College of Medicine, National Yang-Ming Chiao Tung University, Taipei, Taiwan, [3]Division of Cancer Prevention, Department of Oncology, Taipei Veterans General Hospital, Taipei, Taiwan, [4]Division of General Surgery, Department of Surgery, Taipei Veterans General Hospital, Taipei, Taiwan, [5]Division of Transfusion Medicine, Department of Medicine, Taipei Veterans General Hospital, Taipei, Taiwan, [6]Division of Medical Oncology, Department of Oncology, Taipei Veterans General Hospital, Taipei, Taiwan, [7]Institute of Clinical Medicine, School of Medicine, National Yang Ming Chiao Tung University, Taipei, Taiwan, [8]Department of Pathology and Laboratory Medicine, Taipei Veterans General Hospital, Taipei, Taiwan, [9]Medical Affairs, Novartis (Taiwan) Co. Ltd, Taipei, Taiwan, [10]Institute of Epidemiology and Preventive Medicine, College of Public Health, National Taiwan University, Taipei, Taiwan

Background: Breast cancer is the most common cancer type that affects women. In hormone receptor–positive (HR+), human epidermal growth factor receptor 2 –negative (HER2–) advanced breast cancer (ABC), phosphatidylinositol-4,5-bisphosphate 3-kinase catalytic subunit alpha (*PIK3CA)* is the most frequently mutated gene associated with poor prognosis. This study evaluated the frequency of *PIK3CA* mutations in the Taiwanese breast cancer population.

Methodology: This is a retrospective study; patient data were collected for 2 years from a next-generation sequencing database linked to electronic health records (EHRs). The primary endpoint was the regional prevalence of *PIK3CA* mutation. The secondary endpoints were to decipher the mutation types across breast cancer subtype, menopausal status, and time to treatment failure after everolimus (an mTOR inhibitor) or cyclin-dependent kinase 4/6 (CDK4/6) inhibitor treatment.

Results: *PIK3CA* mutations were identified in 278 of 728 patients (38%). *PIK3CA* mutations were reported in 43% of patients with HR–/HER2+ subtype and 42% of patients with HR+/HER2– postmenopausal status. A lower prevalence of *PIK3CA* mutations was observed in triple-negative (27%) and HR+/HER2– premenopausal patients (29%). The most common mutation was at exon 20 (H1047R mutation, 41.6%), followed by exon 9 (E545K mutation, 18.9% and E542K mutation, 10.3%). Among patients treated with CDK4/6 inhibitors, the median time to treatment failure was 12 months (95% CI: 7-21 months) in the *PIK3CA* mutation cohort and 16 months (95% CI: 11-23 months) in the *PIK3CA* wild-type cohort, whereas patients receiving an mTOR inhibitor reported a

median time to treatment failure of 20.5 months (95% CI: 8-33 months) in the *PIK3CA* mutation cohort and 6 months (95% CI: 2-9 months) in the *PIK3CA* wild-type cohort.

Conclusion: A high frequency of *PIK3CA* mutations was detected in Taiwanese patients with breast cancer, which was consistent with previous studies. Early detection of *PIK3CA* mutations might influence therapeutic decisions, leading to better treatment outcomes.

KEYWORDS

advanced breast cancer, *PIK3CA* mutations, hotspot mutations, next-generation sequencing, Taiwanese population

1 Introduction

Breast cancer is the most commonly diagnosed cancer and one of the leading causes of cancer death among women in Taiwan. In 2019, Taiwan reported 14,856 new cases of breast cancer and 2633 deaths that occurred due to breast cancer (1). Despite the wide range of therapeutic interventions available for breast cancer, important current advances are focused on genetic profiling to allow a mutation-driven, targeted, and effective therapeutic approach.

Phosphoinositide 3-kinase (PI3K) is the most frequently disrupted signaling pathway in hormone receptor–positive (HR+) breast cancer (2). Phosphatidylinositol 3-kinase alpha (PI3Kα) is a heterodimeric protein complex composed of the catalytic subunit p110α (coded by the phosphatidylinositol-4,5-bisphosphate 3-kinase catalytic subunit alpha [*PIK3CA*] gene) and the regulatory subunit p85α (coded by the *PIK3R1* gene) (3). Mutations of the *PIK3CA* gene, inducing hyperactivation of the alpha isoform (p110α) of PI3K, occur in 28% to 46% of patients with HR+/human epidermal growth factor receptor-2–negative (HER2–) advanced breast cancer (ABC) (4, 5). This variant is associated with poor response to HER2 targeted therapy, endocrine therapy, and chemotherapy (6). The presence of an oncogenic PI3K mutation has also been correlated with a worse clinical outcome in patients with ABC receiving cyclin-dependent kinase 4/6 (CDK4/6) inhibitors (7). The main "hotspots" reported for *PIK3CA* mutations are E542K and E545K of the helical domain on exon 9 and H1047R of the kinase domain on exon 20 (8–10). Advancement in next-generation sequencing (NGS) technologies has made gene sequencing and mutation analysis feasible and effective for clinical application in breast cancer. NGS is helpful in identifying the key mutations for guiding personalized therapy (11). A study conducted by Huang et al. in Taiwanese patients with breast cancer identified *PIK3CA* as one of the most frequently mutated genes in 38% of the study population, followed by *ERBB2* (23%), *ESR1* (10%), *AKT1* (6%), and *BRCA2* (5%) mutations (12).

Alpelisib, a selective PI3K inhibitor, showed efficacy in patients with *PIK3CA*-mutated HR+/HER2– ABC in the SOLAR-1 trial, with a median progression-free survival (PFS) of 11.0 months (95% confidence interval [CI]: 7.5-14.5) (13). Based on these results, alpelisib was approved in Taiwan since December 2020 for the treatment of postmenopausal women and men, with HR+/HER2–, *PIK3CA*-mutated, locally advanced or metastatic breast cancer following progression on or after an endocrine-based regimen (14). Because the data on the prevalence of *PIK3CA* mutations in the Taiwanese population are limited, this study aimed to evaluate the frequency of *PIK3CA* mutation status, thereby determining the patient pool that might benefit from a personalized treatment plan. Here, we report the results from a single-center observational study that investigated the frequency of *PIK3CA* mutations in Taiwanese patients with all subtypes of breast cancer using NGS over a period of 24 months.

2 Methods

This is a retrospective, single-center study investigating the prevalence of *PIK3CA* mutations in female patients diagnosed with breast cancer in Taiwan.

2.1 Trial design

Taipei Veterans General Hospital, Taiwan, has an ongoing project (VGH-TAYLOR) performing comprehensive genomic profiling on tumor tissues from patients with breast cancer via NGS, which is sponsored by the YongLin Healthcare Foundation. The VGH-TAYLOR study aimed to discover potential biomarkers for recurrence, diagnosis, and prognosis of breast cancer that may enable personalized medicine and improvement in breast cancer treatment; the rationale and design of the study protocol have been previously described (15). Patient and genomic data were collected from the NGS database linked with electronic health records (EHRs) to investigate the mutation prevalence in various subtypes and stages of breast cancer.

In the NGS database, medical records of patients with advanced/metastatic breast cancer who were treated with an mTOR inhibitor or CDK4/6 inhibitor, with treatment initiation (index date) from January 1, 2018 to January 30, 2020, were included in the study once the inclusion/exclusion criteria were met. The EHRs were retrieved 3 years

prior to the index date, from January 1, 2015 to January 1, 2018, for baseline characteristics and breast cancer recurrence data collection (Figure 1). Patients with information of first prescription of mTOR or CDK4/6 inhibitors during the 4-year EHR data collection period were also included for analysis for time to treatment failure. The study protocol was approved by the ethics committee of the Taipei Veterans General Hospital.

The pathological features of the tissue samples were determined using immunohistochemistry (IHC) assay. At least 1% of nuclei staining–positive results were defined as ER-positive. As per the American Society of Clinical Oncology (ASCO) and College of American Pathologists (CAP) guidelines, IHC 3+ and IHC 2+ with fluorescence *in situ* hybridization (FISH) amplification indicated HER2 overexpression. An IHC score of 0 to 1+ is called HER2– and a score of 3+ is called HER2+. A FISH HER2:CEP17 signal ratio >2.2 is called amplification whereas, ratio between 1.8-2.2 is equivocal and <1.8 is non-amplification

2.2 Patients

Inclusion criteria were defined as follows: (1) female patients aged ≥20 years; (2) patients with confirmed diagnosis of primary invasive breast cancer who are planning to receive treatment for breast cancer; (3) patients who have breast cancer recurrence at screening or Stage IV patients who have received or are currently receiving treatments for breast cancer; (4) Eastern Cooperative Oncology Group (ECOG) performance status ≤3; and (5) life expectancy ≥3 months.

Patients were excluded if they had a primary cancer other than breast cancer within 5 years prior to screening. Archival samples from the biobank (retrospective cohort) will be withdrawn if: (1) tumor content of the FFPE sample is lower than the specified percentage according to the standard of the central laboratory; (2) FFPE samples failed the DNA/RNA quality check. The criteria of the DNA/RNA quality check will follow the standard of the central laboratory. Enrolled patients will be withdrawn if one of the following conditions occurs: (1) patient withdraws consent; (2) patient refuses to provide specimens for evaluation after enrollment; (3) patient for which all samples/specimens fail the DNA/RNA quality check. The criteria of the DNA/RNA quality check will follow the standard of the central laboratory; (4) patient who does not have sufficient FFPE samples, tissues or blood samples for genetic profiling analysis by principal investigator's discretion; (5) patient who does not return to the clinical site for more than 6 months (based on their medical records) will be considered as lost to follow-up. However, whether this subject should be withdrawn will be based on the PI's discretion (15).

In this study we retrospectively analyze the database from VGH-TAILOR project (Group 1,2,3). Enrolled patients were categorized into 4 major groups, presented in Figure 2.

2.2.1 Group 1

• Group 1A (early breast cancer): patients who were planning to receive surgery as the first-line treatment followed by adjuvant therapy.

• Group1B (advanced breast cancer): patients with recurrence at screening, who had received surgery for primary breast cancer within 3 years prior to screening, and with primary tumor formalin-fixed paraffin-embedded (FFPE) tissues available.

2.2.2 Group 2 (early breast cancer)

Patients who were planning to receive neoadjuvant therapy as the first-line treatment for breast cancer and followed by surgery.

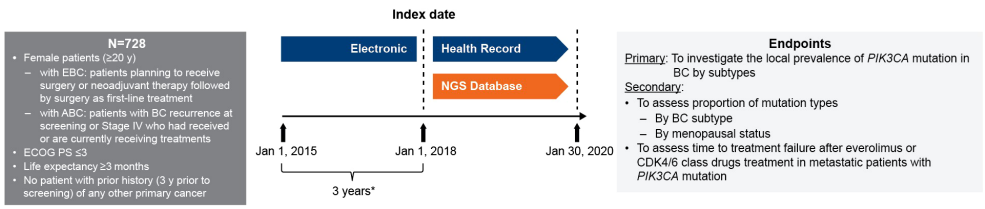

FIGURE 1
Study design. * Baseline characteristics collection period from HER. ABC, advanced breast cancer; BC, breast cancer; CDK4/6, cyclin-dependent 4 or 6 kinase; EBC, early breast cancer; ECOG PS, Eastern Cooperative Oncology Group performance status; EHC, electronic health record; NGS, next-generation sequencing; *PIK3CA*, phosphatidylinositol-4,5-bisphosphate 3-kinase catalytic subunit alpha; y, years.

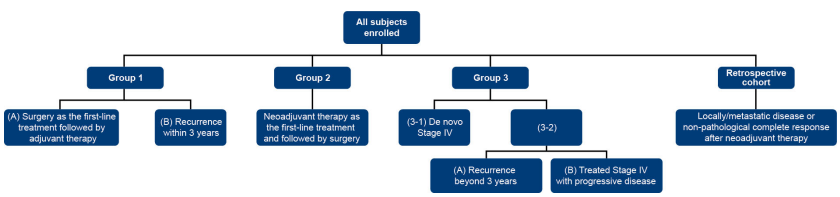

FIGURE 2
Patient distribution.

2.2.3 Group 3 (advanced breast cancer)

- Group 3-1: patients diagnosed with *de novo* and treatment naïve stage IV breast cancer.
- Group 3-2: patients diagnosed with a stage IV breast cancer and with recurrence beyond 3 years after surgery (Group 3-2A) or stage IV subjects who had received or are currently receiving treatments for breast cancer (Group 3-2B).

2.2.4 Retrospective cohort

Samples were collected from the biobank of the patients with local/metastatic disease or non-pathological complete response after neoadjuvant therapy

2.3 Endpoints

The primary endpoint was the regional prevalence of *PIK3CA* mutation in breast cancer and by breast cancer subtypes in overall patients with breast cancer, patients with HR+/HER2–, HR–/HER2+, HR+/HER2+ and triple-negative breast cancer. Because the pre- and postmenopausal status present different biological and genetic characteristics in HR+/HER2– breast cancer, the prevalence of *PIK3CA* mutations was further analyzed by menopausal status in HR+/HER2– breast cancer. Menopause is usually a clinical diagnosis made after ≥12 months of amenorrhea (16).

Secondary endpoints were to assess the frequency of mutation types by breast cancer subtype and by menopausal status and time to treatment failure after mTOR or CDK4/6 inhibitor in metastatic patients stratified by *PIK3CA* mutation status. Time to treatment failure is defined as the time from the date of first dose of treatment of interest to the date of the patient discontinuing treatment for any reason; the Kaplan-Meier (KM) method was used for the estimation.

2.4 Sample preparation

The genetic profiles were determined through NGS of FFPE samples. For screening and recruitment of patients for Group 1B and Group 3-2, paired FFPE primary and recurrent tumor samples were collected and sequenced, and for Group 2, paired FFPE diagnostic and post-neoadjuvant specimens were assayed.

The preparation of FFPE was done under standard conditions at the trial site. The DNA/RNA extraction and hematoxylin and eosin (H&E) staining were performed in accordance with the laboratory manual under the guidance of a certified pathologist in the central laboratory. Quality checks for DNA/RNA were performed as per the manual of the Thermo Fisher™ Oncomine™ (TMO) Comprehensive Assay requirement (see below) and additional samples were collected in case of failure. Of the seven unstained FFPE sections retrieved (per subject), one section was prepared for H&E staining and six sections were prepared for TMO comprehensive assay.

2.5 Oncomine™ comprehensive assay (TMO comprehensive assay)

Oncomine™ comprehensive assay (TMO comprehensive assay, Thermo Fisher Scientific, Waltham, MA) was used to profile thousands of variants across 161 cancer-relevant genes using FFPE tissues (17). Analyses of TMO comprehensive assay included identification of genes and detection of mutation types such as frameshift, missense, synonymous, single nucleotide variation (SNV), insertion/deletion (Indel), and copy number variation (CNV) observed in individual subject.

Amplicon libraries were constructed with multiplex polymerase chain reaction (PCR) primers for preparation of DNA and RNA (for fusion genes) from FFPE samples. Sequencing was performed with the Ion Gene Studio S5 System and Ion 540 Chips. Raw data process, alignment, and variant calling were performed with Torrent Suite™ Software, with variant calling using the Torrent Variant Caller plug-in. Further management was proceeded by Ion Reporter™ Software with workflow "Oncomine Comprehensive v3 - w3.2 - DNA and Fusions - Single Sample" version 5.10 selected and filter chain "Oncomine Variants" version 5.10 applied. Reference genome was hg19.

2.6 Variables

Preindex variables, including demographics of all patients, menopausal status, primary diagnosis, previous medical history/comorbidities, and family history of cancer, were extracted from the NGS database, whereas the treatment response of previous breast cancer was taken from the EHRs.

Postindex variables in the follow-up period, including breast cancer genetic mutations, treatment, and treatment response from previous lines if any, were extracted from the NGS database, and breast cancer recurrence data were also extracted from the EHRs.

2.7 Statistical analysis

All statistical tests were conducted with a two-sided alternative hypothesis, and a significance level of 0.05 and a P value of <0.05 were considered statistically significant, unless otherwise specified. Mutations in the PIK3/AKT/mTOR pathway were deciphered. The prevalence of *PIK3CA* mutations was calculated as the number of *PIK3CA* mutations divided by the number of patients with breast cancer in the populations stated above. The 95% CIs were presented as appropriate. Analysis of the primary endpoint was descriptive in nature, and no statistical hypothesis or testing was performed. The enrolled set was adopted for both primary and secondary endpoints unless otherwise specified.

3 Results

3.1 Patient demographics and baseline characteristics

A total of 728 patients were included for the *PIK3CA* mutation analysis, most of whom were categorized into Group 1A (481 patients, 66.07%), followed by Group 2 (93 patients, 12.77%), Group 3-2 (59 patients, 8.10%), Group 3-1 (42 patients, 5.77%), and Group 1B (20 patients, 2.75%), please refer to Figure 2 for what each group stands for. The mean age in all the groups at the time of testing was 51 to 57 years of age. A total of 548 patients (76.2%) with HR+ and 149 patients (20.8%) with HER2+ status were reported. Patient demographic characteristics are detailed in Table 1.

3.2 Prevalence and characteristics of *PIK3CA* mutations

Overall, 403 of 728 patients (55%) had mutations in the PI3K/AKT/mTOR pathway, of which the 3 most commonly detected mutations were *PIK3CA* (57%), *AKT3* (14%), and *PTEN* (10%) (Figure 3).

A total of 278 of 728 patients (38%) harbored *PIK3CA* mutations. With respect to the IHC phenotypes, 29 patients (43.0%) were HR−/HER2+, 96 patients (42.0%) were HR+/HER2− (postmenopausal), and 34 patients (41.0%) were HR+/HER2+. The prevalence of *PIK3CA* mutation was relatively lower in triple-negative breast cancer (27.0%) and premenopausal patients with HR+/HER2− status (29.0%). The prevalence of *PIK3CA* mutation by IHC status is presented in Figure 4.

The majority of the *PIK3CA* mutations were clustered in exon 9 and exon 20, helical and kinase domains, respectively. Among 278 patients with *PIK3CA* mutations, the most frequently observed mutations were in exon 20 (H1047R, 41.6%) and exon 9 (E545K, 18.9% and E542K, 10.3%); these are presented in Figure 5A.

The distribution of *PIK3CA* mutation types is presented in Figure 5B. A total of 27 of 278 patients (9.7%) harbored multiple *PIK3CA* mutations within one sample. Mutual exclusivity was observed between *PIK3CA* and *AKT1* ($P<0.001$), *PIK3CA* and *AKT3* ($P<0.001$), and *PIK3CA* and *PIK3R1* ($P=0.007$).

3.3 *PIK3CA* mutations in patients with HR+/HER2− breast cancer by menopausal status

PIK3CA hotspot mutations (H1047R, E545K, and E542K) were found in 63.5% of premenopausal patients with breast cancer and in 56.2% of postmenopausal patients with HR+/HER2− breast cancer.

TABLE 1 Patient demographic characteristics (excluding retrospective cohort).

Group	Group 1A	Group 1B	Group 2	Group 3-1	Group 3-2
Case number	481	20	93	42	59
Age, mean (SD)	57 (12)	56 (13)	51 (12)	57 (11)	55 (12)
Age (min-max)	22-93	34-80	27-81	25-83	31-83
Estrogen receptor Positive : Negative Missing	 388:91 2	 11:8 1	 55:38 0	 27:15 0	 41:13 4
HER2 Positive : Equivocal (IHC2+):Negative Missing	 72:6:400 3	 7:1:10 2	 31:0:62 0	 16:1:25 0	 15:1:35 8
Stage					
I	182	5	1	0	4
II	289	9	82	0	11
III	0	0	10	0	0
IV	0	0	0	42	37
Missing	10	6	0	0	7
Grade					
I	83	0	6	2	2
II	256	9	68	30	22
III	135	7	18	10	17
Missing	7	4	1	0	18

Staging of group 1B and 3-2 indicated original stages of primary tumor.
HER2 Positive: IHC2+: Negative: Missing → Positive: Equivocal: Negative: Missing
Equivocal: HER2 immunohistochemical stain score 2+ without in situ hybridization testing; IHC2: without FISH testing.
FISH, fluorescence in situ hybridization; HER2, human epidermal growth factor receptor 2; IHC, immunohistochemistry; SD, standard deviation.

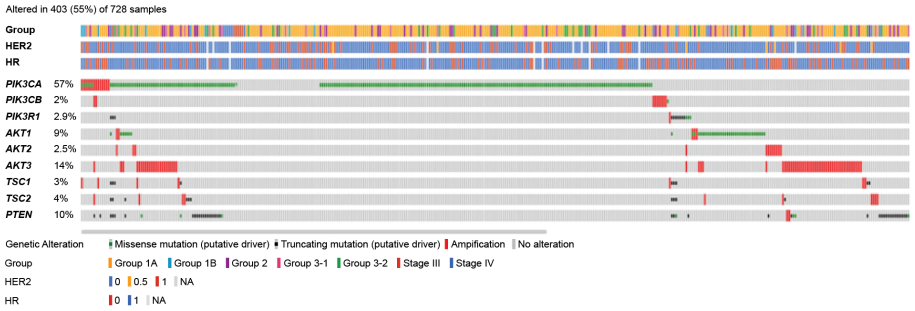

FIGURE 3
Mutation map of genes in the PI3K/AKT/mTOR pathway. *AKT*, serine/threonine kinase; HR, hormone receptor; HER2, human epidermal growth factor receptor 2; mTOR, mammalian target of rapamycin; PI3K, phosphoinositide 3-kinase; *PIK3CA/PIK3CB*, phosphatidylinositol-4,5-bisphosphate 3-kinase catalytic subunit alpha/beta; *PIK3R1*, phosphoinositide-3-kinase regulatory subunit 1; *PTEN*, phosphatase and TENsin homolog; *TSC*, tuberous sclerosis complex.

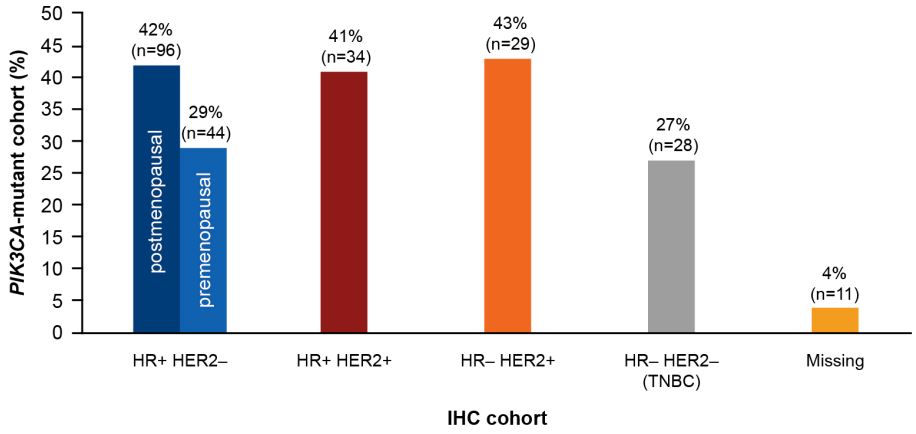

FIGURE 4
Prevalence of *PIK3CA* mutation in each IHC cohort. HR, hormone receptor; HER2, human epidermal growth factor receptor 2; IHC, immunohistochemistry; *PIK3CA*, phosphatidylinositol-4,5-bisphosphate 3-kinase catalytic subunit alpha; TNBC, triple-negative breast cancer.

Among the premenopausal *PIK3CA*-mutated patients, H1047R and E545K mutations were the most common (27% each), followed by the E542K mutation (9.5%). A similar distribution was seen in postmenopausal patients, where the H1047R mutation was the most common mutation (32%), followed by E545K (14.5%) and E542K mutations (9.7%).

3.4 Time to treatment failure in patients with *PIK3CA* mutation after CDK4/6 inhibitors or mTOR inhibitor

A total of 19 patients (22.62%) with advanced breast cancer who received CDK4/6 inhibitors (n=84, ribociclib=47, palbociclib=32, abemaciclib=5) and 3 patients (18.75%) who received an mTOR inhibitor (n=16) were reported to have a *PIK3CA* mutation. For patients treated with CDK4/6 inhibitors, the median time to treatment failure was 16 months (95% CI: 11-23 months) in the *PIK3CA* wild-type cohort and 12 months (95% CI: 7-21 months) in the *PIK3CA* mutation cohort, with a hazard ratio (HR) of 1.670 (95% CI: 0.908-3.069) (Figure 6A; Table 2). The data demonstrated a trend of shorter treatment duration with CDK4/6 inhibitors in patients with *PIK3CA* mutation. For patients receiving mTOR inhibitor, the median time to treatment failure was 20.5 months (95% CI: 8-33 months) in the *PIK3CA* mutation cohort and 6 months (95% CI: 2-9 months) in the *PIK3CA* wild-type cohort, with an HR of 0.244 (95% CI: 0.031-1.922) (Figure 6B; Table 2).

4 Discussion

PIK3CA mutations are significantly associated with breast cancer occurrence and provide a growth advantage to cancer cells, which leads to progression and drug resistance (18). Hence, early detection of *PIK3CA* mutations may help in identifying patients who might benefit from a more effective personalized targeted therapy (19). In the present study, we reported the prevalence of *PIK3CA* mutations in Taiwanese patients with breast cancer stratified by IHC subtypes using an NGS database. In addition, we assessed the impact of *PIK3CA* mutation status on time to treatment failure of CDK4/6 and mTOR inhibitors in patients with metastatic breast cancer.

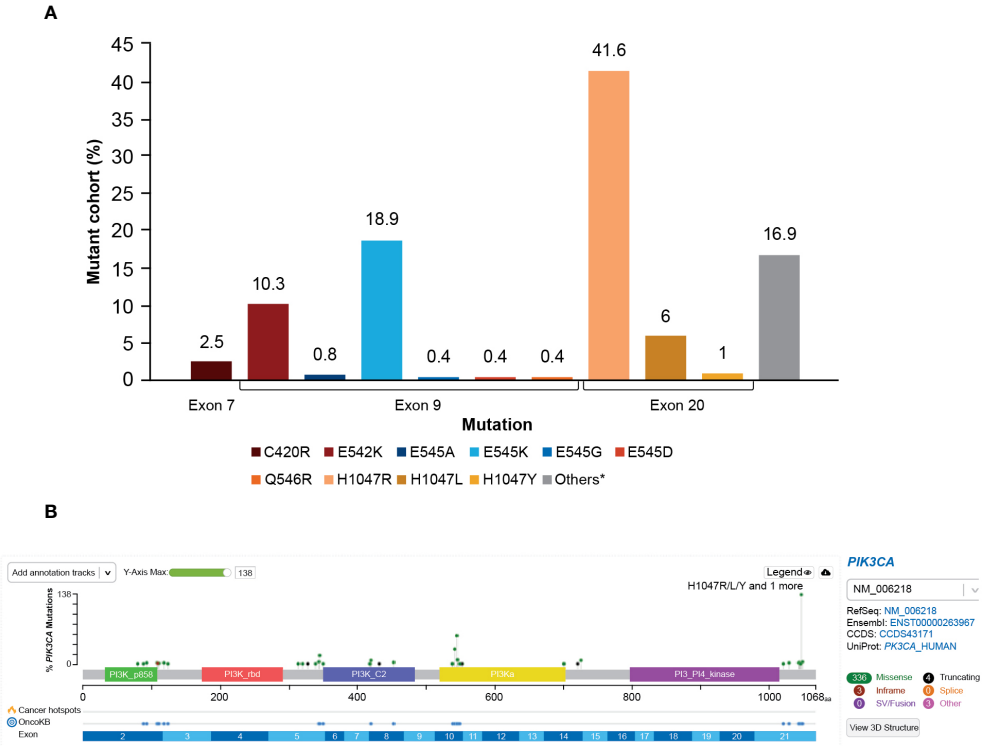

FIGURE 5
(A) Distribution of *PIK3CA* variants frequency. *A total of 16.9% of mutations in patients from this study were not captured by the therascreen *PIK3CA* Rotor-Gene Q (RGQ) PCR Kit. The most frequent mutations not captured were E726K (2.8%) and N345K (5.3%). Mutation Q546E was not detected (0%) at exon 9. **(B)** OncoPrinter plot of *PIK3CA* mutations. PI3K, phosphoinositide 3-kinase; *PIK3CA*, phosphatidylinositol-4,5-bisphosphate 3-kinase catalytic subunit alpha.

In this study, genes in PIK3/AKT/mTOR pathway were deciphered, and *PIK3CA* mutations were identified as the most frequent genetic alterations observed in 38% of Taiwanese patients with breast cancer. Similarly, an earlier study by Huang et al. reported *PIK3CA* mutation as the most frequent mutation occurring in 38% of Taiwanese patients with breast cancer (12). The differences in the *PIK3CA* mutation frequency observed between the 2 studies could be attributed to the different sampling sizes and techniques of analysis.

The frequency of *PIK3CA* mutations varied by breast cancer subtype and menopausal status. A high prevalence of *PIK3CA* mutations was observed in patients with HR−/HER2+ status (43%) and HR+/HER2− postmenopausal status (42%), followed by HR+/HER2+ patients (41%). A comparatively lower prevalence was seen in HR+/HER2− premenopausal patients (29%), followed by patients with triple-negative breast cancer (27%). Although there is no consensus about a predisposition of *PIK3CA* mutation by breast cancer subtype, several studies have reported that 13.3% to 61.5% of HR+/HER2− ABC tumors and 12% to 25% of HER2+ tumors had *PIK3CA* mutations, whereas triple-negative breast cancer harbors the lowest rates of *PI3KCA* mutations (20, 21). A recent-published study (AURORA, BIG 14-01) analyzed 339 patients treated with first-line endocrine therapy plus CDK4/6 inhibitor, and found that *PIK3CA* mutation rate was 40%, which was similar to our findings (42% in HR+/HER2− patients). These mutations were not associated with first-line outcome (HR: 1.07 [95% CI: 0.66-1.75], *P*=0.65) (22). In our study with limited case numbers (n=84) and heterogenous characteristics (CDK4/6 inhibitors not purely first-line), it is difficult to compare the outcome in patients with *PIK3CA* mutations in these two studies. In our study, the most commonly reported hotspot mutations were H1047R (41.6%), followed by E545K (18.9%) and E542K (10.3%). These results were consistent with prior findings that reported H1047R, E545K, and E542K as the most common hotspots for *PIK3CA* mutations (5, 8, 9).

In the present study, 27 patients were reported with multiple *PIK3CA* mutations. Of note, a prior report by Vasan et al. indicated markedly increased sensitivity of multiple *PIK3CA*-mutant tumors to PI3K inhibitors, compared with a single hotspot mutation (23). In the Taiwanese population, *PIK3CA* and *PIK3R1* mutations were observed to be mutually exclusive. This mutual exclusivity of *PIK3CA* and *PIK3R1* mutations was reported earlier, leading to oncogenesis and activation of the PI3K pathway (24).

In a recent study by Pavithran et al., the presence of *PIK3CA* mutations was associated with reduced sensitivity to CDK4/6 inhibitors (25). In the present study, the median time to treatment failure of CDK4/6 inhibitors was much lower in patients with *PIK3CA* mutations than those without *PIK3CA* mutations (12 months vs 16 months; HR: 1.670; 95% CI: 0.908-3.069). However, this profile was shorter than that in another study that reported a time to treatment failure of 19.7 months where they used CDK4/6 inhibitors as the first-line therapy (26). This

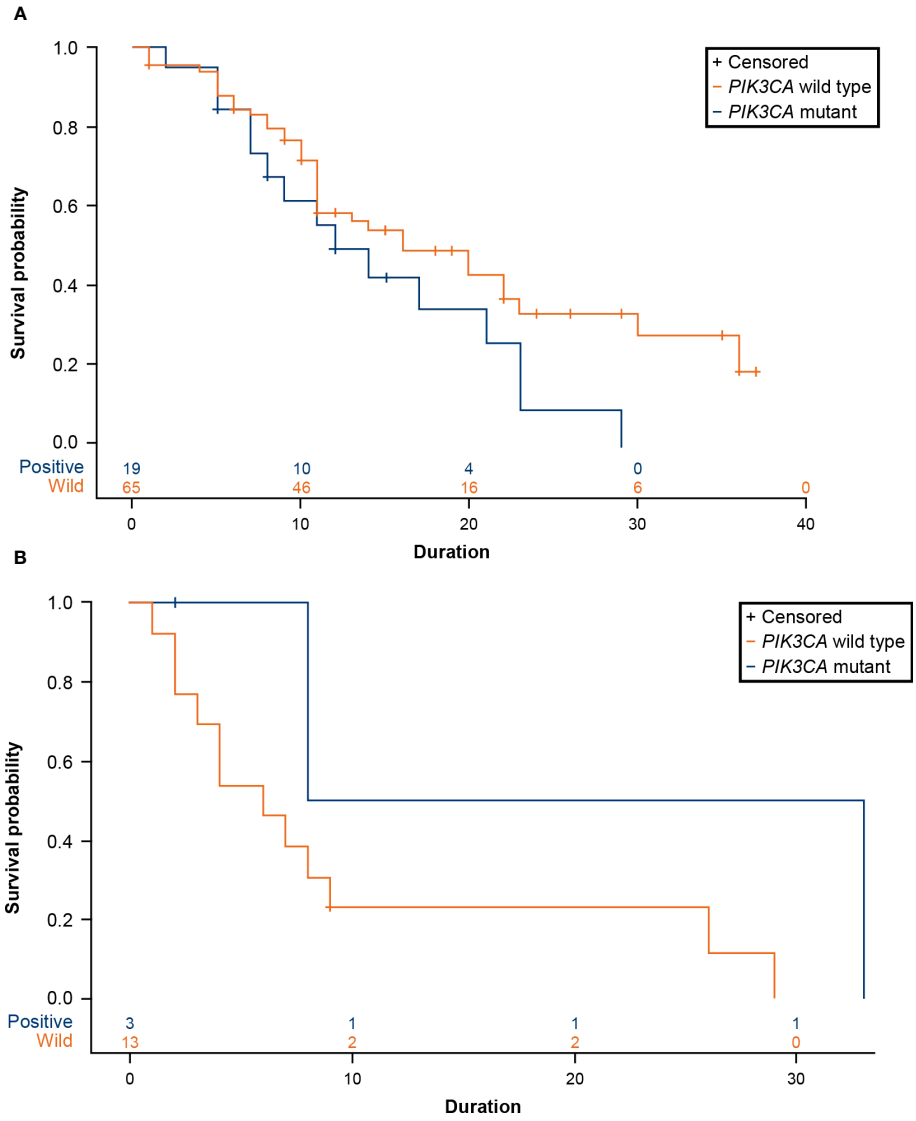

FIGURE 6
(A) Product-limit survival estimates of CDK4/6 inhibitors. **(B)** Product-limit survival estimates of everolimus (an mTOR inhibitor). CDK4/6, cyclin-dependent 4 and 6 kinase; mTOR, mammalian target of rapamycin; *PIK3CA*, phosphatidylinositol-4,5-bisphosphate 3-kinase catalytic subunit alpha.

TABLE 2 CDK4/6 and mTOR inhibitors on patients with *PIK3CA* mutation*.

Drug	Patient number	Median number of lines of therapy	Median time to treatment failure (months)		Hazard ratio, 95% CI
			PIK3CA mutant	*PIK3CA* wild type	
CDK4/6 inhibitors	84	1 (1-5)	12 (n=19, 95% CI: 7-21)	16 (n=65, 95% CI: 11-23)	1.670, 0.908-3.069
mTOR inhibitor (Everolimus)	16	2 (1-6)	20.5 (n=3, 95% CI: 8-33)	6 (n=13, 95% CI: 2-9)	0.244, 0.031-1.922

*Patients with treatment exposure of <1 month were excluded.
CDK4/6, cyclin-dependent 4 and 6 kinase; CI, confidence interval; mTOR, mammalian target of rapamycin; *PIK3CA*, phosphatidylinositol-4,5-bisphosphate 3-kinase catalytic subunit alpha.

difference may be attributed to the discrepancy in patient characteristics, follow-up period, or sample size (24). Findings from the MONALEESA-7 study evaluating ribociclib in premenopausal or perimenopausal women with HR+/HER2– ABC showed a shorter PFS in patients with *PIK3CA* mutations than those without, although this difference was not statistically significant (27). Collectively, multiple studies demonstrated numerical trends towards shorter PFS in patients with *PIK3CA* mutations, which might indicate that the presence of *PIK3CA* mutations may influence the sensitivity to CDK4/6 inhibitors.

Mutations in *PIK3CA* often result in hyperactivation of the PI3K/mammalian target of rapamycin (mTOR) pathway and may predict response to mTOR inhibitors. In the present study, the median time to treatment failure of an mTOR inhibitor (everolimus) was comparably longer in patients with *PIK3CA* mutations than those without (20.5 months vs 6 months; HR: 0.244; 95% CI: 0.031-1.922). Further research is required to validate these findings owing to the small sample size of the *PIK3CA*-mutant cohort (n=3). A combined analysis from BOLERO-1 and BOLERO-3 suggested that patients having tumors with *PIK3CA* mutations or hyperactive PI3K pathway derived PFS benefit from everolimus, whereas patients having tumors without these molecular alterations did not (28). Moynahan et al. reported that this survival benefit with everolimus was maintained irrespective of the type of *PIK3CA* genotype in BOLERO-2 (29). This further supports the findings of the current study. The earlier detection of *PIK3CA* mutations may help oncologists in treatment decisions and thereby help in providing an effective personalized targeted therapy to the patients.

The present study has a few limitations that are worth noting. This was a retrospective, single-center study and was prone to selection bias. Therefore, the actual frequency of genetic alterations observed in the study may not fully represent the general population in Taiwan. Lastly, the small sample size of patients receiving targeted therapies warrants further studies to validate these findings, especially in the case of time to treatment failure.

5 Conclusion

Consistent with previous studies, we identified a high prevalence of *PIK3CA* mutations in 38% of the Taiwanese patients with breast cancer (12). The lower prevalence in premenopausal patients and patients with triple-negative breast cancer warrants further studies. Most of the mutations were in exon 9 and exon 20, with H1047R, E545K, and E542K being the hotspots. A longer time to treatment failure in wild-type *PIK3CA* cohorts treated with CDK4/6 inhibitors was reported, which demonstrated the better efficacy of CDK4/6 inhibitors in wild-type *PIK3CA* cohorts than that in the *PIK3CA*-mutant cohort. Everolimus, an mTOR inhibitor, reported a longer time to treatment failure in the *PIK3CA*-mutant cohort and demonstrated better efficacy. Cumulatively, this indicated variations in the prevalence of *PIK3CA* mutation based on breast cancer IHC phenotype. Detection of mutations at an earlier stage can help in making appropriate therapeutic decisions, thus saving time and resulting in better outcomes for the Taiwanese breast cancer population.

Data availability statement

The original contributions presented in the study are included in the article/supplementary material. Further inquiries can be directed to the corresponding authors.

Ethics statement

The studies involving humans were approved by ethics committee of the Taipei Veterans General Hospital. The studies were conducted in accordance with the local legislation and institutional requirements. The participants provided their written informed consent to participate in this study.

Author contributions

All authors critically reviewed, provided feedback at each stage of the manuscript, approved the final version and agreed to be accountable for all aspects of the work.

Acknowledgments

The authors would like to express their gratitude to the Taiwan Clinical Oncology Research Foundation, the Melissa Lee Cancer Foundation, the YongLin Healthcare Foundation, and Mr Morris Chang for their kind support during the study. The authors thank the patients and study investigators involved. The authors thank Caamin Arora for medical writing assistance.

Conflict of interest

Author JL is full time employee of Novartis.

The remaining authors declare that the research was conducted in the absence of any commercial or financial relationships that could be construed as a potential conflict of interest.

The authors declare his study was supported by Novartis Pharmaceuticals Corporation. The funder was involved in the study design and medical writing assistance was provided by Caamin Arora, M Pharm, from Novartis Pharmaceuticals Corporation, India.

Publisher's note

References

1. Shih N-C, Kung P-T, Kuo W-Y, Tsai W-C. Association of treatment delay and stage with mortality in breast cancer: a nationwide cohort study in Taiwan. *Sci Rep* (2022) 12(1):18915. doi: 10.1038/s41598-022-23683-y

2. Hosford SR, Miller TW. Clinical potential of novel therapeutic targets in breast cancer: CDK4/6, Src, JAK/STAT, PARP, HDAC, and PI3K/AKT/mTOR pathways. *Pharmgenomics Pers Med* (2014) 7:203–15. doi: 10.2147/PGPM.S52762

3. Vasan N, Toska E, Scaltriti M. Overview of the relevance of PI3K pathway in HR-positive breast cancer. *Ann Oncol* (2019) 30(Suppl_10):x3–x11. doi: 10.1093/annonc/mdz281

4. André F, Ciruelos EM, Juric D, Loibl S, Campone M, Mayer IA, et al. Alpelisib plus fulvestrant for PIK3CA-mutated, hormone receptor-positive, human epidermal growth factor receptor-2-negative advanced breast cancer: final overall survival results from SOLAR-1. *Ann Oncol* (2021) 32(2):208–17. doi: 10.1016/j.annonc.2020.11.011

5. Martínez-Sáez O, Chic N, Pascual T, Adamo B, Vidal M, González-Farré B, et al. Frequency and spectrum of PIK3CA somatic mutations in breast cancer. *Breast Cancer Res* (2020) 22(1):45. doi: 10.1186/s13058-020-01284-9

6. Rodon J, Dienstmann R, Serra V, Tabernero J. Development of PI3K inhibitors: lessons learned from early clinical trials. *Nat Rev Clin Oncol* (2013) 10(3):143–53. doi: 10.1038/nrclinonc.2013.10

7. Del Re M, Crucitta S, Lorenzini G, De Angelis C, Diodati L, Cavallero D, et al. PI3K mutations detected in liquid biopsy are associated to reduced sensitivity to CDK4/6 inhibitors in metastatic breast cancer patients. *Pharmacol Res* (2021) 163:105241. doi: 10.1016/j.phrs.2020.105241

8. Zhao L, Vogt PK. Helical domain and kinase domain mutations in p110α of phosphatidylinositol 3-kinase induce gain of function by different mechanisms. *Proc Natl Acad Sci* (2008) 105(7):2652–7. doi: 10.1073/pnas.0712169105

9. Mangone FR, Bobrovnitchaia IG, Salaorni S, Manuli E, Nagai MA. PIK3CA exon 20 mutations are associated with poor prognosis in breast cancer patients. *Clinics (Sao Paulo)* (2012) 67(11):1285–90. doi: 10.6061/clinics/2012(11)11

10. Kang S, Bader AG, Vogt PK. Phosphatidylinositol 3-kinase mutations identified in human cancer are oncogenic. *Proc Natl Acad Sci USA* (2005) 102(3):802–7. doi: 10.1073/pnas.0408864102

11. Tripathy D, Harnden K, Blackwell K, Robson M. Next generation sequencing and tumor mutation profiling: are we ready for routine use in the oncology clinic? *BMC Med* (2014) 12(1):140. doi: 10.1186/s12916-014-0140-3

12. Huang C-C, Tsai Y-F, Liu C-Y, Chao T-C, Lien P-J, Lin Y-S, et al. Comprehensive molecular profiling of Taiwanese breast cancers revealed potential therapeutic targets: prevalence of actionable mutations among 380 targeted sequencing analyses. *BMC Cancer* (2021) 21(1):199. doi: 10.1186/s12885-021-07931-4

13. André F, Ciruelos E, Rubovszky G, Campone M, Loibl S, Rugo HS, et al. Alpelisib for PIK3CA-mutated, hormone receptor–positive advanced breast cancer. *New Engl J Med* (2019) 380(20):1929–40. doi: 10.1056/NEJMoa1813904

14. *Taiwan Food and Drug Administration: Assessment Report* . Available at: https://www.google.com/url?sa=t&rct=j&q=&esrc=s&source=web&cd=&ved=2ahUKEwiUytLHwtL5AhXqglYBHbAEBDwQFnoECCIQAQ&url=https%3A%2F%2Fwww.fda.gov.tw%2Ftc%2Fincludes%2FGetFile.ashx%3Fmid%3D189%26id%3D36084%26t%3Ds&usg=AOvVaw1atEjQQExVG92i10vpWwob (Accessed August 19, 2022).

15. Liu CY, Huang CC, Tsai YF, Chao TC, Lien PJ, Lin YS, et al. VGH-TAYLOR: Comprehensive precision medicine study protocol on the heterogeneity of Taiwanese breast cancer patients. *Future Oncol* (2021) 17(31):4057–69 . doi: 10.2217/fon-2021-0131

16. *National Comprehensive Cancer Network. Breast Cancer (Version 1.2023)* (2023). Available at: https://www.nccn.org/store/Login/Register.aspx.

17. Hovelson DH, McDaniel AS, Cani AK, Johnson B, Rhodes K, Williams PD, et al. Development and validation of a scalable next-generation sequencing system for assessing relevant somatic variants in solid tumors. *Neoplasia* (2015) 17(4):385–99. doi: 10.1016/j.neo.2015.03.004

18. Fusco N, Malapelle U, Fassan M, Marchiò C, Buglioni S, Zupo S, et al. PIK3CA mutations as a molecular target for hormone receptor-positive, HER2-negative metastatic breast cancer. *Front Oncol* (2021) 11. doi: 10.3389/fonc.2021.644737

19. Ferreira-Gonzalez A. Plasma PIK3CA mutation testing in advanced breast cancer patients for personalized medicine: A value proposition. *J Appl Lab Med* (2020) 5(5):1076–89. doi: 10.1093/jalm/jfaa117

20. Anderson EJ, Mollon LE, Dean JL, Warholak TL, Aizer A, Platt EA, et al. A systematic review of the prevalence and diagnostic workup of PIK3CA mutations in HR+/HER2- metastatic breast cancer. *Int J Breast Cancer* (2020) 2020:3759179. doi: 10.1155/2020/3759179

21. Castaneda CA, Lopez-Ilasaca M, Pinto JA, Chirinos-Arias M, Doimi F, Neciosup SP, et al. PIK3CA mutations in Peruvian patients with HER2-amplified and triple negative non-metastatic breast cancers. *Hematology/Oncol Stem Cell Ther* (2014) 7 (4):142–8. doi: 10.1016/j.hemonc.2014.09.007

22. Sotiriou C, Ignatiadis M, Crestani TA, Venet D, Tyekucheva S, Irrthum A, et al. Clinico-molecular characteristics associated with outcomes in breast cancer patients treated with CDK4/6 inhibitors: Results from the AURORA Molecular Screening Initiative. *J Clin Oncol* (2023) 41(Suppl 16):1019. doi: 10.1200/JCO.2023.41.16_suppl.1019

23. Vasan N, Razavi P, Johnson JL, Shao H, Shah H, Antoine A, et al. Double PIK3CA mutations in cis increase oncogenicity and sensitivity to PI3Kα inhibitors. *Science* (2019) 366(6466):714–23. doi: 10.1126/science.aaw9032

24. Huang CS, Liu CY, Lu TP, Huang CJ, Chiu JH, Tseng LM, et al. Targeted sequencing of Taiwanese breast cancer with risk stratification by the concurrent genes signature: A feasibility study. *J Pers Med* (2021) 11(7):1-9.. doi: 10.3390/jpm11070613

25. Pavithran K, Jayamohanan H, Jose WM, Soman S, Vijaykumar DK, Ariyannur PS, et al. PI3K mutation is associated with reduced sensitivity to CDK4/6 inhibitors in metastatic breast cancer. *Ann Oncol* (2021) 32(5):S457–515. doi: 10.1016/j.annonc.2021.08.539

26. Giridhar KV, Choong GM, Leon-Ferre RA, O'Sullivan CC, Ruddy KJ, Haddad TC, et al. Abstract P6-18-09: Clinical management of metastatic breast cancer (MBC) after CDK 4/6 inhibitors: A retrospective single-institution study. *Poster Session Abstracts* (2019) 79(Suppl 4):P6-18-09. doi: 10.1158/1538-7445.SABCS18-P6-18-09

27. Bardia A, Su F, Solovieff N, Im S-A, Sohn J, Lee KS, et al. Genomic profiling of premenopausal HR+ and HER2– metastatic breast cancer by circulating tumor DNA and association of genetic alterations with therapeutic response to endocrine therapy and ribociclib. *JCO Precis Oncol* (2021) 5:1408–20. doi: 10.1200/PO.20.00445

28. André F, Hurvitz S, Fasolo A, Tseng L-M, Jerusalem G, Wilks S, et al. Molecular alterations and everolimus efficacy in human epidermal growth factor receptor 2–overexpressing metastatic breast cancers: combined exploratory biomarker analysis from BOLERO-1 and BOLERO-3. *J Clin Oncol* (2016) 34(18):2115–24. doi: 10.1200/JCO.2015.63.9161

29. Moynahan ME, Chen D, He W, Sung P, Samoila A, You D, et al. Correlation between PIK3CA mutations in cell-free DNA and everolimus efficacy in HR+, HER2–advanced breast cancer: results from BOLERO-2. *Br J Cancer* (2017) 116(6):726–30. doi: 10.1038/bjc.2017.25

frontiers | Frontiers in Oncology

TYPE Case Report
PUBLISHED 28 August 2023
DOI 10.3389/fonc.2023.1245701

OPEN ACCESS

EDITED BY
Zheng Wang,
Shanghai Jiao Tong University, China

REVIEWED BY
Xiaoqing Cai,
Sun Yat-sen University, China
Ruo Wang,
Shanghai Jiao Tong University, China

*CORRESPONDENCE
Wei Li
liwei7769@163.com

†These authors have contributed equally to this work

RECEIVED 23 June 2023
ACCEPTED 14 August 2023
PUBLISHED 28 August 2023

CITATION
Qu F, Liu Q, Lu R and Li W (2023) Disitamab Vedotin (RC48) combined with bevacizumab for treatment of HR-negative/HER2-positive metastatic breast cancer with liver and brain involvement: A case report.
Front. Oncol. 13:1245701.
doi: 10.3389/fonc.2023.1245701

Disitamab Vedotin (RC48) combined with bevacizumab for treatment of HR-negative/HER2-positive metastatic breast cancer with liver and brain involvement: A case report

Fei Qu[1,2†], Qian Liu[1,2†], Rongrong Lu[1,2] and Wei Li[1*]

[1]Department of Oncology, The First Affiliated Hospital of Nanjing Medical University, Nanjing, China, [2]The First Clinical College of Nanjing Medical University, Nanjing, China

Background: The overexpression of human epidermal growth factor receptor 2 (HER2) is strongly correlated with an elevated risk of developing distant metastases, particularly brain metastases, in breast cancer (BC) cases. RC48 (also known as Disitamab vedotin), represents a promising antibody-drug conjugate (ADC), that comprises three well-defined components: hertuzumab against the prominent tumor target-HER2, monomethyl auristatin E (MMAE) and a cleavable linker. Preclinical studies have demonstrated its robust antitumor activity in BC patient-derived xenograft models with HER2-positive or HER2-low expression. Additionally, antiangiogenic drugs like bevacizumab have shown potential efficacy on advanced BC *via* inhibiting pathological neovascularizationits.

Case presentation: Here, we will share our experience in treating a 49-year-old woman initially diagnosed with stage IV breast cancer characterized by hormone receptor (HR)-negativity and HER2-positivity. This complex case entailed brain and liver metastases, and the patient exhibited resistance to various HER2-targeted treatment regimens. Finally, the patient received RC48 plus bevacizumab as the advanced forth-line treatment, which was well tolerated with no observed toxicities. Subsequent radiological assessments revealed remarkable regression in the brain metastatic lesions, classified as having partial response based on the RECIST 1.1 system. The period of progression-free survival (PFS) was 7 months.

Conclusion: The present study underscores the efficacy of systemic treatment with RC48 in conjunction, showcasing substantial enhancement in both radiographic indicators and clinical symptomatology among patients with brain metastatic breast cancer (BMBC). More specifically, the sequential application of ADCs in combination with antiangiogenics presents a novel avenue for advancing the treatment landscape of metastatic BC.

KEYWORDS

HER2-positive, brain metastatic breast cancer, anti-angiogenesis, RC48, case report

Introduction

Breast cancer is now ranked first in terms of incidence and second as the leading cause of mortality among women worldwide. Within this context, HER2-positive BC comprises approximately 25% of all subtypes (1). These tumors express high levels of HER2, which is recognized as a cancer-driving gene and an independent prognostic determinant for BC (2). The emergence of brain metastases (BMs) presents a major clinical challenge that tends to develop in up to approximately 40% of individuals with HER2-positive status. To date, the treatment options for BMBC patients remain limited, focusing on local treatment, including whole-brain radiotherapy (WBRT) and, if applicable, surgical removal of the intracranial metastatic lesions (3). While initially effective, these interventions are linked to significant neurological or systemic repercussions attributed to the metastatic and infiltrative growth patterns, subsequently undermining the overall quality of life and offering limited scope for substantial prognosis enhancement (4). Hence, additional treatment options, including systemic therapy, are warranted to prolong survival. Several retrospective research findings have shown that patients with BMs who received HER2-targeted therapy experienced a prolonged median survival period compared to those who did not receive HER2-targeted therapy (5). The concurrent administration of docetaxel alongside trastuzumab and pertuzumab has emerged as a recommended standard front-line treatment option for patients with HER2-positive metastatic breast cancer (mBC) (6). However, the efficacy of this regimen within the context of BM patients is significantly limited due to the prevailing notion that monoclonal antibodies, as biomolecules, encounter difficulties in traversing the blood-brain barrier (BBB). In recent times, the field of clinical practice has witnessed the introduction of ado-trastuzumab (T-DM1), trastuzumab deruxtecan (T-DXd, DS8201), and a regimen based on the tyrosine kinase inhibitor pyrotinib. These have demonstrated encouraging results as second-line therapies for patients with untreated BMs. However, third-line therapy in HER2-positive BMBC patients has been met with controversies (7), and the identification of new therapeutic strategies is urgently required.

In the early 1900s, Paul Ehrlich conceptualized the notion of a "magic bullet". Against this historical backdrop, a novel category of medications for solid and hematologic malignancies emerged: namely, antibody-drug conjugates (ADCs) (8). Following drug administration, the ADC formulation contains three predominant circulating components: the conjugate (which constitutes the majority of the composition), specific antibodies, and free payload molecules. ADCs are created with the purpose of directly accomplishing their desired cell-structural objectives while being non-aggressive to healthy tissues, thereby mitigating systemic toxicities. Disitamab Vedotin (RC48), as a Chinese original HER2-targeting ADC, developed by Rongchang Biology, has shown promising potential in HER2-overexpressing locally advanced or metastatic gastric cancer and uroepithelial cancer, based on the results of RC48 C008, C005 and C009 studies (9). RC48 not only destroys cancer cells accurately and directly but also has the capacity to exert a "bystander effect" on neighboring cells (10, 11). This characteristic of internalized ADCs necessitates the diffusion of lipophilic payloads through cell membranes thereby playing a pivotal role in the efficacy of RC48 against malignancies characterized by heterogeneous target antigen expression. The pooled results of two studies (C001 and C003 CANCER) presented in the 2021 American Society of Clinical Oncology (ASCO) Meeting, provide compelling insights. Among 118 mBC patients treated with RC48, 70 cases were HER2-positive and 48 cases had low expression of HER2. Notably, 47 patients had previously undergone treatment with three or more chemotherapy regimens (12). The use of RC48 monotherapy exhibited discernible indicators of therapeutic efficacy, resulting in complete or partial remission for nearly 40% of patients undergoing treatment in later-line stages. In June 2021, the Center for Drug Evaluation in China granted a new indication for RC48 as a prospective breakthrough therapy for HER2-positive mBC patients with liver metastases who had been previously treated with trastuzumab and paclitaxel.

In addition, tumors require a constant and abundant supply of blood to sustain cellular replication and energy metabolism. Vascular endothelial growth factor (VEGF) is critical in modulating angiogenesis both in physiologic and pathologic conditions. Excessive VEGF signaling can induce abnormal angiogenesis within tumor tissues, due to increased tumor vessel dilatation, permeability, and leakage (12). Substantial support from laboratory and clinical investigations has highlighted the inverse relationship between VEGF expression levels and the clinical outcomes of breast cancer (BC) patients. Moreover, in preclinical models, brain metastases from BC were found to display higher microvessel density compared to their corresponding primary tumors (13), supporting the hypothesis that brain metastases may be more dependent on angiogenesis than extracranial breast tumors. A study of the possible influence of T-DM1 on blood vessels of HER2-amplified breast cancer brain metastasis model revealed a trend towards reduced vessel diameter and vascular fraction, thus preventing the formation of brain metastases and delaying their growth rate (14). In HER2-positive BMBC patients, the interplay between HER2 and VEGF pathways has laid a theoretical foundation for potentially effective therapies combining antiangiogenic drugs with HER2-targeting therapies (15, 16). The novel antiangiogenic drug bevacizumab, which is an intravenously administered recombinant monoclonal antibody was developed with VEGF in mind (17). In clinical practice, bevacizumab has exhibited impressive efficacy alongside manageable safety profiles in heavily treated patients with metastatic breast cancer (18).

However, to our knowledge, there are no published reports documenting the application of RC48 combined with antiangiogenic drugs for BC treatment. This report will present visible tumor shrinkage and substantial clinical improvement in responding to RC48 combined with bevacizumab treatment in one BC patient with brain and liver metastases.

Case presentation

In June 2019, a 49-year-old female patient presented at Jiangsu Province Hospital, Nanjing Medical University (Nanjing, China), with complaints of fatigue and thickening of the skin on her breasts.

The patient reported no discomfort such as obvious local aching or distending pain during the menstrual phase. Upon physical examination, a palpable, firm, and irregular mass was detected in the right breast, accompanied by skin erythema. Ultrasound examination of the breast identified a 4.7×4.6×2.7 cm^3 mass in the right breast, classified as level 6 according to the breast imaging reporting and data system (BI-RADS). Additionally, enlarged lymph nodes were observed in regions I, II, and III on the right axilla, suggesting a high probability of metastasis. Pathological analysis of the core needle biopsy specimen extracted from the mass revealed non-specific invasive breast cancer. Immunohistochemistry (IHC; HercepTest, Dako, Denmark) confirmed estrogen receptor (ER) -negative/progesterone receptor (PR) -negative and HER2 (3+) disease with Ki-67 of 25%+. A computed tomography (CT) scan revealed multiple metastases in the liver (Figure 1A), while a whole-body bone scintigraphy using 99m Tc-MDP did not reveal any notable abnormalities. The patient had no family history of breast or ovarian cancer, no medical history of radiation or hormonal replacement therapy, and no history of smoking, drinking, or other harmful behaviors. Ultimately, the patient was diagnosed with grade 3 invasive breast cancer, accompanied by right axillary lymph node and liver metastasis, cT2N2M1, stage IV.

Starting from July 6, 2019, until March 10, 2020, the patient underwent advanced first-line treatment with the TCbH regimen, a combination of nab–docetaxel, carboplatin, and trastuzumab. Efficacy evaluation was a partial response (PR) at that time. However, by February 2020, the patient began to experience lower limb muscle strength dysfunction, dizziness, and impaired fine motor coordination skills in both hands. Subsequently, a contrast–enhanced brain magnetic resonance imaging (MRI) revealed multiple brain metastases situated in the right parietal lobe and the left fronto-temporo-parieto-occipital lobe. The lesions were accompanied by obvious edema and the midline structure shifted to the right; the left lateral ventricle moved to the right under pressure. Despite substantial primary tumor and brain metastases growth and extensive tumor burden, the metastatic lesions in the liver gradually shrank and disappeared (Figure 1B). The final assessment of therapeutic efficacy resulted in the identification of progressive disease (PD). After a multi-disciplinary discussion, consideration was given to the following points: i) Radiographic examination revealed approximately five huge brain metastases. These metastases were surrounded by marked edema with a high risk of raised intracranial pressure; ii) Two ulcerations were detected in tumors in the upper-outer quadrant of the breast, accompanied by persistent malodorous surface discharge. The Breast Surgery department indicated that it might be able to perform palliative surgery, but the patient's condition should be fully informed; iii) systemic chemotherapy was necessary.

After careful consideration, the patient and the patient's family accepted our comprehensive treatment regimens. The patient accepted the standard second-line chemotherapy combining pyrotinib and capecitabine, starting on March 22, 2020. Concurrently, the patient received WBRT (54 Gy total, administered in 20 fractions, five times a week) and was administered with mannitol and dexamethasone to reduce intracranial pressure. On June 19, 2020, a modified radical mastectomy was performed and sent for histopathological examination. The postoperative TNM classification was ypT2N1aM1 G3 R0. The tumor was ER (-), PR (-), Her-2 (2+) and Ki67 (40%+). FISH analysis confirmed HER2 amplification. Notably, a BRCA test was not conducted. Postoperatively, the patient continued to be treated with the "pyrotinib + capecitabine" regimen. However, CA-153 levels elevated continuously and an MRI reexamination indicated enlarged and increased brain metastases on February 23, 2021, again indicating PD. Systemic CT suggested that liver metastases remained stable.

T-DXd, as the advanced third-line treatment was applied from March 2021. The initial dose of T-DXd was 200mg, administered every three weeks. In addition, the patient underwent gamma knife treatment for cerebellar metastasis on September 24, 2021. Enhanced CT and MRI with dynamic review during chemotherapy revealed a reduction in the size of intracranial and extracranial lesions. Overall, the best follow-up evaluations, conducted every two months, suggested a stable disease (SD) and the PFS was 11.5 months for the third-line treatment. In February 2022, MRI showed that the brain metastases were enlarged (Figure 2A), representing tumor progression. RC48 was begun

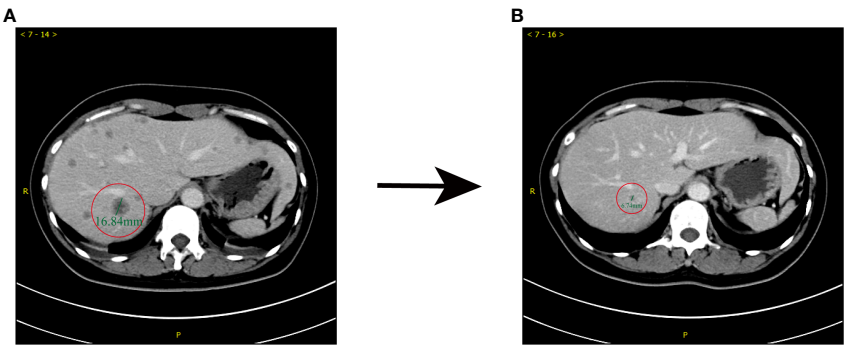

FIGURE 1
Comparison of enhanced CT prior to (June, 2019) and after (December, 2019) first-line treatment. **(A)** Before the administration of TCbH, abnormal small nodular signals were observed in the right lobe of the liver, which was 16 mm in diameter. **(B)** After 5 cycles of TCbH, shrinkage of the liver metastasis was observed; the diameter of the lesion was 6 mm.

after obtaining informed consent. RC48 (116mg, q2w) combined with bevacizumab (290 mg, q2w) as the advanced forth-line treatment, was administered. Notably, within two months, a reduction in size was observed on MRI scans, transitioning from 2.6 x 2.5 cm^2 to 1.5 x 1.3 cm^2 within the right parietal lobe (Figure 2B). As of June 28, 2022, the MRI demonstrated a further decrease in the dimensions of residual lesions (Figure 2C). At the time of writing, due to the re-progression of brain metastases (Figure 2D), the patient was treated with RC48 combined with bevacizumab and pyrotinib. This marked the start of the fifth-line treatment, from September 2022.

Furthermore, we systematically reviewed routine blood tests, tumor markers, biochemical indexes, as well as liver and kidney function electrolyte indicators during the administration of RC48 and bevacizumab, all of which were within the normal range, although they were changeset at different stages of the treatment. Apart from minor liver injury and nausea, which were controlled by symptomatic treatment, no other obvious drug-related toxicity was reported during the treatment. The therapeutic effect was that of partial remission. The patient received a total of 13 cycles of RC48 combined with bevacizumab and had a PFS (from treatment initiation to progression of BM) of 7 months. The summary of the patient's post-RC48 plus bevacizumab treatment results for key indicators is provided in Table 1, while Table 2 outlines the patient's treatment timeline. Notably, the patient has provided her consent for the publication of this case report.

Discussion

Brain metastases are a prevalent form of malignant intracranial tumors in adults, often leading to severe complications for individuals with solid cancers, ultimately impacting their survival prospects and quality of life. While trastuzumab-based therapy has demonstrated noteworthy advancements in the survival rates of patients with HER2-positive breast cancer subtypes, its role in preventing disease recurrence or progression into the brain remains limited (19). This phenomenon has been coined the "HER2 paradigm," wherein patients who exhibit exceptional systemic disease control or the absence of extracranial disease paradoxically experience an increase in the incidence of brain metastases (20). A possible reason for the "HER2 paradigm" is that some novel compounds including trastuzumab do not, or only partially, penetrate the BBB, effectively. The potential for the brain to serve as a "sanctuary site" for cancer arises from the possibility that therapeutic agents may not effectively target tumor cells that have successfully infiltrated the brain. Therefore, the treatment of HER2-targeting drug-resistant patients is an important clinical challenge.

Studies on antibody-drug conjugates (ADCs) targeting HER2, such as T-DM1 and T-DXd have reported promising outcomes. An exploratory analysis of central nervous system metastasis in the KAMILLA study, a prospective, single-arm phase IIIb clinical trial (21), shows that T-DM1 may prolong PFS and OS among patients with BMBC and is well-tolerated in this population. Moreover, T-DXd is characterized by a novel enzyme-cleavable linker and the payload (DXd) with high membrane permeability, thus emerging as a promising agent for the treatment of HER2+ mBC, supported by a series of clinical trials. The DESTINY-Breast 03 study, which included a subgroup of patients with stable brain metastases at baseline, revealed indicated that T-DXd achieved encouraging therapeutic outcomes for BMBC patients, with an mPFS of 15 months (22). TUXEDO-1, a prospective, single-arm, phase II clinical trial, verified the efficacy of T-DXd in HER2+ BCBM patients who were untreated or had progressed after prior local treatment (23). Among 15 eligible patients, the intracranial response rate (RR) was 73.3% (11/15) and the clinical benefit rate (CBR) was 92.9% (13/14).

The impact of BBB breakdown on the efficacy of systemic therapies against brain metastases remains a topic of debate. However, recent findings suggest that BBB disruption occurs during the progression of brain metastases, thereby facilitating the enhanced penetration of numerous drugs. Radiolabeling studies of ADCs showed drug aggregation in HER2-positive BMBC, suggesting that the compromised BBB may allow for the passage of ADCs (24). Furthermore, the pathological effects of WBRT on

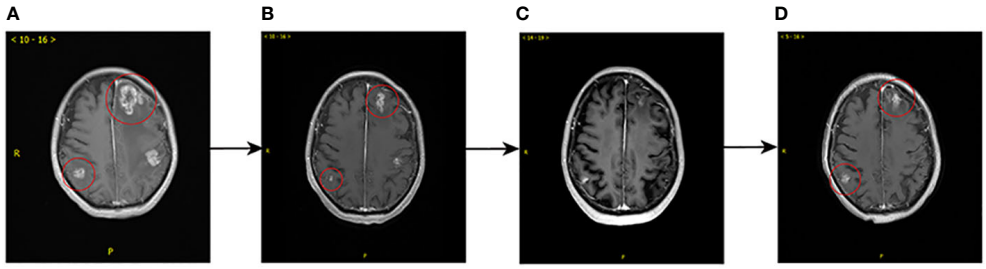

FIGURE 2
Comparison of brain MRI prior to (February, 2022) and after (September, 2022) forth-line treatment. **(A)** Before the administration RC48 plus bevacizumab, multiple brain metastases in the bilateral cerebellar hemispheres, the right parietal lobe and the left fronto-temporo-parieto-occipital lobe were observed, with obviously annular and nodular enhancement, the larger of which measured 2.6 x 2.5 cm2. **(B)** After 4 cycles, shrinkage of the brain metastases was observed, the larger of which measured 1.5 x 1.3 cm2, with diminished enhancement of some lesions. **(C)** After 7 cycles, further shrinkage of the brain metastases was observed. **(D)** After 13 cycles, MRI showed the volume of some brain metastatic sites increased with marked annular and nodular enhancement, the larger of which measured 1.7 x 1.3 cm2, which suggested local progression of tumor.

TABLE 1 Laboratory data of the patient after RC48 plus bevacizumab administration (September 21, 2022).

Hematology		Normal range	Biochemistry		Normal range
White blood cell	4.64×10^9/L	3.50–9.50	Total protein	63.3↓g/L	65.0–85.0
Neutrophil	41.10%	40.00–75.00	Albumin	38.6↓g/L	40.0–55.0
Eosinophil	2.60%	0.40–8.00	Total bilirubin	11.2μmol/L	5.1–19.0
Basophil	2.20↑%	0.00–1.00	AST	26.9U/L	13.0–35.0
Monophil	8.10%	3.00–10.00	ALT	38.7U/L	7.0–40.0
Lymphocyte	36.20%	20.00–50.00	LDH	194U/L	140–271
Red blood cell	3.84x10^12/L	3.80–5.10	UA	255μmol/L	155–357
Hemoglobin	112↓g/L	115–150	Creatinine	48.2μmol/L	44.0–133.0
Platelet	346x10^9/L	125–350	Na	142.5mmol/L	137.0-147.0
Hematology		Normal range	K	3.56mmol/L	3.50-5.30
CEA	7.16↑ng/ml	<4.7	Ca	2.21mmol/L	2.20-2.65
CA15-3	20.90U/ml	<25.0			
CA125	7.8U/ml	<35.00			

the BBB may increase the permeability of the drugs to exert therapeutic effects. As described by Stemmler et al., elevated levels of trastuzumab in cerebrospinal fluid (CSF) in the presence of impaired BBB following WBRT. Specifically, the serum/CSF trastuzumab ratio before and after WBRT was 420: 1 and 76:1 under conditions of impairment of the BBB, respectively (25). These data theoretically indicate that patients with HER2-positive BMBC can benefit from subsequent anti-HER2 therapy based on WBRT.

In addition, angiogenesis is closely related to HER2 signal transduction at the molecular level. In a preclinical study, the authors observed that VEGFR2-positive stromal vessel counts were higher in HER2-positive BC compared to other subtypes (26). In other words, the influence of HER2 on oncogenesis and metastasis may be partially mediated by the stimulation of angiogenesis, providing a solid theoretical basis for the use of antiangiogenic drugs in HER2-positive BC. Preclinical cancer models have suggested that antiangiogenic agents may facilitate ADC penetration and exposure of tumor cells by starving cancer cells and normalizing the aberrant structure and function of tumor vasculature (27). The blend of anetumab ravtansine or mirvetuximab soravtansine with bevacizumab has yielded potent effects and complete responses in preclinical ovarian cancer models (28, 29). These preclinical findings were recapitulated by a Phase 1b trail evaluating the clinical activity and safety of mirvetuximab soravtansine in combination with bevacizumab in heavily pretreated, platinum-resistant, FRα-positive, ovarian cancer patients, with a confirmed ORR of 39% and a median PFS of 6.9 months, which was superior to the benchmark values of the pivotal AURELIA trial (27%). The combination was more favorable in patients who were bevacizumab-naïve, less heavily pretreated (1-2 prior lines), and whose tumors exhibited medium/high FRα expression (ORR, 56%; PFS, 9.9 months). Reportably, only 4.5% of patients were observed to have grade 3 thrombocytopenia and 1.5% to have neutropenia, the anticipated overlapping toxicities (30).

In this context, we present a case in which the combination of RC48 with bevacizumab showed effectiveness in one patient with HER2-positive BC and effectively controlled refractory brain metastases after the failure of pyrotinib treatment. In addition, the patient also received WBRT and gamma knife radiotherapy for brain metastases before RC48 treatment. Surprisingly, this combination regimen produced remarkable results. Brain MRI indicated that the reduction of the brain metastases from breast cancer and alleviation of the brain edema lasted 7 months. The patient's headache and vomiting symptoms improved significantly. This may be due to the synergistic antitumor effect of ADC and antiangiogenic drugs through the BBB.

TABLE 2 Treatment history of the patient.

Line	1st	2nd	3rd	4th
Regimen	TCbH	Pyrotinib + Capecitabine	T-DXd	RC48+bevacizumab
Treatment period (months)	9	11	11	7
Best of response	PR	PR	SD	PR

Moreover, as more and more ADCs are developed and enter clinical settings, some of which target the same antigen or have comparable payloads, determining the optimal therapeutic sequencing of these agents represents an upcoming challenge. Sequential ADC administration may be practical and efficient. In the present case, RC48 has demonstrated activity in the patient who had previously received T-DXd, most likely due to the different mechanisms underpinning the payloads of these two ADCs. Other reasons for the phenomenon are unclear and warrant further exploration.

Therefore, based on the above analysis, there is reason to believe that administering RC48 with bevacizumab is feasible and effective. Combined therapy can enhance the activity of a single drug, reduce the risk of drug resistance and further improve its efficacy (31). Moreover, ongoing efforts encompass an array of combinatorial strategies, extensively explored through both preclinical models and clinical investigations, including coadministration with immune checkpoint inhibitors (ICIs), tyrosine kinase inhibitors (TKIs), large or small molecule anti-angiogenic drugs, DNA-damage response agents, and metronomic chemotherapy, thus integrating and optimizing existing clinical treatment options.

Conclusion

In recent times, there has been a notable surge of interest among clinicians in addressing the challenges posed by patients grappling with HR-negative/HER2-positive brain metastatic breast cancer (BMBC), particularly owing to the involvement of multiple organs and poor physical condition. The application of RC48 is anticipated to exert a substantial and meaningful influence on the prognosis of these individuals. Additional translational and clinical investigations are imperative to ascertain whether RC48's impact on BMBC will culminate in enduring advantages for disease management. Furthermore, it is crucial to identify optimal partners that offer additive or synergistic benefits, devoid of overlapping toxicities when administered alongside ADCs.

Data availability statement

The original contributions presented in the study are included in the article/supplementary material. Further inquiries can be directed to the corresponding author.

Ethics statement

Written informed consent was obtained from the individual(s) for the publication of any potentially identifiable images or data included in this article.

Author contributions

FQ and QL analyzed the cases and radiological images. FQ and RL participated in writing. WL reviewed the manuscript. All authors contributed to the article and approved the submitted version.

Conflict of interest

The authors declare that the research was conducted in the absence of any commercial or financial relationships that could be construed as a potential conflict of interest.

Publisher's note

References

1. Ferrando-Díez A, Felip E, Pous A, Bergamino Sirven M, Margeli M. Targeted therapeutic options and future perspectives for HER2-positive breast cancer. *Cancers (Basel).* (2022) 14(14):3305. doi: 10.3390/cancers14143305

2. Rinnerthaler G, Gampenrieder SP, Greil R. HER2 directed antibody-drug-conjugates beyond T-DM1 in breast cancer. *Int J Mol Sci* (2019) 20(5):1115. doi: 10.3390/ijms20051115

3. Galanti D, Inno A, La Vecchia M, Borsellino N, Incorvaia L, Russo A, et al. Current treatment options for HER2-positive breast cancer patients with brain metastases. *Crit Rev Oncol Hematol* (2021) 161:103329. doi: 10.1016/j.critrevonc.2021.103329

4. Deluche E, Antoine A, Bachelot T, Lardy-Cleaud A, Dieras V, Brain E, et al. Contemporary outcomes of metastatic breast cancer among 22,000 women from the multicentre ESME cohort 2008-2016. *Eur J Cancer* (2020) 129:60–70. doi: 10.1016/j.ejca.2020.01.016

5. Chiec L, Kumthekar P. Targeting HER2+ Breast cancer brain metastases: A review of brain-directed HER2-directed therapies. *CNS Drugs* (2022) 36(2):167–79. doi: 10.1007/s40263-021-00894-x

6. Swain SM, Miles D, Kim SB, Im YH, Im SA, Semiglazov V, et al. Pertuzumab, trastuzumab, and docetaxel for HER2-positive metastatic breast cancer (CLEOPATRA): end-of-study results from a double-blind, randomised, placebo-controlled, phase 3 study. *Lancet Oncol* (2020) 21(4):519–30. doi: 10.1016/S1470-2045(19)30863-0

7. Ferrario C, Christofides A, Joy AA, Laing K, Gelmon K, Brezden-Masley C. Novel therapies for the treatment of HER2-positive advanced breast cancer: A Canadian perspective. *Curr Oncol* (2022) 29(4):2720–34. doi: 10.3390/curroncol29040222

8. Tarantino P, Carmagnani Pestana R, Corti C, Modi S, Bardia A, Tolaney SM, et al. Antibody-drug conjugates: Smart chemotherapy delivery across tumor histologies. *CA Cancer J Clin* (2022) 72(2):165–82. doi: 10.3322/caac.21705

9. Peng Z, Liu T, Wei J, Wang A, He Y, Yang L, et al. Efficacy and safety of a novel anti-HER2 therapeutic antibody RC48 in patients with HER2-overexpressing, locally advanced or metastatic gastric or gastroesophageal junction cancer: a single-arm phase II study. *Cancer Commun (Lond).* (2021) 41(11):1173–82. doi: 10.1002/cac2.12214

10. Shi F, Liu Y, Zhou X, Shen P, Xue R, Zhang M. Disitamab vedotin: a novel antibody-drug conjugates for cancer therapy. *Drug Deliv.* (2022) 29(1):1335–44. doi: 10.1080/10717544.2022.2069883

11. Li L, Xu MZ, Wang L, Jiang J, Dong LH, Chen F, et al. Conjugating MMAE to a novel anti-HER2 antibody for selective targeted delivery. *Eur Rev Med Pharmacol Sci* (2020) 24(24):12929–37. doi: 10.26355/eurrev_202012_24196

12. Gyamfi J, Eom M, Koo JS, Choi J. Multifaceted roles of interleukin-6 in adipocyte-breast cancer cell interaction. *Transl Oncol* (2018) 11(2):275–85. doi: 10.1016/j.tranon.2017.12.009

13. Monsky WL, Mouta Carreira C, Tsuzuki Y, Gohongi T, Fukumura D, Jain RK. Role of host microenvironment in angiogenesis and microvascular functions in human breast cancer xenografts: mammary fat pad versus cranial tumors. *Clin Cancer Res* (2002) 8(4):1008–13.

14. Askoxylakis V, Ferraro GB, Kodack DP, Badeaux M, Shankaraiah RC, Seano G, et al. Preclinical efficacy of ado-trastuzumab emtansine in the brain microenvironment. *J Natl Cancer Inst* (2016) 108(2):djv313. doi: 10.1093/jnci/djv313

15. Izumi Y, Xu L, di Tomaso E, Fukumura D, Jain RK. Tumour biology: herceptin acts as an anti-angiogenic cocktail. *Nature* (2002) 416(6878):279–80. doi: 10.1038/416279b

16. Alameddine RS, Otrock ZK, Awada A, Shamseddine A. Crosstalk between HER2 signaling and angiogenesis in breast cancer: molecular basis, clinical applications and challenges. *Curr Opin Oncol* (2013) 25(3):313–24. doi: 10.1097/CCO.0b013e32835ff362

17. Oguntade AS, Al-Amodi F, Alrumayh A, Alobaida M, Bwalya M. Anti-angiogenesis in cancer therapeutics: the magic bullet. *J Egypt Natl Canc Inst* (2021) 33(1):15. doi: 10.1186/s43046-021-00072-6

18. Li Z, Guo F, Han Y, Wang J, Xu B. Efficacy and safety of bevacizumab in pretreated metastatic breast cancer: A systematic review and meta-analysis. *Oncol Res Treat* (2022) 45(10):608–17. doi: 10.1159/000525882

19. Wang Y, Ye F, Liang Y, Yang Q. Breast cancer brain metastasis: insight into molecular mechanisms and therapeutic strategies. *Br J Cancer* (2021) 125(8):1056–67. doi: 10.1038/s41416-021-01424-8

20. Lin NU, Winer EP. Brain metastases: the HER2 paradigm. *Clin Cancer Res* (2007) 13(6):1648–55. doi: 10.1158/1078-0432.CCR-06-2478

21. Montemurro F, Delaloge S, Barrios CH, Wuerstlein R, Anton A, Brain E, et al. Trastuzumab emtansine (T-DM1) in patients with HER2-positive metastatic breast cancer and brain metastases: exploratory final analysis of cohort 1 from KAMILLA, a single-arm phase IIIb clinical trial(☆). *Ann Oncol* (2020) 31(10):1350–8. doi: 10.1016/j.annonc.2020.06.020

22. Hurvitz S, Kim SB, Chung WP, Im SA, Park YH, Hegg R, et al. Trastuzumab deruxtecan (T-DXd; DS-8201a) vs. trastuzumab emtansine (T-DM1) in patients (pts) with HER2+ metastatic breast cancer (mBC): subgroup analyses from the randomized phase 3 study DESTINY-Breast03. *Cancer Res* (2022) 82(4 SUPPL):GS3-01. doi: 10.1158/1538-7445.SABCS21-GS3-01

23. Bartsch R, Berghoff AS, Furtner J, Marhold M, Bergen ES, Roider-Schur S, et al. 165MO Trastuzumab-deruxtecan (T-DXd) in HER2-positive breast cancer patients (pts) with active brain metastases: Primary outcome analysis from the TUXEDO-1 trial. *Ann Oncol* (2022) 33(suppl_3):S194–S223. doi: 10.1016/j.annonc.2022.03.184

24. Keith KC, Lee Y, Ewend MG, Zagar TM, Anders CK. ACTIVITY OF TRASTUZUMAB-EMTANSINE (TDM1) IN HER2-POSITIVE BREAST CANCER BRAIN METASTASES: A CASE SERIES. *Cancer Treat Commun* (2016) 7:43–6. doi: 10.1016/j.ctrc.2016.03.005

25. Stemmler HJ, Schmitt M, Willems A, Bernhard H, Harbeck N, Heinemann V. Ratio of trastuzumab levels in serum and cerebrospinal fluid is altered in HER2-positive breast cancer patients with brain metastases and impairment of blood-brain barrier. *Anticancer Drugs* (2007) 18(1):23–8. doi: 10.1097/01.cad.0000236313.50833.ee

26. Nasir A, Holzer TR, Chen M, Man MZ, SChade AE. Differential expression of VEGFR2 protein in HER2 positive primary human breast cancer: potential relevance to anti-angiogenic therapies. *Cancer Cell Int* (2017) 17:56. doi: 10.1186/s12935-017-0427-5

27. Fuentes-Antrás J, Genta S, Vijenthira A, Siu LL. Antibody-drug conjugates: in search of partners of choice. *Trends Cancer* (2023) 9(4):339–54. doi: 10.1016/j.trecan.2023.01.003

28. Quanz M, Hagemann UB, Zitzmann-Kolbe S, Stelte-Ludwig B, Golfier S, Elbi C, et al. Anetumab ravtansine inhibits tumor growth and shows additive effect in combination with targeted agents and chemotherapy in mesothelin-expressing human ovarian cancer models. *Oncotarget* (2018) 9(75):34103–21. doi: 10.18632/oncotarget.26135

29. Ponte JF, Ab O, Lanieri L, Lee J, Coccia J, Bartle LM, et al. Mirvetuximab soravtansine (IMGN853), a folate receptor alpha-targeting antibody-drug conjugate, potentiates the activity of standard of care therapeutics in ovarian cancer models. *Neoplasia* (2016) 18(12):775–84. doi: 10.1016/j.neo.2016.11.002

30. O'Malley DM, Matulonis UA, Birrer MJ, Castro CM, Gilbert L, Vergote I, et al. Phase Ib study of mirvetuximab soravtansine, a folate receptor alpha (FRα)-targeting antibody-drug conjugate (ADC), in combination with bevacizumab in patients with platinum-resistant ovarian cancer. *Gynecol Oncol* (2020) 157(2):379–85. doi: 10.1016/j.ygyno.2020.01.037

31. Park S, Jiang Z, Mortenson ED, Deng L, Radkevich-Brown O, Yang X, et al. The therapeutic effect of anti-HER2/neu antibody depends on both innate and adaptive immunity. *Cancer Cell* (2010) 18(2):160–70. doi: 10.1016/j.ccr.2010.06.014

frontiers | Frontiers in Oncology

TYPE Original Research
PUBLISHED 28 August 2023
DOI 10.3389/fonc.2023.1216438

OPEN ACCESS

EDITED BY
Deniz Can Guven,
Hacettepe University, Türkiye

REVIEWED BY
Wanjian Gu,
Affiliated Hospital of Nanjing University of Chinese Medicine, China
Hongmei Cui,
Lanzhou University, China

*CORRESPONDENCE
Gulnihal Ozcan
guozcan@ku.edu.tr

RECEIVED 03 May 2023
ACCEPTED 09 August 2023
PUBLISHED 28 August 2023

CITATION
Ozcan G (2023) *PTCH1* and *CTNNB1* emerge as pivotal predictors of resistance to neoadjuvant chemotherapy in ER+/HER2- breast cancer.
Front. Oncol. 13:1216438.
doi: 10.3389/fonc.2023.1216438

PTCH1 and *CTNNB1* emerge as pivotal predictors of resistance to neoadjuvant chemotherapy in ER+/HER2- breast cancer

Gulnihal Ozcan[1,2]*

[1]Department of Medical Pharmacology, Koç University School of Medicine, Istanbul, Türkiye, [2]Koç University Research Center for Translational Medicine (KUTTAM), Istanbul, Türkiye

Introduction: Endeavors in the molecular characterization of breast cancer opened the doors to endocrine therapies in ER+/HER2- breast cancer, increasing response rates substantially. Despite that, taxane-based neoadjuvant chemotherapy is still a cornerstone for achieving breast-conserving surgery and complete tumor resection in locally advanced cancers with high recurrence risk. Nonetheless, the rate of chemoresistance is high, and deselecting patients who will not benefit from chemotherapy is a significant task to prevent futile toxicities. Several multigene assays are being used to guide decisions on chemotherapy. However, their development as prognostic assays but not predictive assays limits predictive strength, leading to discordant results. Moreover, high costs impediment their use in developing countries. For global health equity, robust predictors that can be cost-effectively incorporated into routine clinical management are essential.

Methods: In this study, we comprehensively analyzed 5 GEO datasets, 2 validation sets, and The Cancer Genome Atlas breast cancer data to identify predictors of resistance to taxane-based neoadjuvant therapy in ER+/HER2- breast cancer using efficient bioinformatics algorithms.

Results: Gene expression and gene set enrichment analysis of 5 GEO datasets revealed the upregulation of 63 genes and the enrichment of CTNNB1-related oncogenic signatures in non-responsive patients. We validated the upregulation and predictive strength of 18 genes associated with resistance in the validation cohort, all exhibiting higher predictive powers for residual disease and higher specificities for ER+/HER2- breast cancers compared to one of the benchmark multi-gene assays. Cox Proportional Hazards Regression in three different treatment arms (neoadjuvant chemotherapy, endocrine therapy, and no systemic treatment) in a second comprehensive validation cohort strengthened the significance of *PTCH1* and *CTNNB1* as key predictors, with hazard ratios over 1.5, and 1.6 respectively in the univariate and multivariate models.

Discussion: Our results strongly suggest that PTCH1 and CTNNB1 can be used as robust and cost-effective predictors in developing countries to guide decisions on chemotherapy in ER +/HER2- breast cancer patients with a high risk of

recurrence. The dual function of PTCH1 as a multidrug efflux pump and a hedgehog receptor, and the active involvement of CTNNB1 in breast cancer strongly indicate that *PTCH1* and *CTNNB1* can be potential drug targets to overcome chemoresistance in ER +/HER2- breast cancer patients.

KEYWORDS

breast cancer, chemoresistance, taxane-based neoadjuvant chemotherapy, predictive markers, precision medicine, bioinformatics

1 Introduction

Breast Cancer is the most frequent cancer and the leading cause of mortality from cancer in women worldwide (1). Elaborate investigation of the molecular mechanisms revealed the significance of estrogen receptor (ER), progesterone receptor (PR), and human epidermal growth factor receptor (HER2) in breast cancer. This knowledge enabled the classification of breast cancer into three subtypes; ER+/HER2-, HER2+, and triple-negative breast cancer (TNBC) which lacks all three receptors.

ER+/HER2- breast cancers constitute more than 70% of breast cancer cases, mainly consisting of luminal A and luminal B PAM50 intrinsic subtypes (2). Luminal A-type breast cancer is characterized by ER positivity, HER2 negativity, high expression of PR, and low Ki67. Luminal B-type breast cancers are also ER+ cancers but HER2 status may be negative or positive, PR expression may be low, and Ki67 may be high, in contrast to the luminal A-type (3, 4).

The mainstay of systemic therapy in ER+/HER2- breast cancers is endocrine therapy. However, resistance to endocrine therapy is a handicap in locally advanced breast cancer patients with high risk, leading to inadmissible recurrence rates (5). In this patient group taxane-based neoadjuvant chemotherapy is crucial to prevent relapse, especially in luminal B-type ER+/HER2- breast cancers. Neoadjuvant chemotherapy is crucial for down-staging the tumors to achieve complete tumor resection and breast-conserving surgery in locally advanced breast cancer patients with high recurrence risk. Moreover, neoadjuvant chemotherapy may provide a chance to guide decisions on adjuvant chemotherapy based on the response to neoadjuvant therapy (3, 5, 6). Nonetheless, response rates to taxane-based neoadjuvant chemotherapy are low in ER+/HER2- breast cancer patients compared to HER2+ breast cancers and TNBC (4, 6, 7). Since chemotherapeutics come with a cost of non-specific toxicities to normal tissues, deselecting patients who will not benefit from neoadjuvant chemotherapy is crucial to refrain from the unnecessary toxicities of chemotherapeutics.

The last two decades had witnessed intensive efforts to develop multi-gene assays for guiding decisions on therapy for breast cancer patients. Among several of these, Oncotype DX, MammaPrint, Endopredict, Prosigna, and Breast Cancer Index are incorporated into treatment guidelines as tools that may be used in patients where decisions on systemic chemotherapy are indefinite after primary clinical assessment (4). However, these multi-gene expression assays were originally developed as prognostic assays to estimate the risk of recurrence after endocrine therapy, but not to predict whether high-risk patients will respond to chemotherapy. Later trials on their predictive utility proposed these tests as tools that can provide insight for decisions on systemic chemotherapy. Despite that, the risk scores predicted by different multi-gene assays are commonly discordant and the benefits they provide over the 4-gene IHC assay (IHC4), which involves immunohistochemical analysis of the ER, PR, HER2, and the proliferation marker Ki67, is unclear. For instance, one of the most used benchmark assays, Oncotype Dx, consists of two main gene groups: ER-related genes and Ki67-related genes. If the expression of ER-related genes is high, the patient is considered low risk and undergoes endocrine therapy. On the other hand, patients with a high expression of Ki67-related genes are considered high risk and undergo neoadjuvant chemotherapy (8–12).

Another obstacle to the use of these multi-gene assays is their costs. Although, countries in which public health insurance systems reimburse these tests, like the United Kingdom and Germany, got benefit in the prediction of patients who will not respond to therapy (13, 14), limited coverage of health insurance systems in many developing countries impediment the chance of incorporating these tests into routine clinical management (15). For global health equity, the identification of robust predictors of resistance that can be cost-effectively incorporated into clinical management is required in breast cancer. Such predictive markers may also provide a chance for the selection of patients eligible for newly developed molecular targeted agents in the first-line setting, before subjecting them to the effects of chemotherapeutics.

In this study, we aimed to identify pivotal predictors for resistance to taxane-based neoadjuvant therapy in ER+/HER2- breast cancer that would guide decisions on neoadjuvant chemotherapy. To this end, we analyzed five GEO breast cancer datasets including a total of 513 patients. We identified the enrichment of β-catenin (CTNNB1)-related oncogenic signatures and 63 commonly upregulated genes associated with resistance. For validation of the upregulation and predictive strength of these 63 genes, we utilized a cohort of 512 ER+/HER2- patients who had undergone taxane-based systemic therapy in the ROC plotter database developed by Fekete & Győrffy for the validation of predictive markers in cancer (16). We validated that, 18 genes out of 63 upregulated genes had high and significant predictive values for residual disease in ER+/HER2- breast cancer. We comparatively analyzed these 18 genes with the most used multi-gene assay

signatures in this validation cohort and The Cancer Genome Atlas (TCGA) dataset. With further analysis in a second cohort of 316 ER+/HER2- breast cancer patients who underwent neoadjuvant therapy in the KM plotter database by Győrffy et al. (17, 18), we validated the significance of 4 out of 18 genes together with CTNNB1 in relapse-free survival. Lastly, Cox Proportional Hazards Regression put forward PTCH1 and CTNNB1 as key markers of resistance to neoadjuvant therapy in ER+/HER2- breast cancer. Figure 1 summarizes the algorithms we used to identify these 2 robust predictors.

2 Materials and methods

2.1 Data collection and identification of differentially expressed genes

To investigate the markers of resistance to taxane-based neoadjuvant chemotherapy in ER+/HER2- breast cancer, we analyzed GSE20194, GSE20271, GSE25055, GSE25065, and GSE32646 datasets in GEO (https://www.ncbi.nlm.nih.gov/geo/). All datasets included mRNA-sequencing data from fine needle aspiration biopsy (FNA) or core biopsy (CBX) samples collected from patients before surgery and any systemic therapy (19–25). Only patients with ER-positivity and HER2-negativity were included in the analysis. We did not include patients with other receptor subtypes of breast cancer, patients who did not receive taxane-based neoadjuvant therapy, or for whom information on the chemotherapy and the response to therapy was not available. Pathological complete response (pCR) was accepted as the surrogate of sensitivity to chemotherapy and residual disease (RD) was accepted as the surrogate of chemoresistance. Information on the number of patients with RD or pCR, chemotherapy regimens, and PAM50 intrinsic subtypes is summarized in Supplementary Table 1.

To identify differentially expressed genes (DEGs) in chemoresistant patients compared with chemosensitive patients, we used the GEO2R web tool (https://www.ncbi.nlm.nih.gov/geo/geo2r/). In total, we analyzed samples from 468 chemoresistant and 45 chemosensitive patients with ER+/HER2- breast cancer. Since response rates to taxane-based chemotherapy are low in ER+/HER2- breast cancer, the number of chemosensitive patients was much lower compared to the number of chemoresistant patients in all datasets. To avoid bias that could be caused by the imbalance in the number of resistant vs. sensitive patients or the inhomogeneous distribution of data, we applied log transformation and force normalization to all datasets. The p-value cut-off was selected as 0.05 for statistical significance. Genes with a log-fold change smaller than -0.2 were accepted as downregulated genes and genes with a log-fold change greater than 0.2 were accepted as upregulated genes. The volcano plots for DEGs were plotted on Image GP (http://www.ehbio.com/ImageGP). To identify the DEGs

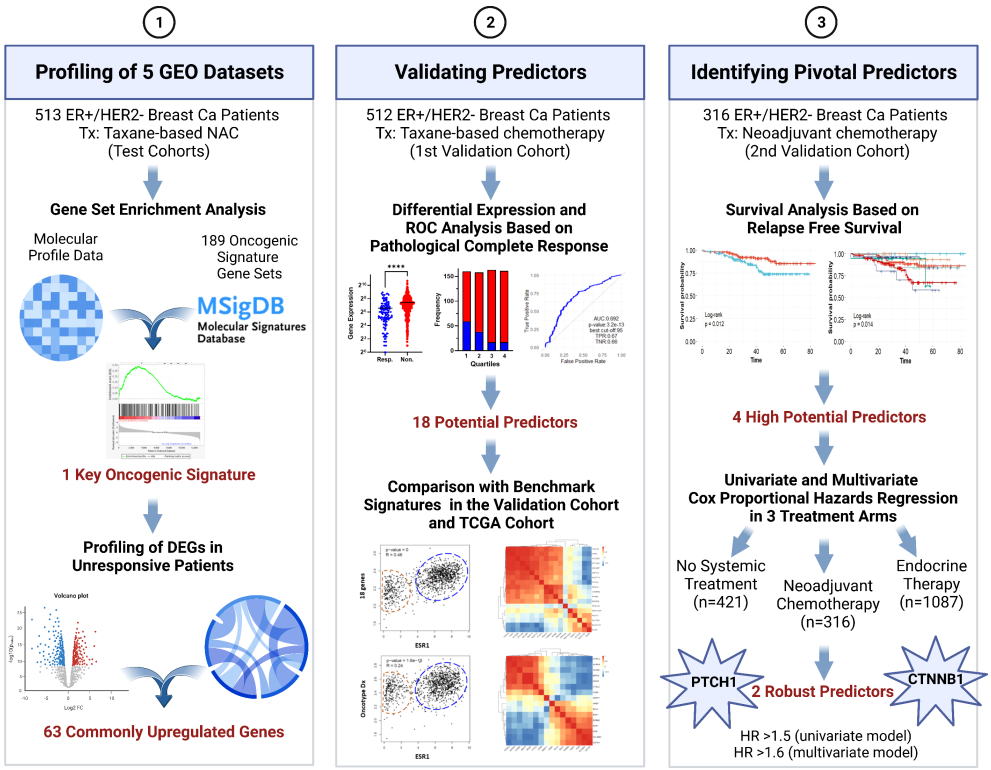

FIGURE 1
The algorithm used in the study for identifying pivotal predictors in ER+/HER2- breast cancer. DEG, differentially expressed genes; NAC, neoadjuvant chemotherapy; ROC, Receiver/Relative-operating characteristics; Tx, treatment. Created with BioRender.com.

and ontologies shared by different datasets we analyzed the data on Metascape (26) (https://metascape.org) and extracted the circos plots.

2.2 Gene set enrichment analysis

To dissect the enriched hallmark gene sets and oncogenic signature gene sets in ER+/HER2- breast tumors resistant to taxane-based neoadjuvant chemotherapy, we performed gene set enrichment analysis on Gene Set Enrichment Analysis software GSEA_4.2.3 (27). First, we prepared the list of t values calculated in GEO2R for the differential expression of each gene in non-responsive patients compared to the responsive patients in each dataset. Then we uploaded the pre-ranked t-value lists for each dataset separately to the GSEA_4.2.3. We have chosen hallmark gene sets (50 sets) or oncogenic signature gene sets (189 sets) from Molecular Signatures Database (MSigDB) and ran the GSEA-Preranked tool (28, 29). We evaluated the GSEA plots, enrichment scores, normalized enrichment scores, and p-values for each reference gene set to find out statistically enriched hallmark genes and oncogenic signatures in 5 GEO datasets.

2.3 Functional annotation, enrichment, and hierarchical clustering analysis

To identify the gene ontologies and pathways that the DEGs were enriched, we analyzed the list of 63 commonly upregulated genes in non-responsive patients on The Database for Annotation, Visualization, and Integrated Discovery (DAVID) (Version 6.8) (https://david.ncifcrf.gov/). The gene ontologies (GO-CC: cellular compartments, GO-MF: molecular functions, and GO-BP: biological processes) and Kyoto Encyclopedia of Genes and Genomes (KEGG) pathways listed in the top enrichment clusters were explored (p-value significance cut-off: 0.05).

2.4 Gene expression profiling and receiver operating characteristic analysis

To validate the upregulation of key genes in patients who did not respond to taxane-based therapy, and demonstrate their specificity to ER+/HER2- breast cancer, we analyzed the data for 512 ER+/HER2- patients (437 non-responders vs 75 responders), 71 HER2+/ER- patients (31 non-responders vs. 40 responders), 204 TNBC patients (125 non-responders vs. 79 responders) who received taxane-based chemotherapy on the ROC-plotter database (16). The patients who received endocrine therapy or anti-HER2 therapy were not included in the gene expression profiling and ROC curve analysis. Pathological complete response was considered as the surrogate for responsiveness in both analysis types.

We evaluated the fold-change in gene expression in non-responders vs. responders and p-values calculated with the Mann-Whitney test (p-value cut-off=0.05). We also evaluated the frequency of responders and non-responders at each quartile of gene expression. The graphs for this analysis were plotted in GraphPad Prism 9. To validate the value of the key markers in predicting resistance to taxane-based chemotherapy, we analyzed the Receiver/Relative Operating Characteristic (ROC) curves of the genes in the ROCplotter (16). The data for the true positive rate (TPR), and true negative rate (TNR) calculated by the "pROC" package in R was used to plot ROC curves with the "ggplot2" package in R. We evaluated the area under the curve (AUC), ROC p-values, and calculated the positive predictive values (PPV) and negative predictive values (NPV) using the TPR, and TNR values extracted from the ROC analysis.

2.5 Kaplan Meier survival analysis and Cox proportional hazards regression

To investigate the effect of upregulated genes on survival we analyzed the KM-survival for 316 ER+/HER2- breast cancer patients who underwent neoadjuvant chemotherapy on the Kaplan-Meier Plotter database (17). For all genes, we downloaded the gene expression data (both categorical and continuous data) and relapse-free survival data for these 316 patients to perform KM survival analysis and Cox Proportional Hazards Regression. We built the univariate and multivariate survival models and Cox Proportional Hazards models with these genes using the 'survival' package in R. In KM analysis we included categorical expression of genes as high or low. We plotted the KM-survival plots using the 'survminer' and 'ggplot2' packages in R. We extracted the log-rank p-values for each model. The Proportional Hazards assumption for Cox models was tested with the Schoenfeld test in R using the 'survival' and 'survminer' packages in R. The FDR-adjusted p-values for Cox Proportional Hazards models were calculated by the 'p.adjust' package in R using the "Benjamini-Hochberg" method.

To validate the potential of *PTCH1*, and *CTNNB1* as predictors in ER+/HER2- breast cancer patients, we additionally extracted data for 421 ER+/HER2- patients who had not undergone any systemic therapy and 1087 ER+/HER2- patients who underwent endocrine therapy in KM plotter database. We established Cox Proportional Hazards models using *PTCH1*, and *CTNNB1* as covariates in three treatment arms: no systemic therapy, neoadjuvant chemotherapy, and endocrine therapy. To build Cox models, we used the 'survival' package in R and included gene expression values as log2-normalized continuous variables. We extracted the concordance and log-rank p-values for each model. We also compared the goodness of fit of each model compared to the null model with ANOVA. We extracted the chi-square and p-values as an output of this analysis.

2.6 Gene signature and gene correlation analysis

We analyzed the correlation of the 18 gene list with Oncotype Dx, EndoPredict, or MammaPrint signatures in TCGA breast cancer data using the correlation analysis tool of GEPIA2 (http://gepia2.cancer-pku.cn) (30). The Pearson method was used for

correlation analysis. The housekeeping/reference genes in the signatures were excluded from the analysis. The correlation of the 18 gene list and Oncotype Dx, and EndoPredict signatures with *ESR1, ERBB2*, or *ESR1* plus *ERBB2* were also analyzed in GEPIA2. For the Oncotype Dx signature, the *ESR1, ERBB2*, or *ESR1* plus *ERBB2* was not included in the signature when correlation with *ESR1, ERBB2*, or *ESR1* plus *ERBB2* was analyzed respectively.

To investigate the correlation between the expression of each gene in the 18 gene list and Oncotype Dx genes, we extracted the data for 316 ER+/HER2- breast cancer patients who underwent neoadjuvant chemotherapy on the Kaplan-Meier Plotter database. We performed the hierarchical clustering analysis of the correlation matrices on Image GP using both the Pearson and the Spearman methods (http://www.ehbio.com/ImageGP) (31). Additionally, we extracted the data for correlation coefficients between all signature genes in all breast cancer patients (n=1100), patients with luminal A-type (n=568), and luminal B-type (n=219) breast cancer patients in the TCGA dataset from TIMER.2.0 (http://timer.cistrome.org) (32). We performed the hierarchical clustering analysis of the correlation matrices on Image GP using the Spearman method.

3 Results

3.1 Oncogenic signatures and upregulated genes associated with resistance to taxane-based neoadjuvant chemotherapy

To identify the markers associated with resistance to taxane-based neoadjuvant chemotherapy in ER+/HER2- breast cancer, we analyzed GSE20194, GSE20271, GSE25055, GSE25065, and GSE32646 datasets in GEO2R. These datasets included gene profiling data from breast cancers with different subtypes (19–25). We included and analyzed a total of 468 chemoresistant and 45 chemosensitive patients with ER+/HER2- breast cancer who underwent taxane-based neoadjuvant chemotherapy. We considered pathological complete response (pCR) as the surrogate of chemosensitivity and residual disease (RD) as the surrogate of chemoresistance. Supplementary Table 1 lists the number of patients with RD or pCR in each dataset, with information on the source of samples, PAM50 intrinsic classes, and chemotherapy regimens.

First, we performed gene set enrichment analysis for each dataset to find out hallmark genes and oncogene signatures commonly enriched in patients resistant to therapy. We utilized 50 hallmark gene sets, and 189 oncogenic signature gene sets from Molecular Signatures Database (MSigDB) (27–29). Although we could not detect a hallmark gene set commonly enriched in all 5 GEO datasets, oncogenic signature gene sets "MTOR UP.N4.V1_DN" and "CYCLIN_D1.KE.V1.DN" were enriched at least in 3 out of 5 GEO datasets (Figures 2A, B).

"MTOR_UP.N4.V1_DN" signature consists of genes downregulated upon treatment of CEM-C1 T cell leukemia cells with an MTOR inhibitor rapamycin (33). "CYCLIN_D1.KE.V1.DN" gene signature includes genes downregulated in MCF-7 breast cancer cells heterogeneously over-expressing a mutant form of Cyclin D1 (K112E) lacking the ability to activate cyclin-dependent kinase 4 (CDK4) (34). Based on the significance of MTOR and CCND1 in tumor progression and resistance to therapy in cancer including breast cancer (35–38), we investigated whether *MTOR* and *CCND1* have a predictive significance for the pathological complete response to taxane-based chemotherapy, in 437 non-responsive vs. 75 responsive ER+/HER2- breast cancers patients in the ROC Plotter cohort. These two genes were not differentially expressed in non-responsive patients (Figures 2C, D), nor exhibit a predictive power in ROC analysis (Figures 2E, F). High expression of these genes in 316 ER+/HER2- breast cancer patients who had undergone neoadjuvant chemotherapy was not associated with a decreased relapse-free survival in the KM Plotter cohort (Figures 2G, H).

Interestingly, we observed three different β-Catenin (CTNNB1)-related oncogenic signatures, "BCAT_GDS748_UP", "BCAT.100_UP.V1_UP" "BCAT_BILD_ET_AL _DN" enriched in GSE20194, GSE20271, and GSE25055 datasets, although a single β-Catenin-related oncogenic signature is not commonly enriched among the datasets (Figures 3A, B). "BCAT_GDS748_UP" and "BCAT.100_UP.V1_UP" signatures consist of genes upregulated in HEK293 cells which express a constitutively active β-Catenin (39). "BCAT_BILD_ET_AL _DN" is established from the down-regulated genes in a primary epithelial breast cancer cell model that overexpresses active β-Catenin (40). β-Catenin is a crucial component of E-cadherin-mediated cell-cell adhesion and canonical WNT pathway which has high significance in mammary tissue development, breast cancer formation, and metastasis (41). Unexpectedly, our analysis of ER+/HER2- breast cancer patients in the ROC plotter cohort exhibited down-regulation of β-Catenin in patients with residual disease (Figure 3C). Despite that, the genes that are upregulated or downregulated in the presence of constitutively active CTNNB1 are enriched in non-responders in GEO datasets (Figures 3A, B), *CTNNB1* exhibited a significant predictive value in the ROC analysis (Figure 3D), and high expression of the *CTNNB1* was associated with decreased relapse-free survival in ER+/HER2- breast cancer patients who received neoadjuvant chemotherapy (Figure 3E). Since relapse-free survival is a better surrogate for response to therapy we evaluated these results in favor of the possible involvement of *CTNNB1* in resistance to taxane-based chemotherapy. These results also suggested the importance of the activity status of CTNNB1 besides the gene expression levels.

Then we explored upregulated genes and ontologies in chemoresistant patients in GEO datasets (Supplementary Figures 1A-E). A low number of upregulated genes were shared in all 5 datasets (1 gene: *XIST*), or 4 datasets (4 genes: *MLH3, TNFRSF25, SNX1, RBM5*). However, the overlap between the ontologies that the upregulated genes enriched was high in all 5 datasets (Supplementary Figure 1F). To investigate and compare the potential predictive power of a larger list of genes, we compiled the list of genes upregulated in 3 or more datasets, which included 63 coding genes.

3.2 Functionally enriched gene ontologies and pathways associated with resistance to taxane-based neoadjuvant chemotherapy

To identify the pathways and gene ontologies at which the 63 upregulated genes were enriched, we performed functional

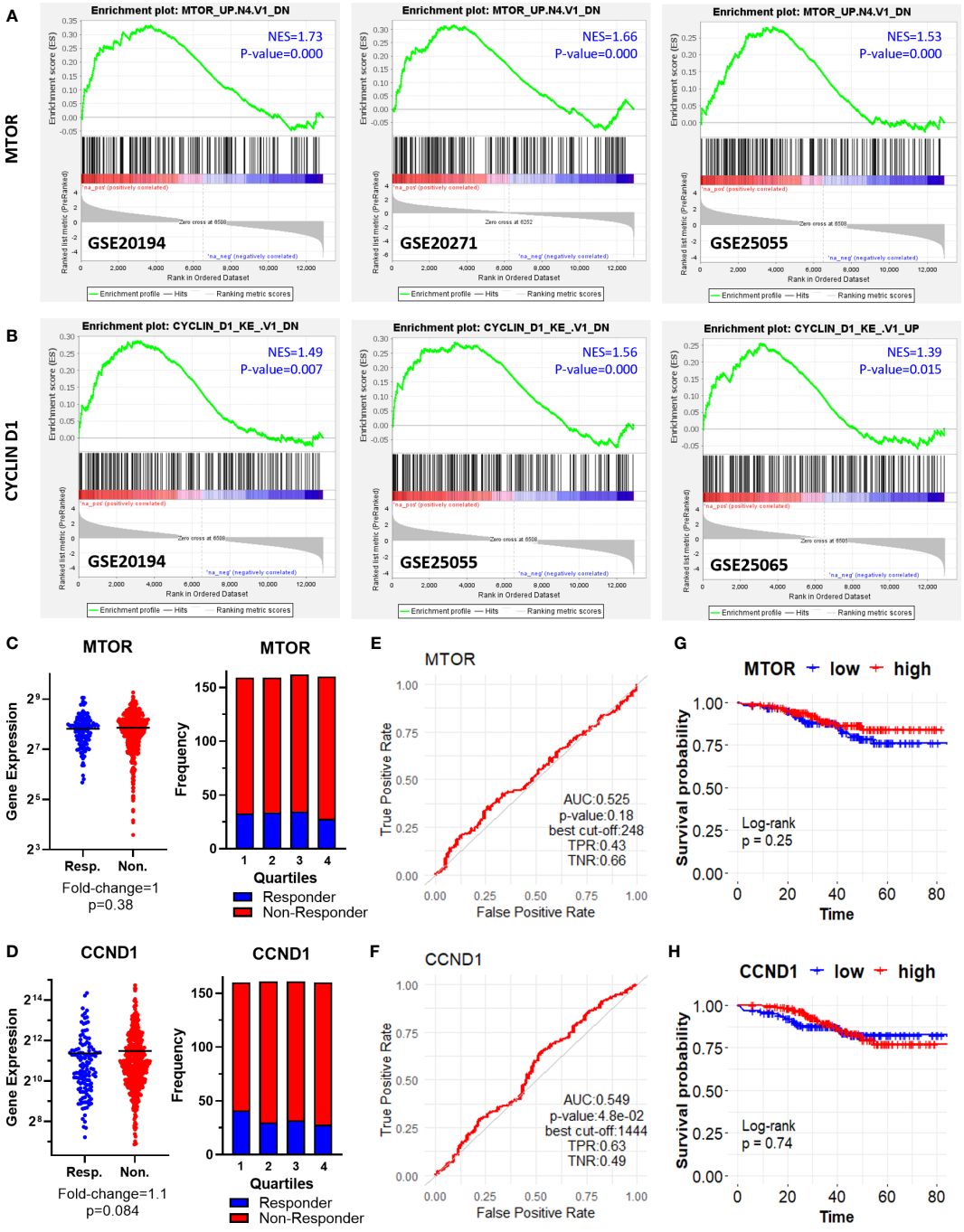

FIGURE 2
Oncogenic signature genes enriched in ER+/HER2- breast cancer patients resistant to taxane-based neoadjuvant chemotherapy. GSEA enrichment plots for **(A)** "MTOR_UP.N4.V1_DN" and **(B)** "CYCLIN_D1.KE.V1.DN" oncogenic signature gene sets in GSE20194, GSE20271, GSE25055, and GSE25065 datasets. The differential expression plot (left), and the frequency of responders and non-responders at each quartile of gene expression (right) for **(C)** MTOR and **(D)** CCND1; and the ROC plots for **(E)** MTOR and **(F)** CCND1 in 437 non-responsive vs. 75 responsive ER+/HER2- breast cancer patients who received taxane-based chemotherapy (ROC Plotter database). The pathological response was used as the surrogate of response to chemotherapy. The KM plots for **(G)** MTOR and **(H)** CCND1 in 316 ER+/HER2- breast cancer patients who received taxane-based neoadjuvant chemotherapy (KM Plotter database). AUC, Area under the curve; TPR, true positive rate; TNR, true negative rate; NES, normalized enrichment score.

annotation and clustering analysis in The Database for Annotation, Visualization, and Integrated Discovery (DAVID) (Version 6.8) (https://david.ncifcrf.gov/) (42). The 63 upregulated genes clustered in 5 annotation clusters. The top annotation cluster with the highest enrichment score included "protein kinase activity" and "protein phosphorylation" as the most prominent biological processes and molecular functions (Supplementary Table 2). Ontologies related to "endocytosis" and "regulation of transcription" were the other prominent processes and molecular functions that the upregulated genes enriched in other clusters.

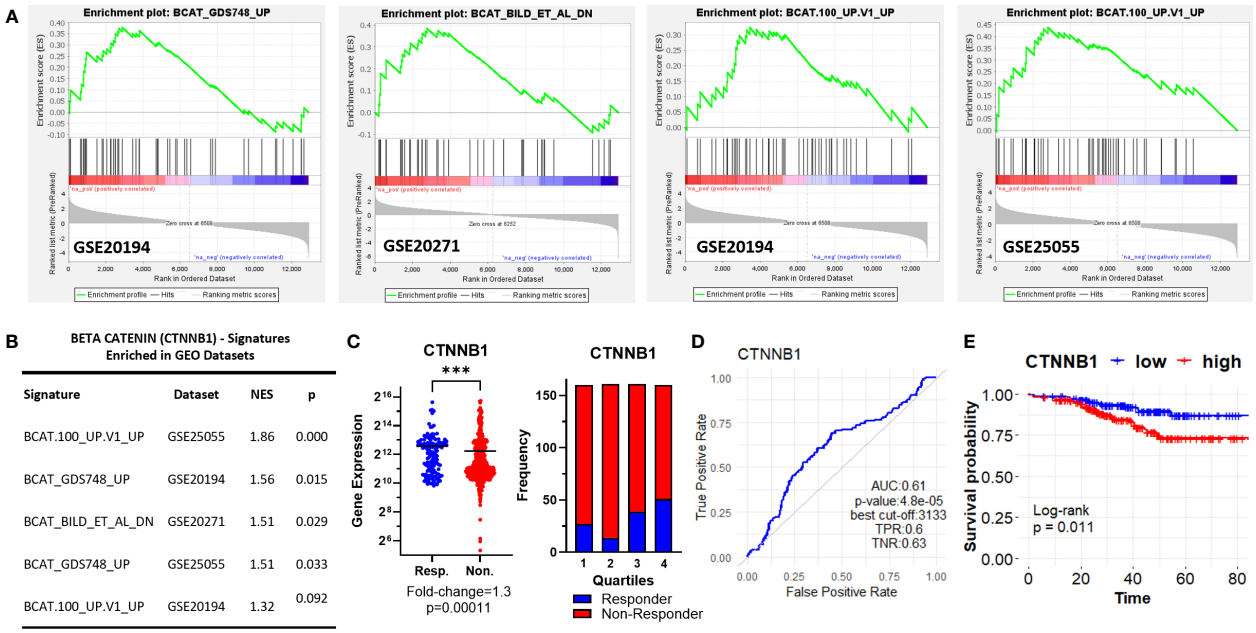

FIGURE 3
β-Catenin-related oncogenic signature genes enriched in ER+/HER2- breast cancer patients resistant to taxane-based therapy. **(A)** GSEA enrichment plots for β-Catenin-related oncogenic signature genes in GSE20194, GSE20271, and GSE25055 datasets with **(B)** the table of statistical parameters. **(C)** The differential expression (left), the frequency of responders and non-responders at each quartile of gene expression (right), and **(D)** the ROC curves for CTNNB1 in 437 non-responsive vs. 75 responsive ER+/HER2- breast cancer patients who received taxane-based chemotherapy (ROC Plotter database). **(E)** The KM plot for CTNNB1 in 316 ER+/HER2- breast cancer patients who received taxane-based neoadjuvant chemotherapy (KM Plotter database). AUC, Area under the curve; TPR, true positive rate; TNR, true negative rate; NES, normalized enrichment score.

3.3 Validation of the differential expression and predictive power of upregulated genes

To validate the upregulation of the 63 genes in chemoresistant patients and investigate their predictive value for resistance to taxane-based chemotherapy, we analyzed their differential expression and ROC plots in a large cohort of breast cancer patients in the ROC plotter developed by Fekete and Győrffy (16). Among these 63 genes, we validated the significant upregulation of 18 genes in non-responders to taxane-based chemotherapy (Figure 4). The ROC plots of these 18 genes also demonstrated a statistically significant power to predict resistance to taxane-based therapy in 437 non-responsive vs. 75 responsive ER+/HER2- breast cancer patients (Figure 5). The area under the ROC curves (AUC) was significantly higher than 0.5 for all 18 genes ($p<0.01$ for 2 genes and $p<0.001$ for 16 genes). These genes with functional annotations are listed in Supplementary Table 3. Among the 18 validated genes, *BLOC1S1, AP3B2, ZNF609, ZFYVE9*, and *RAP1GAP* were the top 5 genes with the highest PPV and NPV (Table 1).

3.4 The specificity of the 18 upregulated genes to ER+/HER2- breast cancer

Breast cancer is a heterogeneous disease with different responses to treatment in different subtypes (4, 7). Therefore, distinct gene lists may have different predictive strengths in different subtypes. To test whether the predictive value of the 18 upregulated genes we identified is specific to the ER+/HER2- breast cancer, we tested the predictive power of each gene also in HER2+/ER- and triple-negative breast cancers (Table 1).

Among the 18 genes, fewer genes exhibited significant predictive value in HER2+ cancers and TNBC, compared with ER+/HER2- breast cancer. Despite the p-values for AUCs of some genes such as *AP3B2, BLOC1S1, NUDT13, PTCH1*, and *ZNF609* being statistically significant in all three breast cancer subtypes, their significance in HER2+ cancers and TNBC were much lower compared to that in ER+/HER2- breast cancer patients. PPV and NPVs were also lower compared to that in ER+/HER2- breast cancer. These results showed that the 18 gene signature has higher predictive value and specificity in ER+/HER2- breast cancer.

3.5 Comparative analysis of the 18 upregulated genes with prognostic signatures in breast cancer

Several multi-gene assays such as Oncotype Dx, EndoPredict, and MammaPrint are being used as complementary tools to guide decisions in the clinical management of breast cancer patients. Although their primary benefit is to estimate the risk of recurrence after endocrine therapy in ER+/HER2- breast cancers, some studies suggested their utility also as predictive tools to estimate response to systemic chemotherapy (10, 43–45). Therefore, we investigated the correlation of our 18 gene list with these signatures. The analysis of TCGA dataset demonstrated that the expression of the 18 genes is

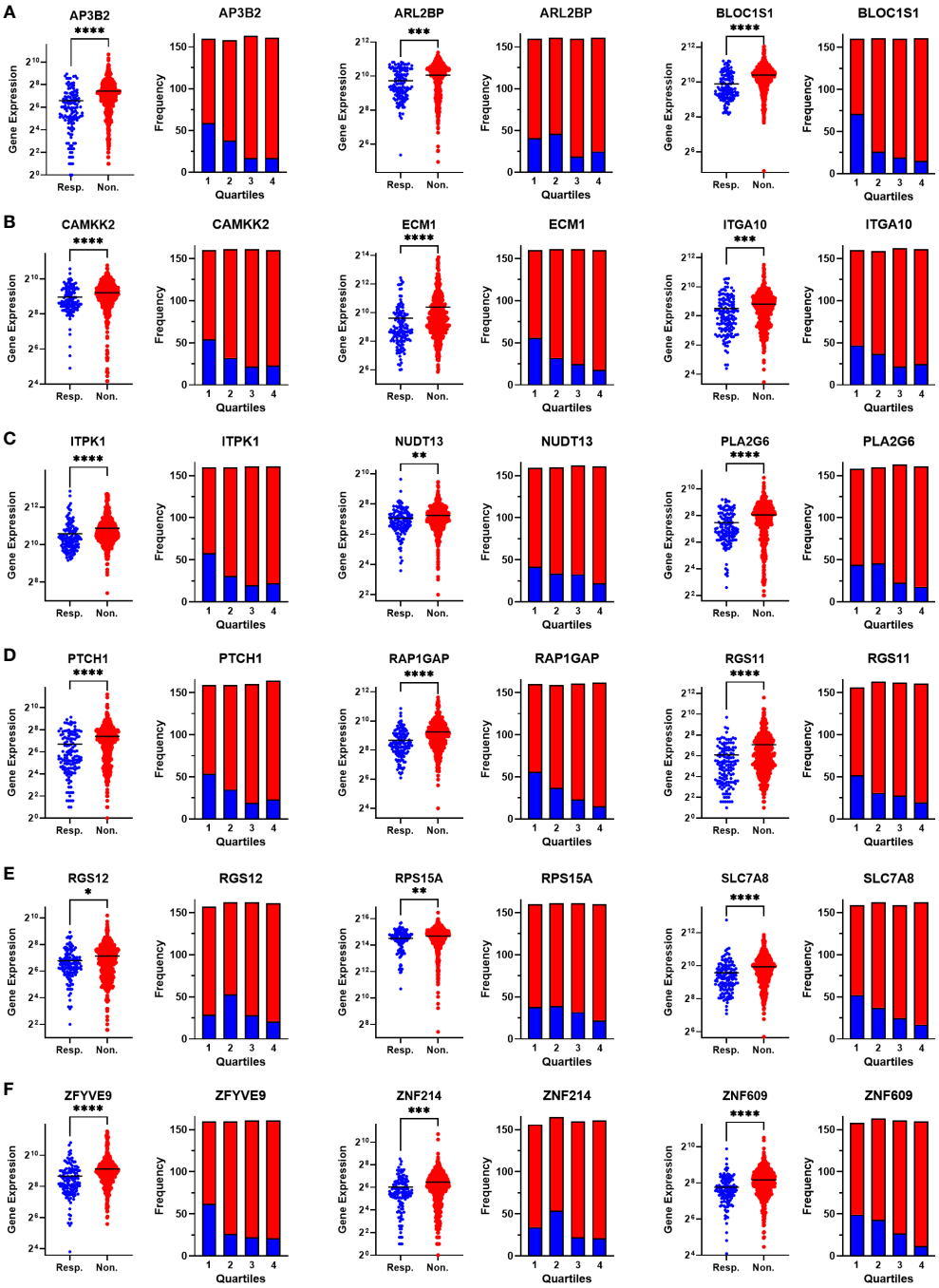

FIGURE 4
Validating the differential expression of the 18 upregulated genes in non-responders. The differential expression (left), and the frequency of responders and non-responders at each quartile of gene expression (right) for **(A)** AP3B2, ARL2BP, BLOC1S1, **(B)** CAMKK2, ECM1, and ITGA10, **(C)** ITPK1, NUDT13, PLA2G6, **(D)** PTCH1, RAP1GAP, and RGS11, **(E)** RGS12, RPS15A, SLC7A8, **(F)** ZFYVE9, ZNF214, and ZNF609. The analysis was performed on data for 437 non-responsive vs. 75 responsive ER+/HER2- breast cancer patients who received taxane-based chemotherapy in the ROCplotter cohort. The pathological response was used as the surrogate of response to chemotherapy. Resp.: Responders (blue), Non.:Non-responders (red). *: p<0.05, **: p<0.01, ***: p<0.001, ****: p<0.0001.

correlated with the expression of Oncotype Dx, EndoPredict, and MammaPrint signatures in 1100 breast cancer patients. The correlation of the 18 gene list was highest with the Oncotype Dx (Figure 6A).

Then we compared the correlation of the 18 genes, Oncotype Dx and EndoPredict signatures with the expression of ER (*ESR1*), HER2 (*ERBB2*), and ER plus HER2 in breast cancer patients in TCGA dataset. The 18 genes and the two signatures were correlated with the expression of ER and ER plus HER2 in breast cancer patients (Figures 6B–D). The correlation with HER2 was significant only for the EndoPredict signature. It was noticeable that the clustering pattern of patients in correlation analysis with ER,

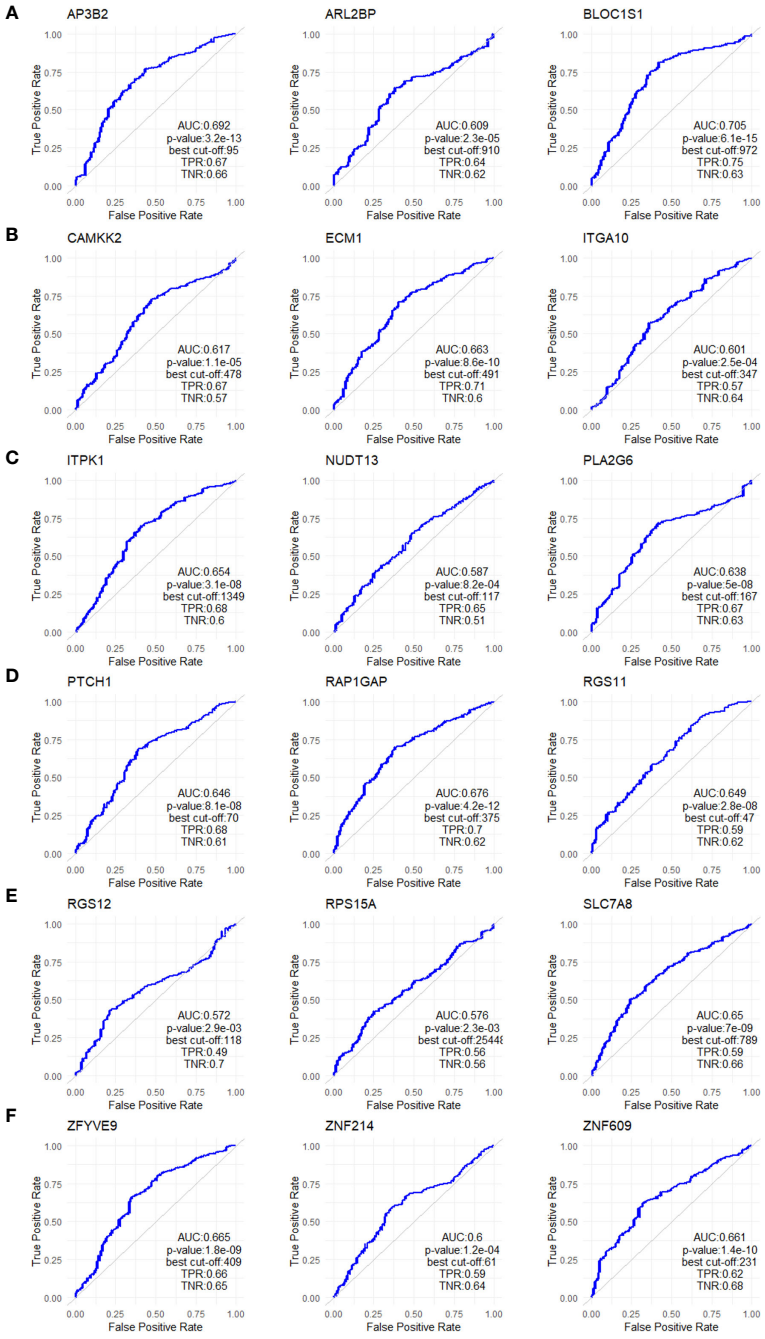

FIGURE 5
ROC analysis of the 18 upregulated genes in non-responders. ROC plots for **(A)** AP3B2, ARL2BP, BLOC1S1, **(B)** CAMKK2, ECM1, and ITGA10, **(C)** ITPK1, NUDT13, PLA2G6, **(D)** PTCH1, RAP1GAP, and RGS11, **(E)** RGS12, RPS15A, SLC7A8, **(F)** ZFYVE9, ZNF214, and ZNF609. The analysis was performed on data for 437 non-responsive vs. 75 responsive ER+/HER2- breast cancer patients who received taxane-based chemotherapy in the ROCplotter cohort. The pathological response was used as the surrogate of response to chemotherapy.

HER2, and ER plus HER2 were very similar for the 18 gene list (Figure 6B) and the two signatures (Figures 6C, D). Since the correlation of the 18 genes was highest with Oncotype Dx (Figure 6A), and the Oncotype Dx signature bears a comparable number of genes (16 marker genes + 5 reference genes), we further analyzed the characteristics of our 18 gene list comparatively with Oncotype Dx.

3.6 Comparative analysis of the 18 gene list with the Oncotype Dx signature in breast cancer

Despite that multi-gene signatures are used to calculate recurrence scores based on multivariate statistical equations (8), we wondered whether the individual predictive powers of the 18

TABLE 1 The predictive power of the 18 upregulated genes in different breast cancer subtypes.

	ER +/HER2 -				HER2 +/ER -				TNBC			
Genes	AUC	P-value	PPV	NPV	AUC	P-value	PPV	NPV	AUC	P-value	PPV	NPV
AP3B2	**0.692**	**3.2E-13**	**0.663**	**0.667**	0.623	4.3E-03	0.625	0.598	0.596	2.3E-03	0.580	0.580
ARL2BP	**0.609**	**2.3E-05**	**0.627**	**0.633**	0.537	2.2E-01	0.600	0.574	0.523	2.5E-01	0.564	0.541
BLOC1S1	**0.705**	**6.1E-15**	**0.670**	**0.716**	0.604	1.5E-02	0.624	0.626	0.587	5.3E-03	0.584	0.586
CAMKK2	**0.617**	**1.1E-05**	**0.609**	**0.633**	0.545	1.8E-01	0.632	0.568	0.539	1.3E-01	0.564	0.557
ECM1	**0.663**	**8.6E-10**	**0.640**	**0.674**	0.502	4.8E-01	0.568	0.540	0.550	7.3E-02	0.608	0.570
ITGA10	**0.601**	**2.5E-04**	**0.613**	**0.598**	0.591	2.9E-02	0.632	0.581	0.557	5.0E-02	0.563	0.549
ITPK1	**0.654**	**3.1E-08**	**0.630**	**0.652**	0.614	7.7E-03	0.588	0.616	0.552	6.2E-02	0.573	0.559
NUDT13	**0.587**	**8.2E-04**	**0.570**	**0.593**	0.623	4.4E-03	0.639	0.663	0.585	5.3E-03	0.567	0.563
PLA2G6	**0.638**	**5.0E-08**	**0.644**	**0.656**	0.553	1.4E-01	0.598	0.568	0.523	2.5E-01	0.528	0.532
PTCH1	**0.646**	**8.1E-08**	**0.636**	**0.656**	**0.666**	**1.6E-04**	**0.663**	**0.667**	0.597	2.1E-03	0.576	0.627
RAP1GAP	**0.676**	**4.20E-12**	**0.648**	**0.674**	0.569	7.6E-02	0.578	0.607	0.532	1.8E-01	0.542	0.561
RGS11	**0.649**	**2.8E-08**	**0.608**	**0.602**	0.577	5.5E-02	0.588	0.630	**0.627**	**6.4E-05**	**0.586**	**0.584**
RGS12	0.572	2.9E-03	0.620	0.579	0.503	4.7E-01	0.587	0.574	0.564	3.0E-02	0.571	0.569
RPS15A	0.576	2.3E-03	0.560	0.560	0.532	2.6E-01	0.570	0.545	0.561	3.6E-02	0.563	0.580
SLC7A8	**0.65**	**7.0E-09**	**0.634**	**0.617**	0.560	1.0E-01	0.600	0.560	0.561	3.6E-02	0.549	0.551
ZFYVE9	**0.665**	**1.8E-09**	**0.653**	**0.657**	0.556	1.2E-01	0.579	0.620	**0.611**	**4.9E-04**	**0.607**	**0.636**
ZNF214	**0.6**	**1.2E-04**	**0.621**	**0.610**	0.531	2.7E-01	0.519	0.521	0.551	6.8E-02	0.552	0.548
ZNF609	**0.661**	**1.4E-10**	**0.660**	**0.642**	0.621	4.9E-03	0.600	0.611	0.595	2.2E-03	0.577	0.573

The results for which the p-value for AUC was 0.001<p<0.05 were underlined, and p<0.001 were written in bold. Number of patients: ER+/HER2-: non-responders: 437, responders: 75; HER2 +/ER-: non-responders: 31, responders:40; TNBC: non-responders:125, responders:79. Analysis was performed on ROC Plotter database.

gene list we identified are similar to the individual predictive powers of Oncotype Dx genes in different subtypes of breast cancer. Hence, we investigated the individual predictive powers of Oncotype Dx genes in three breast cancer subtypes in the ROC plotter database. The AUCs were significantly higher than 0.5 for only 8 genes (p<0.05 for 2 genes and p<0.001 for 6 genes) in ER+/HER2- breast cancer patients who received taxane-based chemotherapy (Table 2). *BCL2*, *ERBB2*, *GRB7*, and *SCUBE2* exhibited highest predictive strength. *SCUBE2* also emerged as a key predictor of chemoresistance in breast cancer in our recent study (46). Only one or two Oncotype Dx genes exhibited predictive value in HER2 +/ER- and TNBC subtypes, suggesting specificity of the signature for the ER+/HER2- subtype. However, nearly half of the Oncotype Dx genes did not exhibit a predictive value in ER+/HER2- breast cancer.

Then we compared the differential expression of the 18 gene list and Oncotype Dx signature in chemoresistant patients with different breast cancer subtypes in the ROC plotter dataset. All the genes in the 18 gene list were significantly increased in the ER +/HER2- subtype and most of the fold changes (FCs) in HER2 +/ER- and TNBC subtypes were insignificant (Table 3). The FC for almost all the Oncotype Dx genes was also insignificant in HER2 +/ER- and TNBC subtypes. However, only 7 out of 16 Oncotype Dx genes were significantly upregulated in ER+/HER2- breast cancer. These results, together with the comparison of the results in Tables 1, 2 suggest that the 18 genes we identified exhibit higher individual predictive values and higher specificity to ER+/HER2- breast cancer patients.

After that, we analyzed the Pearson correlation between each gene in the 18 gene list (Figure 7A) and the Oncotype Dx signature (Figure 7B) in 316 ER+/HER2- breast cancer patients who underwent neoadjuvant chemotherapy. The 18 gene list formed 3 main clusters: a cluster of positively correlated genes (*ITPK1*, *ITGA10*, *ZFYVE9*, *PLA2G6, ARL2BP*, and *RGS12*), a cluster of uncorrelated or poorly correlated genes (*AP3B2*, *CAMKK2, ZNF214, NUDT13, PTCH1*, and *ZNF609*) and a cluster of genes negatively correlated with others in the 18 gene-list (*RAP1GAP, BLOC1S1, ECM1, RGS11, SLCA78*, and *RPS15A*). Oncotype Dx genes also formed 3 main clusters but with a different pattern: a cluster of positively correlated genes (*CCNB1, AURKA, MYBL2, BIRC5, MKI67*, and *CTSL2*), a cluster of uncorrelated or poorly correlated genes (*CD68, MMP11, BCL2, BAG1*, and *GRB7*), and a second cluster of positively correlated genes (*ERBB2, ESR1, GSTM1, SCUBE2*, and *PGR*).

Although linear correlation for some genes is poor, they may exhibit concordant increases or decreases in expression in tumor samples. To investigate these kinds of monotonic relationships we analyzed the Spearman correlation between each gene in the 18 gene list (Figure 7C) and the Oncotype Dx signature (Figure 7D) in 316 ER+/HER2- breast cancer patients. The 18 genes constituted

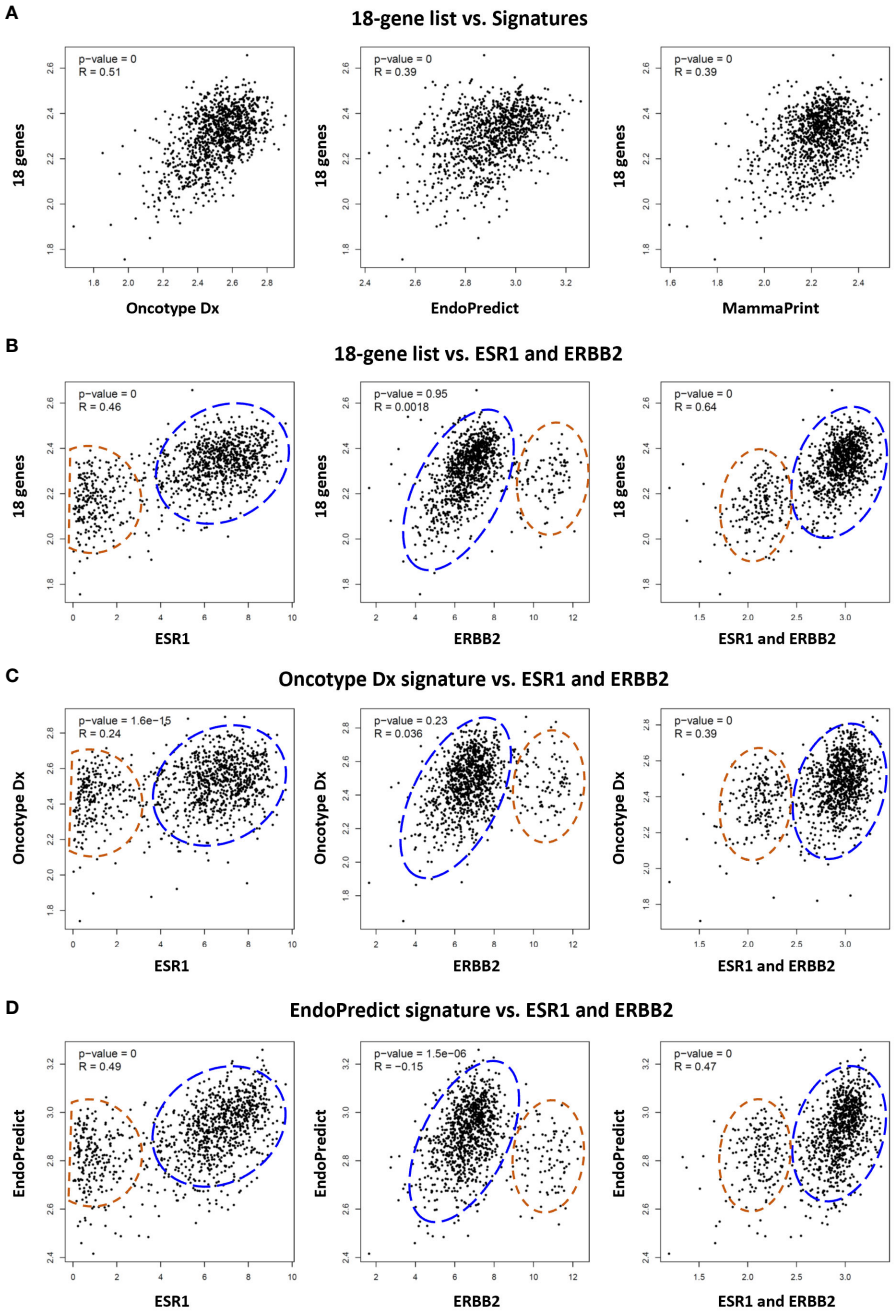

FIGURE 6
Comparative analysis of the 18 gene list with multi-gene assay signatures in TCGA breast cancer patients. **(A)** Correlation between the 18 gene list and Oncotype Dx, EndoPredict, and MammaPrint signatures respectively in 1100 breast cancer patients in TCGA dataset. Correlation of **(B)** 18 gene list, **(C)** Oncotype Dx, and **(D)** EndoPredict signatures with ER (ESR1), HER2 (ERBB2), and ER plus ERBB2 respectively in breast cancer patients. The housekeeping/reference genes in all the signatures were excluded from the analysis. For the Oncotype Dx signature, the ESR1, ERBB2, or ESR1 plus ERBB2 was not included in the signature when correlation with ESR1, ERBB2, or ESR1 plus ERBB2 was analyzed respectively in (6c). The blue dashed circles show the main cluster of patients with high expression of 18-genes or two signatures in the y-axis, together with high ESR1 expression (left graph), low ERBB2 expression (middle), and high ESR1+ERBB2 expression (right graph) in the x-axis. The red dashed circles show patients with lower expression of the 18 genes or two signatures in the y-axis, and low ESR1(left), high ERBB2 (middle), and low ESR1+ERBB2 (right) expression in the x-axis. x- and y-axis represent log(transcript per million) values for gene expression.

two main clusters of positively and monotonically correlated genes. The larger cluster included *ITGA10, ITPK1, PLA2G6, ZFYVE9, ARLB2BP, ZNF214, NUDT13, PTCH1, RGS12, CAMKK2, AP3B2,* and *ZNF609*. The smaller cluster consisted of *RAP1GAP, RGS11, SLC7A8, BLOC1S1*, and *ECM1* (Figure 7C). The Oncotype Dx signature exhibited 2 clusters of positively and monotonically changing clusters of similar size. These 2 clusters, one composed of *ESR1*-related genes, and the other composed of genes associated with proliferation like *MKI67* and *CCNB1* exhibited changes in the opposite direction in ER+/HER2- breast cancer patients (Figure 7D).To understand whether this pattern of correlation within the 18-gene list and Oncotype Dx is specific to ER

TABLE 2 The predictive power of Oncotype Dx genes in different breast cancer subtypes.

	ER +/HER2 -				HER2 +/ER -				TNBC			
Genes	AUC	P-value	PPV	NPV	AUC	P-value	PPV	NPV	AUC	P-value	PPV	NPV
AURKA	0.579	3.5E-03	0.588	0.616	0.527	2.9E-01	0.548	0.542	0.503	4.6E-01	0.523	0.527
BAG1	0.558	1.6E-01	0.677	0.585	0.646	1.1E-02	0.757	0.638	0.531	3.3E-01	0.596	0.585
BCL2	**0.701**	**3.7E-14**	**0.651**	**0.670**	0.559	1.1E-01	0.587	0.594	0.553	6.1E-02	0.545	0.545
BIRC5	0.513	3.3E-01	0.535	0.526	0.502	4.8E-01	0.546	0.554	0.51	3.8E-01	0.538	0.532
CCNB1	0.574	7.7E-02	0.596	0.628	0.503	4.8E-01	0.576	0.537	0.596	9.4E-02	0.621	0.593
CD68	0.531	1.4E-01	0.535	0.535	0.561	1.0E-01	0.571	0.622	0.537	1.4E-01	0.584	0.553
CTSL2	**0.6**	**1.5E-04**	**0.605**	**0.571**	0.545	1.8E-01	0.619	0.555	0.544	1.0E-01	0.552	0.558
ERBB2	**0.644**	**2.3E-08**	**0.626**	**0.645**	0.551	4.1E-01	0.569	0.533	0.511	3.7E-01	0.521	0.519
ESR1	**0.595**	**6.2E-04**	**0.571**	**0.569**	0.555	1.3E-01	0.582	0.554	0.582	8.1E-03	0.624	0.591
GRB7	**0.646**	**1.7E-08**	**0.657**	**0.663**	0.54	2.1E-01	0.566	0.574	0.571	1.8E-02	0.588	0.565
GSTM1	NA	NA	NA	NA	NA	NA	NA	NA	NA	NA	NA	NA
MKI67	0.506	4.2E-01	0.513	0.517	0.522	3.3E-01	0.571	0.552	0.506	4.3E-01	0.546	0.544
MMP11	0.531	1.5E-01	0.527	0.523	0.562	9.9E-02	0.545	0.545	0.532	1.8E-01	0.548	0.579
MYBL2	0.549	3.9E-02	0.545	0.556	0.52	3.4E-01	0.524	0.517	0.528	2.0E-01	0.538	0.533
PGR	0.531	2.9E-01	0.568	0.554	0.53	3.4E-01	0.571	0.579	0.599	8.5E-02	0.638	0.653
SCUBE2	**0.628**	**6.7E-07**	**0.590**	**0.641**	0.557	1.2E-01	0.581	0.561	0.534	1.6E-01	0.538	0.532

The results for which the p-value for AUC was 0.001<p<0.05 were underlined, and p<0.001 were written in bold. The housekeeping/reference genes ACTB, GAPDH, GUSB, RPLP0, and TFRC in Oncotype Dx signature were excluded from the analysis, and the data was not available (NA) for GSTM1. Number of patients: ER+/HER2-:non-responders: 437, responders: 75; HER2+/ER-: non-responders: 31, responders:40; TNBC: non-responders:125, responders:79.

+/HER2- breast cancer patients, we performed a similar Spearman correlation analysis in TCGA breast cancer data (Figure 8).

We observed that the pattern of correlation of 18 genes was different in all breast cancer patients in the TCGA dataset with lower correlation coefficients in general (Figure 8A) compared to that in the cohort of ER+/HER2- breast cancer patients (Figure 7C). The pattern of the Spearman correlation matrix was also different in luminal A- or luminal B- type breast cancers in the TCGA dataset (Figures 8 B, C). On the other hand, the Oncotype Dx signature exhibited nearly the same correlation pattern in all TCGA breast cancer patients and luminal A-type breast cancer patients (Figures 8D, E) as in the cohort of ER+/HER2- breast cancer patients (Figure 7D). The pattern in luminal B-type breast cancer was different from that in other cohorts (Figure 8F). These results suggested that the 18 gene list we identified may be more representative of ER+/HER2- breast cancer patients, while Oncotype Dx similarly represents all breast cancer subtypes, Luminal A type, and ER+/HER2- breast cancer.

3.7 The effect of 18 genes in the relapse free survival of ER+/HER2- breast cancer patients

Pathological complete response is often used as a surrogate of treatment response to neoadjuvant chemotherapy. Since its assessment within the period of clinical studies is relatively easy, pCR gained widespread use as a primary endpoint in many clinical trials to facilitate and accelerate the drug discovery process. However, recent studies question its efficacy as a predictor of patient survival and reveal varying surrogacy of pCR in distinct breast cancer subtypes (47–49). To identify reliable predictors of resistance to neoadjuvant chemotherapy we investigated the effect of 18 genes in relapse-free survival of 316 ER-/HER2- patients in the KM plotter cohort. We validated that high expression of 4 out of 18 genes, namely *AP3B2, ITGA10, ITPK1*, and *PTCH1* is associated with a significantly decreased relapse-free survival (Figures 9A–E).

Then we performed multivariate survival analysis using these four genes as categorical variates (Figures 9F–O). The survival models were statistically significant for gene combinations *AP3B2/ITPK1*, *AP3B2/PTCH1, ITPK1/PTCH1, AP3B2/ITGA10/ITPK1, AP3B2/ITPK1/PTCH1*, and *ITGA10/ITPK1/PTCH1* (Figures 9G, H, K, L, N, O). *AP3B2/ITPK1* model remarkably had the greatest significance in the log-rank test (Figure 9G).

3.8 The effect of AP3B2, ITGA10, ITPK1, PTCH1 and CTNNB1 as continuous covariates in the relapse free survival of ER+/HER2- breast cancer patients

Despite that KM survival curves are efficient tools to assess the impact of gene expression on patient outcome, the cut-offs used to allocate patients to low-expression and high-expression groups

TABLE 3 The differential expression of 18 gene list vs. Oncotype Dx signature genes in taxane-resistant patients with different breast cancer subtypes.

18-gene	ER +/HER2 -		HER2 +/ER -		TNBC		Oncotype Dx	ER +/HER2 -		HER2 +/ER -		TNBC	
Genes	FC	P-value	FC	P-value	FC	P-value	Genes	FC	P-value	FC	P-value	FC	P-value
AP3B2	**1.8**	**1.2E-11**	1.3	1.1E-02	1.3	5.2E-03	**AURKA**	**1.2**	**5.2E-03**	1.1	5.8E-01	1	9.2E-01
ARL2BP	**1.5**	**1.2E-06**	1.1	4.4E-01	1.1	5.1E-01	**BAG1**	1.2	2.9E-01	1.7	3.4E-02	1.3	6.8E-01
BLOC1S1	**1.4**	**3.9E-13**	1.1	3.3E-02	1.1	1.1E-02	**BCL2**	**2.1**	**1.2E-12**	1	2.3E-01	1.2	1.3E-01
CAMKK2	**1.2**	**4.0E-04**	1.1	3.5E-01	1.1	2.6E-01	**BIRC5**	1	6.4E-01	1	9.6E-01	1	7.7E-01
ECM1	**1.2**	**5.3E-08**	1.2	9.7E-01	1.1	1.5E-01	**CCNB1**	1.3	1.8E-01	1	9.7E-01	1.5	2.1E-01
ITGA10	**1.2**	**3.8E-04**	1.3	6.0E-02	1.1	9.4E-02	**CD68**	1.1	2.8E-01	1.2	2.1E-01	1.3	2.8E-01
ITPK1	**1.6**	**2.6E-07**	1.2	1.9E-02	1.1	1.3E-01	**CTSL2**	**1.2**	**4.3E-04**	1.1	3.6E-01	1.1	2.0E-01
NUDT13	1.1	7.4E-03	1.3	1.1E-02	1.3	1.3E-02	**ERBB2**	**1.3**	**3.3E-07**	1	8.2E-01	1.1	7.4E-01
PLA2G6	**1.3**	**1.4E-08**	1.3	2.7E-01	1.1	5.0E-01	**ESR1**	**1.2**	**8.3E-04**	1.1	2.5E-01	1.1	1.7E-02
PTCH1	**1.3**	**1.2E-07**	**1.6**	**6.4E-04**	1.4	4.6E-03	**GRB7**	**1.5**	**2.6E-07**	1	4.1E-01	1.2	4.0E-02
RAP1GAP	**1.7**	**7.6E-09**	1.2	1.5E-01	1.0	3.5E-01	**GSTM1**	NA	NA	NA	NA	NA	NA
RGS11	1.1	2.1E-03	1.1	1.1E-01	**1.7**	**2.1E-04**	**MKI67**	1.1	8.2E-01	1	6.5E-01	1	8.7E-01
RGS12	**1.3**	**1.2E-04**	1.0	9.5E-01	1.2	6.2E-02	**MMP11**	1	2.8E-01	1.5	2.0E-01	1.1	3.5E-01
RPS15A	1.3	1.1E-02	1.1	5.1E-01	1.1	7.6E-02	**MYBL2**	1.1	8.2E-02	1	6.9E-01	1.1	4.1E-01
SLC7A8	**2**	**1.4E-07**	1.2	2.1E-01	1.2	7.5E-02	**PGR**	1	5.8E-01	1	6.6E-01	1.1	1.9E-01
ZFYVE9	**1.4**	**5.0E-09**	1.3	2.5E-01	1.3	1.2E-03	**SCUBE2**	**1.7**	**6.0E-06**	1.1	2.4E-01	1.3	3.3E-01
ZNF214	**1.2**	**3.6E-05**	1.3	5.3E-01	1.4	1.4E-01							
ZNF609	**1.5**	**4.8E-10**	1.2	1.3E-02	1.3	5.5E-03							

The results for which the p-value for FC (fold-change) was 0.001<p<0.05 were underlined, and p<0.001 were written in bold. The housekeeping/reference genes ACTB, GAPDH, GUSB, RPLP0, and TFRC in Oncotype Dx signature were excluded from the analysis, and the data was not available (NA) for GSTM1. Number of patients: ER+/HER2-:non-responders: 437, responders: 75; HER2+/ER-: non-responders: 31, responders:40; TNBC: non-responders:125, responders:79.

substantially affect the results. To assess the impact of gene expression on patient outcomes independent of cut-offs, we performed Cox Proportional Hazards regression using *AP3B2, ITGA10, ITPK1*, and *PTCH1* as continuous covariates. We also included *CTNNB1* in the analysis since *CTNNB1*-related signatures were enriched in ER+/HER2- breast cancer patients resistant to taxane-based therapy and high expression of *CTNNB1* was associated with decreased survival in ER+/HER2- breast cancer patients (Figures 3A, B, D). We established univariate and multivariate Cox Proportional Hazards regression models of these genes using the relapse-free survival data of 316 ER+/HER2- Breast Cancer patients who underwent neoadjuvant chemotherapy (Table 4). Nearly half of the univariate and multivariate models fitted survival data significantly, and nearly all of them achieved significantly better fits compared to the null model in ANOVA.

The Cox models which included *PTCH1* and *CTNNB1* like *PTCH1+CTNNB1, AP3B2+PTCH1+CTNNB1, ITGA10+PTCH1 +CTNNB1*, and *ITPK1+ PTCH1+CTNNB1* achieved the best concordance and Log-rank p values (Table 4). Moreover, *PTCH1* and *CTNNB1* displayed the highest hazard ratios, 1.534 and 1.563 respectively in the univariate Cox Proportional Hazards with significant p- and adjusted p-values (Table 5). Their hazard ratios increased further in the multivariate model including *AP3B2, ITGA10, ITPK1*, *PTCH1*, and *CTNNB1* as covariates and the Schoenfeld test validated the proportional hazards assumption (Supplementary Figure 2). These results put forth *PTCH1* and *CTNNB1* as the markers with the highest predictive potential.

Lastly, we validated the potential of *PTCH1* and *CTNNB1* as predictive biomarkers for neoadjuvant chemotherapy in ER +/HER2- breast cancer patients, by performing Cox Proportional Hazards Regression in two additional treatment arms: patients with no systemic therapy and patients who underwent endocrine therapy (Table 6). *PTCH1* and *CTNNB1* were associated with increased risk specifically in ER+/HER2- breast cancer patients who underwent neoadjuvant chemotherapy, while their hazard ratios were smaller than 1 and/or statistically insignificant in patients with no systemic therapy and patients who underwent endocrine therapy (Table 6). These findings supported that *PTCH1* and *CTNNB1* have predictive significance rather than prognostic significance. The hazard ratios for *PTCH1* and *CTNNB1* in the neoadjuvant chemotherapy arm further increased in the multivariate model suggesting an interaction between these two genes. These findings indicated that *PTCH1* and *CTNNB1* may have a high potential as predictors of resistance to taxane-based neoadjuvant chemotherapy.

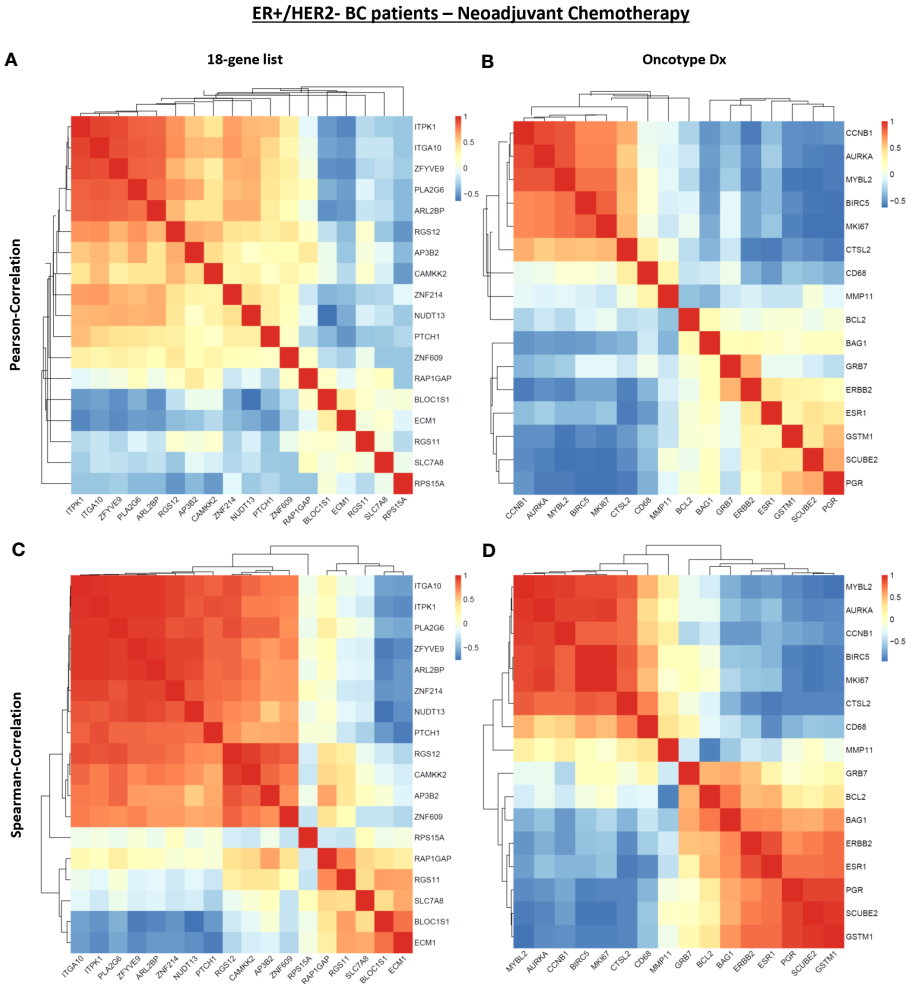

FIGURE 7
The correlation between genes in the 18 gene list and the Oncotype Dx signature in ER+/HER2- breast cancer patients. Pearson correlation between the expression of **(A)** 18 genes and **(B)** Oncotype Dx genes in 316 ER+/HER2- breast cancer patients who underwent neoadjuvant chemotherapy (KM plotter database). Spearman correlation between the expression of **(C)** 18 genes and **(D)** Oncotype Dx genes in 316 ER+/HER2- breast cancer patients who underwent neoadjuvant chemotherapy (KM plotter database). The housekeeping/reference genes ACTB, GAPDH, GUSB, RPLP0, and TFRC in the Oncotype Dx signature were excluded from the analysis.

4 Discussion

Several multi-gene assays have been developed over the last two decades to guide decisions on systemic therapy (12). The gene signatures in these assays were derived from mixed cohorts of breast cancer patients for prognostic purposes to estimate the risk of recurrence and distant metastasis after therapy (50). Based on the risk scores calculated with these assays, the ER+/HER2- breast cancer patients undergo only endocrine therapy in the low-risk group, or systemic chemotherapy in the high-risk group (4). However, the prognostic value of these assays does not necessarily indicate a predictive value. The discordance in the risk scores calculated with different assays and the lack of regimen-specific predictions for chemotherapy are big limitations. Additionally, breast cancer is a heterogeneous disease with variant responses to treatment in different subtypes (8, 12, 43). Distinct gene signatures may have different predictive strengths in different breast cancer subtypes. Therefore, predictors specific to distinct molecular subtypes of breast cancer are crucial. Moreover, high costs make it impossible to incorporate multi-gene assays into routine clinical practice in developing countries. These limitations were the primary motives for us to conduct this study.

In this study, we focused specifically on the ER+/HER2- breast cancer and markers specific to taxane-based chemotherapy. We analyzed multiple cohorts of ER+/HER2- breast cancer patients who underwent taxane-based neoadjuvant therapy. Our analysis revealed 18 markers of resistance to taxane-based chemotherapy, all of which are significantly upregulated in chemoresistant patients and have statistically significant positive predictive and negative predictive powers. Furthermore, we validated that the predictive strength of the 18 genes is specific to ER+/HER2- breast cancer patients.

In clinical practice, Oncotype Dx and MammaPrint are the most frequently used first-generation multi-gene assays, and EndoPredict and Prosigna are the most used second-generation multi-gene assays for ER+/HER2- breast cancer (4). The accuracy of

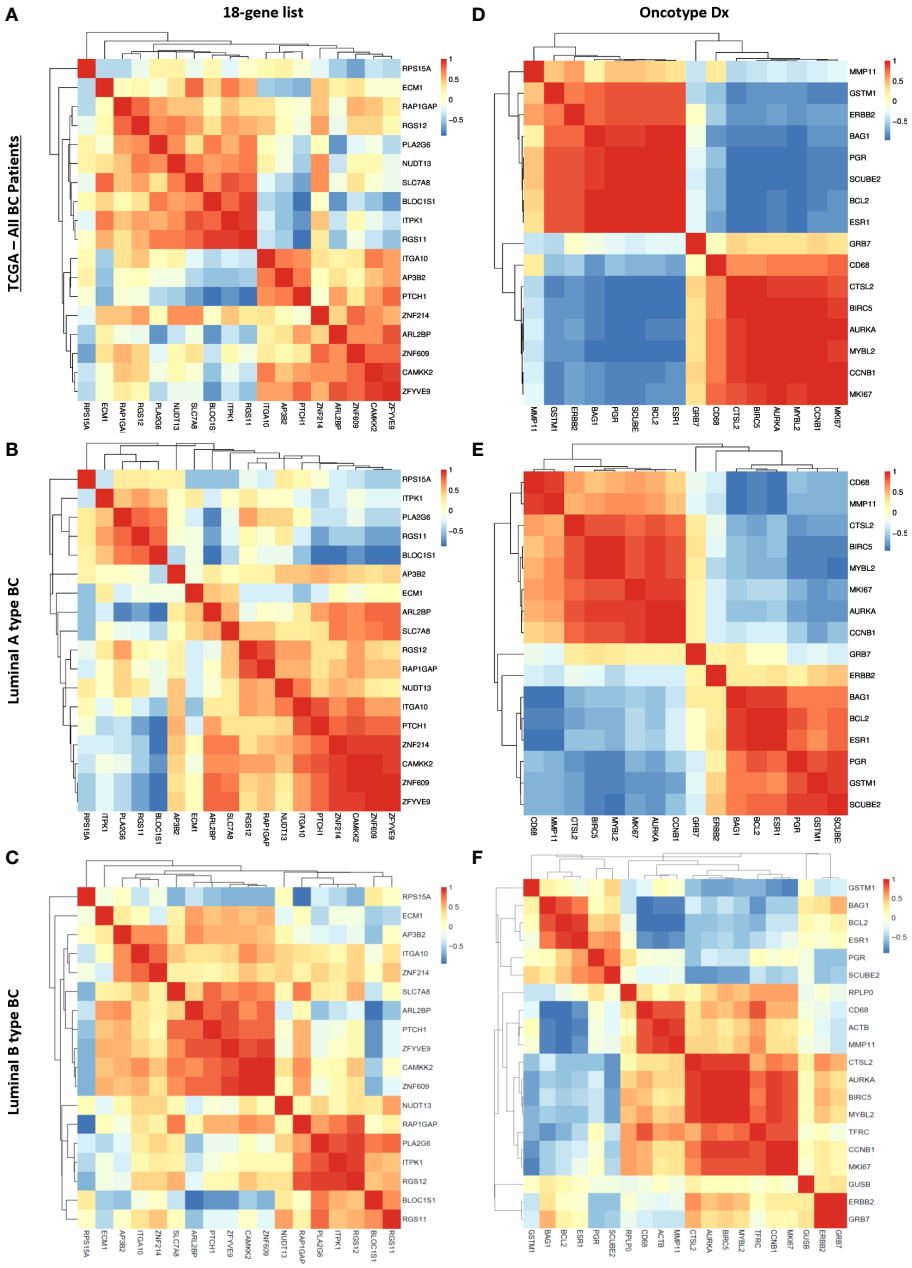

FIGURE 8
Correlation between genes in the 18 gene list and the Oncotype Dx signature in TCGA breast cancer patients. Spearman correlation heatmap of the expression of 18 genes in TCGA **(A)** all breast cancer patients (n=1100), **(B)** luminal-A type breast cancer patients (n=568), and **(C)** luminal-B type breast cancer patients (n=219). Spearman correlation heatmap of the expression of Oncotype Dx genes in TCGA **(D)** all breast cancer patients (n=1100), **(E)** luminal-A type breast cancer patients (n=568), and **(F)** luminal-B type breast cancer patients (n=219). The housekeeping/reference genes ACTB, GAPDH, GUSB, RPLP0, and TFRC in the Oncotype Dx signature were excluded from the analysis.

the first-generation multi-gene assays to predict recurrence after endocrine therapy is higher in the first five years after treatment. The second-generation multi-gene assays like EndoPredict are more accurate in predicting late recurrences compared to the first-generation tests (8). Since first- and second-generation tests offer different accuracies, and each test uses a non-overlapping set of genes, we investigated the correlation of our 18-gene list with multi-gene assays of different generations. Our analysis suggested a higher correlation of the 18-gene list with Oncotype Dx in breast cancer patients.

Oncotype Dx signature is predominated by two groups of genes, one group related to hormone receptors, and another group of proliferation markers. It is now widely accepted that high expression of ER and the related genes is associated with better prognosis and sensitivity to endocrine therapy in breast cancer. On the other hand, high expression of proliferation markers such as Ki67 is associated with a worse prognosis but sensitivity to chemotherapy (4, 8). This information is the basis for the IHC4 assay of ER, PR, HER2, and Ki67. Oncotype Dx draws expression data from a set of genes highly clustered with ER and Ki67, instead

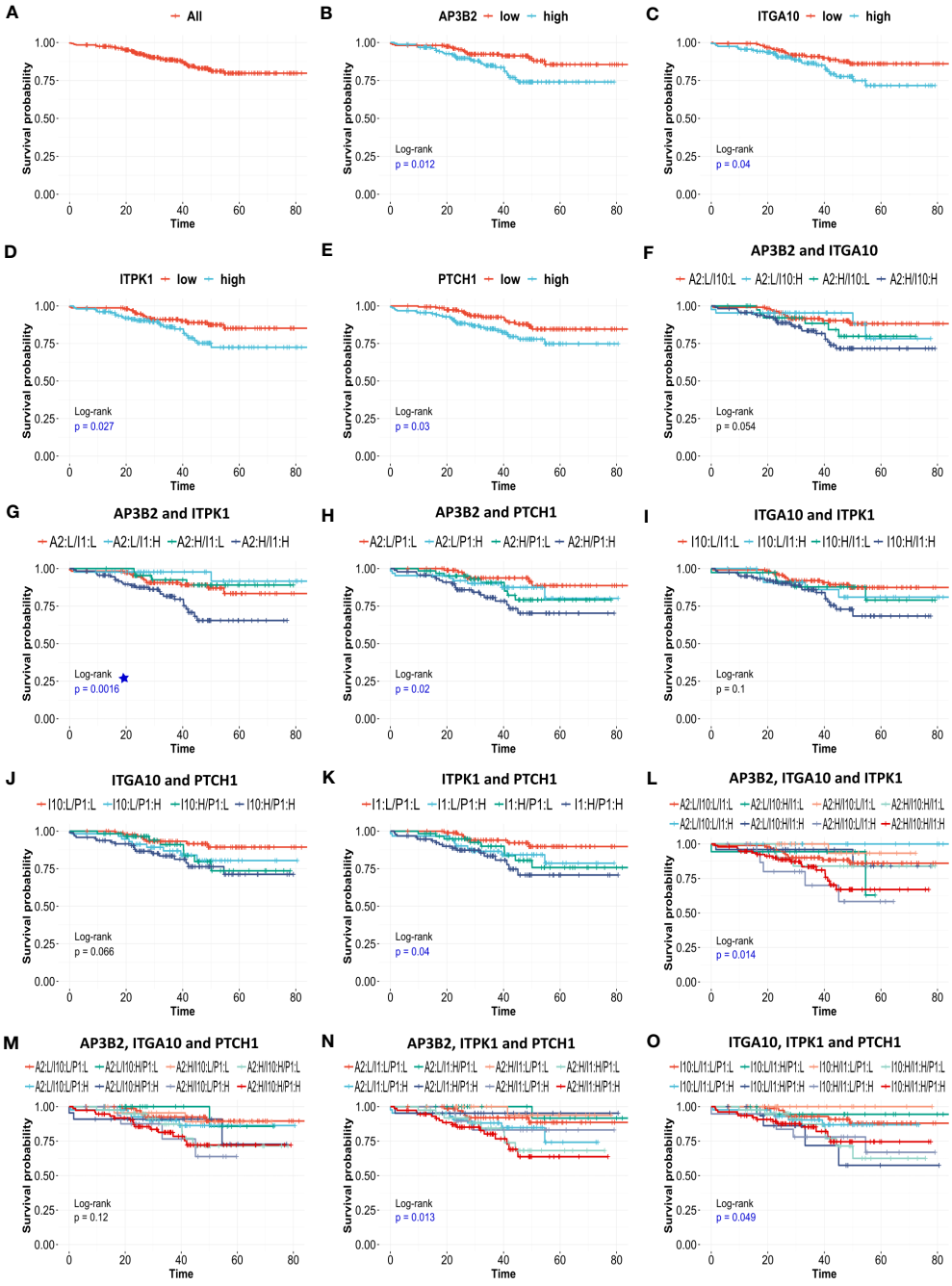

FIGURE 9
The effects of AP3B2, ITGA10, ITPK1, and PTCH1 on relapse-free survival of ER+/HER2- breast cancer patients. KM survival plots for the **(A)** null model, **(B)** AP3B2, **(C)** ITGA10, **(D)** ITPK1, **(E)** PTCH1, **(F)** AP3B2 and ITGA10, **(G)** AP3B2 and ITPK1, **(H)** AP3B2 and PTCH1, **(I)** ITGA10 and ITPK1, **(J)** ITGA10 and PTCH1, **(K)** ITPK1 and PTCH1, **(L)** AP3B2, ITGA10, and ITPK1, **(M)** AP3B2, ITGA10, and PTCH1, **(N)** AP3B2, ITPK1, and PTCH1, **(O)** ITGA10, ITPK1, and PTCH1, in 316 ER+/HER2- breast cancer patients who underwent neoadjuvant chemotherapy. H: high, L: low.

of testing only these individual genes like the IHC4 assay. This may provide some robustness to Oncotype Dx (8, 51). However, our analysis in the validation set of ER+/HER2- breast cancer patients and the 1100 breast cancers in TCGA dataset demonstrated that the expressions of the ER group genes in the Oncotype Dx signature are substantially correlated with each other, and proliferation markers are strongly correlated with each other, these two clusters being negatively correlated. Therefore, in practice, the predictive advantage of Oncotype Dx over IHC4 may be limited.

The 18 gene list we identified in this study may have several advantages over multigene assays like Oncotype Dx. First, the constituents of the 18 gene list are highly independent in terms of biological functions compared to the components of the Oncotype Dx signature. Therefore, it may capture information from an extensive subset of biological processes associated with chemoresistance. Secondly, the Oncotype Dx may be more efficient in predicting resistance to endocrine therapy rather than chemotherapy, since ER-related genes constitute a big part of the

TABLE 4 The statistical significance measures for Cox Proportional Hazards Regression Models.

Gene/Genes	COX-PH Model Fit			ANOVA		
	Concordance	Log-rank p	Sig.	Chi-Sqr	Pr(>|Chi|)	Sig.
AP3B2	0.559	1		0.0008	0.978	
ITGA10	0.556	0.4		0.8412	<2e-16	***
ITPK1	0.603	0.2		0.5873	<2e-16	***
PTCH1	0.625	0.01	*	6.4123	<2e-16	***
CTNNB1	0.602	0.02	*	2.4801	<2e-16	***
AP3B2 + ITGA10	0.540	0.5		4.0103	0.045	*
AP3B2 + ITPK1	0.597	0.4		0.4428	<2e-16	***
AP3B2 + PTCH1	0.630	0.02	*	4.975	<2e-16	***
ITGA10 + ITPK1	0.606	0.5		5.3101	<2e-16	***
ITGA10 + PTCH1	0.626	0.03	*	6.4228	<2e-16	***
ITPK1 + PTCH1	0.633	0.03	*	0.2529	<2e-16	***
AP3B2 + CTNNB1	0.624	0.05		2.3355	<2e-16	***
ITGA10 + CTNNB1	0.616	0.02	*	1.9464	<2e-16	***
ITPK1 + CTNNB1	0.625	0.04	*	0.6459	<2e-16	***
PTCH1 + CTNNB1	0.660	0.003	**	6.7732	<2e-16	***
AP3B2 + ITGA10 + ITPK1	0.579	0.6		11.8057	0.0005	***
AP3B2 + ITGA10 + PTCH1	0.619	0.06		6.4765	<2e-16	***
AP3B2 + ITPK1 + PTCH1	0.630	0.05		0.2698	<2e-16	***
ITGA10 + ITPK1 + PTCH1	0.635	0.07		0.6456	<2e-16	***
AP3B2 + ITGA10 + CTNNB1	0.613	0.06		0.2395	<2e-16	***
AP3B2 + ITPK1 + CTNNB1	0.625	0.09		0.8286	<2e-16	***
AP3B2 + PTCH1 + CTNNB1	0.661	0.008	**	6.7832	<2e-16	***
ITGA10 + ITPK1 + CTNNB1	0.616	0.06		6.022	<2e-16	***
ITGA10 + PTCH1 + CTNNB1	0.669	0.006	**	6.5044	<2e-16	***
ITPK1 + PTCH1 + CTNNB1	0.672	0.007	**	0.0773	<2e-16	***
AP3B2 + ITGA10 + ITPK1 + PTCH1	0.627	0.1		5.4122	0.020	*
AP3B2 + ITGA10 + ITPK1 + CTNNB1	0.614	0.1		0.7987	<2e-16	***
AP3B2 + ITGA10 + PTCH1 + CTNNB1	0.664	0.01	*	6.4861	<2e-16	***
AP3B2 + ITPK1 + PTCH1 + CTNNB1	0.669	0.02	*	0.2227	<2e-16	***
ITGA10 + ITPK1 + PTCH1 + CTNNB1	0.672	0.01	*	0.0798	<2e-16	***
AP3B2 + ITGA10 + ITPK1 + PTCH1 + CTNNB1	0.666	0.03	*	0.2139	0.643	

Sig., significance; *, p<0.05; **, p<0.01; ***, p<0.001.

signature. On the other hand, the 18 gene list we derived specifically from the data of patients who underwent taxane-based chemotherapy may be more accurate in predicting resistance to chemotherapy. Therefore, these 18 genes may have a higher predictive strength to guide the clinical decision on systemic chemotherapy in ER+/HER2- breast cancer patients. However, the size of the cohorts was a limitation to validate that. Therefore, prospective studies in larger cohorts are needed.

One other limitation of the development of predictive gene signatures is the use of pathological complete response as the surrogate of responsiveness to the therapy. Since the observation and evaluation of the pathological complete response after therapy are advantageous over the follow-up of relapse-free or overall survival, it is commonly used as the primary outcome in clinical studies to speed up the drug discovery process. However, emerging evidence suggests that its surrogacy may be different in distinct

TABLE 5 Hazard Ratios for AP3B2, ITGA10, ITPK1, PTCH1, and CTNNB1 in univariate and multivariate Cox Proportional Hazards Regression Models.

Gene	Univariate Models					Multivariate Model				
	HR	Lower 95.	Upper 95.	Pr(>|z|)	Adj.p	HR	Lower 95.	Upper 95.	Pr(>|z|)	Adj.p
AP3B2	1.004	0.780	1.292	0.978	0.978	0.920	0.646	1.309	0.641	0.792
ITGA10	1.213	0.795	1.851	0.370	0.462	1.200	0.618	2.331	0.591	0.792
ITPK1	1.236	0.864	1.770	0.246	0.410	1.069	0.653	1.751	0.792	0.792
PTCH1	1.534	1.109	2.123	0.009	0.045	1.541	1.073	2.214	0.019	0.047
CTNNB1	1.563	1.074	2.273	0.019	0.047	1.667	1.106	2.512	0.014	0.047

HR, Hazards ratio; Lower 95. and Upper 95. represent lower and upper boundaries of 95% confidence interval, Adj.p: FDR adjusted p-values calculated by the "Benjamini-Hochberg" method.

breast cancer subtypes, with questionable efficacy as a predictor of patient survival (47–49). Since publicly available datasets mostly report pathological complete response as the surrogate of therapy response and the number of patients in the datasets which included relapse-free survival or overall survival was limited, the initial steps of our algorithm for feature selection were mostly based on pathological response as the surrogate of response. This further limit the strength of the 18 genes we identified in this study. However, regarding this limitation, we further analyzed the impact of these 18 genes on relapse-free survival in another validation cohort with data on relapse-free survival.

Our KM-survival analysis of 316 ER+/HER2-patients who had undergone neoadjuvant chemotherapy validated the poor prognostic effect of *AP3B2, ITGA10, ITPK1*, and *PTCH1* as categorical variates out of 18 genes (Figures 9A–E). The multivariate survival models which included these four genes as dual or triple combinations were also significant mostly (Figures 9F–O), *AP3B2/ITPK1* gene pair achieving the lowest log-rank p-values (Figure 9G). These findings suggested that *AP3B2, ITGA10, ITPK1*, and *PTCH1* may be markers of resistance to taxane-based neoadjuvant chemotherapy in ER+/HER2- breast cancer patients. However, the evidence for their use as markers is insufficient yet. Therefore, a thorough investigation of both expression and mutation status together with molecular interactors of these genes should be performed to understand their role in chemoresistance in breast cancer.

The key finding of this study is the emergence of *PTCH1* and *CTNBB1* as key predictors for resistance to taxane-based neoadjuvant therapy in ER+/HER2- breast cancer. Our Cox Proportional Hazards analysis revealed that *PTCH1* and *CTNBB1* pose the highest risk for resistance, with hazard ratios over 1.5 in ER +/HER2- breast cancer patients. Their hazard ratios further increased over 1.6 in the multivariate model in the neoadjuvant therapy group. *PTCH1* and *CTNNB1* did not exhibit an increased risk in the control group and endocrine therapy group, further strengthening the predictive potential of *PTCH1* and *CTNNB1* in ER+/HER2- breast cancer. These findings together with the knowledge on the biology of these genes strongly support their predictor role in chemoresistance.

PTCH1 is a transmembrane receptor for sonic hedgehog (SHH). In the unbound form, PTCH1 captures the protein "smoothened" (SMO) which has proliferative action. The binding of SHH leads to the degradation of PTCH1, hence releasing the SMO. Then SMO dissociates Glioma-associated oncogene GLI from SUFU, activating the transcription of target genes with tumorigenic action. Due to this mechanism, PTCH1 is known as a tumor suppressor (52). However, increased expression of PTCH1 was detected in several cancers including ovarian carcinoma, lung,

TABLE 6 The hazard ratios for PTCH1, and CTNNB1 in three different arms of treatment in ER+/HER2- breast cancer patients.

Treatment Arms Gene	Univariate Models				Multivariate Model			
	HR	Lower 95.	Upper 95.	Pr(>|z|)	HR	Lower 95.	Upper 95.	Pr(>|z|)
No systemic tx (n=421)								
PTCH1	0.875	0.752	1.018	0.084	0.873	0.749	1.018	0.082
CTNNB1	0.846	0.647	1.106	0.221	0.843	0.645	1.105	0.217
Neoadjuvant Ctx (n=361)								
PTCH1	**1.534**	**1.109**	**2.123**	**0.009**	**1.605**	**1.133**	**2.273**	**0.007**
CTNNB1	**1.563**	**1.074**	**2.273**	**0.019**	**1.630**	**1.109**	**2.395**	**0.012**
Endocrine tx (n=1087)								
PTCH1	0.927	0.835	1.029	0.153	0.931	0.838	1.035	0.187
CTNNB1	0.779	0.654	0.928	0.005	0.782	0.657	0.932	0.005

HR: Hazards ratio, Lower 95. and Upper 95. represent lower and upper boundaries of 95% confidence interval respectively.
The results for which there is a statistically significant increase in HR are written in bold.

and prostate cancer (53, 54). More importantly, PTCH1 acts as a multidrug resistance pump, expelling chemotherapeutics like doxorubicin, and dyes like Hoesct33342, hence inducing chemoresistance (55). Since taxanes share important drug efflux pumps with doxorubicin and Hoesct33342 such as MDR1 (56), there is a high probability that taxanes can be substrates for efflux by PTCH1. Hence, *PTCH1* may be a crucial marker of resistance to taxanes and other chemotherapeutics like anthracyclines used in taxane-based chemotherapy. Moreover, targeting PTCH1 may be a key strategy to overcome taxane resistance in cancer. Accordingly, paclitaxel was shown to increase PTCH1 expression, and inhibition of proteasome suppressed PTCH1 levels and increased sensitivity of ovarian cancer cells to the paclitaxel (57). Furthermore, mutated *PTCH1* was proposed as a strong predictor of recurrence in breast cancer (58), and fusion of *PTCH1* with glioma-associated proteins was associated with oncogenic activation in different tumors (59). All these findings indicate a significant potential for PTCH1 in chemoresistance via its functions as a drug efflux pump and a hedgehog receptor.

CTNNB1 encodes β-Catenin which is a crucial component of E-cadherin-mediated cell-cell adhesion and a downstream mediator of canonical WNT pathway. β-Catenin is significantly involved in mammary tissue development, breast cancer formation, and metastasis. Alterations in the gene expression and the localization of β-Catenin are frequently reported in breast cancer. However, the involvement of the WNT/β-Catenin pathway in breast cancer is intricate, and the expression level of β-Catenin provides incomplete information without investigation of its activity and subcellular localization (41). Therefore, there is still a discrepancy in the exact mechanisms by which WNT/β-Catenin signaling plays a role in breast cancer (60).

Similar to the controversial effects of the WNT/β-Catenin pathway reported in the literature, we observed that the signature genes that are upregulated or downregulated in the presence of constitutively active CTNNB1 were enriched in ER+/HER2- breast cancer patients with incomplete pathological response to taxane-based chemotherapy in GEO datasets (Figures 3A, B). However, CTNNB1 was down-regulated in ER+/HER2- breast cancer patients with incomplete pathological response to taxane-based chemotherapy in the validation cohort (Figure 3C). This discrepancy pointed out the necessity of investigating the activity and subcellular localization of this molecule in patient samples, besides gene expression levels, to achieve a complete understanding of the involvement of β-Catenin in chemoresistance. Despite this discrepancy in differential expression in test and validation cohorts, the high expression of *CTNNB1* was associated with decreased survival in KM-survival analysis (Figure 3E) and *CTNNB1* demonstrated the highest hazards ratio and significance in Cox proportional hazards regression (Tables 4, 5). Therefore, our results suggested the involvement of CTNNB1 in resistance to taxane-based neoadjuvant chemotherapy in ER+/HER2- breast cancer patients.

PTCH1 and CTNNB1 take role in distinct oncogenic signaling pathways. However, our Cox Proportional Hazard models suggested an interaction between these two genes. Therefore, we searched the relevant literature to find out biological interactions between these two molecules. The non-canonical hedgehog pathway was reported to increase the expression of WNT through the involvement of PTCH1 in colon carcinoma (61). Moreover, the WNT/B-catenin pathway was reported to regulate the SHH pathway at multiple levels in different studies (62). These observations suggest that the crosstalk between SHH/PTCH1 and WNT/β-Catenin pathway may have a pivotal role in chemoresistance in ER+/HER2- breast cancer. In our prospective studies, we will dissect the mechanisms by which these pathways play a role in chemoresistance, considering the mutation status, activity, subcellular localization, and interactors of each molecule in ER+/HER2- breast cancer.

In conclusion, *PTCH1* and *CTNBB1* emerge as key markers of resistance to taxane-based neoadjuvant chemotherapy in ER+/HER2- breast cancer patients. Future studies in larger cohorts may present them as predictive markers cost-effectively incorporated into clinics to guide decisions on taxane-based chemotherapy. Detailed investigation of their molecular mechanisms may also enable the development of new molecular-targeted agents for overcoming chemoresistance in ER+/HER2- breast cancer patients. This will be addressed in our future studies.

Data availability statement

The original contributions presented in the study are included in the article/Supplementary Material. Further inquiries can be directed to the corresponding author.

Ethics statement

Ethical approval was not required for the study involving humans in accordance with the local legislation and institutional requirements. Written informed consent to participate in this study was not required from the participants or the participants' legal guardians/next of kin in accordance with the national legislation and the institutional requirements.

Author contributions

GO conceptualized the study, analyzed, and interpreted the genomic data to identify key markers of resistance to taxane-based neoadjuvant chemotherapy in ER+/HER2-breast cancer. GO conducted the whole study and wrote the manuscript. The author confirms being the sole contributor of this work and has approved it for publication.

Funding

The author declares that there is no funding used for the current study.

Acknowledgments

The author gratefully acknowledges the use of services and facilities of the Koç University Research Center for Translational Medicine (KUTTAM), funded by the Presidency of Turkey, Presidency of Strategy and Budget.

Conflict of interest

The author declares that the research was conducted in the absence of any commercial or financial relationships that could be construed as a potential conflict of interest.

Publisher's note

Supplementary material

The Supplementary Material for this article can be found online at: https://www.frontiersin.org/articles/10.3389/fonc.2023.1216438/full#supplementary-material

References

1. Sung H, Ferlay J, Siegel RL, Laversanne M, Soerjomataram I, Jemal A, et al. Global cancer statistics 2020: GLOBOCAN estimates of incidence and mortality worldwide for 36 cancers in 185 countries. *CA: A Cancer J Clin* (2021) 71(3):209–49. doi: 10.3322/caac.21660

2. Cheang MC, Martin M, Nielsen TO, Prat A, Voduc D, Rodriguez-Lescure A, et al. Defining breast cancer intrinsic subtypes by quantitative receptor expression. *Oncologist* (2015) 20(5):474–82. doi: 10.1634/theoncologist.2014-0372

3. Harbeck N, Penault-Llorca F, Cortes J, Gnant M, Houssami N, Poortmans P, et al. Breast cancer. *Nat Rev Dis Primers.* (2019) 5(1):66. doi: 10.1038/s41572-019-0111-2

4. Cardoso F, Kyriakides S, Ohno S, Penault-Llorca F, Poortmans P, Rubio IT, et al. Early breast cancer: ESMO Clinical Practice Guidelines for diagnosis, treatment and follow-up†. *Ann Oncol* (2019) 30(8):1194–220. doi: 10.1093/annonc/mdz173

5. Szostakowska M, Trębińska-Stryjewska A, Grzybowska EA, Fabisiewicz A. Resistance to endocrine therapy in breast cancer: molecular mechanisms and future goals. *Breast Cancer Res Treat* (2019) 173(3):489–97. doi: 10.1007/s10549-018-5023-4

6. Waks AG, Winer EP. Breast cancer treatment: A review. *JAMA* (2019) 321 (3):288–300. doi: 10.1001/jama.2018.19323

7. Burguin A, Diorio C, Durocher F. Breast cancer treatments: updates and new challenges. *J Pers Med* (2021) 11(8). doi: 10.3390/jpm11080808

8. Győrffy B, Hatzis C, Sanft T, Hofstatter E, Aktas B, Pusztai L. Multigene prognostic tests in breast cancer: past, present, future. *Breast Cancer Res* (2015) 17 (1):11. doi: 10.1186/s13058-015-0514-2

9. Iwata H, Masuda N, Yamamoto Y, Fujisawa T, Toyama T, Kashiwaba M, et al. Validation of the 21-gene test as a predictor of clinical response to neoadjuvant hormonal therapy for ER+, HER2-negative breast cancer: the TransNEOS study. *Breast Cancer Res Treat* (2019) 173(1):123–33. doi: 10.1007/s10549-018-4964-y

10. Sparano JA, Gray RJ, Makower DF, Pritchard KI, Albain KS, Hayes DF, et al. Adjuvant chemotherapy guided by a 21-gene expression assay in breast cancer. *N Engl J Med* (2018) 379(2):111–21. doi: 10.1056/NEJMoa1804710

11. Bhargava R, Esposito NN, O'Connor SM, Li Z, Turner BM, Moisini I, et al. Magee Equations™ and response to neoadjuvant chemotherapy in ER+/HER2-negative breast cancer: a multi-institutional study. *Mod Pathol* (2021) 34(1):77–84. doi: 10.1038/s41379-020-0620-2

12. Buus R, Sestak I, Kronenwett R, Ferree S, Schnabel CA , Baehner FL, et al. Molecular drivers of oncotype DX, prosigna, endoPredict, and the breast cancer index: A transATAC study. *J Clin Oncol* (2021) 39(2):126–35. doi: 10.1200/jco.20.00853

13. Lux MP, Minartz C, Müller-Huesmann H, Sandor MF, Herrmann KH, Radeck-Knorre S, et al. Budget impact of the Oncotype DX® test compared to other gene expression tests in patients with early breast cancer in Germany. *Cancer Treat Res Commun* (2022) 31:100519. doi: 10.1016/j.ctarc.2022.100519

14. Crolley VE, Marashi H, Rawther S, Sirohi B, Parton M, Graham J, et al. The impact of Oncotype DX breast cancer assay results on clinical practice: a UK experience. *Breast Cancer Res Treat* (2020) 180(3):809–17. doi: 10.1007/s10549-020-05578-6

15. Özmen V, Çakar B, Gökmen E, Özdoğan M, Güler N, Uras C, et al. Cost effectiveness of gene expression profiling in patients with early-stage breast cancer in a middle-income country, Turkey: results of a prospective multicenter study. *Eur J Breast Health* (2019) 15(3):183–90. doi: 10.5152/ejbh.2019.4761

16. Fekete JT, Győrffy B. ROCplot.org: Validating predictive biomarkers of chemotherapy/hormonal therapy/anti-HER2 therapy using transcriptomic data of 3,104 breast cancer patients. *Int J Cancer.* (2019) 145(11):3140–51. doi: 10.1002/ijc.32369

17. Győrffy B, Lanczky A, Eklund AC, Denkert C, Budczies J, Li Q, et al. An online survival analysis tool to rapidly assess the effect of 22,277 genes on breast cancer prognosis using microarray data of 1,809 patients. *Breast Cancer Res Treat* (2010) 123 (3):725–31. doi: 10.1007/s10549-009-0674-9

18. Lánczky A, Győrffy B. Web-based survival analysis tool tailored for medical research (KMplot): development and implementation. *J Med Internet Res* (2021) 23(7): e27633. doi: 10.2196/27633

19. Popovici V, Chen W, Gallas BG, Hatzis C, Shi W, Samuelson FW, et al. Effect of training-sample size and classification difficulty on the accuracy of genomic predictors. *Breast Cancer Res* (2010) 12(1):R5. doi: 10.1186/bcr2468

20. Shi L, Campbell G, Jones WD, Campagne F, Wen Z, Walker SJ, et al. The MicroArray Quality Control (MAQC)-II study of common practices for the development and validation of microarray-based predictive models. *Nat Biotechnol* (2010) 28(8):827–38. doi: 10.1038/nbt.1665

21. Hatzis C, Pusztai L, Valero V, Booser DJ, Esserman L, Lluch A, et al. A genomic predictor of response and survival following taxane-anthracycline chemotherapy for invasive breast cancer. *Jama* (2011) 305(18):1873–81. doi: 10.1001/jama.2011.593

22. Itoh M, Iwamoto T, Matsuoka J, Nogami T, Motoki T, Shien T, et al. Estrogen receptor (ER) mRNA expression and molecular subtype distribution in ER-negative/progesterone receptor-positive breast cancers. *Breast Cancer Res Treat* (2014) 143 (2):403–9. doi: 10.1007/s10549-013-2763-z

23. Tabchy A, Valero V, Vidaurre T, Lluch A, Gomez H, Martin M, et al. Evaluation of a 30-gene paclitaxel, fluorouracil, doxorubicin, and cyclophosphamide chemotherapy response predictor in a multicenter randomized trial in breast cancer. *Clin Cancer Res* (2010) 16(21):5351–61. doi: 10.1158/1078-0432.Ccr-10-1265

24. Shen K, Song N, Kim Y, Tian C, Rice SD, Gabrin MJ, et al. A systematic evaluation of multi-gene predictors for the pathological response of breast cancer patients to chemotherapy. *PloS One* (2012) 7(11):e49529. doi: 10.1371/journal.pone.0049529

25. Miyake T, Nakayama T, Naoi Y, Yamamoto N, Otani Y, Kim SJ, et al. GSTP1 expression predicts poor pathological complete response to neoadjuvant chemotherapy in ER-negative breast cancer. *Cancer Sci* (2012) 103(5):913–20. doi: 10.1111/j.1349-7006.2012.02231.x

26. Zhou Y, Zhou B, Pache L, Chang M, Khodabakhshi AH, Tanaseichuk O, et al. Metascape provides a biologist-oriented resource for the analysis of systems-level datasets. *Nat Commun* (2019) 10(1):1523. doi: 10.1038/s41467-019-09234-6

27. Subramanian A, Tamayo P, Mootha VK, Mukherjee S, Ebert BL, Gillette MA, et al. Gene set enrichment analysis: a knowledge-based approach for interpreting genome-wide expression profiles. *Proc Natl Acad Sci U S A.* (2005) 102(43):15545–50. doi: 10.1073/pnas.0506580102

28. Liberzon A, Birger C, Thorvaldsdóttir H, Ghandi M, Mesirov JP, Tamayo P. The Molecular Signatures Database (MSigDB) hallmark gene set collection. *Cell Syst* (2015) 1(6):417–25. doi: 10.1016/j.cels.2015.12.004

29. Liberzon A, Subramanian A, Pinchback R, Thorvaldsdóttir H, Tamayo P, Mesirov JP. Molecular signatures database (MSigDB) 3.0. *Bioinformatics* (2011) 27 (12):1739–40. doi: 10.1093/bioinformatics/btr260

30. Tang Z, Kang B, Li C, Chen T, Zhang Z. GEPIA2: an enhanced web server for large-scale expression profiling and interactive analysis. *Nucleic Acids Res* (2019) 47 (W1):W556–w60. doi: 10.1093/nar/gkz430

31. Chen T, Liu Y-X, Huang L. ImageGP: An easy-to-use data visualization web server for scientific researchers. *iMeta* (2022) 1(1):e5. doi: 10.1002/imt2.5

32. Li T, Fu J, Zeng Z, Cohen D, Li J, Chen Q, et al. TIMER2.0 for analysis of tumor-infiltrating immune cells. *Nucleic Acids Res* (2020) 48(W1):W509–w14. doi: 10.1093/nar/gkaa407

33. Wei G, Twomey D, Lamb J, Schlis K, Agarwal J, Stam RW, et al. Gene expression-based chemical genomics identifies rapamycin as a modulator of MCL1 and glucocorticoid resistance. *Cancer Cell* (2006) 10(4):331–42. doi: 10.1016/j.ccr.2006.09.006

34. Lamb J, Ramaswamy S, Ford HL, Contreras B, Martinez RV, Kittrell FS, et al. A mechanism of cyclin D1 action encoded in the patterns of gene expression in human cancer. *Cell* (2003) 114(3):323–34. doi: 10.1016/s0092-8674(03)00570-1

35. Murugan AK. mTOR: Role in cancer, metastasis and drug resistance. *Semin Cancer Biol* (2019) 59:92–111. doi: 10.1016/j.semcancer.2019.07.003

36. Bièche I, Olivi M, Noguès C, Vidaud M, Lidereau R. Prognostic value of CCND1 gene status in sporadic breast tumours, as determined by real-time quantitative PCR assays. *Br J Cancer.* (2002) 86(4):580–6. doi: 10.1038/sj.bjc.6600109

37. Dong C, Wu J, Chen Y, Nie J, Chen C. Activation of PI3K/AKT/mTOR pathway causes drug resistance in breast cancer. *Front Pharmacol* (2021) 12:628690. doi: 10.3389/fphar.2021.628690

38. Lundberg A, Lindström LS, Li J, Harrell JC, Darai-Ramqvist E, Sifakis EG, et al. The long-term prognostic and predictive capacity of cyclin D1 gene amplification in 2305 breast tumours. *Breast Cancer Res* (2019) 21(1):34. doi: 10.1186/s13058-019-1121-4

39. Chamorro MN, Schwartz DR, Vonica A, Brivanlou AH, Cho KR, Varmus HE. FGF-20 and DKK1 are transcriptional targets of beta-catenin and FGF-20 is implicated in cancer and development. *EMBO J* (2005) 24(1):73–84. doi: 10.1038/sj.emboj.7600460

40. Bild AH, Yao G, Chang JT, Wang Q, Potti A, Chasse D, et al. Oncogenic pathway signatures in human cancers as a guide to targeted therapies. *Nature* (2006) 439(7074):353–7. doi: 10.1038/nature04296

41. Xu X, Zhang M, Xu F, Jiang S. Wnt signaling in breast cancer: biological mechanisms, challenges and opportunities. *Mol Cancer.* (2020) 19(1):165. doi: 10.1186/s12943-020-01276-5

42. Sherman BT, Hao M, Qiu J, Jiao X, Baseler MW, Lane HC, et al. DAVID: a web server for functional enrichment analysis and functional annotation of gene lists (2021 update). *Nucleic Acids Res* (2022) 50(W1):W216–21. doi: 10.1093/nar/gkac194

43. Soliman H, Wagner S, Flake DD 2nd, Robson M, Schwartzberg L, Sharma P, et al. Evaluation of the 12-gene molecular score and the 21-gene recurrence score as predictors of response to neo-adjuvant chemotherapy in estrogen receptor-positive, HER2-negative breast cancer. *Ann Surg Oncol* (2020) 27(3):765–71. doi: 10.1245/s10434-019-08039-7

44. Bear HD, Wan W, Robidoux A, Rubin P, Limentani S, White RL Jr., et al. Using the 21-gene assay from core needle biopsies to choose neoadjuvant therapy for breast cancer: A multicenter trial. *J Surg Oncol* (2017) 115(8):917–23. doi: 10.1002/jso.24610

45. Cardoso F, van't Veer LJ, Bogaerts J, Slaets L, Viale G, Delaloge S, et al. 70-gene signature as an aid to treatment decisions in early-stage breast cancer. *N Engl J Med* (2016) 375(8):717–29. doi: 10.1056/NEJMoa1602253

46. Özcan G. SCUBE2 as a marker of resistance to taxane-based neoadjuvant chemotherapy and a potential therapeutic target in breast cancer. *Eur J Breast Health* (2023) 19(1):45–54. doi: 10.4274/ejbh.galenos.2022.2022-8-2

47. Conforti F, Pala L, Sala I, Oriecuia C, De Pas T, Specchia C, et al. Evaluation of pathological complete response as surrogate endpoint in neoadjuvant randomised clinical trials of early stage breast cancer: systematic review and meta-analysis. *BMJ* (2021) 375:e066381. doi: 10.1136/bmj-2021-066381

48. Wang-Lopez Q, Chalabi N, Abrial C, Radosevic-Robin N, Durando X, Mouret-Reynier M-A, et al. Can pathologic complete response (pCR) be used as a surrogate marker of survival after neoadjuvant therapy for breast cancer? *Crit Rev Oncology/Hematol* (2015) 95(1):88–104. doi: 10.1016/j.critrevonc.2015.02.011

49. Davey MG, Browne F, Miller N, Lowery AJ, Kerin MJ. Pathological complete response as a surrogate to improved survival in human epidermal growth factor receptor-2-positive breast cancer: systematic review and meta-analysis. *BJS Open* (2022) 6(3). doi: 10.1093/bjsopen/zrac028

50. Buus R, Szijgyarto Z, Schuster EF, Xiao H, Haynes BP, Sestak I, et al. Development and validation for research assessment of Oncotype DX® Breast Recurrence Score, EndoPredict® and Prosigna®. *NPJ Breast Cancer.* (2021) 7(1):15. doi: 10.1038/s41523-021-00216-w

51. Yeo B, Zabaglo L, Hills M, Dodson A, Smith I, Dowsett M. Clinical utility of the IHC4+C score in oestrogen receptor-positive early breast cancer: a prospective decision impact study. *Br J Cancer.* (2015) 113(3):390–5. doi: 10.1038/bjc.2015.222

52. Niyaz M, Khan MS, Mudassar S. Hedgehog signaling: an achilles' Heel in cancer. *Transl Oncol* (2019) 12(10):1334–44. doi: 10.1016/j.tranon.2019.07.004

53. Karin-Kujundzic V, Covarrubias-Pinto A, Skrtic A, Vranic S, Serman L. New insight into the role of PTCH1 protein in serous ovarian carcinomas. *Int J Oncol* (2022) 61(6):145. doi: 10.3892/ijo.2022.5435

54. Gonnissen A, Isebaert S, Perneel C, McKee CM, Van Utterbeeck F, Lerut E, et al. Patched 1 expression correlates with biochemical relapse in high-risk prostate cancer patients. *Am J Pathol* (2018) 188(3):795–804. doi: 10.1016/j.ajpath.2017.11.019

55. Hasanovic A, Mus-Veteau I. Targeting the multidrug transporter ptch1 potentiates chemotherapy efficiency. *Cells* (2018) 7(8):107. doi: 10.3390/cells7080107

56. Wind NS, Holen I. Multidrug resistance in breast cancer: from *in vitro* models to clinical studies. *Int J Breast Cancer.* (2011) 2011:967419. doi: 10.4061/2011/967419

57. Steg AD, Burke MR, Amm HM, Katre AA, Dobbin ZC, Jeong DH, et al. Proteasome inhibition reverses hedgehog inhibitor and taxane resistance in ovarian cancer. *Oncotarget* (2014) 5(16):7065–80. doi: 10.18632/oncotarget.2295

58. Wang C-Y, Chang Y-C, Kuo Y-L, Lee K-T, Chen P-S, Cheung CHA, et al. Mutation of the PTCH1 gene predicts recurrence of breast cancer. *Sci Rep* (2019) 9(1):16359. doi: 10.1038/s41598-019-52617-4

59. Alwaqfi RR, Samuelson MI, Guseva NN, Ouyang M, Bossler AD, Ma D. PTCH1-GLI1 fusion-positive ovarian tumor: report of a unique case with response to tyrosine kinase inhibitor pazopanib. *J Natl Compr Canc Netw* (2021) 19(9):998–1004. doi: 10.6004/jnccn.2021.7058

60. Van Schie EH, Van Amerongen R. Aberrant WNT/CTNNB1 signaling as a therapeutic target in human breast cancer: weighing the evidence. *Front Cell Dev Biol* (2020) 8:25. doi: 10.3389/fcell.2020.00025

61. Regan JL, Schumacher D, Staudte S, Steffen A, Haybaeck J, Keilholz U, et al. Non-canonical hedgehog signaling is a positive regulator of the WNT pathway and is required for the survival of colon cancer stem cells. *Cell Rep* (2017) 21(10):2813–28. doi: 10.1016/j.celrep.2017.11.025

62. Kumar V, Vashishta M, Kong L, Wu X, Lu JJ, Guha C, et al. The role of notch, hedgehog, and wnt signaling pathways in the resistance of tumors to anticancer therapies. *Front Cell Dev Biol* (2021) 9:650772. doi: 10.3389/fcell.2021.650772

frontiers | Frontiers in Oncology

TYPE Review
PUBLISHED 27 September 2023
DOI 10.3389/fonc.2023.1253191

OPEN ACCESS

EDITED BY
Zheng Wang,
Shanghai Jiao Tong University, China

REVIEWED BY
Pai-Sheng Chen,
National Cheng Kung University, Taiwan
Yuqi Yang,
St. John's University, United States

*CORRESPONDENCE
Zhiqun Cao
caozhiqun@163.com

†These authors have contributed equally to this work and share first authorship

RECEIVED 05 July 2023
ACCEPTED 06 September 2023
PUBLISHED 27 September 2023

CITATION
Zhou J, Xiang H and Cao Z (2023) Dual mechanism of Let-7i in tumor progression. *Front. Oncol.* 13:1253191. doi: 10.3389/fonc.2023.1253191

Dual mechanism of Let-7i in tumor progression

Jiapei Zhou[1†], Hongjie Xiang[2†] and Zhiqun Cao[1*]

[1]First Clinical Medical College, Shandong University of Traditional Chinese Medicine, Jinan, China, [2]Department of Traditional Chinese Medicine, The First Affiliated Hospital of Shandong First Medical University & Shandong Provincial Qianfoshan Hospital, Jinan, China

Let-7i regulates tumors primarily by binding to the 3′ untranslated region (3′ UTR) of mRNA, which indirectly regulates post-transcriptional gene expression. Let-7i also has an epigenetic function via modulating DNA methylation to directly regulate gene expression. Let-7i performs a dual role by inducing both the promotion and inhibition of various malignancies, depending on its target. The mechanism of Let-7i action involves cancer cell proliferation, migration, invasion, apoptosis, epithelial-mesenchymal transition, EV transmission, angiogenesis, autophagy, and drug resistance sensitization. Let-7i is closely related to cancer, and hence, is a potential biomarker for the diagnosis and prognosis of various cancers. Therapeutically, it can be used to promote an anti-cancer immune response by modifying exosomes, thus exerting a tumor-suppressive effect.

KEYWORDS

Let-7i, cancer, promoter, inhibitor, dual mechanism

1 Introduction

MicroRNA (miRNA) refers to short non-coding RNA with a length of 19–25 nucleotides that functions as a conservative post-transcriptional regulator of gene expression. It recruits Argonaute proteins to form the RNA-induced silencing complex (RISC), which regulates RNA via base-complementary pairing. The combination of miRNA and RISC can inhibit mRNA translation without destroying the stability of mRNA as well as silence unwanted genetic material and transcripts (1, 2). When the miRNA and mRNA involved are entirely complementary, the complex can also mediate mRNA degradation to inhibit transcription (3), thereby regulating the production of the resulting protein. In addition, it has been found that mature miRNAs have the ability to enter the nucleus, directly combine with the original components of gene promoter regions, and contribute to the regulation of non-classical gene transcription (4). MiRNA is involved in almost all biological processes, including cell growth, proliferation, differentiation, metabolism, and the development of organisms (5). Each miRNA binds to hundreds of different mRNAs, and miRNA controls more than half of human protein-coding genes (6). Therefore, the dysregulation of miRNA expression is closely related to the occurrence of various diseases, including cancer (7).

MiRNA biogenesis requires a series of sequential processing events. First, miRNA is transcribed as long primary transcripts (pri-miRNA). This pri-miRNA is subsequently

trimmed to 70-nucleotide (nt) pre-miRNAs in the nucleus. Then, the trimmed pre-miRNA is exported to the cytoplasm and synergized by Dicer and Drosha, which are both members of the RNase III superfamily of bidentate nucleases. This cleavage event yields mature miRNA molecules that are approximately 22 nt in length (8–11).

Let-7 was first found in the nematode and identified as a key developmental regulator (12). It is one of the two first known microRNAs (the other one being Lin-4) and the first known human miRNA. The Let-7 family is often present in multiple copies in a genome (13). To distinguish between its multiple subtypes, a letter is placed after Let-7 to represent its various sequences, while numbers at the end of the name indicate that the same sequence exists in multiple genomic locations (13, 14). There are 10 mature Let-7 family sequences in humans that arise from 13 precursor sequences and function in similar ways (13).

Let-7 expression is reportedly downregulated in several human cancers, including esophageal, lung, and breast cancers. As a tumor suppressor, Let-7 miRNA targets various oncogenic molecules (including RAS, HMGA 2, and cell cycle and apoptosis regulators) and exerts its anti-tumor effect by preventing proliferation, promoting apoptosis, inhibiting angiogenesis, and reducing immune surveillance (15–17).

Small differences in the sequence of Let-7 can alter the affinity for its target sequences, thereby resulting in differences in its function or employed mechanism (18). The expression of different family members also varies significantly between tumors. Most Let-7i family members exert an anti-tumor effect to function as tumor suppressors (19), but interestingly, recent studies have found that Let-7i may also act as an oncogene to promote the occurrence and development of cancer (20, 21). Let-7i has been shown to have tumor-suppressive as well as tumor-promoting properties simultaneously. To clarify the specific mechanisms differentiating between the tumor-suppressing and tumor-promoting roles of Let-7i, the current Review summarizes previous studies to provide guidance for further targeted precision therapies in a clinical setting.

2 Tumor suppressor function

Let-7i has been widely recognized and studied as a tumor suppressor. Its mechanism of inhibiting tumor development involves not only the modulation of cell proliferation, metastasis, and changes in the tumor cells themselves (such as autophagy, apoptosis, and stem cell properties) but also changes in the tumor microenvironment, such as alterations to immunity and angiogenesis.

2.1 Regulation of malignant phenotypes: proliferation, migration, invasion, and apoptosis

Let-7i regulates gene expression to control the processes that underpin malignant phenotypes, such as tumor cell proliferation, migration, invasion, and apoptosis. Let-7i can regulate gene expression indirectly via the classical mRNA regulatory pathway or directly via the non-canonical epigenetic regulation pathway.

2.1.1 mRNA regulation

The regulation of protein levels by specifically binding to the mRNA 3′ UTR is the classic mechanism employed by Let-7i. Let-7i reduces melanoma cell proliferation and metastasis by upregulating KISS1 expression (22), inhibits the proliferation and invasion of osteosarcoma by downregulating the expression of Aurora B (a member of the serine/threonine protein kinase family) (23), inhibits the survival, proliferation, and motility of gastric cancer cells by downregulating the expression of COL1A1 (24), and promotes the DDP-induced apoptosis of esophageal cancer cells by downregulating the expression of ABCC10 (25). In the process of suppressing the occurrence and development of colorectal cancer, Let-7i can not only specifically bind to serine protease (KLK6) mRNA to inhibit its transcription (26) but also inhibits the activity of the ERK signaling pathway by inhibiting the expression of CCND1 (27). In glioblastoma, a study by Xiaopeng Sun et al. found that Let-7i-5p could downregulate the levels of cyclin-dependent kinases (CDK2 and CDK4), cyclin A2, and BCL-2 by silencing GALE, thereby inducing cell cycle arrest and a reduction in proliferation (28). Furthermore, according to experiments by Lobna Elkhadragy, ERK3 and BMI1 are both highly expressed in head and neck cancer and BMI1 upregulates ERK3 by suppressing the expression of Let-7i, ultimately facilitating the migration of head and neck cancer cells (29). Therefore, we speculated that Let-7i can prevent head and neck cancer cells from migrating by reducing the activity of ERK3.

2.1.2 Epigenetic alterations

DNA, histones, non-histone proteins, and a small amount of RNA can all bind and interact with chromatin, which is a linear complex structure containing the genetic material of interphase cells (30). Epigenetics refers to heritable modifications of gene function that ultimately alter phenotype but do not entail changes to the DNA sequence itself. DNA methylation, histone modification, non-coding RNA regulation, and chromatin remodeling are all examples of epigenetic processes. Let-7i may play a tumor-regulating role by modulating epigenetics.

Let-7i acts on histone lysine demethylase to achieve tumor suppression through structural modification. In esophageal cancer, KDM5B, a histone 3 lysine 4 (H3K4) methylation regulator (31), can be downregulated by Let-7i to encourage the tri-methylation of H3K4 (H3K4me3) in the promoter region, consequently promoting the expression of the tumor suppressor SOX17 (32). Overexpressed SOX17 can then silence the tumor promoter GREB1, thereby reducing the proliferation and invasion of esophageal cancer cells and exerting anti-tumor efficacy *in vitro* (32, 33). In lung cancer, Let-7i enhances DCLK1 expression by interacting with endogenous KDM3A, allowing KDM3A to bind to the promoter region of DCLK1 and removing histone H3K9me2 (34). The enhancement of DCLK1 expression promotes the expression of FXYD3, which reduces the ability of lung cancer cells to proliferate, migrate, and invade, thereby exerting its anti-tumor effect. The above mechanisms have been confirmed *in vitro* and *in vivo* (34). Yawen Liu et al. suggested that Lin28B upregulates the level of

TET3 by blocking Let-7i, while TET3 catalyzes the conversion of 5-methylcytosine to 5-hydroxymethylcytosine, resulting in DNA depletion and pancreatic cell carcinoma (35). Through a feedback mechanism, TET3 and Let-7i can also promote the expression of Lin28B (35, 36).

High mobility group proteins A1 and 2 (HMGA1, 2) are members of the HMGA family that are a class of non-histone chromatin structural proteins with no transcriptional activity, which primarily regulate transcription by altering DNA conformation (37). HMGA1 exerts its tumor-regulating effects via multiple pathways, including DNA phosphorylation, acetylation, and methylation (37). Qin et al. illustrated that by targeting HMGA1, Let-7i suppressed the malignant phenotype of bladder cancer cell lines T24 and 5637 (38). According to Ravindresh Chhabra's study, Let-7i-5p overexpression and SOX2 silencing could both decrease the number of spheroids formed in the cervical cancer cell lines HeLa and CaSki, while HMGA2 and SOX2 expression were significantly reduced in CaSki following Let-7i-5p overexpression (39). HMGA2 has been shown to induce SOX2; therefore, we speculate that Let-7i-5p can disrupt the stem cell phenotype, alter the conformation of DNA, and downregulate SOX2 expression by targeting HMGA2 expression (39–41). Figure 1 shows a schematic diagram illustrating the way in which Let-7i regulates epigenetics.

2.2 Tumor microenvironment pathway regulation

2.2.1 Epithelial-mesenchymal transition and mesenchymal phenotype

Epithelial-mesenchymal transition (EMT) is the process by which epithelial cells lose polarity and transform into motile mesenchymal cells, acquiring a mesenchymal phenotype (42). This process mediates tumor metastasis by blocking connections between cells, reorganizing the cytoskeleton, altering cell shape, and encoding gene expression to enhance cell motility, migration, and invasion. In addition, EMT promotes stem cell likeness and plays a key role in the processes of treatment resistance, embryonic development, and organ fibrosis (42–44). Epithelial cadherin (E-cadherin) degradation is a fundamental mechanistic feature that deconstructs intercellular links and induces EMT, leading to tumor metastasis (42).

Hypoxia is a common feature of the tumor microenvironment. It can activate hypoxia-inducible factor-1α (HIF-1α) to further regulate the expression levels of Nur77 (45) and TWIST1 (46). Nur77 is a distinct nuclear receptor, the low expression of which can cause E-cadherin to be downregulated, causing more dispersed colonies to form and triggering EMT and typical mesenchymal morphology (45). Let-7i-5p plays a key role in this process. Under

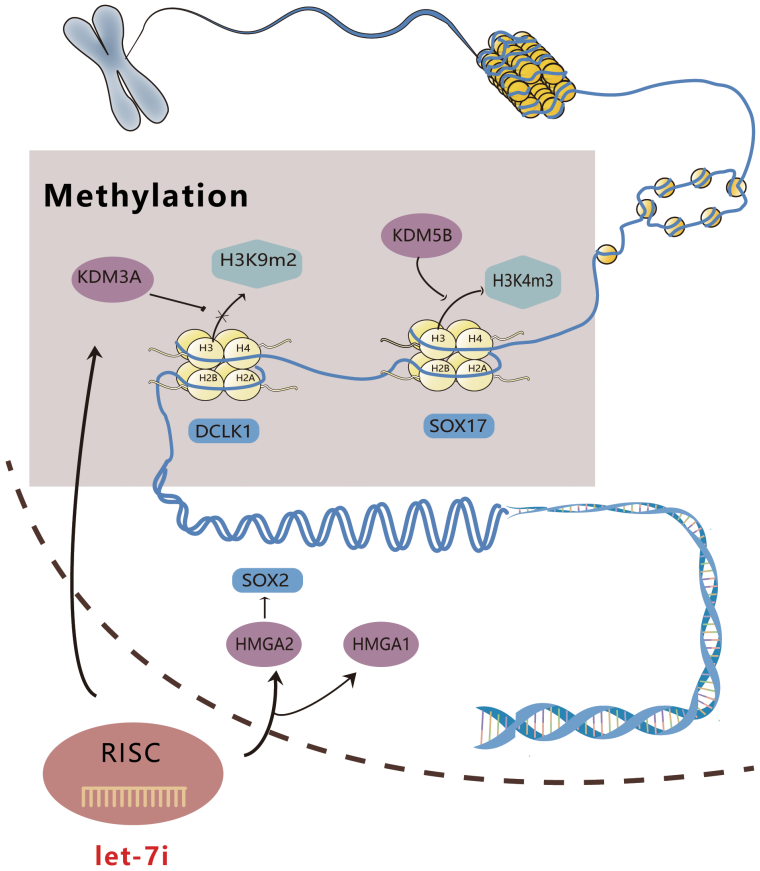

FIGURE 1
Schematic diagram of Let-7i regulating epigenetics. Let-7i can enter the nucleus to combine with KDM3A and KDM5B, affect DNA methylation, and directly interfere with gene expression. Additionally, it can act on HMGA1 and 2, modify the conformation of DNA, and directly regulate gene expression.

hypoxia, Nur77 interacts with p63 to specifically inhibit Dicer, which affects the maturation of Let-7i-5p from precursor (pre)-Let-7i, resulting in a decrease in Let-7i-5p levels (45). Let-7i-5p binds p110α mRNA on the 3′ untranslated region (UTR) and promotes its degradation, while low expression of Let-7i-5p reduces the degradation of PI3K-p110α to increase its level and activates the Akt signaling pathway. Additionally, the low expression of Let-7i-5p affects the phosphorylation of downstream mTORC1 and its target proteins p70S6K and 4E-BP1, thereby inducing colorectal cancer (CRC) EMT (45). Figure 2 provides an intuitive illustration of the above mechanism.

TWIST1, a basic helix-loop-helix (bHLH) transcription factor, is a master regulator of EMT (46–48). It is regulated by HIF-1α, regulates BMI1 levels, and cooperates with BMI1 to inhibit E-cadherin expression to induce EMT (49). Let-7i expression can be co-repressed by TWIST1 and BMI1 simultaneously, while low Let-7i levels can increase cell invasiveness. Let-7i downregulation changes the morphology of head and neck squamous cell carcinoma (HNSCC) OECM-1 cells, causing them to adopt an elongated shape with pseudopodia protrusions, which promotes the interstitial cell pattern, ultimately increasing their capacity to move and invade. In addition, downregulating Let-7i increases the expression of NEDD9 and DOCK3, activates RAC1, drives interstitial movement, and further enhances the invasive phenotype (50).

Moreover, in human glioma cells, Yuan et al. confirmed that Let-7i directly targets IKBKE (inhibitor of nuclear factor kappa-B kinase subunit epsilon) to upregulate E-cadherin expression and suppress EMT (51). In endometrial cancer cells, Let-7i is expressed at low levels under the control of DICER1, and low levels of Let-7i have been found to downregulate the expression of EZH2 to affect the methylation of histone H3 at arginine 27 as well as total H3 acetylation, thereby inhibiting the expression of E-cadherin and encouraging EMT (52). In head and neck squamous cell carcinoma (HNSCC), Let-7i inhibits MBP4 to alter cell morphology, turn slender cells round, and decrease interstitial movement, ultimately preventing local invasion (53).

2.2.2 Extracellular vesicles

Extracellular vesicles (EVs), including exosomes and shed microvesicles (sMVs), mediate intercellular trafficking and are crucial for enabling bidirectional communication between cells and the microenvironment at both the paracrine and systemic levels (54). Studies have repeatedly demonstrated the close connection between EVs and the emergence of cancer. EVs transport a wide range of molecules from donor cells to recipient

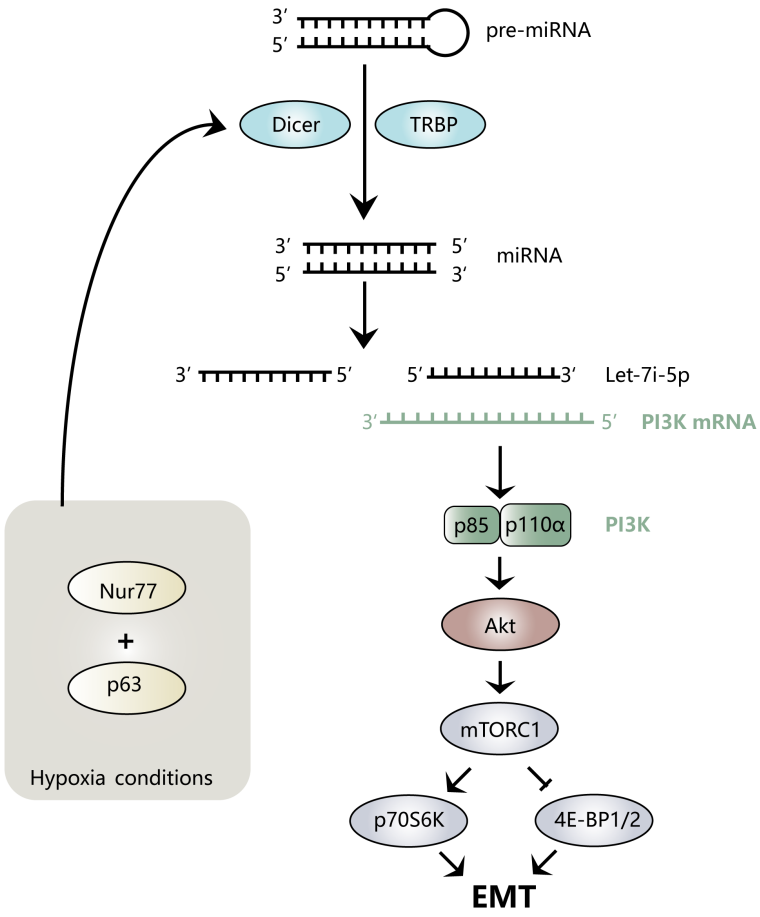

FIGURE 2
Mechanism diagram of Let-7i regulating EMT. Nur77 binds to p63 under hypoxic conditions, inhibits the maturation of Let-7i-5p, prevents the degradation of PI3K mRNA, activates the Akt signaling pathway, and regulates downstream mTORC1, p70S6K, and 4E-BP1/2, thereby inducing the EMT process.

cells, including proteins (such as oncoproteins and oncopeptides), RNAs (such as microRNA and mRNA), DNA fragments, and lipids; this process profoundly alters the phenotype of the tumor microenvironment (54–56). Adeleh Taghi Khani et al. confirmed by *in vivo* and *in vitro* experiments that Let-7i can be delivered by the intercellular delivery system-EV, exerting its tumor suppressive effect in breast cancer cells (57). Experiments conducted by Jiefeng Liu et al. demonstrated that Let-7i inhibits the malignant phenotype of lung cancer through EV transport (34). Additionally, results from a study by Deyi Xiao et al. suggest that Let-7i may act on LIN28B and HMGA2 to alter the expression of EMT markers, thereby inhibiting exosome-mediated melanocyte invasion by suppressing EMT-like effects (58).

3 Tumor promoter function

Although Let-7i is widely recognized as a tumor suppressor, increasingly more studies in recent years have found that Let-7i also has a tumor-promoting effect. Moreover, it appears to promote tumor growth and development through different pathways in different tumors.

3.1 Classical pathways to modulating malignant phenotypes: proliferation, migration, invasion, and apoptosis

Let-7i promotes hepatocellular carcinoma (HCC) by targeting TSP1. By conducting *in vitro* experiments, Hee Doo Yang et al. found that Let-7i-5p rescued a range of tumor suppressive effects of HDAC6, while the ectopic expression of a Let-7i-5p antisense inhibitor (AS-Let-7i-5p) inhibited tumor cell proliferation, induced apoptosis, and prevented migration under chemotactic stimulation, revealing that Let-7i-5p promotes HCC (20). The thrombospondin-1 gene (THBS1) 3′ UTR was cloned into a reporter vector and detected using an AS-Let-7i-5p dual-luciferase reporter assay, after which, there was an observed increase in the relative luciferase activity (20). In addition, we observed that AS-Let-7i-5p transfection increased thrombospondin-1 protein (TSP1) secretion in the conditioned medium of HCC cells. It has been proposed that Let-7i-5p can interact directly with the transcript 3′ UTR to selectively regulate the expression of THBS1, thereby regulating TSP1 secretion. The inhibition of Let-7i-5p can upregulate the level of TSP1 and inhibit both tumor growth and invasion (20). Therefore, we hypothesized that Let-7i-5p may contribute to tumor growth by suppressing the expression of THBS1 and lowering TSP1 levels. In nasopharyngeal carcinoma (NPC), Let-7i-5p has been demonstrated to act not only as an oncogene to promote cancer but also as a valuable biomarker to evaluate its end stage, predict its recurrence, and predict its metastasis risk. Bo You et al. revealed that Let-7i-5p expression was upregulated in NPC and was significantly associated with clinical stage, recurrence, and metastasis. Patients with a higher ISH staining score exhibited higher Let-7i expression, while patients with higher Let-7i-5p expression displayed worse overall survival (OS) and progression-free survival (DFS) rates (59). Simultaneously, the study confirmed the faciliatory effect of Let-7i-5p on the proliferation and migration of NPC cells through several *in vitro* experiments (59). Results obtained from luciferase gene assays showed that Let-7i-5p binds to the 3′ UTR of ATG10 and ATG16L1, revealing the direct targeting effect on genes (59). Let-7i-5p promotes tumor cell proliferation and migration, while the knockdown of ATG10 and/or ATG16L1 abolished this effect, indicating that Let-7i-5p exerts its effect by controlling ATG10 and ATG16L1 (59). In renal clear cell carcinoma (ccRCC), Let-7i-5p is also highly expressed as an oncogene, and its expression level is strongly associated with the pathological stage. Experiments conducted by Yujie Liu et al. showed that the level of Let-7i differed significantly across different pathological stages and different AJCC stages, allowing it to be used as a prognostic marker for ccRCC (21). Meanwhile, the same research showed that Let-7i-5p can promote malignant phenotypes by directly targeting hyaluronan-binding protein 4 (HABP4) (21). HABP4 is a nuclear and cytoplasmic regulatory protein involved in the regulation of gene expression at the transcriptional and mRNA levels. Additionally, it regulates the cell cycle and apoptosis to modulate cell proliferation (60). Downregulating the level of HABP4 to regulate the cell cycle may therefore be the mechanism by which Let-7i promotes ccRCC (21).

Interestingly, Let-7i can promote or suppress hepatocellular carcinoma growth by acting on different targets. Let-7i promotes HCC proliferation and invasion by upregulating the expression of THBS1 and TSP1. Conversely, it also inhibits the malignant phenotype of HCC cells via multiple pathways. A study by Injie Omar Fawzy et al. indicated that Let-7i can inhibit the viability and colony-forming ability of HCC cells either by directly targeting IGF1R or by indirectly reducing IGF1R expression via regulating the expression of insulin-like growth factor 2-mRNA-binding proteins (IGF2BP) 1, 2, and 3 (61). Alternatively, Let-7i can mediate the downregulation of the apoptosis protein Bcl-xL, thereby inhibiting HCC (62). Figure 3 features a schematic diagram that summarizes the classical mechanism of action of Let-7i.

3.2 Angiogenesis and extracellular vesicles

Angiogenesis in tumor tissue is an important prerequisite for rapid tumor proliferation. Tumor tissue blood vessels originate from the pre-existing vasculature and serve as a source of nutrients and oxygen for the tumor cells to ensure their rapid proliferation. The development of vascular architecture in the tumor microenvironment depends on the coordination of pro- and anti-angiogenic factors (63). Hee Doo Yang et al. treated HCC cells with AS-Let-7i-5p and rTSP1, finding that the *in vitro* development of microtubule cells was noticeably suppressed. This effect was successfully rescued by combining the treatment with the TSP1 antibody C-terminal domain to the CD47 receptor (3F352). The research elucidated the following mechanism: the downregulation of Let-7i-5p levels mediates TSP1 binding to the cell surface receptor CD47 to exert anti-angiogenic activity (20). We thus

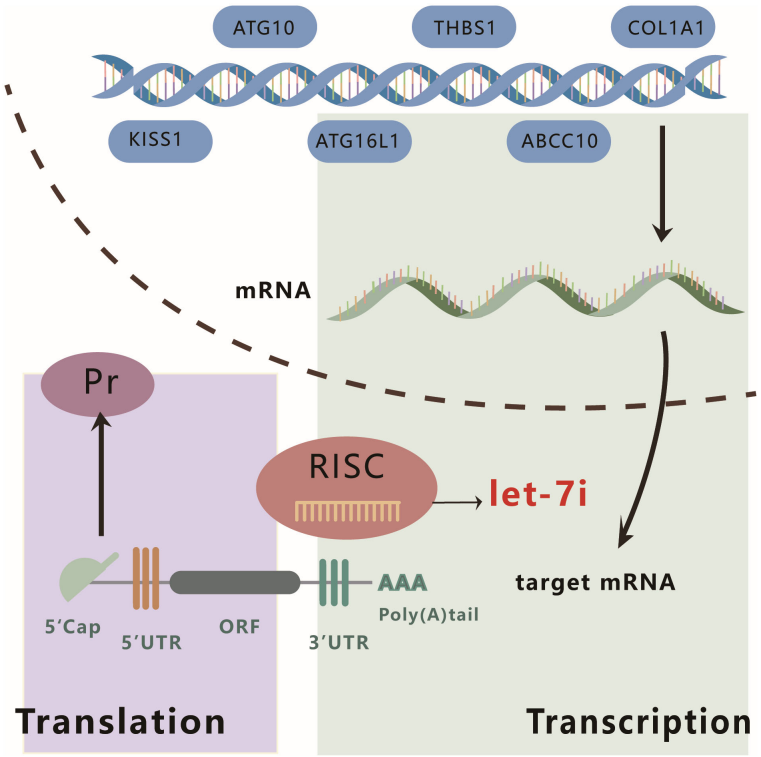

FIGURE 3
Schematic diagram of the mechanism of action of Let-7i. Let-7i can regulate the expression of KISS, ATG10, ATG16L1, THBS1, ABCC10, and COL1A1 at the post-transcriptional level by binding to the 3′ UTR of mRNA.

concluded that Let-7i contributes to the promotion of angiogenesis during the development of tumors.

In a study by Hee Doo Yang et al. (20), exosomes were isolated and purified from HCC cell culture medium, from which Let-7i-5p was detected by qPCR, and donor cell fractions were analyzed. The results of the study showed that Let-7i-5p was mainly present in the exosomes but not in the donor cells of HCC cells. The exosomes were then fluorescently labeled with PKH67 dye and incubated with the receptor system. Measurements found that the expression of Let-7i-5p in the receptor cells was significantly enhanced, suggesting that in HCC, Let-7i-5p facilitates communication between liver cancer cells and normal cells via exosomes, subsequently promoting the malignant transformation of cells and the development of cancer (20).

3.3 Regulation of autophagy

Autophagy is an intracellular degradation process that fuses autophagosomes and lysosomes by the action of various autophagy genes. It hydrolyzes damaged organelles and macromolecules by hydrolases (64). Autophagy plays a complex dual role in tumors, not only by inducing programmed death to eliminate tumor cells but also by promoting cancer cell-stroma communication to promote tumorigenesis and development, supporting tumor growth in a nutrient-limited environment (65, 66). Cancer autophagy is affected by factors such as nutrient availability, microenvironmental stress, and the immune system (65). Numerous studies have documented how miRNAs regulate autophagy and how autophagy affects tumor progression (67, 68).

In NPC, Bo You et al. found that the transfection of NPC cells with a Let-7i-5p inhibitor could inhibit their proliferation and migration ability via autophagy (59). The research also found that silencing the expression of Let-7i-5p induced LC3 aggregation and increased the number of both yellow fluorescent autophagosomes and red fluorescent autolysosomes in the autophagic flux assay, indicating that Let-7i-5p can inhibit the formation of the autophagy phagosome and inhibit the autophagic flux of NPC cells (59). Furthermore, after knocking out Let-7i-5p, western blot showed that the expression levels of the autophagy marker LC3-II and the autophagy-related gene *ATG5* were significantly increased, while the level of the autophagy substrate p62 was decreased (59). The modulation of autophagy by Let-7i was also observed in non-small cell lung cancer (NSCLC). The transfection of a Let-7i-5p inhibitor into NSCLC cells resulted in an increase in the LC3-II/LC3-I ratio and an increase in the number of autophagosomes, while p62 levels were decreased, suggesting that Let-7i-5p negatively regulates autophagy (69). Taken together, Let-7i-5p exerts a tumorigenic role in NPC through the inhibition of autophagy activity (59).

3.4 Regulation of immune escape

As an important part of the immune system, innate immunity is the first line of defense against infection and malignant cell transformation (70). Macrophages can act as antigen-presenting cells (APCs) in innate immunity, processing and cross-presenting antigens to T cells to activate adaptive immunity (71). In addition, macrophages have the ability to mediate phagocytosis, involving multiple cell processes such as target cell recognition, phagocytosis, and lysosomal digestion, which are essential for the programmed clearance of damaged and foreign cells (72). Phagocytosis depends on the relative expression of pro- and anti-phagocytic signals on target cells. Tumor cells have been shown to evade macrophage phagocytosis by expressing anti-phagocytic signals, including CD200 and CD47 (73).

In hepatocellular carcinoma (HCC), TSP1 can prevent the interaction between CD47 and SIRPα, disrupt the "don't eat me" signal between hepatoma cells and macrophages, and prevent immune escape (20). SIRPα is a signal-regulating protein that is mainly expressed on the surface of myeloid cells such as macrophages. It binds to the transmembrane protein CD47 and is activated to initiate a signal transduction cascade, resulting in the inhibition of phagocytosis (74). It has been reported that cell migration ability was significantly inhibited following the treatment of HCC cells with a Let-7i-5p antisense inhibitor and recombinant TSP1, whereas combined treatment with 3F352 rescued these responses, suggesting the existence of an autocrine/paracrine TSP1-CD47 mechanism in HCC cells (20). Then, co-cultured mouse peritoneal macrophages and HCC cells were treated with a Let-7i-5p antisense inhibitor and recombinant TSP1, and consequently, an increase in the phagocytic index and enhanced macrophage phagocytic activity were observed. This suggests that TSP1 can compete with SIRPα for CD47, convert the CD47-SIRP interaction between HCC and macrophages into the CD47-TSP1 interaction, activate the "eat me" signal, and restart macrophage phagocytosis. However, Let-7i could target and downregulate the levels of TSP1, inhibiting the competitive binding of TSP1, which suppressed the immune response, mediated immune escape, and encouraged the development of tumors (20).

Figure 4 illustrates the mechanisms by which Let-7i suppresses immunological response, promotes angiogenesis, inhibits autophagy, and delivers via exosomes.

4 Diagnostic and prognostic biomarkers

Although there is an extensive body of research on cancer and a deep understanding of its development, numerous challenges remain regarding its diagnosis. Most cancers occur insidiously but develop rapidly, and when diagnosed, they are often already at an advanced stage, which is greatly related to an untimely diagnosis. Therefore, it is of great significance to improve the diagnostic methods, establish convenient, accurate, and efficient diagnostic biomarkers, detect lesions in a timely manner, and follow up and confirm diagnoses at an early stage.

In almost all cancer types, miRNA signatures are enriched for proteoglycan-related proteins. Proteoglycans are macromolecules

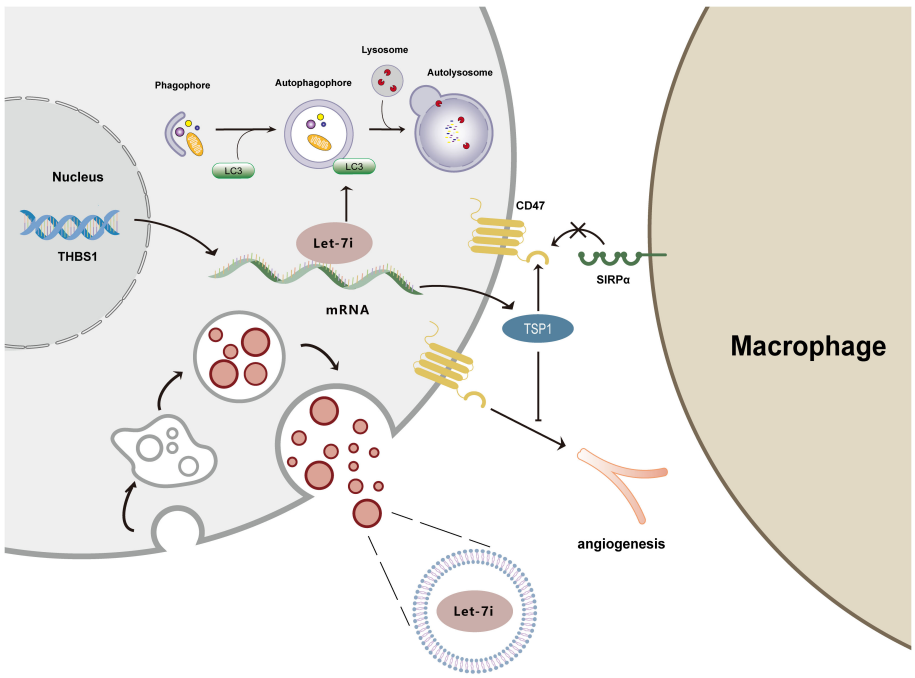

FIGURE 4
Mechanism diagram of Let-7i regulating autophagy, angiogenesis, immune response, and exosomes. Let-7i suppresses autophagy by reducing LC3 aggregation. Let-7i blocks the immune response and initiates immune evasion by downregulating TSP1. Additionally, Let-7i inhibits the anti-angiogenic effects of TSP1. Furthermore, Let-7i transmits between cells through exosomes.

that are major components of the extracellular matrix, and alterations in their expression correlate with the prognosis of malignant tumors (75, 76). Specific miRNA signatures regulate proteoglycan and stem cell pluripotency in the tumor microenvironment, which may have profound implications for early cancer detection.

Sathipati et al. (77) suggested that the recognition of Let-7i signatures by CancerSig miRNAs can be used as a basis for predicting the development and stage of various types of cancers, which can help in early cancer identification and stratification. In experiments conducted by Liang Li et al. (78), serum Let-7i was detected in preclinical HCC patients and has the potential to be used in the screening of CHB patients at high risk of developing HCC 6–12 months after the measurement of miRNAs. Cochetti (79) used Let-7i to differentiate patients with prostate cancer from those with benign prostatic hyperplasia and found that the expression level of Let-7i decreased with increasing malignancy of prostate cancer, which led to the suggestion that Let-7i may be a potential marker for high-risk disease. In addition, Let-7i was found to be a potential biomarker for smoking-associated pneumonia (80). The nucleotide diversity of Let-7i can also affect the risk of cervical cancer, head and neck cancer, and many other cancers by influencing Let-7i levels (81, 82).

The issue of tumor prognosis, which considers tumor recurrence and metastasis, is still the focus of attention in the prevention and treatment of malignant tumors, as it seriously affects the survival time and quality of life of affected patients. Therefore, there is an urgent need to identify a biological marker to monitor the effect of tumor treatment and determine prognosis to intervene early, adjust the treatment plan in time, and select the optimal treatment. Let-7i has been extensively studied as a candidate prognostic biomarker for clinical applications. For pancreatic neuroendocrine tumors, Let-7i predicts metabolic aggressiveness and contributes to pancreatic neuroendocrine tumor (PanNET) stratification by peptide receptor radionuclide therapy (PRRT) (83). Let-7i was found to be significantly associated with hepatitis infection and overall survival in patients with hepatocellular carcinoma and was an independent factor in the development of hepatocellular carcinoma (HCC) in patients with chronic hepatitis B (CHB) and chronic hepatitis C (CHC) (84). Let-7i is an early predictor of HCC development after antiviral therapy, and circulating Let-7i levels can be used for the early surveillance of CHB and CHC with HCC risk and as a non-invasive biomarker to predict the risk of hepatocellular carcinoma after antiviral therapy in patients with chronic hepatitis B and C (84). Moreover, Let-7i is associated with poorer overall cancer survival (OS) and could be a potential biomarker for prognostic survival in individuals with tumors (85). Let-7i has been demonstrated to be a good predictor of overall survival (OS) in metastatic renal cancer (86), recurrence-free survival (RFS) in oral cancer (87), progression-free survival (PFS) in advanced ovarian cancer (88), and liver metastasis-free survival (HFS) in colorectal cancer (89). Let-7i not only predicts OS in gastric cancer but also predicts the sensitivity of gastric cancer to chemotherapy (90). Similarly, Let-7i can be predictive of chemotherapy resistance in ovarian and breast cancer cells (88). The potential biomarker role of Let-7i renders it relevant for clinical studies. A proportional risk model for COX has been developed using the expression of miRNAs, including Let-7i, to robustly predict the high and low risk of distant metastasis in nasopharyngeal carcinoma patients (91).

5 Clinical target

Owing to the important role of Let-7i in tumorigenesis and development, research on its utility as a therapeutic target is progressively expanding. Let-7i can enable the cell-cell delivery of Let-7i via exosomes (20). Additionally, it can effectively induce dendritic cell (DC) maturation, which plays a key role in generating an anti-tumor immune response. Based on this, Let-7i-modified exosomes have emerged as a primary therapeutic direction, and this technology can be administered by either intramuscular or intraperitoneal injection to target DCs and promote their maturation as well as enhance the proliferation of T-cells and regulate the release of cytokines, thus exerting a powerful anti-tumor response through enhancing the immune response and remodeling the tumor microenvironment (57, 92). Let-7i-modified exosomes also hold promise in the development of a novel cell-free vaccine for cancer therapy (92).

In addition, Let-7i has been extensively studied for its ability to enhance the sensitivity of cancer cells to chemotherapeutic drugs (93). Let-7i can inhibit the transcription of lncRNA XIST and downregulate the expression of XIST (94). LncRNA XIST has been shown to confer chemoresistance to cancer cells via a variety of pathways, including improved DNA repair and apoptosis regulation (93). Therefore, the downregulation of lncRNA XIST can reduce the proliferation and anti-apoptotic ability of lung adenocarcinoma (LAD) cells, enhance LAD sensitivity to cisplatin, and improve the drug resistance of cancer cells (94). Yan-Ling Ren et al. (95) confirmed that propofol is not only useful as an intravenous anesthetic but also exerts non-anesthetic effects by interacting with various signaling pathways, thereby participating in the regulation of various human malignant tumors. Propofol can reduce HOXA11-AS expression and upregulate Let-7i to regulate the expression of ABCC10 and alleviate the resistance of colon cancer to chemotherapy (95). Nenghui Liu et al. illustrated that a MUC1 aptamer-Let-7i chimera can enhance the sensitivity of epithelial ovarian cancer cells to paclitaxel by downregulating the expression levels of cyclin D1, cyclin D2, Dicer 1, and PGRMC1 (96).

6 Article summary

By reviewing the role and mechanism of Let-7i in various tumors, we conclude that Let-7i not only plays a tumor suppressor role but also acts as an oncogenic factor to promote the occurrence and development of cancer. Let-7i employs multiple mechanisms of action across different cancers in a cancer-specific manner. Furthermore, for the same cancer cell, depending on the

target, it also plays a different role in promotion and inhibition. Multiple processes underlying the cancer phenotype, including cancer cell growth, migration, invasion, apoptosis, stem cell-likeness, epithelial-mesenchymal transition, EV transmission, angiogenesis, immune evasion, and autophagy, are all regulated by Let-7i. Furthermore, Let-7i is a potential biomarker for the diagnosis or prognosis of various diseases. Therapeutically, Let-7i can modulate the anti-cancer immune response by modifying exosomes while also contributing to the sensitivity of cancer cells to chemotherapeutic drugs to varying degrees. The mechanism of Let-7i is complex and detailed. Table 1 summarizes different aspects of the mechanism of Let-7i in this paper, providing a theoretical basis and reference for the future use of Let-7i as a clinical target in the treatment of cancer.

Author contributions

The idea comes from ZC and JZ, the article is written by JZ, article modification is by HX, all authors reviewed the article. All authors contributed to the article and approved the submitted version.

Funding

This work was supported by the National Natural Science Foundation of China (82104723); Natural Science Foundation of Shandong Province Project (ZR2021LZY019); Key Project Subject of Traditional Chinese Medicine Science and Technology Development in Shandong Province (2020Z14); Shandong Provincial Key Discipline

TABLE 1 Summary of the Let-7i mechanism.

Cancer type	The role of Let-7i	Direct target	Expression status	Downstream pathways involved	Involved phenotype
Hepatocellular carcinoma	Promoter	THBS1	Downregulate	TSP1	Proliferation, migration, apoptosis, angiogenesis, immune escape
	Inhibitor	Bcl-xL	Downregulate		Proliferation, apoptosis
	Inhibitor	IGF1R	Downregulate		Proliferation, migration, Invasion
	Inhibitor	IGF2BPs	Downregulate	IGF1R	Proliferation, migration, Invasion
Nasopharyngeal carcinoma	Promoter	ATG10, ATG16L1	Downregulate		Proliferation, migration
Clear cell renal cell carcinoma	Promoter	HABP4	Downregulate		Proliferation, migration, invasion
Melanoma	Inhibitor	KISS1	Upregulate		Proliferation, migration,
Osteosarcoma	Inhibitor	Aurora B	Downregulate		Migrate, Invasion
Stomach cancer	Inhibitor	COL1A1	Downregulate		Proliferation, migration,
Esophageal cancer	Inhibitor	ABCC10	Downregulate		Apoptosis
		KDM5B	Downregulate	SOX17, GREB1	proliferation, migration, Invasion, apoptosis
Colorectal cancer	Inhibitor	KLK6	Downregulate	Caspase signaling pathway	Proliferation, migration, Invasion, apoptosis
		CCND1	Downregulate	ERK signaling pathway	Proliferation, migration, invasion
		p110α	Downregulate	Akt	migrate, Invasion
Glioblastoma	Inhibitor	GALE	Downregulate	CDK2, CDK4, BCL-2, Cyclin A2	Proliferation, migration, angiogenesis
		IKBKE	Downregulate		migrate, Invasion
Head and neck cancer	Inhibitor	ERK3	Downregulate		Migrate
		NEDD9, DOCK3	Downregulate	RAC1	Invasion
		MBP4	Downregulate		Migrate
Lung cancer	Inhibitor	KDM3A	Downregulate	DCLK1, FXYD3	Proliferation, migration, Invasion
Lung adenocarcinoma	Inhibitor	XIST	Downregulate		Proliferation, apoptosis, drug resistance
Pancreatic cancer	Inhibitor	TET3	Downregulate		Proliferation, invasion
Bladder Cancer	Inhibitor	HMGA1	Downregulate		Proliferation, migration, Invasion
Cervical cancer	Inhibitor	HMGA2	Downregulate	SOX2	Cell stemness
Endometrial cancer	Inhibitor	EZH2	Downregulate		Invasion

Construction Project of Traditional Chinese Medicine (Clinical Discipline of Integrated Traditional Chinese and Western Medicine).

Conflict of interest

The authors declare that the research was conducted in the absence of any commercial or financial relationships that could be construed as a potential conflict of interest.

Publisher's note

References

1. Lu TX, Rothenberg ME. MicroRNA. *J Allergy Clin Immunol* (2018) 141(4):1202–7. doi: 10.1016/j.jaci.2017.08.034

2. Ha M, Kim VN. Regulation of microRNA biogenesis. *Nat Rev Mol Cell Biol* (2014) 15(8):509–24. doi: 10.1038/nrm3838

3. Lim LP, Lau NC, Garrett-Engele P, Grimson A, Schelter J M, Castle J, et al. Microarray analysis shows that some microRNAs downregulate large numbers of target mRNAs. *Nature* (2005) 433(7027):769–73. doi: 10.1038/nature03315

4. Guo H, Pu M, Tai Y, Chen Y, Lu H, Qiao J, et al. Nuclear miR-30b-5p suppresses TFEB-mediated lysosomal biogenesis and autophagy. *Cell Death differentiation* (2021) 28(1):320–36. doi: 10.1038/s41418-020-0602-4

5. Ameres SL, Zamore PD. Diversifying microRNA sequence and function. *Nat Rev Mol Cell Biol* (2013) 14(8):475–88. doi: 10.1038/nrm3611

6. Friedman RC, Farh KK, Burge CB, et al. Most mammalian mRNAs are conserved targets of microRNAs. *Genome Res* (2009) 19(1):92–105. doi: 10.1101/gr.082701.108

7. Sayed D, Abdellatif M. MicroRNAs in development and disease. *Physiol Rev* (2011) 91(3):827–87. doi: 10.1152/physrev.00006.2010

8. Lee Y, Jeon K, Lee JT, Kim S, Kim V N. MicroRNA maturation: stepwise processing and subcellular localization. *EMBO J* (2002) 21(17):4663–70. doi: 10.1093/emboj/cdf476

9. Lee Y, Ahn C, Han J, Choi H, Kim J, Yim J, et al. The nuclear RNase III Drosha initiates microRNA processing. *Nature* (2003) 425(6956):415–9. doi: 10.1038/nature01957

10. Hutvágner G, McLachlan J, Pasquinelli AE, Bálint E, Tuschl T, Zamore PD. A cellular function for the RNA-interference enzyme Dicer in the maturation of the Let-7 small temporal RNA. *Sci (New York NY)* (2001) 293(5531):834–8. doi: 10.1126/science.1062961

11. Bernstein E, Caudy AA, Hammond SM, Hannon GJ. Role for a bidentate ribonuclease in the initiation step of RNA interference. *Nature* (2001) 409(6818):363–6. doi: 10.1038/35053110

12. Reinhart BJ, Slack FJ, Basson M, Pasquinelli AE, Bettinger JC, Rougvie AE, et al. The 21-nucleotide Let-7 RNA regulates developmental timing in Caenorhabditis elegans. *Nature* (2000) 403(6772):901–6. doi: 10.1038/35002607

13. Roush S, Slack FJ. The Let-7 family of microRNAs. *Trends Cell Biol* (2008) 18 (10):505–16. doi: 10.1016/j.tcb.2008.07.007

14. Lee H, Han S, Kwon CS, Lee D. Biogenesis and regulation of the Let-7 miRNAs and their functional implications. *Protein Cell* (2016) 7(2):100–13. doi: 10.1007/s13238-015-0212-y

15. Johnson CD, Esquela-Kerscher A, Stefani G, Byrom M, Kelnar K, Ovcharenko D, et al. The Let-7 microRNA represses cell proliferation pathways in human cells. *Cancer Res* (2007) 67(16):7713–22. doi: 10.1158/0008-5472.CAN-07-1083

16. Johnson SM, Grosshans H, Shingara J, Byrom M, Jarvis R, Cheng A, et al. RAS is regulated by the Let-7 microRNA family. *Cell* (2005) 120(5):635–47. doi: 10.1016/j.cell.2005.01.014

17. Wang T, Wang G, Hao D, Liu X, Wang D, Ning N, et al. Aberrant regulation of the LIN28A/LIN28B and Let-7 loop in human Malignant tumors and its effects on the hallmarks of cancer. *Mol Cancer* (2015) 14:125. doi: 10.1186/s12943-015-0402-5

18. Chirshev E, Oberg KC, Ioffe YJ, Unternaehrer JJ. Let-7 as biomarker, prognostic indicator, and therapy for precision medicine in cancer. *Clin Trans Med* (2019) 8(1):24. doi: 10.1186/s40169-019-0240-y

19. Chirshev E, Suzuki T, Wang H, Nguyen A, Hojo N, Sanderman L, et al. Let-7i reduces aggressive phenotype and induces BRCAness in ovarian cancer cells. *Cancers* (2021) 13(18):4617. doi: 10.3390/cancers13184617

20. Yang HD, Kim HS, Kim SY, Na M J, Yang G, Eun J W, et al. HDAC6 suppresses let-7i-5p to elicit TSP1/CD47-mediated anti-tumorigenesis and phagocytosis of hepatocellular carcinoma. *Hepatol (Baltimore Md)* (2019) 70(4):1262–79. doi: 10.1002/hep.30657

21. Liu Y, Hu X, Hu L, Xu C, Liang X. Let-7i-5p enhances cell proliferation, migration and invasion of ccRCC by targeting HABP4. *BMC Urol* (2021) 21(1):49. doi: 10.1186/s12894-021-00820-9

22. Alkafaji HA, Raji A, Rahman HS, Zekiy A O, Adili A, Jalili M, et al. Up-regulation of KISS1 as a novel target of Let-7i in melanoma serves as a potential suppressor of migration and proliferation in *vitro*. *J Cell Mol Med* (2021) 25(14):6864–73. doi: 10.1111/jcmm.16695

23. Zhang GM, Long XH, Liu JM, Zhu L B, Chen X Y, Huang S H, et al. Let-7i inhibits the Malignant phenotype of osteosarcoma cells by targeting Aurora-B. *Mol Med Rep* (2015) 12(3):3543–8. doi: 10.3892/mmr.2015.3798

24. Shi Y, Duan Z, Zhang X, Zhang X, Wang G, Li F. Down-regulation of the Let-7i facilitates gastric cancer invasion and metastasis by targeting COL1A1. *Protein Cell* (2019) 10(2):143–8. doi: 10.1007/s13238-018-0550-7

25. Wu K, Yang Y, Zhao J, Zhao S. BAG3-mediated miRNA Let-7g and Let-7i inhibit proliferation and enhance apoptosis of human esophageal carcinoma cells by targeting the drug transporter ABCC10. *Cancer Lett* (2016) 371(1):125–33. doi: 10.1016/j.canlet.2015.11.031

26. Song J, Wang L, Ma Q, Yang Y, Yang Z, Wang B, et al. Let–7i–5p inhibits the proliferation and metastasis of colon cancer cells by targeting kallikrein–related peptidase 6. *Oncol Rep* (2018) 40(3):1459–66. doi: 10.3892/or.2018.6577

27. Tu F, Li M, Chen Y, Chu H, Wang S, Hai L, et al. Let-7i-3p inhibits the cell cycle, proliferation, invasion, and migration of colorectal cancer cells *via* downregulating CCND1. *Open Med (Warsaw Poland)* (2022) 17(1):1019–30. doi: 10.1515/med-2022-0499

28. Sun X, Xue H, Xiong Y, Yu R, Gao X, Qian M, et al. GALE promotes the proliferation and migration of glioblastoma cells and is regulated by miR-let-7i-5p. *Cancer Manage Res* (2019) 11:10539–54. doi: 10.2147/CMAR.S221585

29. Elkhadragy L, Chen M, Miller K, Yang MH, Long W. A regulatory BMI1/Let-7i/ERK3 pathway controls the motility of head and neck cancer cells. *Mol Oncol* (2017) 11 (2):194–207. doi: 10.1002/1878-0261.12021

30. van Steensel B. Chromatin: constructing the big picture. *EMBO J* (2011) 30 (10):1885–95. doi: 10.1038/emboj.2011.135

31. Xhabija B, Kidder BL. KDM5B is a master regulator of the H3K4-methylome in stem cells, development and cancer. *Semin Cancer Biol* (2019) 57:79–85. doi: 10.1016/j.semcancer.2018.11.001

32. Yang Y, Li W, Wei B, Wu K, Liu D, Zhu D, et al. MicroRNA let-7i inhibits histone lysine demethylase KDM5B to halt esophageal cancer progression. *Mol Ther Nucleic Acids* (2020) 22:846–61. doi: 10.1016/j.omtn.2020.09.012

33. Tan DS, Holzner M, Weng M, Srivastava Y, Jauch R. SOX17 in cellular reprogramming and cancer. *Semin Cancer Biol* (2020) 67(Pt 1):65–73. doi: 10.1016/j.semcancer.2019.08.008

34. Liu J, Feng Y, Zeng X, He M, Gong Y, Liu Y. Extracellular vesicles-encapsulated Let-7i shed from bone mesenchymal stem cells suppress lung cancer *via* KDM3A/DCLK1/FXYD3 axis. *J Cell Mol Med* (2021) 25(4):1911–26. doi: 10.1111/jcmm.15866

35. Liu Y, Wang D, Zhou M, Chen H, Wang H, Min J, et al. The KRAS/Lin28B axis maintains stemness of pancreatic cancer cells *via* the Let-7i/TET3 pathway. *Mol Oncol* (2021) 15(1):262–78. doi: 10.1002/1878-0261.12836

36. Subramanian M, Francis P, Bilke S, Li X L, Hara T, Lu X, et al. A mutant p53/Let-7i-axis-regulated gene network drives cell migration, invasion and metastasis. *Oncogene* (2015) 34(9):1094–104. doi: 10.1038/onc.2014.46

37. Wang L, Zhang J, Xia M, Liu C, Zu X, Zhong J. High mobility group A1 (HMGA1): structure, biological function, and therapeutic potential. *Int J Biol Sci* (2022) 18(11):4414–31. doi: 10.7150/ijbs.72952

38. Qin MM, Chai X, Huang HB, Feng G, Li X N, Zhang J, et al. Let-7i inhibits proliferation and migration of bladder cancer cells by targeting HMGA1. *BMC Urol* (2019) 19(1):53. doi: 10.1186/s12894-019-0485-1

39. Chhabra R. Let-7i-5p, miR-181a-2-3p and EGF/PI3K/SOX2 axis coordinate to maintain cancer stem cell population in cervical cancer. *Sci Rep* (2018) 8(1):7840. doi: 10.1038/s41598-018-26292-w

40. Chien CS, Wang ML, Chu PY, Chang YL, Liu WH, Yu CC, et al. Lin28B/let-7 regulates expression of oct4 and sox2 and reprograms oral squamous cell carcinoma

cells to a stem-like state. *Cancer Res* (2015) 75(12):2553–65. doi: 10.1158/0008-5472.CAN-14-2215

41. Lee YS, Dutta A. The tumor suppressor microRNA Let-7 represses the HMGA2 oncogene. *Genes Dev* (2007) 21(9):1025–30. doi: 10.1101/gad.1540407

42. Lamouille S, Xu J, Derynck R. Molecular mechanisms of epithelial-mesenchymal transition. *Nat Rev Mol Cell Biol* (2014) 15(3):178–96. doi: 10.1038/nrm3758

43. Gupta PB, Onder TT, Jiang G, Tao K, Kuperwasser C, Weinberg RA, et al. Identification of selective inhibitors of cancer stem cells by high-throughput screening. *Cell* (2009) 138(4):645–59. doi: 10.1016/j.cell.2009.06.034

44. Mani SA, Guo W, Liao MJ, Eaton EN, Ayyanan A, Zhou AY, et al. The epithelial-mesenchymal transition generates cells with properties of stem cells. *Cell* (2008) 133 (4):704–15. doi: 10.1016/j.cell.2008.03.027

45. Shi Z, To SKY, Zhang S, Deng S, Artemenko M, Zhang M, et al. Hypoxia-induced Nur77 activates PI3K/Akt signaling *via* suppression of Dicer/Let-7i-5p to induce epithelial-to-mesenchymal transition. *Theranostics* (2021) 11(7):3376–91. doi: 10.7150/thno.52190

46. Yang MH, Wu MZ, Chiou SH, Chen PM, Chang SY, Liu CJ, et al. Direct regulation of TWIST by HIF-1alpha promotes metastasis. *Nat Cell Biol* (2008) 10 (3):295–305. doi: 10.1038/ncb1691

47. Furlong EE, Andersen EC, Null B, White KP, Scott MP. Patterns of gene expression during Drosophila mesoderm development. *Sci (New York NY)* (2001) 293 (5535):1629–33. doi: 10.1126/science.1062660

48. Yang J, Mani SA, Donaher JL, Ramaswamy S, Itzykson RA, Come C, et al. Twist, a master regulator of morphogenesis, plays an essential role in tumor metastasis. *Cell* (2004) 117(7):927–39. doi: 10.1016/j.cell.2004.06.006

49. Yang MH, Hsu DS, Wang HW, Wang HJ, Lan HY, Yang WH, et al. Bmi1 is essential in Twist1-induced epithelial-mesenchymal transition. *Nat Cell Biol* (2010) 12 (10):982–92. doi: 10.1038/ncb2099

50. Yang WH, Lan HY, Huang CH, Tai SK, Tzeng CH, Kao SY, et al. RAC1 activation mediates Twist1-induced cancer cell migration. *Nat Cell Biol* (2012) 14 (4):366–74. doi: 10.1038/ncb2455

51. Tian Y, Hao S, Ye M, Zhang A, Nan Y, Wang G, et al. MicroRNAs Let-7b/i suppress human glioma cell invasion and migration by targeting IKBKE directly. *Biochem Biophys Res Commun* (2015) 458(2):307–12. doi: 10.1016/j.bbrc.2015.01.105

52. Li B, Lu W, Qu J, Zhang Y, Wan X. DICER1 regulates endometrial carcinoma invasion *via* histone acetylation and methylation. *J Cancer* (2017) 8(6):933–9. doi: 10.7150/jca.17435

53. Yang WH, Lan HY, Tai SK, Yang MH. Repression of bone morphogenetic protein 4 by Let-7i attenuates mesenchymal migration of head and neck cancer cells. *Biochem Biophys Res Commun* (2013) 433(1):24–30. doi: 10.1016/j.bbrc.2013.02.076

54. Xu R, Rai A, Chen M, Suwakulsiri W, Greening DW, Simpson RJ, et al. Extracellular vesicles in cancer - implications for future improvements in cancer care. *Nat Rev Clin Oncol* (2018) 15(10):617–38. doi: 10.1038/s41571-018-0036-9

55. Luga V, Zhang L, Viloria-Petit AM, Ogunjimi AA, Inanlou MR, Chiu E, et al. Exosomes mediate stromal mobilization of autocrine Wnt-PCP signaling in breast cancer cell migration. *Cell* (2012) 151(7):1542–56. doi: 10.1016/j.cell.2012.11.024

56. Fang T, Lv H, Lv G, Li T, Wang C, Han Q, et al. Tumor-derived exosomal miR-1247-3p induces cancer-associated fibroblast activation to foster lung metastasis of liver cancer. *Nat Commun* (2018) 9(1):191. doi: 10.1038/s41467-017-02583-0

57. Khani AT, Sharifzad F, Mardpour S, Hassan ZM, Ebrahimi M. Tumor extracellular vesicles loaded with exogenous Let-7i and miR-142 can modulate both immune response and tumor microenvironment to initiate a powerful anti-tumor response. *Cancer Lett* (2021) 501:200–9. doi: 10.1016/j.canlet.2020.11.014

58. Xiao D, Barry S, Kmetz D, Egger M, Pan J, Rai SN, et al. Melanoma cell-derived exosomes promote epithelial-mesenchymal transition in primary melanocytes through paracrine/autocrine signaling in the tumor microenvironment. *Cancer Lett* (2016) 376 (2):318–27. doi: 10.1016/j.canlet.2016.03.050

59. You B, Zhang P, Gu M, Yin H, Fan Y, Yao H, et al. Let-7i-5p promotes a Malignant phenotype in nasopharyngeal carcinoma *via* inhibiting tumor-suppressive autophagy. *Cancer Lett* (2022) 531:14–26. doi: 10.1016/j.canlet.2022.01.019

60. Saito Â, Souza EE, Costa FC, Meirelles GV, Gonçalves KA, Santos MT, et al. Human regulatory protein ki-1/57 is a target of SUMOylation and affects PML nuclear body formation. *J Proteome Res* (2017) 16(9):3147–57. doi: 10.1021/acs.jproteome.7b00001

61. Fawzy IO, Hamza MT, Hosny KA, Esmat G, Abdelaziz AI. Abrogating the interplay between IGF2BP1, 2 and 3 and IGF1R by Let-7i arrests hepatocellular carcinoma growth. *Growth factors (Chur Switzerland)* (2016) 34(1-2):42–50. doi: 10.3109/08977194.2016.1169532

62. Wu L, Wang Q, Yao J, Jiang H, Xiao C, Wu F. MicroRNA Let-7g and Let-7i inhibit hepatoma cell growth concurrently *via* downregulation of the anti-apoptotic protein B-cell lymphoma-extra large. *Oncol Lett* (2015) 9(1):213–8. doi: 10.3892/ol.2014.2706

63. Abdalla AME, Xiao L, Ullah MW, Yu M, Ouyang C, Yang G. Current challenges of cancer anti-angiogenic therapy and the promise of nanotherapeutics. *Theranostics* (2018) 8(2):533–48. doi: 10.7150/thno.21674

64. Kaur J, Debnath J. Autophagy at the crossroads of catabolism and anabolism. *Nat Rev Mol Cell Biol* (2015) 16(8):461–72. doi: 10.1038/nrm4024

65. Amaravadi R, Kimmelman AC, White E. Recent insights into the function of autophagy in cancer. *Genes Dev* (2016) 30(17):1913–30. doi: 10.1101/gad.287524.116

66. Levy JMM, Towers CG, Thorburn A. Targeting autophagy in cancer. *Nat Rev Cancer* (2017) 17(9):528–42. doi: 10.1038/nrc.2017.53

67. Yin S, Jin W, Qiu Y, Fu L, Wang T, Yu H. Solamargine induces hepatocellular carcinoma cell apoptosis and autophagy *via* inhibiting LIF/miR-192-5p/CYR61/Akt signaling pathways and eliciting immunostimulatory tumor microenvironment. *J Hematol Oncol* (2022) 15(1):32. doi: 10.1186/s13045-022-01248-w

68. Yu T, Guo F, Yu Y, Sun T, Ma D, Han J, et al. Fusobacterium nucleatum promotes chemoresistance to colorectal cancer by modulating autophagy. *Cell* (2017) 170(3):548–63.e16. doi: 10.1016/j.cell.2017.07.008

69. Li C, Chen L, Song W, Peng B, Zhu J, Fang L. DICER activates autophagy and promotes cisplatin resistance in non-small cell lung cancer by binding with Let-7i-5p. *Acta histochemica* (2021) 123(7):151788. doi: 10.1016/j.acthis.2021.151788

70. Dranoff G. Cytokines in cancer pathogenesis and cancer therapy. *Nat Rev Cancer* (2004) 4(1):11–22. doi: 10.1038/nrc1252

71. Iwasaki A, Medzhitov R. Control of adaptive immunity by the innate immune system. *Nat Immunol* (2015) 16(4):343–53. doi: 10.1038/ni.3123

72. Jutras I, Desjardins M. Phagocytosis: at the crossroads of innate and adaptive immunity. *Annu Rev Cell Dev Biol* (2005) 21:511–27. doi: 10.1146/annurev.cellbio.20.010403.102755

73. Chao MP, Majeti R, Weissman IL. Programmed cell removal: a new obstacle in the road to developing cancer. *Nat Rev Cancer* (2011) 12(1):58–67. doi: 10.1038/nrc3171

74. Logtenberg MEW, Scheeren FA, Schumacher TN. The CD47-SIRPα Immune checkpoint. *Immunity* (2020) 52(5):742–52. doi: 10.1016/j.immuni.2020.04.011

75. Theocharis AD, Skandalis SS, Tzanakakis GN, Karamanos NK. Proteoglycans in health and disease: novel roles for proteoglycans in Malignancy and their pharmacological targeting. *FEBS J* (2010) 277(19):3904–23. doi: 10.1111/j.1742-4658.2010.07800.x

76. Sofeu Feugaing DD, Götte M, Viola M. More than matrix: the multifaceted role of decorin in cancer. *Eur J Cell Biol* (2013) 92(1):1–11. doi: 10.1016/j.ejcb.2012.08.004

77. Yerukala Sathipati S, Tsai MJ, Shukla SK, Ho SY. Artificial intelligence-driven pan-cancer analysis reveals miRNA signatures for cancer stage prediction. *HGG Adv* (2023) 4(3):100190. doi: 10.1016/j.xhgg.2023.100190

78. Li L, Chen J, Chen X, Tang J, Guo H, Wang X, et al. Serum miRNAs as predictive and preventive biomarker for pre-clinical hepatocellular carcinoma. *Cancer Lett* (2016) 373(2):234–40. doi: 10.1016/j.canlet.2016.01.028

79. Cochetti G, Poli G, Guelfi G, Boni A, Egidi MG, Mearini E. Different levels of serum microRNAs in prostate cancer and benign prostatic hyperplasia: evaluation of potential diagnostic and prognostic role. *OncoTargets Ther* (2016) 9:7545–53. doi: 10.2147/OTT.S119027

80. Huang J, Wu J, Li Y, Li X, Yang T, Yang Q, et al. Deregulation of serum microRNA expression is associated with cigarette smoking and lung cancer. *BioMed Res Int* (2014) 2014:364316. doi: 10.1155/2014/364316

81. Yerukala Sathipati S, Ho SY. Novel miRNA signature for predicting the stage of hepatocellular carcinoma. *Sci Rep* (2020) 10(1):14452. doi: 10.1038/s41598-020-71324-z

82. Liu J, Ni S. Association between genetic polymorphisms in the promoters of Let-7 and risk of cervical squamous cell carcinoma. *Gene* (2018) 642:256–60. doi: 10.1016/j.gene.2017.11.038

83. Bocchini M, Tazzari M, Ravaioli S, Piccinini F, Foca F, Tebaldi M, et al. Circulating hsa-miR-5096 predicts (18)F-FDG PET/CT positivity and modulates somatostatin receptor 2 expression: a novel miR-based assay for pancreatic neuroendocrine tumors. *Front Oncol* (2023) 13:1136331. doi: 10.3389/fonc.2023.1136331

84. Tsai YS, Huang CI, Tsai PC, Yeh ML, Huang CF, Hsieh MH, et al. Circulating Let-7 Family Members as Non-Invasive Biomarkers for Predicting Hepatocellular Carcinoma Risk after Antiviral Treatment among Chronic Hepatitis C Patients. *Cancers* (2022) 14(8):2023. doi: 10.3390/cancers14082023

85. Ding HX, Lv Z, Yuan Y, Xu Q. MiRNA polymorphisms and cancer prognosis: A systematic review and meta-analysis. *Front Oncol* (2018) 8:596. doi: 10.3389/fonc.2018.00596

86. Du M, Giridhar KV, Tian Y, Tschannen MR, Zhu J, Huang CC, et al. Plasma exosomal miRNAs-based prognosis in metastatic kidney cancer. *Oncotarget* (2017) 8 (38):63703–14. doi: 10.18632/oncotarget.19476

87. Falzone L, Lupo G, La Rosa GRM, Crimi S, Anfuso CD, Salemi R, et al. Identification of novel microRNAs and their diagnostic and prognostic significance in oral cancer. *Cancers* (2019) 11(5):610. doi: 10.3390/cancers11050610

88. Yang N, Kaur S, Volinia S, Greshock J, Lassus H, Hasegawa K, et al. MicroRNA microarray identifies Let-7i as a novel biomarker and therapeutic target in human epithelial ovarian cancer. *Cancer Res* (2008) 68(24):10307–14. doi: 10.1158/0008-5472.CAN-08-1954

89. Coebergh van den Braak RRJ, Sieuwerts AM, Lalmahomed ZS, Smid M, Wilting SM, Bril SI, et al. Confirmation of a metastasis-specific microRNA signature in primary colon cancer. *Sci Rep* (2018) 8(1):5242. doi: 10.1038/s41598-018-22532-1

90. Liu K, Qian T, Tang L, Wang J, Yang H, Ren J. Decreased expression of microRNA Let-7i and its association with chemotherapeutic response in human gastric cancer. *World J Surg Oncol* (2012) 10:225. doi: 10.1186/1477-7819-10-225

91. Zhao L, Fong AHW, Liu N, Cho WCS. Molecular subtyping of nasopharyngeal carcinoma (NPC) and a microRNA-based prognostic model for distant metastasis. *J Biomed Sci* (2018) 25(1):16. doi: 10.1186/s12929-018-0417-5

92. Taghikhani A, Hassan ZM, Ebrahimi M, Moazzeni SM. microRNA modified tumor-derived exosomes as novel tools for maturation of dendritic cells. *J Cell Physiol* (2019) 234(6):9417–27. doi: 10.1002/jcp.27626

93. Zhou X, Ao X, Jia Z, Li Y, Kuang S, Du C, et al. Non-coding RNA in cancer drug resistance: Underlying mechanisms and clinical applications. *Front Oncol* (2022) 12:951864. doi: 10.3389/fonc.2022.951864

94. Sun J, Pan LM, Chen LB, Wang Y. LncRNA XIST promotes human lung adenocarcinoma cells to cisplatin resistance *via* Let-7i/BAG-1 axis. *Cell Cycle (Georgetown Tex)* (2017) 16(21):2100–7. doi: 10.1080/15384101.2017.1361071

95. Ren YL, Zhang W. Propofol promotes apoptosis of colorectal cancer cells *via* alleviating the suppression of lncRNA HOXA11-AS on miRNA Let-7i. *Biochem Cell Biol = Biochimie biologie cellulaire* (2020) 98(2):90–8. doi: 10.1139/bcb-2018-0235

96. Liu N, Zhou C, Zhao J, Chen Y. Reversal of paclitaxel resistance in epithelial ovarian carcinoma cells by a MUC1 aptamer-Let-7i chimera. *Cancer Invest* (2012) 30 (8):577–82. doi: 10.3109/07357907.2012.707265

frontiers | Frontiers in Oncology

TYPE Original Research
PUBLISHED 19 December 2023
DOI 10.3389/fonc.2023.1272586

OPEN ACCESS

EDITED BY
Zheng Wang,
Shanghai Jiao Tong University, China

REVIEWED BY
Francesco Pepe,
University of Naples Federico II, Italy
Suhail Muzaffar,
University of Alabama at Birmingham, United States

*CORRESPONDENCE
Hongfu Cai
caihongfu31@126.com
Maobai Liu
liumaobai@126.com

†These authors have contributed equally to this work

RECEIVED 04 August 2023
ACCEPTED 28 November 2023
PUBLISHED 19 December 2023

CITATION
Zeng W, Cao X, Lin J, Zheng B, Li N, Liu M and Cai H (2023) Cost-effectiveness analysis of elacestrant versus standard endocrine therapy for second-/third-line treatment of patients with HR+/HER2- advanced or metastatic breast cancer: a US payer perspective. *Front. Oncol.* 13:1272586. doi: 10.3389/fonc.2023.1272586

Cost-effectiveness analysis of elacestrant versus standard endocrine therapy for second-/third-line treatment of patients with HR+/HER2- advanced or metastatic breast cancer: a US payer perspective

Wanxian Zeng[1,2†], Xueqiong Cao[1,2†], Jingwen Lin[1,2], Bin Zheng[1,2], Na Li[1,2], Maobai Liu[1,2*] and Hongfu Cai[1,2*]

[1]Affiliated Union Hospital of Fujian Medical University, Fuzhou, Fujian, China, [2]The School of Pharmacy, Fujian Medical University, Fuzhou, Fujian, China

Background: This study evaluated the cost-effectiveness of elacestrant (ELA) and standard-of-care (SOC) as second-/third-line treatment for pretreated estrogen receptor (ER)– positive/human epidermal growth factor receptor 2 (HER2)–negative advanced or metastatic breast cancer (A/MBC) in the US.

Methods: The 3 health states partitioned survival model (PSM) was conducted from the perspective of the US third-party payers. The time horizon for the model lasted 10 years. Effectiveness and safety data were derived from the EMERALD trial (NCT03778931). Costs were derived from the pricing files of Medicare and Medicaid Services, and utility values were derived from published studies. One-way sensitivity analysis as well as probabilistic sensitivity analysis were performed to observe model stability.

Result: ELA led to an incremental cost-effectiveness ratio (ICER) of $8,672,360/quality-adjusted life year (QALY) gained compared with SOC in the overall population and $2,900,560/QALY gained compared with fulvestrant (FUL) in the ESR1(estrogen receptor 1) mutation subgroup. The two ICERs of ELA were significantly higher than the willingness-to-pay (WTP) threshold values of $150,000/QALY.

Conclusions: ELA was not cost-effective for the second-/third-line treatment of patients with ER+/HER2–A/MBC compared with SOC in the US.

KEYWORDS

cost-effectiveness, elacestrant, partitioned survival model, advanced breast cancer, oncology

1 Introduction

Breast cancer (BC) is one of the most commonly diagnosed cancers (11.7% of total cases) and the leading cause of cancer-related death among women globally (1). Since 2020, BC represents the second most diagnosed cancer (2), becoming the leading cause of cancer death among women aged 20–49 years in this year (3). According to the National Cancer Institute, BC is the most common cancer in US women except for nonmelanoma of the skin, accounting for 15% of new annual female cancer cases today (2). In addition, it is the second leading cause of cancer death among women in the US. Since 2004, The incidence rates of invasive breast cancer continue to increase by about 0.5% per year. As of January 1, 2022, there were approximately 4.1 million women with a history of breast cancer living in the United States, and approximately 4% of them present with metastatic disease (4). The survival of breast cancer patients differs from the stage at the time of diagnosis (4). A/MBC remains a virtually incurable disease, with a median overall survival (OS) of about 3 years and a 5-year survival rate of around 25%, even in countries without major accessibility problems (5).

After diagnosing BC, the neoplasm will be further checked for the expression of biological markers, which jointly define the subtypes of BC (2). Such as ER, progesterone receptor (PR), and HER2 (5). ER-positive/HER2-negative are the most common subset of breast cancers, accounting for 65% of cases of breast cancer among women less than 50 years of age and 75% of cases among older women (6).

29% of A/MBC women were originally diagnosed with IV-stage cancers (4). 60% of patients with stage IV BC receive noncurative-intent radiation and/or chemotherapy, but the efficacy is limited, and the prognosis is poor. A recent clinical study by Khan SA et al. (7) found that the survival rate of women with metastatic disease did not benefit from surgery of the primary tumor. Whereas, further expansion to targeted therapies, especially for HR-positive and HER2-positive disease, has improved survival for the metastatic disease over the past 3 decades (6, 8, 9). So far, the National Comprehensive Cancer Network Clinical Practice Guidelines in Oncology (NCCN Guidelines) (10) recommend endocrine therapy, with either aromatase inhibitors (AIs) or FUL, plus a cyclin-dependent kinase 4/6 (CDK4/6) inhibitor as first-line SOC for locally metastatic ER–positive/HER2–negative breast cancer, and sequential endocrine therapy or tamoxifen as a way of later-line therapy. However, endocrine monotherapy had shown limited activity in patients who have received prior CDK4/6 or mammalian targets of rapamycin inhibition (11). Novel therapeutic strategies that target this condition must be developed to address an important unmet clinical need for the vast majority of patients currently on A/MBC therapy.

ELA was a novel, oral selective ER degrader that demonstrated activity in early studies (12–14). What's more, ELA was the first oral SERD that has demonstrated improved efficacy compared to SOC endocrine therapy in patients with advanced breast cancer. In 2002, FUL was approved for patients with ER-positive metastatic breast cancer. It has been almost 20 years since this last type of endocrine therapy was approved. On January 27, 2023, ELA was approved by the Food and Drug Administration (FDA) to treat postmenopausal women and adult men living with A/MBC that has tested positive for an ESR1 mutation with disease progression following treatment with at least one hormonal therapy based on the EMERALD clinical trial (15). Mutations in ESR1 gene lead to estrogen-independent ER activation. As a result, resistance to AIs but not ER inhibitors (e.g. selective ER degraders [SERDs] and selective ER modulators). The subgroup was included to compare the effectiveness of treatment between different groups of patients with detectable ESR1 mutations (16). EMERALD was an international, randomized, open-label, active-controlled, Phase III clinical study (11) (NCT03778931) accessing the efficacy and safety of an investigational oral hormone therapy, ELA (RAD1901), to the SOC hormone therapy options of FUL or an AI in patients with A/MBC that expresses the ER-positive and does not express HER2. In the EMERALD trial, patients treated with ELA had better progression-free survival (PFS) than patients treated with FUL. In addition to improved efficacy, ELA provides an oral treatment option instead of FUL's intramuscular injection. The results showed that patients receiving ELA had superior PFS compared with those receiving SOC (in overall population = 2.8 months *vs.* 1.9 months or ESR1 mutation cohort = 3.8 months *vs.* 1.9 months). However, both groups experienced an initial decrease in PFS, the single median PFS in the overall population or ESR1 mutation cohort may not be sufficient to measure efficacy. Rather, more importantly, hazard ratio (HR) and landmark analyses at 6 and 12 months were used to assess efficacy over a longer period in this population. The HR reflected a 30% reduction in progression or death in the entire cohort and a relative reduction of 45% in the ESR1-mutant cohort. Landmark analyses at 6 and 12 months showed that the use of ELA significantly improved PFS at these later time points. This exciting result may mark the beginning of a paradigm shift in oral SERD therapy for estrogen receptor-positive breast cancer (17). ESR1 mutations result in estrogen-independent endoplasmic reticulum activation and therefore resistance to AIs, but not to endoplasmic reticulum inhibitors (e.g., selective endoplasmic SERDs and selective endoplasmic reticulum modulators). And in patients who have previously received CDK4/6 or mammalian target of rapamycin inhibition, ELA can fulfill this need for limited clinical activity of endocrine monotherapy (16). Although ELA has markedly contributed to A/MBC therapy, the high cost ($22511.06 for 30 tablets, 345mg per tablet) may be a heavy burden for patients and families. Thus, a cost-effectiveness analysis of ELA *vs.* SOC is necessary. The present study investigated the economic outcomes of implementing ELA or SOC regimens as a later-line therapy for patients who were previously treated, with estrogen receptor–positive/human epidermal growth factor receptor 2–negative advanced breast cancer from third-party payers in the United States. We provided the following articles according to the request of the CHEERS 2022 report list (18).

2 Methods

2.1 Cohort patients

The eligible population in this study utilized the sample characteristics of the EMERALD clinical trial: Participants were advanced/metastatic ER+/HER2- breast cancer; Their disease has

progressed or relapsed on or after 1 or 2 lines of endocrine therapy, 1 of which was given in combination with a CDK4/6 inhibitor, for advanced or metastatic breast cancer; The ECOG PS 0 or 1 (11).

2.2 Interventions

According to the EMERALD clinical trial, the intervention group receives ELA 400 mg orally once daily, with reductions to 300 mg or 200 mg daily permitted for toxicity. The control group received SOC treatment, with FUL, anastrozole, letrozole, or exemestane monotherapy by per investigator's choice. FUL was administered intramuscularly (IM) into the buttocks as 500mg dissolved into two 5 mL injections on C1D1 (cycle 1, day 1), C1D15, and C2D1 and Day 1 of every subsequent 28-day cycle; Anastrozole was given 1 mg/day orally on a continuous dosing schedule; Letrozole was given 2.5 mg/day orally on a continuous dosing schedule and exemestane was given 25 mg/day orally on a continuous dosing schedule, respectively (11). Since the clinical trial articles did not provide specific information regarding the percentage of each drug considered standard of care (SOC), except for mentioning that FUL was used in 165 patients (69.33%), we adopted the approach of assuming that the remaining three drugs in SOC were utilized equally (i.e., 30.67% * 1/3 = 10.22% of each drug).Treatment was continued until the disease progressed, the unacceptable adverse event, the withdrawal of consent, or the investigator's decision, etc. Follow-up treatment was selected for patients who have progression of the disease, which was composed of anthracyclines, taxanes, anti-metabolites, vinca alkaloids, hormones, HER2-targeted therapies, and non-HER2-targeted therapies. The proportions of these therapies were derived from the study of Sorensen et al. (19, 20).

2.3 Model

2.3.1 Model approach

The model of cost-effectiveness analysis (CEA) was based on a PSM that has three mutually exclusive health states (progression-free, post-progression, and death). The PSM uses the area under curves to represent the number of patients in each state. It is mainly used to evaluate the impact of interventions that can prolong the patients' lives on their expected lifetime and quality of lives of the patients (21). Survival data in each arm were extracted in digital forms from the survival curves of EMERALD via GetData Graph Digitizer software (version 2.26;http://www.getdata-graph-digitizer.com/download.php). According to the method developed by Guyot et al. (22), Kaplan–Meier survival curves were reconstructed by R software (version 3.5.1) to obtain the new survival curves. There are 5 fitted distribution functions: Weibull, log-logistic, log-normal, Gompertz, and Gamma (23). Akaike information criterion (AIC), Bayesian information criterion (BIC), and visual simulation methods were used to check the goodness of fit. Thus, distribution functions with lower AIC and BIC and better visual simulation were selected as fitting curves, which were extrapolated to obtain long-term clinical survival results (24). The AIC and BIC values of the fitting results of each function were shown in Supplementary Figures S1, S2, and the selected fitting curves and data are shown in Table 1. The median PFS was in good agreement with the results observed in EMERALD (ELA PFS/FUL PFS: 3.37/1.94 *vs.* 2.8/1.9; 3.76/1.83 *vs.* 3.8/1.9), which ensure the practicability of the model (Supplementary Figures S3, 4).

2.3.2 Model structure

The PS model assumed that all patients were in the PF health state at the beginning and were able to maintain their particular health state or progress into healthy state in each cycle (Figure 1). The probability of the PF state transitioning to the death state was assumed to be natural mortality (35). The model was built by TreeAge Pro2022 software and analyzed statistically. The proportion of members was determined in each status from the survival curves base on the PS model. The cycle of the model was set to 1 month for the case of calculation, which was also consistent with the dosing schedule of FUL in EMERALD. The 5-year relative survival rate for women with metastatic breast cancer in the U.S. is 30%. The 5-year survival rate for men with metastatic breast cancer is 19%; thus, the time horizon was set to 10 years, which was sufficient to model an OS of patients with A/MBC (35). Patients entered the model and started cycling into different states until death, incurring treatment costs and health effects. The primary outcomes included total cost, quality-adjusted life-years (QALYs), and incremental cost-effectiveness ratio (ICER), which is expressed as the cost per QALY. All of them were discounted by 3% according to Weinstein M C et al.'s recommendations (36).

2.4 Cost

All relevant data have been listed in Table 1. As we adopted the perspective of American payers, we only consider direct healthcare costs, including drug acquisition costs, administration and medical fees for each state, end-of-life care costs, and costs associated with MAEs. The drug unit costs were obtained from the Centers for Medicare & Medicaid Services and AWP&AAC Medicaid, while all other costs were derived from published economic articles on similar drugs, and the cost per cycle was calculated. Since there is no clear median time for drug administration in EMERALD, it was assumed that the duration of treatments continues until the patients' PD. According to the recommendations of the NCCN guidelines, progression after second/third-line treatment should be managed as supportive care. FUL monotherapy is administered via injection, thus drug management costs should also be taken into consideration. It was assumed equal opportunities for anastrozole, letrozole, or exemestane monotherapy by the investigator's choice. Patients in the PF state require being followed up and monitored until disease progression, which mainly included laboratory scans and tests as well as bone metastasis treatment. The costs for patients in the PD include subsequent drug treatment costs and best supportive care costs, calculated by multiplying the cost of each cycle by the number of cycles. The impact of grade 3 or 4 adverse events (≥5%) and a difference in the incidence of >50% between the arms were

10.3389/fonc.2023.1272586

TABLE 1 Model parameters and ranges used in the sensitivity analysis.

Variable	Baseline Value	Range		Reference
PFS survival model for all patients				
ELA (log-Normal)	meanlog=1.414933; sdlog=0.958343			
SOC (log-Logistic)	shape =2.24661; scale =2.73599			
FUL (log-Logistic)	shape =2.22577; scale =2.71317			
OS survival model for all patients				
ELA (log-Normal)	meanlog=3.192779; sdlog=0.851157			
SOC (log-Normal)	meanlog=3.09129; sdlog=1.09301			
PFS survival model for patients with ESR1 Mutation				
ELA (log-Normal)	meanlog=1.63382; sdlog=1.03730			
SOC (log-Logistic)	shape =2.42158; scale =2.57804			
FUL (log-Logistic)	shape =2.40911; scale =2.63315			
OS survival model for patients with ESR1 Mutation				
ELA (log-Normal)	meanlog=3.339774; sdlog=0.858537			
SOC (log-Normal)	meanlog=2.982833; sdlog=0.867711			
Drug cost, US $				
ELA per mg	2.175	1.088	2.610	(25)
FUL per 25mg	3.915	4.698	3.132	(26)
Anastrozole per mg	0.107	0.086	0.128	(27)
Exemestane per 25mg	0.713	0.571	0.855	(27)
Letrozole per 2.5mg	0.106	0.085	0.127	(27)
After progression	6,549	5,240	7,859	(20)
Subsequent treatment	9,061	7,248	10,873	(20)
End-of-life care	2,601	2,081	3,121	(20)
Follow-up visit	2,959	2,367	3,551	(28)
Administration	702	561	842	(29)
MAEs cost per event, First cycle only, US $				
Nausea	2,586	2,069	3,103	(30)
Back pain	2,501	2001	3001	(31)
Risk of MAEs in ELA (grade 3/4)				
Nausea	0.025	0.020	0.030	(11)
Back pain	0.025	0.020	0.030	(11)
Risk of MAEs in SOC (grade 3/4)				
Nausea	0.0090	0.0072	0.1080	(11)
Back pain	0.0040	0.0032	0.0048	(11)
Risk of MAEs in FUL (grade 3/4)				
Back pain	0.0060	0.0048	0.0072	(11)
QoL utility (per year)				
PF	0.837	0.753	0.921	(32)

(Continued)

TABLE 1 Continued

Variable	Baseline Value	Range		Reference
PD	0.443	0.399	0.487	(33)
Disutilities of MAEs (per year)				
Nausea	0.05	0.02	0.10	(30)
Back pain	0.07	0.05	0.09	(34)
Other Parameters				
Discount rate	3%	0%	5%	(32)

MAEs, main adverse events; SOC, standard-of-care; OS, overall survival; ELA, elacestrant; FUL, fulvestrant; PD, progressed disease; PF, progression-free disease; PFS, progression-free survival.

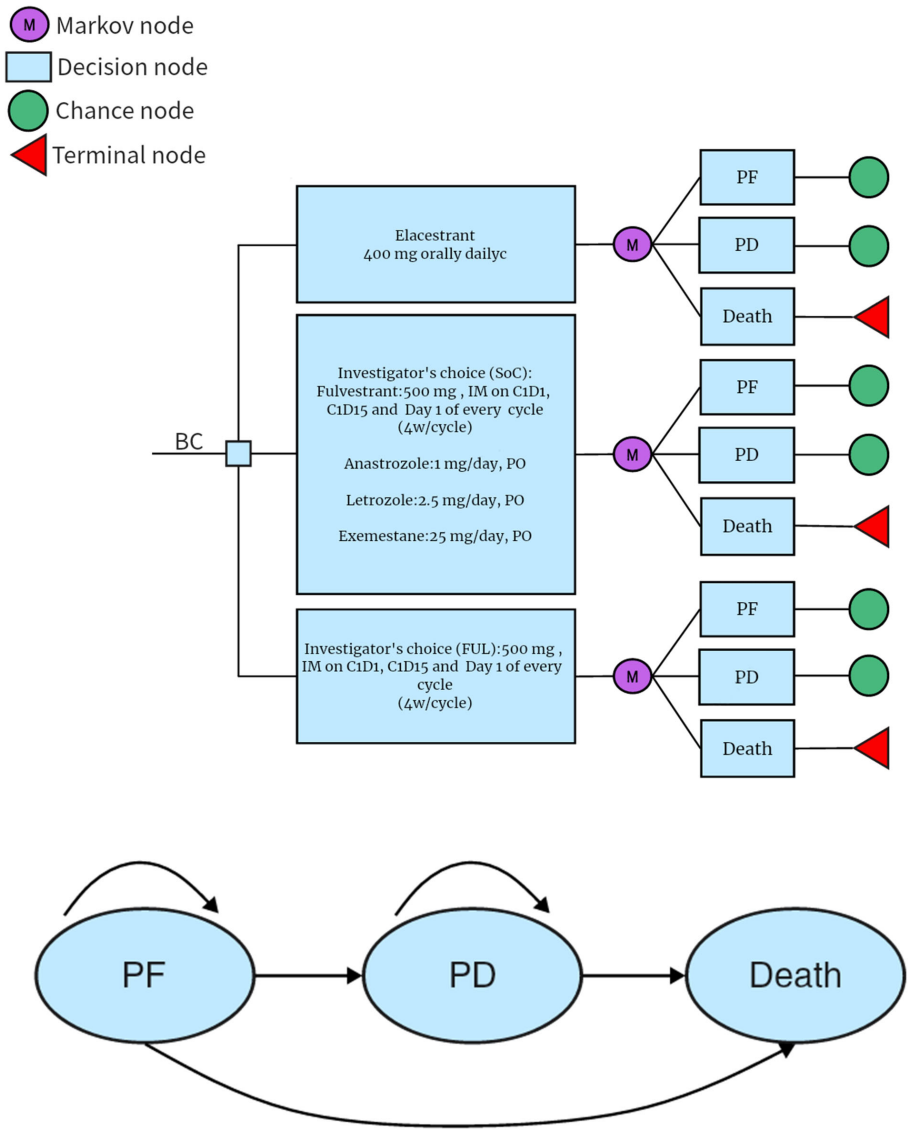

FIGURE 1
PSM simulating the results of the EMERALD clinical trial. All patients started in the PFD and received appropriate treatment. Patients could enter the PFD state and subsequently move to the death state. PD, progressed disease: PF, progression-free disease.

considered in our study. The associated costs are sourced from published literature. The application of AE cost was limited to the first cycle of the model and assumes a monthly occurrence rate of only once.

2.5 Utility

The utility values for PF were derived from the study conducted by Mistry et al. (32). The utility was calculated using the latest UK value set, with data collected from the EuroQol 5-Dimension 5-Level (EQ-5D5L) data collected in the MONALEESA-2 trial. The utility values for PD were sourced from the study reported by Lloyd et al. (33), which used standard gambling techniques to report estimated health state utility values. The disutilities of adverse events were obtained from published literature. The calculation of the MAEs per cycle's disutilities was determined by multiplying the probability of the AE with its corresponding utility.

2.6 Sensitivity analyses

The impact of different parameters on the stability of the results was evaluated using one-way sensitivity analysis. The prices and variations of ELA, FUL, Anastrozole, Exemestane, and Letrozole were determined based on the FDA recommendations and existing market prices. Administration cost, follow-up cost, adverse event cost, utilities, and discount rates were obtained from published literature. The variation range of the remaining parameters was set at 20%. The results were presented in the form of tornado diagrams. As the drugs used in EMERALD were of fixed dosage, changes in body surface area and weight were not considered.

A second-order Monte Carlo simulation was used for probabilistic sensitivity analysis. Based on the recommendation of the ISPOR-SMDM Modeling Good Research Practice Working Group, costs, incidence of MAEs as well as all utilities were set to gamma, beta, and normal distributions, respectively (37). The utility and the transition probability parameter were assumed to conform to the β distribution, and the cost parameter was assumed to conform to the γ distribution (Briggs et al, 2012) (37). Probabilistic sensitivity analysis (PSA) was conducted with 1000 iterations to examine parameter uncertainty in the entire model. The results were presented in the form of cost-effectiveness acceptability curves and an incremental cost-effectiveness scatter plot. According to the suggestion of Neumann et al., the willingness-to-pay (WTP) threshold for the United States is $150,000 (38).

3 Results

3.1 Base case results

Our study only compared the cost-effectiveness analysis of ELA with SOC. In terms of incremental costs and QALYs, in the overall patient group, ELA increased by0.08 QALY compared to SOC. Additionally, the incremental cost of ELA was $754,158, resulting in an ICER increase of $8,672,360/QALY for the overall population. While in the subgroup, ELA increased by 0.51 QALY compared to SOC. It was associated with the additional cost of $906,533, which led to an ICER of $2,900,560/QALY. (Shown in Table 2) Both ICER values were significantly higher than the threshold value of $150,000/QALY. As for the life years, ELA had an additional 0.01 compared to SOC. while in the subgroups, ELA had an additional 0.78 compared to SOC. which were consistent with the results observed in EMERALD, validating the model.

3.2 One-way sensitivity analysis

The results of the one-way sensitivity analysis were shown in Figure 2. The key model drivers was the cost of ELA, followed by the utility values of PF and PD in both the overall group and subgroup. Other costs such as subsequent treatment cost, cost of after-progression, follow-up and administration, and some additional parameters including the discount rate, and risk of MAEs, such as nausea in SOC also had a slight impact on the ICER.

3.3 Probabilistic sensitivity analysis

In both overall population and subgroup, the probability of ELA being cost-effective *vs.* SOC or FUL at thresholds of $150,000 per

TABLE 2 The results of the base case analysis.

	All patients			Patients with ESR1 MUTATION		
	ELA	SOC	FUL	ELA	SOC	FUL
Total cost ($)	1,260,727	506,569	505,473	1,421,188	416,064	514,654
Incremental costs ($)	754,158	1,096	–	906,533	–	98,590
Total effectiveness (QALYs)	1.36	1.28	1.27	1.59	1.08	1.27
Incremental effectiveness (QALYs)	0.09	0.00	–	0.31	–	0.19
ICER ($/QALY)	8,672,360	236,938	–	2,900,560	–	509,831
LYs	2.53	2.52	2.51	2.88	2.10	2.53

QALYs, quality-adjusted life years; SOC, standard-of-care; Lys, life years; ELA, elacestrant; FUL, fulvestrant.

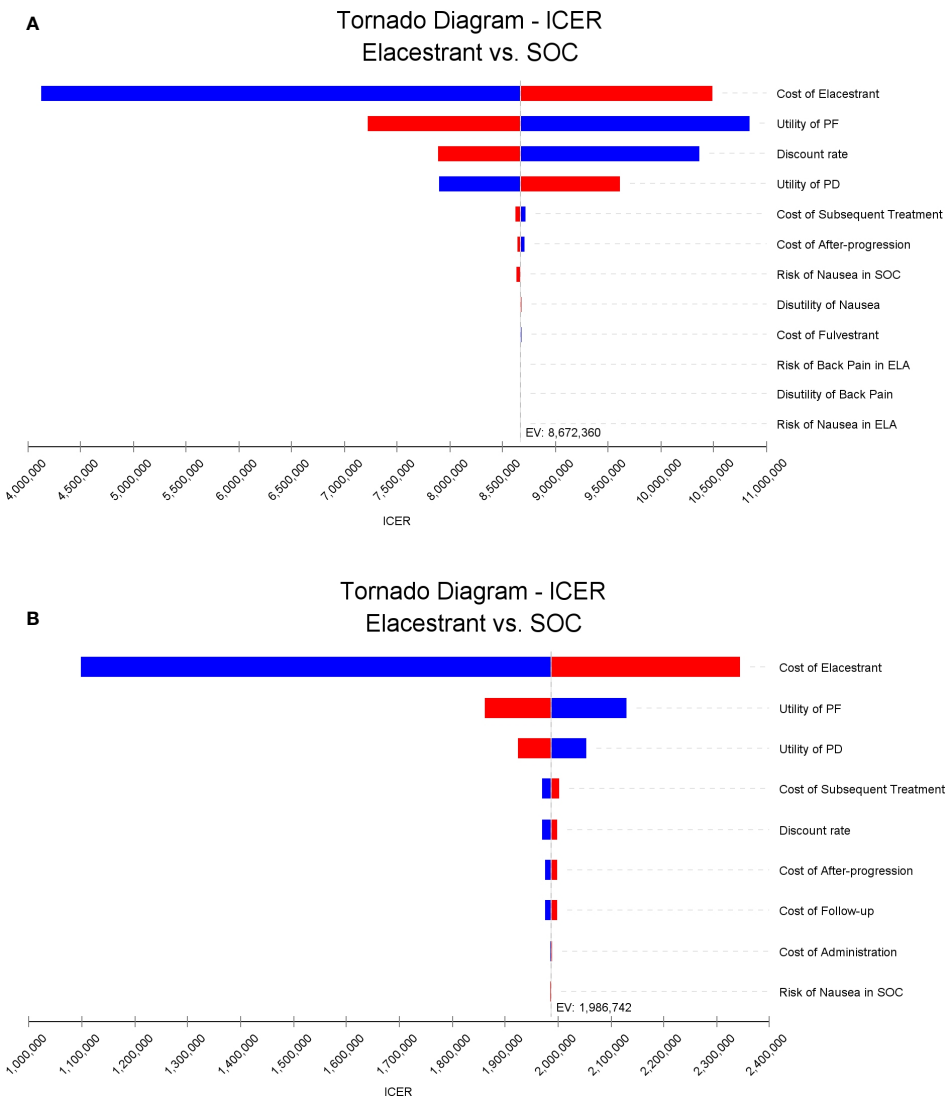

FIGURE 2
Tornado diagrams of one-way sensitivity analyses. **(A, B)** were the results for the overall population and the subgroup, respectively. The dotted line intersecting the blue and red bars represents the ICER of base case results. ICER, incremental cost-effectiveness ratio.

QALY gained was 0%. The cost-effectiveness acceptability curves for three treatments were shown in Figure 3.

4 Discussion

Endocrine therapy stands out as a highly effective treatment for ER+ breast cancer. Nevertheless, the persistent challenge of endocrine resistance in advanced ER+ breast cancer complicates the clinical landscape. Early approved endocrine therapies fall into broad categories, including AIs, selective estrogen receptor modulators (SERMs), and SERDs. These therapies can be utilized with or without ovarian suppression. AIs, administered orally, play a pivotal role in reducing the risk of relapse post curative therapy and represent the standard first-line treatment for metastatic disease. Often, they are employed in conjunction with a CDK4/6 inhibitor. However, AIs are not without side effects, including the exacerbation of menopausal symptoms, vaginal dryness, arthralgia, and accelerated bone loss. Clinical challenges associated with SERDs, like FUL, involve the dual action of antagonizing endoplasmic reticulum transcriptional activity and promoting its degradation. Nevertheless, pharmacologic limitations, including a lack of oral bioavailability, intramuscular injection administration with low patient compliance, and arthralgia-related side effects, impede their widespread use. The activity of FUL or AIs in the context of ESR1 mutations remains incompletely characterized due to limited retrospective datasets. The combination of the low oral bioavailability of FUL and the necessity for intramuscular administration underscores the demand for a more effective oral SERD (17, 39).

The EMERALD study provided a new treatment option for patients with advanced/metastatic ER-positive/HER2-negative breast cancer who had experienced progression after previous endocrine therapy and CDK4/6 inhibitor treatment. It

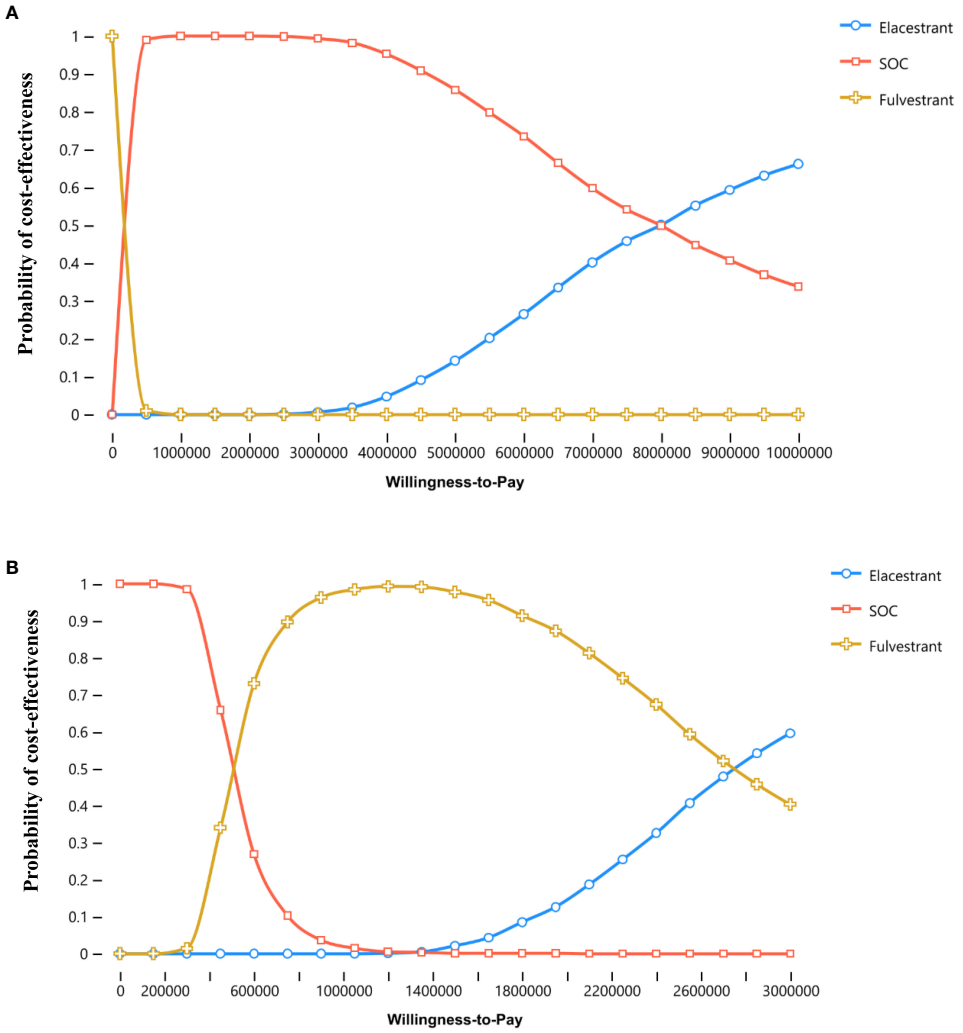

FIGURE 3
Cost-effectiveness acceptability curves. **(A, B)** were the results for the overall population and the subgroup, respectively.

demonstrated that ELA was the first oral SERD that significantly improved PFS compared to SOC. In this study, we evaluated the cost-effectiveness of ELA versus standard-of-care. According to current endocrine therapy guidelines (10), priority was given to AIs and FUL, and there have been related articles on the economy showing that FUL monotherapy was the most cost-effective (in the absence of a combination of drugs) (20). Due to the representation of FUL, we chose to take FUL out from the SOC group and compare it with ELA separately, which was also consistent with the trial design of EMERALD.

Compared with intramuscular injection of FUL, ELA has better therapeutic effects and a more universal and patient-compliant oral administration method. Nevertheless, ELA is a relatively expensive drug. The basic results of this study showed that compared with SOC and FUL, the ICER values of ELA in the overall population and subgroup were $8,672,360/QALY and $2,900,560/QALY, respectively, both of which were significantly higher than the WTP threshold of $150,000/QALY. Accordingly, under the WTP threshold of $150,000/QALY, ELA did not have an economic advantage, indicating that ELA was not a cost-effective choice under the payment willingness of Americans.

In the United States, the traditionally accepted threshold for the cost-effectiveness ratio is $50,000/QALY (38). In basic case analysis, ELA has been found to increase QALYs by 0.09 compared to SOC in the overall population. This was due to ELA extended PFS to a certain degree, and the risk ratio of OS in EMERALD was 0.75, indicating that ELA had an effect in reducing the risk of disease progression or death. In the subgroup analysis, ELA showed a superior effect compared to FUL, with an increase in QALYs of 0.31 and a LYs of 2.88. This was due to ELA's advantage in filling the therapeutic gap for patients with ESR1 mutations. Clinical trial results also indicated that the improvement in PFS may be lower in patients without ESR1 mutations (11). ELA had higher ICER values in both groups, the potential reason was somewhat associated with a higher incidence of MAEs compared to traditional drugs (treatment-related grade 3/4 MAEs occurred in 7.2% receiving ELA and 3.1% receiving SOC). This article did not delve into the economic comparison between SOC and FUL.

The sensitivity analysis of the two groups indicated that, the model was more sensitive to the cost of ELA. Apart from the utility of PF and PD, the cost of subsequent treatment and cost after progression had the greatest impact on the model results. It may result from the fact that the patients included in the clinical trial had already received first/second-line treatment and deteriorated. All patients who entered the PD state in the clinical trial received subsequent treatment until death, or intolerant patients were directly referred to the next level of treatment. Thus, the selection of drugs, the requirements of the medical environment, and the consumption of medical supplies were all more sophisticated and professional, resulting in higher costs.

To the best of our knowledge, this is the first study to explore the cost-effectiveness of ELA This paper evaluated, for the first time, the economic viability of ELA as a treatment for ER-positive/HER2-negative advanced or metastatic breast cancer patients using economic modeling methods. The findings offered the latest evidence for the formulation of relevant medical insurance policies and clinical decisions. However, our research also has some limitations. Firstly, in terms of the collection of cost-effectiveness data on MAEs, no matching reports on nausea were found in the articles on the second-line treatment of breast cancer. Therefore, we used articles on advanced esophageal squamous cell carcinoma and advanced non-small cell lung cancer as the utility and cost parameters of the model, respectively, while the utility of back pain was selected from a Canadian study. Secondly, the management costs of grade 1 and 2 adverse events were not included in this study. However, the result of sensitivity analysis showed that these parameters only have a slight impact. Secondly, EMERALD did not provide the median dosing time, which has caused certain deviations in our drug-cost calculation results. Since the median dosing time was unknown, it was assumed that all patients would receive the assigned drug until PD. Such calculations may not correspond with the actual clinical process. Furthermore, in the SOC group, EMERALD did not provide the proportion or number of per investigator's choices for all drugs except for the number of FUL users. Therefore, for convenience in the calculation, we assumed that the number of patients receiving anastrozole, letrozole, or exemestane monotherapy was the same. These patients were divided into three groups and given the drugs above separately. Nevertheless, such an assumption may deviate from the actual clinical design, and cost calculations may lead to certain biases. Thirdly, after consulting with physicians, we learned that the question of how to proceed with subsequent treatment after disease progression following ELA therapy was extremely complex because it depended on the first/second-line therapeutic regimen. Notably, NCCN has not yet provided new recommendations for subsequent treatment for patients who have progressed after ELA therapy so far. Accordingly, regarding costs other than drug and adverse reaction expenses, we referred to data from pharmacoeconomic articles on FUL (20), which was also a second-line treatment for A/MBC. Whereas, another issue arose: published economic evaluations of the same type of drugs so far required that the patients had not received CDK4/6 inhibitor treatment, which partly deviates from the inclusion criteria of our study. Consequently, the cost of subsequent treatment we reference may include the cost of CDK4/6 inhibitors (40). In the end, though PSM is one of the most popular methods in oncology evaluation including the evaluation of drugs for leukemia treatment currently, the limitations of the PSM arise from its assumption that the survival function is independent. Although the conceptual model includes transitions between different health states, the implemented structure does not explicitly model the disease or estimate transition probabilities for all possible transitions. Therefore, it is incorrect to describe the PSM as a state transition model, as it does not establish a structural connection between health states or estimate transition probabilities for each possible transition. Also, the sensitivity analysis cannot account for variations in drug effectiveness unless bootstrapping is employed (41, 42).

The purpose of this study is to compare the new endocrine therapy with the existing endocrine therapy, rather than evaluating combination therapy. The benefits of ELA relative to FUL and AIs monotherapy in the EMERALD trial also suggest that ELA was a promising strategy as a preferred endocrine backbone therapy in future early combination studies. Therefore, further clinical studies are necessary to evaluate the economic feasibility of comparing ELA/everolimus with exemestane/everolimus combination and ELA/alpelisib with FUL/alpelisib combination. Finally, our team is looking forward to the ultimate OS results being provided when the data is mature in the future so that researchers can obtain more complete data to conduct economic evaluations more professionally and accurately.

5 Conclusion

Based on cost-effectiveness analysis and sensitivity analyses, the results indicate that under the WTP threshold of $150,000, ELA is not a cost-effective option compared to the standard-of-care for second-line treatment of advanced or metastatic ER-positive/HER2-negative breast cancer patients in the United States.

Data availability statement

The original contributions presented in the study are included in the article/Supplementary Material. Further inquiries can be directed to the corresponding authors.

Author contributions

WZ: Formal Analysis, Investigation, Software, Writing – original draft. XC: Conceptualization, Resources, Writing – review & editing. JL: Data curation, Methodology, Writing – original draft. BZ: Validation, Writing – review & editing. NL: Validation, Writing – review & editing. ML: Visualization, Writing – review & editing. HC: Conceptualization, Project administration, Supervision, Writing – review & editing.

Funding

The author(s) declare that no financial support was received for the research, authorship, and/or publication of this article.

Acknowledgments

We thank all of the people who have contributed to this paper.

Conflict of interest

The authors declare that the research was conducted in the absence of any commercial or financial relationships that could be construed as a potential conflict of interest.

Publisher's note

All claims expressed in this article are solely those of the authors and do not necessarily represent those of their affiliated organizations, or those of the publisher, the editors and the reviewers. Any product that may be evaluated in this article, or claim that may be made by its manufacturer, is not guaranteed or endorsed by the publisher.

Supplementary material

The Supplementary Material for this article can be found online at: https://www.frontiersin.org/articles/10.3389/fonc.2023.1272586/full#supplementary-material

References

1. Sung H, Ferlay J, Siegel RL, Laversanne M, Soerjomataram I, Jemal A, et al. Global cancer statistics 2020: GLOBOCAN estimates of incidence and mortality worldwide for 36 cancers in 185 countries. *CA: A Cancer J Clin* (2021) 71(3):209–49. doi: 10.3322/caac.21660

2. Mayrovitz HN ed. *Breast cancer*. Brisbane (AU: Exon Publications Copyright© 2022 Exon Publications (2022).

3. Siegel RL, Miller KD, Wagle NS, Jemal A. Cancer statistics, 2023. *CA: A Cancer J Clin* (2023) 73(1):17–48. doi: 10.3322/caac.21763

4. Giaquinto AN, Sung H, Miller KD, Kramer JL, Newman LA, Minihan A, et al. Breast cancer statistics, 2022. *CA: A Cancer J Clin* (2022) 72(6):524–41. doi: 10.3322/caac.21754

5. Howlader N, Altekruse SF, Li CI, Chen VW, Clarke CA, Ries LA, et al. US incidence of breast cancer subtypes defined by joint hormone receptor and HER2 status. *J Natl Cancer Institute* (2014) 106(5). doi: 10.1093/jnci/dju055

6. Burstein HJ. Systemic therapy for estrogen receptor-positive, HER2-negative breast cancer. *N Engl J Med* (2020) 383(26):2557–70. doi: 10.1056/NEJMra1307118

7. Khan SA, Zhao F, Goldstein LJ, Cella D, Basik M, Golshan M, et al. Early local therapy for the primary site in *de novo* stage IV breast cancer: results of a randomized clinical trial (E2108). *J Clin Oncol* (2022) 40(9):978–87. doi: 10.1200/JCO.21.02006

8. Cortés J, Kim S-B, Chung W-P, Im S-A, Park YH, Hegg R, et al. Trastuzumab deruxtecan versus trastuzumab emtansine for breast cancer. *New Engl J Med* (2022) 386 (12):1143–54. doi: 10.1056/NEJMoa2115022

9. Miles D, Ciruelos E, Schneeweiss A, Puglisi F, Peretz-Yablonski T, Campone M, et al. Final results from the PERUSE study of first-line pertuzumab plus trastuzumab plus a taxane for HER2-positive locally recurrent or metastatic breast cancer, with a multivariable approach to guide prognostication. *Ann Oncol* (2021) 32(10):1245–55. doi: 10.1016/j.annonc.2021.06.024

10. Network. NCC. *NCCN Clinical Practice Guidelines in Oncology: Breast Cancer cancers (Version 4.2023)* (2023). Available at: https://www.nccn.org/professionals/physician_gls/pdf/breast.pdf.

11. Bidard F-C, Kaklamani VG, Neven P, Streich G, Montero AJ, Forget F, et al. Elacestrant (oral selective estrogen receptor degrader) Versus Standard Endocrine Therapy for Estrogen Receptor–Positive, Human Epidermal Growth Factor Receptor 2–Negative Advanced Breast Cancer: Results From the Randomized Phase III EMERALD Trial. *J Clin Oncol* (2022) 40(28):3246–56. doi: 10.1200/JCO.22.00338

12. Varella L, Cristofanilli M. Evaluating elacestrant in the management of ER-positive, HER2-negative advanced breast cancer: evidence to date. *OncoTargets Ther* (2023) 16:189–96. doi: 10.2147/OTT.S400563

13. Wang Y, Tang S-C. The race to develop oral SERDs and other novel estrogen receptor inhibitors: recent clinical trial results and impact on treatment options. *Cancer Metastasis Rev* (2022) 41(4):975–90. doi: 10.1007/s10555-022-10066-y

14. Bardia A, Kaklamani V, Wilks S, Weise A, Richards D, Harb W, et al. Phase I study of elacestrant (RAD1901), a novel selective estrogen receptor degrader, in ER-positive, HER2-negative advanced breast cancer. *J Clin Oncol* (2021) 39(12):1360–70. doi: 10.1200/JCO.20.02272

15. U. S. Food and Drug Administration. *FDA approves elacestrant for ER-positive, HER2-negative, ESR1-mutated advanced or metastatic breast cancer* (2023). Available at: https://www.fda.gov/drugs/resources-information-approved-drugs/fda-approves-elacestrant-er-positive-her2-negative-esr1-mutated-advanced-or-metastatic-breast-cancer.

16. Bidard FC, Kaklamani VG, Neven P, Streich G, Montero AJ, Forget F, et al. Elacestrant (oral selective estrogen receptor degrader) Versus Standard Endocrine Therapy for Estrogen Receptor-Positive, Human Epidermal Growth Factor Receptor 2-Negative Advanced Breast Cancer: Results From the Randomized Phase III EMERALD Trial. *J Clin oncol: Off J Am Soc Clin Oncol* (2022) 40(28):3246–56. doi: 10.1200/JCO.22.00338

17. Lloyd MR, Wander SA, Hamilton E, Razavi P, Bardia A. Next-generation selective estrogen receptor degraders and other novel endocrine therapies for management of metastatic hormone receptor-positive breast cancer: current and emerging role. *Ther Adv Med Oncol* (2022) 14:17588359221113694. doi: 10.1177/17588359221113694

18. Husereau D, Drummond M, Augustovski F, de Bekker-Grob E, Briggs AH, Carswell C, et al. Consolidated Health Economic Evaluation Reporting Standards 2022 (CHEERS 2022) statement: updated reporting guidance for health economic evaluations. *BMJ* (2022) 376:e067975. doi: 10.1016/j.jval.2021.11.1351

19. Sorensen SV, Goh JW, Pan F, Chen C, Yardley D, Martin M, et al. Incidence-based cost-of-illness model for metastatic breast cancer in the United States. *Int J Technol Assess Health Care* (2012) 28(1):12–21. doi: 10.1017/S026646231100064X

20. Wang Y, Rui M, Guan X, Cao Y, Chen P. Cost-effectiveness analysis of abemaciclib plus fulvestrant in the second-line treatment of women with HR +/HER2- advanced or metastatic breast cancer: A US payer perspective. *Front Med (Lausanne)* (2021) 8:658747. doi: 10.3389/fmed.2021.658747

21. Rui M, Wang Y, Fei Z, Zhang X, Shang Y, Li H. Will the Markov model and partitioned survival model lead to different results? A review of recent economic evidence of cancer treatments. *Expert Rev Pharmacoecon Outcomes Res* (2021) 21 (3):373–80. doi: 10.1080/14737167.2021.1893167

22. Guyot P, Ades A, Ouwens MJ, Welton NJ. Enhanced secondary analysis of survival data: reconstructing the data from published Kaplan-Meier survival curves. *BMC Med Res Methodol* (2012) 12(1):9. doi: 10.1186/1471-2288-12-9

23. Ishak KJ, Kreif N, Benedict A, Muszbek N. Overview of parametric survival analysis for health-economic applications. *Pharmacoeconomics* (2013) 31(8):663–75. doi: 10.1007/s40273-013-0064-3

24. Williams C, Lewsey JD, Mackay DF, Briggs AH. Estimation of survival probabilities for use in cost-effectiveness analyses: A comparison of a multi-state modeling survival analysis approach with partitioned survival and markov decision-analytic modeling. *Med Decis Making* (2017) 37(4):427–39. doi: 10.1177/0272989X16670617

25. *Drugs.com. Orserdu prices, coupons and patient assistance programs* (2023). Available at: https://www.drugs.com/price-guide/orserdu#:~:text=Orserdu%20%28elacestrant%29%20is%20a%20member%20of%20the%20estrogen,customers%20and%20are%20not%20valid%20with%20insurance%20plans.

26. Centers for Medicare and Medicaid Services. *ASP drug pricing files* (2023). Available at: https://www.cms.gov/medicare/medicare-part-b-drug-average-sales-price/2023-asp-drug-pricing-files.

27. *Medicaid*. Baltimore, MD: NADAC (National Average DrugAcquisition Cost (2023). Available at: https://data.medicaid.gov/Drug-Pricing-and-Payment/NADAC-National-Average-Drug-Acquisition-Cost-/a4y5-998d.

28. Sorensen SV, Goh JW, Pan F, Chen C, Yardley D, Martín M, et al. Incidence-based cost-of-illness model for metastatic breast cancer in the United States. *Int J Technol Assess Health Care* (2012) 28(1):12–21. doi: 10.1017/S026646231100064X

29. Gauthier G, Gagnon-Sanschagrin P, Guérin A, Burne R, Small T, Niravath P, et al. Economic burden of HR+/HER2- metastatic breast cancer among adult premenopausal women. *Adv Ther* (2018) 35(4):503–14. doi: 10.1007/s12325-018-0689-x

30. Cao X, Cai H, Li N, Zheng B, Zheng Z, Liu M. First-line nivolumab plus ipilimumab or chemotherapy versus chemotherapy alone for advanced esophageal cancer: a cost-effectiveness analysis. *Ther Adv Med Oncol* (2022) 14:17588359221122733. doi: 10.1177/17588359221122733

31. Donga PZ, Bilir SP, Little G, Babinchak T, Munakata J. Comparative treatment-related adverse event cost burden in immune thrombocytopenic purpura. *J Med Econ* (2017) 20(11):1200–6. doi: 10.1080/13696998.2017.1370425

32. Mistry R, May JR, Suri G, Young K, Brixner D, Oderda G, et al. Cost-Effectiveness of Ribociclib plus Letrozole Versus Palbociclib plus Letrozole and Letrozole Monotherapy in the First-Line Treatment of Postmenopausal Women with HR+/HER2- Advanced or Metastatic Breast Cancer: A U.S. Payer Perspective. *J managed Care specialty Pharm* (2018) 24(6):514–23. doi: 10.18553/jmcp.2018.24.6.514

33. Lloyd A, Nafees B, Narewska J, Dewilde S, Watkins J. Health state utilities for metastatic breast cancer. *Br J Cancer* (2006) 95(6):683–90. doi: 10.1038/sj.bjc.6603326

34. Delea TE, Amdahl J, Chit A, Amonkar MM. Cost-effectiveness of lapatinib plus letrozole in her2-positive, hormone receptor-positive metastatic breast cancer in Canada. *Curr Oncol* (2013) 20(5):e371–87. doi: 10.3747/co.20.1394

35. *Breast cancer - metastatic: statistics*. American Society of Clinical Oncology (ASCO (2023). Available at: https://www.cancer.net/cancer-types/breast-cancer-metastatic/statistics.

36. Weinstein MC, Siegel JE, Gold MR, Kamlet MS, Russell LB. Recommendations of the panel on cost-effectiveness in health and medicine. *JAMA* (1996) 276(15):1253–8. doi: 10.1001/jama.1996.03540150055031

37. Briggs AH, Weinstein MC, Fenwick EA, Karnon J, Sculpher MJ, Paltiel AD. Model parameter estimation and uncertainty analysis: a report of the ISPOR-SMDM Modeling Good Research Practices Task Force Working Group-6. *Med decision making: an Int J Soc Med Decision Making* (2012) 32(5):722–32. doi: 10.1177/0272989X12458348

38. Neumann PJ, Cohen JT, Weinstein MC. Updating cost-effectiveness–the curious resilience of the $50,000-per-QALY threshold. *N Engl J Med* (2014) 371(9):796–7. doi: 10.1056/NEJMp1405158

39. Bardia A, Aftimos P, Bihani T, Anderson-Villaluz AT, Jung J, Conlan MG, et al. EMERALD: Phase III trial of elacestrant (RAD1901) vs endocrine therapy for previously treated ER+ advanced breast cancer. *Future Oncol (London England)* (2019) 15(28):3209–18. doi: 10.2217/fon-2019-0370

40. Gye A, Goodall S, De Abreu Lourenco R. Cost-effectiveness analysis of tisagenlecleucel versus blinatumomab in children and young adults with acute lymphoblastic leukemia: partitioned survival model to assess the impact of an outcome-based payment arrangement. *PharmacoEconomics* (2023) 41(2):175–86. doi: 10.1007/s40273-022-01188-w

41. Woods BS, Sideris E, Palmer S, Latimer N, Soares M. Partitioned survival and state transition models for healthcare decision making in oncology: where are we now? *Value health: J Int Soc Pharmacoeconomics Outcomes Res* (2020) 23(12):1613–21. doi: 10.1016/j.jval.2020.08.2094

42. Woods B, Sideris EB, Palmer S, Latimer NR, Soares MO eds. *Nice dsu technical support document 19: partitioned survival analysis for decision modelling in health care: A critical review report by the decision support unit 2 June 20172017*. University of York: NICE Decision Support Unit. (2017).

frontiers | Frontiers in Oncology

TYPE Case Report
PUBLISHED 23 January 2024
DOI 10.3389/fonc.2024.1286910

OPEN ACCESS

EDITED BY
Deniz Can Guven,
Hacettepe University, Türkiye

REVIEWED BY
Claudia Andreetta,
Azienda Sanitaria Universitaria Friuli Centrale (ASU FC), Italy
Prince Kasongo Mwila,
University of the Witwatersrand, South Africa

*CORRESPONDENCE
Nuno Rodrigues Alves
nuno.al113@gmail.com
Diogo Alpuim Costa
diogo.costa@cuf.pt

RECEIVED 31 August 2023
ACCEPTED 03 January 2024
PUBLISHED 23 January 2024

CITATION
Rodrigues Alves N, Duarte AF, Ribeiro DF, Silva RS, Carvalho BA and Alpuim Costa D (2024) Successful management of bilateral orbital metastases from invasive lobular breast cancer with abemaciclib and letrozole: a case report and literature review.
Front. Oncol. 14:1286910.
doi: 10.3389/fonc.2024.1286910

Successful management of bilateral orbital metastases from invasive lobular breast cancer with abemaciclib and letrozole: a case report and literature review

Nuno Rodrigues Alves[1,2*], Ana Filipa Duarte[1,2,3], David Fernandes Ribeiro[4], Rita Sousa Silva[1,2,5], Bruno Almeida Carvalho[3,6] and Diogo Alpuim Costa[7,8,9,10*]

[1]Department of Ophthalmology, Centro Hospitalar Universitário Lisboa Central, Lisbon, Portugal, [2]Department of Ophthalmology, Unidade Local de Saúde de São José, Lisbon, Portugal, [3]Department of Ophthalmology, Hospital CUF Descobertas, Lisbon, Portugal, [4]Department of Anatomical Pathology, Hospital de Montilla, Andaluzia, Spain, [5]Department of Ophthalmology, Hospital Lusíadas de Lisboa, Lisbon, Portugal, [6]Deparment of Ophthalmology, Clínica de São João de Deus, Lisbon, Portugal, [7]Department of Haematology and Oncology, CUF Oncologia, Lisbon, Portugal, [8]Department of Medical Oncology, Hospital de Cascais, Cascais, Portugal, [9]NOVA Medical School (NMS), Faculdade de Ciências Médicas (FCM), Universidade NOVA de Lisboa (UNL), Lisbon, Portugal, [10]Department of Medical Oncology, AIM Cancer Center, Lisbon, Portugal

Breast cancer is a significant global health concern, contributing to substantial morbidity and mortality among women. Hormone receptor-positive (HR+)/HER2-negative (HER2-) breast cancer constitutes a considerable proportion of cases, and significant advancements have been made in its management. CDK4/6 inhibitors (CDK4/6is) are a new targeted therapy that has demonstrated efficacy in adjuvant, advanced and metastatic settings. The propensity of lobular breast carcinomas for estrogen-rich sites, such as periocular tissues and orbital fat, may explain their tendency for orbital metastases. Current treatment strategies for these cases are predominantly palliative, and the prognosis remains poor. This article presents a unique case of a 51-year-old female with progressive right periorbital edema, pain, and limited ocular motility. An imaging work-up showed bilateral intra and extraconal orbital infiltration, which was biopsied. The histopathologic analysis disclosed mild chronic inflammatory infiltrate with thickened fibrous tissue and moderately differentiated lobular carcinoma cells, positive for GATA3 and CK7 markers, with 100% of tumor nuclei expressing estrogen receptors (ER+). A systemic evaluation showed a multicentric nodular formation in both breasts. Further diagnostic assessments unveiled an HR+/HER2- bilateral lobular breast carcinoma with synchronous bilateral orbital metastases. Systemic treatment was initiated with abemaciclib 150mg twice daily and letrozole 2.5mg once a day. However, this regimen was interrupted due to toxicity. After two weeks, treatment was resumed with a reduced abemaciclib dose (100mg twice daily) alongside letrozole, with a reasonable tolerance. Nearly two years after the initial diagnosis of inoperable metastatic cancer, the patient remains on the same systemic treatment regimen with no signs of invasive disease. This case report is the first of a patient

presenting with bilateral orbital metastases from bilateral lobular breast cancer, showing an impressive and sustained response to a first-line treatment regimen combining abemaciclib and letrozole. A literature review on bilateral orbital metastases from breast cancer is also presented.

KEYWORDS

CDK4/6 inhibitor, abemaciclib, letrozole, breast cancer, orbit, metastases, case report, review

1 Introduction

Breast cancer is the most commonly diagnosed cancer globally and is the primary cause of cancer-related mortality in women (1). Categorized by disease stage and histological features, which include morphology and receptor status, breast cancer heterogeneity plays a crucial role in clinical decision-making (2, 3). Hormone receptor-positive (HR+)/HER2-negative (HER2-) breast cancer constitutes the most prevalent subtype, accounting for around 65% of cases (4). Another shared characteristic in luminal HER2- breast cancer is the hyperactivity of the CDK4/6 pathway, which contributes to resistance against endocrine therapy (5).

In recent years, significant strides have been made in the management of HR+/HER2- breast cancer through the introduction of CDK4/6 inhibitors (CDK4/6is), such as palbociclib, ribociclib, and abemaciclib, thereby improving outcomes for adjuvant, advanced and/or metastatic settings (6–15). CDK4/6is can block retinoblastoma protein hyper-phosphorylation, inducing G1 arrest and curtailing proliferation (16, 17). A novel therapeutic approach by abemaciclib (Verzenio; Eli Lilly), an oral selective small molecule targeting the CDK-RB1-E2F pathway pivotal for cell cycle progression, has garnered substantial attention (16). The MONARCH 3 trial, a phase 3, double-blind, randomized study, recently demonstrated that abemaciclib plus nonsteroidal aromatase inhibitor (NSAI - including letrozole) resulted in more prolonged overall survival compared to placebo plus NSAI (absolute improvement of 13.1 months) (hazard ratio, 0.804; 95% CI, 0.637 to 1.015; p= 0.0664; p-value did not reach threshold for statistical significance) and significantly extended progression-free survival (hazard ratio, 0.535; 95% CI, 0.429 to 0.668; p= <0.0001; 29.0 months in the abemaciclib arm, 14.8 months in the placebo arm) (10, 18). Consequently, combining CDK4/6is with endocrine therapy emerged as one of the preferred regimens for patients with advanced and/or metastatic HR+/HER2- breast cancer.

Furthermore, abemaciclib distinguishes itself as the sole CDK4/6 inhibitor examined in a dedicated clinical trial specifically addressing metastatic disease within the central nervous system (CNS) (NCT02308020, phase II trial, encompassing leptomeningeal disease, a criterion indicative of greater severity) (19, 20). In contrast, trials involving palbociclib and ribociclib had limited inclusion or lacked representation of patients with disease at this CNS level (21–23).

To our knowledge, we report the first clinical case of bilateral orbital metastases as the presenting feature of bilateral breast cancer treated with a CDK4/6i and an aromatase inhibitor.

2 Case report

A 51-year-old female presented with a seven-month history of painful progressive periorbital edema and limitation of extraocular movements of the right eye (Figure 1). Her medical history revealed essential hypertension, dyslipidemia, adenomyosis, benign thyroid nodule, gallbladder polyp, major depression, allergic rhinitis, and a smoking history of 32 pack-years. Her pharmacological regimen included candesartan, rosuvastatin, montelukast, paroxetine, lorazepam, mirtazapine, and bupropion. Additionally, she reported an allergy to ibuprofen and had a pertinent family history of prostate cancer in two brothers, diagnosed at 64 and 70 years old. Physical examination revealed inferior dystopia of the right eye with limited horizontal movements on the right eye, without diplopia (Figure 2). The best corrected visual acuity was 20/30 right eye (OD) and 20/20 left eye (OS), Ishihara test 6/10 OD vs. 9/10 OS, and a relative afferent pupillary defect (RAPD) was detected on the right eye. Hertel exophthalmometry showed mild asymmetry of 15mm OD and 16mm OS. In the visual fields, there was an inferonasal paracentral scotoma in the right eye, while the left eye had a normal visual field. Optical coherence tomography (OCT) indicated a mild optic disc edema and a reduction in retinal ganglion cell layer thickness in the right eye, without changes in the nerve fiber layer; no changes were observed in the left eye. Biomicroscopy, intraocular pressure, and ocular fundoscopy findings were unremarkable.

2.1 Diagnostic assessment

After the initial presentation, an orbital and cranial magnetic resonance image (MRI) was requested. An extensive intra- and

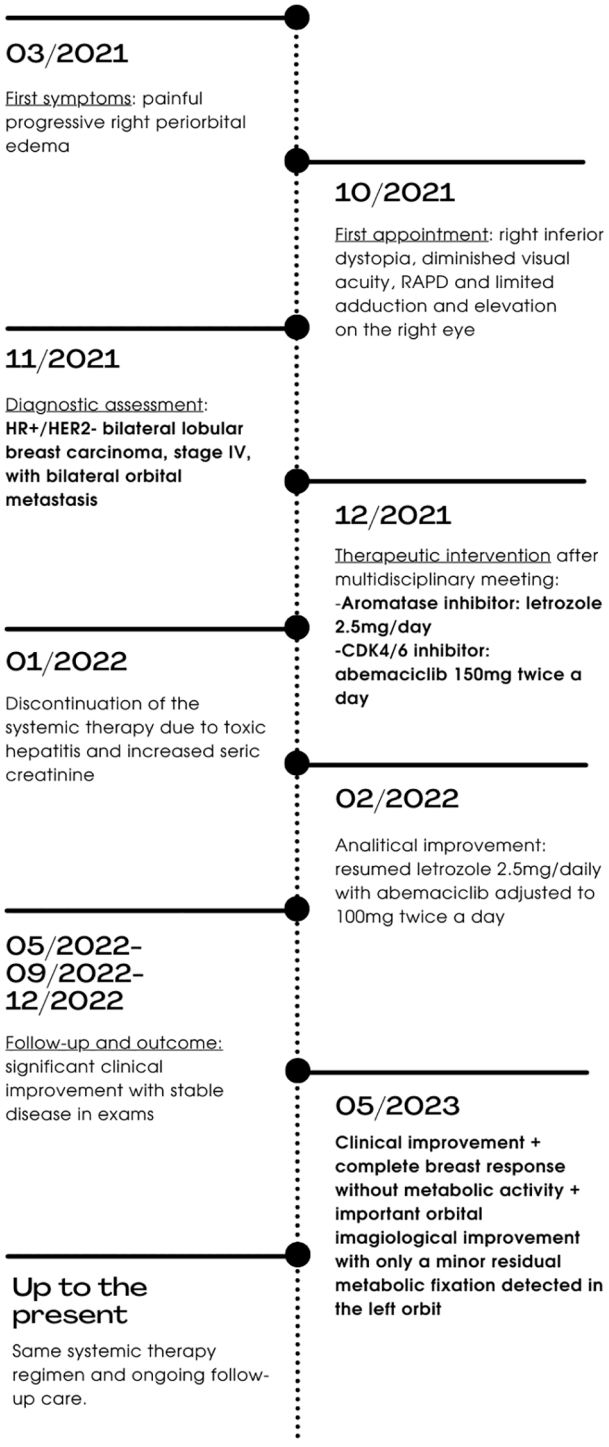

FIGURE 1
Patient timeline.

extraconal orbital infiltration involving the optic nerve, extrinsic ocular musculature, and lacrimal gland was found on the right orbit. Similar discrete signal alterations were identified within the left orbit, mainly between the optic nerve and the medial and inferior rectus muscles (Figure 2).

An incisional biopsy of the right orbit was performed, which included several samples collected from the superior and superior-temporal areas through a lid cease approach. Histopathologic examination revealed moderately differentiated lobular carcinoma cells (Figure 3). Immunohistochemical analysis revealed positivity for GATA3 and CK7 markers, with 100% of tumor nuclei expressing estrogen receptors (ER+) (Figure 3). The c-ERB-B2 (HER2/neu) score was 0, and E-cadherin and PD-L1 (combined positive score) expressions were negative.

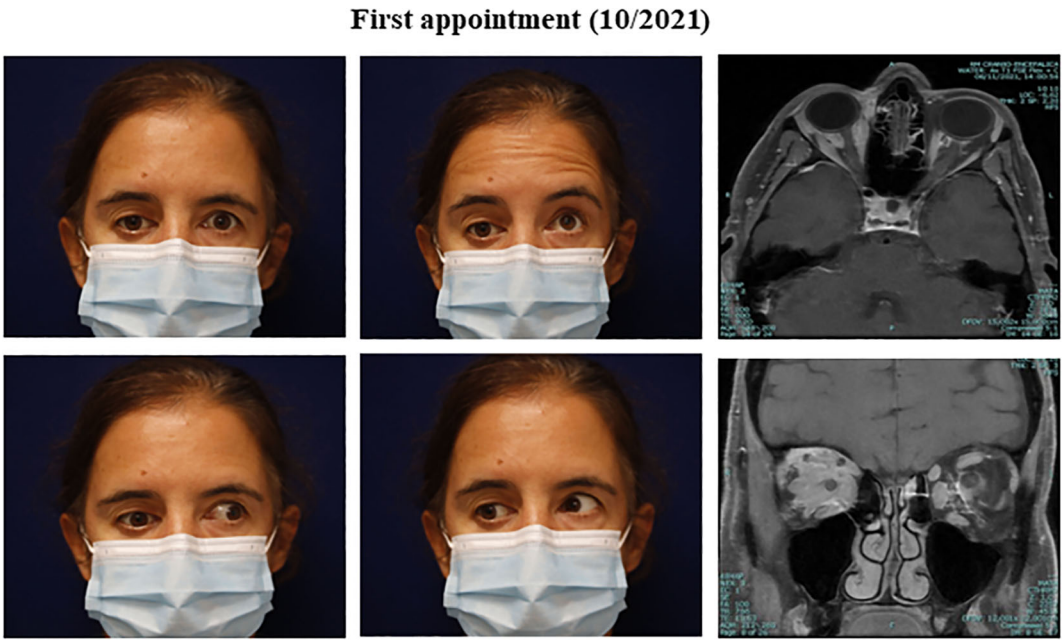

FIGURE 2
Clinical presentation and orbital findings at the initial appointment. (Clinical pictures) Right inferior dystopia with restriction in extraocular elevation and adduction of the right eye. (Orbit Imaging) Orbit axial and coronal T1 MRI showing post-gadolinium enhancing lesions (intra and extra-conal), with mass effect and inflammatory changes of orbital fat.

Following these findings, a comprehensive work-up was initiated to identify the primary tumor. This encompassed breast ultrasonography, mammography, breast MRI, esophagogastroduodenoscopy, gynecological transvaginal ultrasound, lumbar puncture, and positron emission tomography (PET)/CT scan employing 18-fluorodeoxyglucose (18F-FDG). The PET/CT 18-FDG scan revealed moderate heterogeneous radiopharmaceutical uptake in both orbits, the right axillary lymph node, and mild to moderate metabolic activity in the stomach and uterus. Esophagogastroduodenoscopy uncovered hyperemic gastropathy without neoplastic or dysplastic tissue, and transvaginal ultrasonography identified adenomyosis and leiomyomas. A lumbar puncture revealed suspected neoplastic cells, prompting a

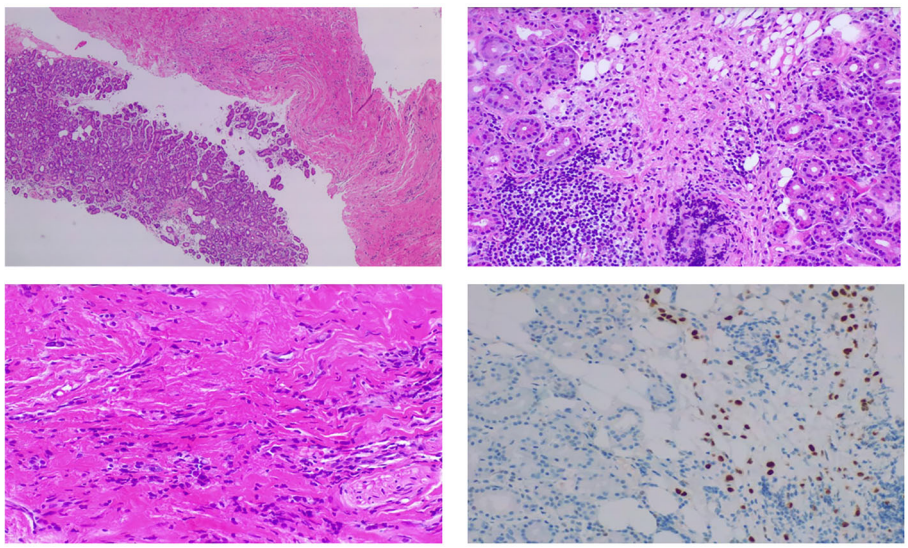

FIGURE 3
Orbital biopsy. (Supero-left) Orbital biopsy comprised soft tissue and lacrimal gland fragments with infiltration by lobular breast carcinoma. (Supero-right) Lacrimal gland showing discohesive cells with nuclear atypia, many resembling signet-ring cells and containing intracellular mucin. (Infero-left) Thickened fibrous tissue where isolated cells and cell rows of similar histologic characteristics are identified. (Infero-right) Infiltrating cells exhibiting immunoreactivity for estrogen receptors, suggesting breast origin.

neuroaxis MRI that showed no suspected invasive disease. Breast imaging unveiled multicentric nodular formations. These solid, irregularly contoured nodules numbered at least three on the right and two on the left, with a larger, coarser superior-external nodule on the right (10mm) along with notably enhancing right axillary lymph nodes, the largest measuring 19 mm. Given the suspicious nature of the findings in both breasts (BI-RADS Category 4), ultrasound-guided core biopsies were performed on two breast nodules and the right axillary node. Histological analysis revealed invasive carcinoma with a lobular pattern, moderately differentiated (Grade 2). ER was positive in 90% of cells, while progesterone receptor (PR) was 100%. HER2 was negative, as was E-cadherin. The dominant lesion in the right breast exhibited a proliferation index (Ki67) of 10%, and in the left breast, it was 7%. Axillary cytology confirmed these findings.

Hence, the patient was diagnosed with metastatic lobular breast cancer, classified as stage IV disease according to the AJCC 8th edition TNM staging (24). The case was discussed in a multidisciplinary breast cancer tumor board, and, given the metastatic and unresectable nature of the disease, coupled with its unsuitability for local intervention, it was decided to initiate systemic treatment with a CDK4/6i plus an aromatase inhibitor.

2.2 Therapeutic intervention

In December of 2021, based on the results of the MONARCH 3 clinical trial (10), the patient initiated abemaciclib 150mg twice daily, combined with letrozole 2.5mg once a day.

2.3 Follow-up and outcome

In January 2022, just a month after starting systemic therapy, the patient developed analytical toxic hepatitis, marked by elevated ALT and AST levels at grade 3, along with GGT elevation at grade 4, as classified by the Common Terminology Criteria for Adverse Events (CTCAE) (25), which contributed to the temporary withdrawal of treatment. Furthermore, this was accompanied by increased serum creatinine (grade 2). After a two-week interval, during which laboratory parameters were reassessed and showed progressive improvement, the patient resumed letrozole, while the dose of abemaciclib was adjusted to 100mg twice a day. Close monitoring of laboratory values was undertaken. Over the subsequent four months, there was a gradual recovery in hepatic parameters, although the serum creatinine level remained at grade 1.

Concomitantly, the patient encountered grade 1 diarrhea, nausea, and asthenia. While adverse effects progressively resolved, grade 1 diarrhea persisted and was effectively managed through interventions such as loperamide administration, oral hydration, and dietary adjustments.

During follow-up, the patient exhibited a marked clinical response to treatment, with significant recovery of visual acuity and extraocular motility, which occurred as early as the first cycle of abemaciclib and continued despite the reduced dosage of 100mg twice daily. The patient underwent repeated orbital MRI, breast MRI, and PET/CT with 18F-FDG imaging, confirming a favorable response, with bilateral tumor size reduction on both orbits and breast areas, without new lesions.

In May 2023, after sixteen months of systemic therapy, the patient achieved a complete response in both breasts and a significant improvement on orbital imaging, with practically complete permeabilization of bilateral intraorbital fat with only a minor residual metabolic fixation detected in the left orbit (Figure 4). Visual acuity remained stable at 20/20 OI, with visual field recovery, and extraocular motility improved with only a mild limitation of right eye adduction (Figure 4). OCT revealed an improvement in retinal ganglion cell layer thickness and normalization of the optic disc in the right eye. Hertel exophthalmometry was 14mm OD and 15mm OS, while the rest of the physical examination yielded unremarkable findings.

The patient continues to adhere to the same systemic therapy regimen, remains resilient with her progress, and actively participates in follow-up care. In the last follow-up, the patient resumed her professional and social activities, not reporting any limitations in daily tasks.

3 Discussion and conclusion

Orbital metastases represent a complex subset, accounting for 1–13% of all orbital neoplasms and affecting around 2–5% of patients diagnosed with systemic malignancies (26). Notably, breast cancer (36%), melanoma (10%), and prostate cancer (8.5%) emerge as the most common primary sources of orbital metastases (27–29). They are typically unilateral, but clinically evident bilateral metastases are reported in 4–20% of cases (30). They are often identified after the primary tumor diagnosis, with a prevailing interval of 3 to 6 years (31, 32). However, exceptional cases have revealed latency extending over decades post-cancer diagnosis, the longest being 42 years after the primary breast carcinoma identification (33). The median age of orbital metastases from breast cancer is 54 (range 28-77 years) (26, 29).

Various tumors and tumor-like lesions can involve the orbit (34), making imaging a crucial step in the initial differential diagnosis of patients with new symptoms or without a previous diagnosis (35). Thyroid eye disease, granulomatosis with polyangiitis, amyloidosis, sarcoidosis, lymphoproliferative disease, orbital inflammatory pseudotumor, IgG4-related disease, as well as solid tumors, infectious and vascular conditions, are always important to consider when radiologic changes are found in the orbital space (36). A biopsy is warranted when clinicoradiologic findings are inconclusive or a previous histological diagnosis is questioned (36, 37).

Intriguingly, orbital metastases can occasionally serve as the inaugural finding of an undetected primary tumor, appearing in an estimated 10% to 31% of cases (31, 38, 39). Considering histological subtypes, lobular breast carcinoma, comprising 10-15% of all breast cancer cases (40), exhibits an increased expression of ER and PR but has decreased HER2 positivity compared to the no special type (NST)/ductal carcinoma (41). In contrast, E-cadherin expression in ductal breast carcinoma limits cellular dispersion, and therefore, orbital metastases from NST are rare (42). Conversely, it is worth noting the propensity of lobular carcinomas for metastases to sites

FIGURE 4
Orbital findings after sixteen months of systemic treatment and clinical presentation in 08/2023. (Orbit Imaging) Orbit axial and coronal T1 MRI showing imaging improvement in the orbital region, marked by permeabilization of bilateral intraorbital fat. (Clinical pictures) Significant clinical improvement in ocular movement restrictions, with only partial limitation remaining on right adduction.

with a substantial supply of estrogen, such as the gastrointestinal and genitourinary tracts (42–47). This could be attributed to the steroid hormone production in periocular tissues and orbital fat, fostering a conducive milieu to metastases of lobular breast carcinoma (45–47).

Despite advances, therapeutic strategies for managing orbital metastases remain a challenge due to the scarcity of data. Current treatment approaches generally lean toward a palliative plan, especially as orbital metastases from breast cancer often arise in the context of advanced end-stage disease (48). Even with treatment, the prognosis for patients diagnosed with orbital metastases yields a mean survival of 31 months (1-116 months) (31, 49).

A review of cases involving bilateral orbital metastases from breast cancer, as reported in English-language literature, was conducted through PubMed, Medline, and Google Scholar databases using the appropriate controlled [MESH] keywords “breast cancer”, “bilateral”, “metastases”, “ocular” and “orbit” and acknowledging references list. The selected articles included case reports and case series that provided detailed clinical, histological, and treatment descriptions (30, 42, 47, 48, 50–77). The summarized findings are presented in Table 1. Forty-two patients, mostly females (95%), were found. The mean age was 59 years (ranging from 36 to 83 years). The majority (64%) had known breast cancer (42, 47, 50, 53, 57, 58, 61, 62, 64–68, 70–73, 76, 77), and orbital metastases were usually identified around 4.8 years after the first diagnosis. Due to the anatomical constraints of the compact orbit space, these metastases usually present as space-occupying lesions, leading to significant clinical symptoms (31). Affected patients commonly exhibit limited ocular motility (55%) (30, 48, 50, 51, 54–58, 60, 61, 64, 65, 67–71, 73–77), vision loss (29%) (51, 53, 54, 56, 57, 59, 63, 64, 68, 71, 75, 77), periorbital edema (24%) (30, 52, 53, 59, 62, 65, 66, 68, 69, 76), diplopia (21%) (48, 55, 57, 58, 64, 67, 70, 71, 73), proptosis (14%) (47, 51–53, 56, 59), ptosis (14%) (53, 54, 69, 73, 75, 77), palpable mass (7%) (54, 63, 70), as well as dystopia (64, 74), and upper lid retraction (53, 67) (both 5%). A notable and intriguing occurrence is enophthalmos, observed in 2 cases (5%) (61, 75). This is likely due to the infiltration of neoplastic cells into the extraocular muscles and retro-bulbar stromal tissues, leading to desmoplasia, fibrosis, and the retraction of the eye globe (78). The majority of orbital metastases exhibit lobular histology (50%) (30, 42, 47, 52, 53, 55, 57, 58, 60, 62, 65–67, 69, 72, 76, 77) vs. ductal (14%) (56, 59, 64, 71, 72, 75) (48, 61, 74) vs. mixed (5%) (72), a trend that is consistent throughout existing literature (42). The immunophenotype of these clinical cases is predominantly hormone receptor-positive in breast cancer, specifically belonging to the luminal subtype (42, 47, 56, 62, 64–66, 69, 72, 76). These metastases often demonstrate a diffuse infiltration pattern within the orbit, affecting bones and extraocular muscles. Invasion of intracranial structures is rare, with brain metastases identified in only 6 cases (14%) (50, 63, 68, 72). Despite various forms of palliative treatment, bilateral orbital metastasis from breast cancer remains a poor prognostic factor, with a mean survival of 16 months following diagnosis (range 0.5 to 41 months) (31).

The emergence of CDK4/6is, such as palbociclib, ribociclib, and abemaciclib, has brought a remarkable shift in the paradigm of the treatment of advanced and/or metastatic HR+/HER2- breast cancer (6–13). Notably, none of the included treatment guidelines name specific CDK4/6is treatments but recommend the class broadly, as there have been no head-to-head clinical trials to date comparing the three approved CDK4/6is, and the efficacy of each appears to be similar (22, 79, 80). Nevertheless, the latest comprehensive survival data imply possible distinctions between the different CDK4/6is, indicating a trend in preferred choices, as palbociclib did not increase overall survival (23).

Notably, abemaciclib has exhibited efficacy in managing intraocular metastases originating from breast cancer, as elucidated in two case reports (81, 82). A woman 57 years old with iris metastases, which regressed within four months and remained undetectable through an eight-month follow-up using a combination of abemaciclib and letrozole (82). In a second case, a

TABLE 1 Literature review of 42 clinical cases of bilateral orbital metastases from breast cancer.

Source	Known previous disease (Y/N)	Ophthalmologic presentation	Other metastatic sites	Orbital imaging at presentation	Histology	Immunophenotype	Treatment	Outcome
Bedford 1960 (50)	Y	Limited ocular motility	Liver, peritoneal carcinomatosis, lymph nodes, skin, brain	NA	NA	NA	NA	Deceased after 2 weeks
Capone 1990 (51)	N	Proptosis, limited ocular motility, pain, vision loss	None	Bilateral diffuse EOM enlargement	NA	NA	Refused treatment	Deceased after 23 months
Glazer 1991 (52)	N	Proptosis, periorbital edema	None	Bilateral enlargement of multiple EOM and anterior soft tissue infiltration	Lobular	NA	RT, HT (tamoxifen) and CHT	Progression (multiple metastases after 1 year)
Rhatigan 1995 (53)	Y	Proptosis, ptosis, periorbital edema, vision loss, upper lid retraction	NA	Soft tissue masses encasing the globes	Lobular	NA	RT	Deceased after 2 weeks
Po 1996 (54)	N	Limited ocular motility, ptosis, palpable mass, vision loss	None	Bilateral diffuse infiltration	NA	NA	CHT	Deceased after 5 months
Zambarakjj 1997 (55)	N	Limited ocular motility, diplopia	Cerebrospinal fluid	Ill-defined 'cuffing' of the globe, optic nerve and EOM	Lobular	NA	RT, CHT (cytarabine, intratectal methotrexate)	Improvement of symptoms
Garcia 1998 (56)	N	Proptosis, limited ocular motility, vision loss	None	Bilateral diffuse infiltration	Ductal	Luminal B	RT, HT (tamoxifen)	Improvement of symptoms
Toller 1998 (57)	Y	Limited ocular motility, pain, vision loss, diplopia	Bone, lymph nodes	Bilateral diffuse enlargement of EOM, infiltration of fat, Tenon capsule, sclera, and eyelid soft tissue	Lobular	NA	Refused treatment	Deceased after 9 months
Lacey 1999 (58)	Y	Enophthalmos, limited ocular motility, diplopia	None	Bilateral nodular enlargement of MR and IR	Lobular	NA	NA	NA
Stuntz 2000 (59)	N	Proptosis, pain, periorbital edema, pain, vision loss	Bone, visceral	Bilateral posterior mass lesions	Ductal	NA	RT, CHT, HT	Progression, deceased after 34 months
Lell 2004 (30)	N	Periorbital edema, limited ocular motility	None	Bilateral diffuse infiltration of the EOM and extra and intraconal compartments	Lobular	NA	NA	NA

(Continued)

10.3389/fonc.2024.1286910

TABLE 1 Continued

Source	Known previous disease (Y/N)	Ophthalmologic presentation	Other metastatic sites	Orbital imaging at presentation	Histology	Immunophenotype	Treatment	Outcome
Gonçalves 2005 (60)	N	Enophtalmos, limited ocular motility	None	Infiltration of both orbits	Lobular	NA	CHT (cyclophosphamide, adriamycin)	Improvement of symptoms and stable after 2 years of follow-up
Spitzer 2005 (48)	N	Limited ocular motility, diplopia	None	Bilateral diffuse EOM enlargement	NA	NA	CHT (cyclophosphamide, doxorubicin) + HT (letrozole) + RT	Improvement of symptoms
Peckham 2005 (61)	Y	Enophtalmos, limited ocular motility	NA	Bilateral thickening of all EOM sparing the anterior tendon.	NA	NA	NA	NA
Kuchel 2006 (62)	Y	Periorbital edema	None	Bilateral inferior extraconal and intraconal mass lesions	Lobular	Luminal	NA	NA
Gasperini 2007 (63)	N	Palpable mass, vision loss	Brain	Infiltration of orbital bone, both optic nerves and left orbital mass lesion lateral to the LR	NA	NA	RT, CHT and optic nerve sheath fenestration	improvement of symptoms
Milman 2008 (64)	Y	Dystopia, limited ocular motility, vision loss, diplopia	Bone, lymph nodes, pancreas	Bilateral nodular enlargement of EOM	Ductal	Luminal	HT (letrozole, anastrozole)	Improvement of symptoms and diminished systemic metastases with letrozole, but progression after 10 months and switch to anastrozole. 15 months free from disease with anastrozole
Kouvaris 2008 (65)	Y	Periorbital edema, limited ocular motility	Bone, lymph nodes, skin	Bilateral nodular enlargement of EOM	Lobular	Luminal A	RT, HT (anastrozole), CHT (vinorelbine, mitomycin), hyperthermia	Improvement of symptoms. Deceased after 13 months
Jaspers 2009 (66)	Y	Periorbital edema	Bone, liver, peritoneal carcinomatosis	Bilateral mass lesions	Lobular	Luminal	CHT (docetaxel), RT	NA
Murthy 2011 (67)	Y	Limited ocular motility, upper lid retraction, diplopia	Lungs	Bilateral diffuse EOM enlargement	Lobular	Triple negative	RT, HT (tamoxifen)	Improvement of symptoms and complete remission after 18 months of follow-up
Kim 2011 (68)	Y	Limited ocular motility, pain, periorbital edema, vision loss	Bone, brain	Bilateral extraconal masses with periostieal thickening	NA	NA	RT	Improvement of symptoms. Deceased after 19 months

(Continued)

10.3389/fonc.2024.1286910

TABLE 1 Continued

Source	Known previous disease (Y/N)	Ophthalmologic presentation	Other metastatic sites	Orbital imaging at presentation	Histology	Immunophenotype	Treatment	Outcome
Kim 2012 (69)	N	Periorbital edema, limited ocular motility, ptosis	Bone, lymph nodes	Bilateral soft tissue mass lesions molding to the globes	Lobular	Luminal	CHT + HT	Undergoing treatment at time of publication
Wiggins 2012 (70)	Y	Palpable mass, limited ocular motility, diplopia	NA	Bilateral fusiform enlargement of the MR, LR muscles sparing the tendons	NA	NA	RT+HT	Improvement of symptoms. Deceased after 8 months
Khan 2015 (71)	Y	Limited ocular motility, vision loss, diplopia	Bone	Mass lesions in the left IR and right LR	Ductal	NA	RT	Partial orbit response. Undergoing treatment at time of publication
Raap 2015 (47)	Y	Proptosis	Liver	Ill-defined mass lesions	Lobular	Luminal	Right enucleation, CHT (paclitaxel)	NA
Raap 2015 (47)	N	NA	NA	NA	NA	Luminal	NA	NA
Jakobiec 2017 (42)	N	NA	NA	NA	Lobular	Triple negative	NA	NA
Jakobiec 2017 (42)	Y	NA	NA	NA	Lobular	Luminal	NA	NA
Blohmer 2020 (72)	Y	NA	Bone, brain, spleen	NA	Ductal	NA	Systemic treatment	Deceased after 2 months
Blohmer 2020 (72)	N	NA	Bone	NA	Lobular	NA	RT, systemic treatment	Deceased after 41 months
Blohmer 2020 (72)	Y	NA	Bone, lymph nodes	NA	Lobular	NA	RT, systemic treatment	Deceased after 12 months
Blohmer 2020 (72)	Y	NA	None	NA	Lobular	NA	RT, systemic treatment	Deceased after 22 months
Blohmer 2020 (72)	Y	NA	Bone	NA	Lobular	NA	RT, systemic treatment	Lost to follow-up
Blohmer 2020 (72)	Y	NA	Rectum	NA	Mixed (lobular-ductal)	Luminal	RT, systemic treatment	Deceased after 25 months
Blohmer 2020 (72)	Y	NA	Bone, brain	NA	Mixed (lobular-ductal)	NA	RT, systemic treatment	Deceased after 9 months

(Continued)

10.3389/fonc.2024.1286910

TABLE 1 Continued

Source	Known previous disease (Y/N)	Ophthalmologic presentation	Other metastatic sites	Orbital imaging at presentation	Histology	Immunophenotype	Treatment	Outcome
Blohmer 2020 (72)	Y	NA	Peritoneal carcinomatosis, gastrointestinal	NA	NA	NA	RT, systemic treatment	Deceased after 4 months
Blohmer 2020 (72)	Y	NA	Bone, brain	NA	NA	NA	RT, systemic treatment	Deceased after 10 months
Marotta 2020 (73)	Y	Limited ocular motility, pain, ptosis, diplopia	Bone, pleural	Nodular enlargement of the left MR, IR and the right SR	NA	NA	CHT (trastuzumab, pertuzumab, docetaxel), RT	Improvement of symptoms
Dimopoulos 2020 (74)	NA	Dystopia,limited ocular motility	NA	Bilateral EOM enlargement and unilateral intraconal mass	NA	NA	NA	NA
Muhammad-Ikmal 2022 (75)	N	Enophthalmos, limited ocular motility, ptosis, vision loss	NA	Infiltrating mass invading the ethmoidal sinuses, frontal sinuses and both orbits	Ductal	NA	CHT+RT	Stable disease control after 1 year
Tsutsui 2022 (76)	Y	Limited ocular motility, periorbital edema	Bone	Bilateral soft tissue, medial and retrobulbar infiltration	Lobular	Luminal A	HT (fulvestrant, abemaciclib)	Progression to orbital metastases.Deceased after 3 months
Karimaghaei 2022 (77)	Y	Limited ocular motility, ptosis, vision loss	None	Bilateral retrobulbar infiltration	Lobular	NA	NA	NA

CHT (chemotherapy), EOM (extraocular muscle), F (female), HT (hormonotherapy), IR (inferior rectus), LR (lateral rectus), M (male), MR (medial rectus), N (no), NA (nonavailable), RT (radiotherapy), SR (superior rectus), and Y (yes).

10.3389/fonc.2024.1286910

woman in her 50s with bilateral choroid metastases stemming from breast cancer positively responded to abemaciclib and fulvestrant within four months after the beginning of treatment (81). The significant response observed to abemaciclib in treating intraocular metastases aligns with preclinical and clinical evidence showing its ability to penetrate the central nervous system (19, 20). This suggests that abemaciclib holds promise as a viable therapeutic option in this specific clinical scenario. No cases of orbital metastases treated with these targeted therapies were found.

To the best of our knowledge, we present the first case of a patient whose initial presentation had bilateral orbital metastases originating from bilateral lobular breast cancer with a substantial and dramatic response to a first-line treatment regimen that combined abemaciclib and letrozole.

Interestingly, our case report emphasizes that even with a reduced dose of 100mg, abemaciclib demonstrated efficacy without compromising the outcome. Similar to the MONALEESA trials, overall survival outcomes for patients with HR+/HER2- advanced breast cancer exhibited comparable results between those who underwent dose reductions of ribociclib and those who received the standard dose (83). This observation prompts the intriguing idea of tailoring treatment by personalizing doses for individual patients, considering their unique responses and tolerances.

Further comprehensive investigations are warranted to fully comprehend the potential of CDK4/6is in managing orbital metastases. It is essential to conduct rigorous studies that evaluate the safety and efficacy of different CDK4/6is through head-to-head comparisons and explore the impact of varying doses. These studies will provide valuable insights into optimizing treatment strategies and potentially improving outcomes for HR+/HER2- breast cancer patients with orbital metastases.

Therefore, the selection of CDK4/6i depends mainly on the toxicity profile and comorbidities of the patient. For instance, it is conceivable to avoid abemaciclib in patients with inflammatory bowel disease, while ribociclib should be avoided in patients with prolonged QT interval alterations on electrocardiogram (23). Conversely, palbociclib should be cautiously approached in patients with compromised bone marrow reserve (23).

Notably, the most frequent adverse effect observed during abemaciclib treatment is diarrhea, primarily of grade 1 severity (10), which aligns with our clinical case. Additionally, our patient exhibited analytical findings of hepatic toxicity and a mild increase in serum creatinine one month after initiating systemic treatment. These events, known and expected in the MONARCH trials (10), resolved upon withdrawal and subsequent reduction of abemaciclib dosage to 100mg twice a day. Adverse events and toxicities have been recognized in certain instances to correlate with positive treatment outcomes in cancer therapy (84, 85). Nevertheless, the current understanding of predictive factors for response to available breast cancer treatments remains insufficient. This uncertainty prompts the exploration of unconventional factors, such as the microbiota's role in offering insights into individual risk and prognosis, pharmacokinetics, pharmacodynamics, and clinical efficacy (86, 87). Recent research has demonstrated the capacity of the gut microbiota to influence the effectiveness and adverse effects of cancer treatments, as both cancer and anticancer therapies have bidirectional interactions with gut microbiota (86, 88, 89).

While the correlation is intriguing, it is essential to acknowledge that it may not be straightforward. The connection between adverse effects and treatment response can be intricate, influenced by various patient-specific elements, tumor characteristics, and the complex interplay of the drug with the body's physiological systems. Thus, while a correlation between diarrhea, changes in hepatic parameters, and treatment response in breast cancer with abemaciclib is captivating, further investigations are imperative to establish a causal relationship and unveil the underlying mechanisms linking these observations.

As we navigate these investigations, we must recognize the limitations inherent in single-case reports and exercise caution in extrapolating results to similar presentations and the long-term effects that may extend beyond sixteen months.

In conclusion, this clinical case underscores the potential of combining CDK4/6is, especially abemaciclib, with endocrine therapy in treating HR+/HER2- orbital metastatic breast cancer. While this case report highlights promising therapeutic avenues, it underscores the need for comprehensive studies, acknowledging the complexities of individual responses and the influence of factors like microbiota. As we advance toward more personalized oncology approaches, these findings encourage us to delve deeper into the interplay between treatments, adverse effects, and patient outcomes to optimize therapeutic strategies in metastatic breast cancer.

Data availability statement

The original contributions presented in the study are included in the article/supplementary material. Further inquiries can be directed to the corresponding authors.

Ethics statement

Written informed consent was obtained from the individual(s) for the publication of any potentially identifiable images or data included in this article.

Author contributions

NRA: Data curation, Formal analysis, Investigation, Methodology, Resources, Validation, Visualization, Writing – original draft, Writing – review & editing, Conceptualization, Supervision. AD: Conceptualization, Data curation, Formal analysis, Resources, Supervision, Validation, Visualization, Writing – review & editing. DR: Data curation, Formal analysis, Investigation, Methodology, Resources, Visualization, Writing – original draft. RS: Data curation, Investigation, Resources, Visualization, Writing – original draft. BC: Data curation, Writing – review & editing. DAC: Conceptualization, Data curation, Formal Analysis, Funding acquisition, Investigation, Methodology, Resources, Supervision, Validation, Visualization, Writing – review & editing.

Funding

The author(s) declare financial support was received for the research, authorship, and/or publication of this article. The funding was for open access publication fee. Payed by CUF Oncology.

Acknowledgments

The authors would like to express their gratitude to Nuno Caçador, MD, neuroradiologist, for his invaluable work and diagnostic assessment.

Conflict of interest

DC has received honoraria from the Portuguese Navy, CUF Oncologia, RiberaSalud, and NTT DATA, and has served as a speaker, advisory board member, or has received research or education funding from AstraZeneca, CUF Oncologia, Daiichi Sankyo, Gilead, Hoffmann-La Roche, Merck KGaA, Merck Sharp & Dohme, Nestlé, Novartis, Pfizer, Nanobiotix, Puma Biotechnology Inc., Sanofi, Seagen Inc., and Uriage. DC is supported by two research grants: AstraZeneca Produtos Farmacêuticos LDA and Grupo José de Mello.

The remaining authors declare that the research was conducted in the absence of any commercial or financial relationships that could be construed as a potential conflict of interest.

Publisher's note

References

1. Sung H, Ferlay J, Siegel RL, Laversanne M, Soerjomataram I, Jemal A, et al. Global cancer statistics 2020: GLOBOCAN estimates of incidence and mortality worldwide for 36 cancers in 185 countries. *CA: A Cancer J Clin* (2021) 71(3):209–49. doi: 10.3322/caac.21660

2. Seung SJ, Traore AN, Pourmirza B, Fathers KE, Coombes M, Jerzak KJ. A population-based analysis of breast cancer incidence and survival by subtype in ontario women. *Curr Oncol* (2020) 27(2):191–8. doi: 10.3747/co.27.5769

3. Blows FM, Driver KE, Schmidt MK, Broeks A, van Leeuwen FE, Wesseling J, et al. Subtyping of breast cancer by immunohistochemistry to investigate a relationship between subtype and short and long term survival: A collaborative analysis of data for 10,159 cases from 12 studies. *PloS Med* (2010) 7(5):e1000279. doi: 10.1371/journal.pmed.1000279

4. NIH SEER Program. *Cancer stat facts: female breast cancer subtypes. 2022. Cancer stat facts: female breast cancer subtypes* . Available at: https://seer.cancer.gov/statfacts/html/breast-subtypes.html (Accessed 1st August 2023).

5. Thangavel C, Dean JL, Ertel A, Knudsen KE, Aldaz CM, Witkiewicz AK, et al. Therapeutically activating RB: reestablishing cell cycle control in endocrine therapy-resistant breast cancer. *Endocr Related Cancer*. (2011) 18(3):333–45. doi: 10.1530/ERC-10-0262

6. Li J, Fu F, Yu L, Huang M, Lin Y, Mei Q, et al. Cyclin-dependent kinase 4 and 6 inhibitors in hormone receptor-positive, human epidermal growth factor receptor-2 negative advanced breast cancer: a meta-analysis of randomized clinical trials. *Breast Cancer Res Treat* (2020) 180(1):21–32. doi: 10.1007/s10549-020-05528-2

7. Hortobagyi GN, Stemmer SM, Burris HA, Yap YS, Sonke GS, Paluch-Shimon S, et al. Ribociclib as first-line therapy for HR-positive, advanced breast cancer. *New Engl J Med* (2016) 375(18):1738–48. doi: 10.1056/NEJMoa1609709

8. Finn RS, Martin M, Rugo HS, Jones S, Im SA, Gelmon K, et al. Palbociclib and letrozole in advanced breast cancer. *New Engl J Med* (2016) 375(20):1925–36. doi: 10.1056/NEJMoa1607303

9. Cristofanilli M, Turner NC, Bondarenko I, Ro J, Im SA, Masuda N, et al. Fulvestrant plus palbociclib versus fulvestrant plus placebo for treatment of hormone-receptor-positive, HER2-negative metastatic breast cancer that progressed on previous endocrine therapy (PALOMA-3): final analysis of the multicentre, double-blind, phase 3 randomised controlled trial. *Lancet Oncol* (2016) 17(4):425–39. doi: 10.1016/S1470-2045(15)00613-0

10. Goetz MP, Toi M, Campone M, Sohn J, Paluch-Shimon S, Huober J, et al. MONARCH 3: abemaciclib as initial therapy for advanced breast cancer. *J Clin Oncol* (2017) 35(32):3638–46. doi: 10.1200/JCO.2017.75.6155

11. Tripathy D, Im SA, Colleoni M, Franke F, Bardia A, Harbeck N, et al. Ribociclib plus endocrine therapy for premenopausal women with hormone-receptor-positive, advanced breast cancer (MONALEESA-7): a randomised phase 3 trial. *Lancet Oncol* (2018) 19(7):904–15. doi: 10.1016/S1470-2045(18)30292-4

12. Im SA, Lu YS, Bardia A, Harbeck N, Colleoni M, Franke F, et al. Overall survival with ribociclib plus endocrine therapy in breast cancer. *New Engl J Med* (2019) 381(4):307–16. doi: 10.1056/NEJMoa1903765

13. Sledge GW, Toi M, Neven P, Sohn J, Inoue K, Pivot X, et al. The effect of abemaciclib plus fulvestrant on overall survival in hormone receptor–positive, ERBB2-negative breast cancer that progressed on endocrine therapy—MONARCH 2. *JAMA Oncol* (2020) 6(1):116. doi: 10.1001/jamaoncol.2019.4782

14. Slamon DJ, Fasching PA, Hurvitz S, Chia S, Crown J, Martín M, et al. Rationale and trial design of NATALEE: a Phase III trial of adjuvant ribociclib + endocrine therapy *versus* endocrine therapy alone in patients with HR+/HER2– early breast cancer. *Ther Adv Med Oncol* (2023) 15:1758835923117781. doi: 10.1177/17588359231178125

15. Johnston SRD, Toi M, O'Shaughnessy J, Rastogi P, Campone M, Neven P, et al. Abemaciclib plus endocrine therapy for hormone receptor-positive, HER2-negative, node-positive, high-risk early breast cancer (monarchE): results from a preplanned interim analysis of a randomised, open-label, phase 3 trial. *Lancet Oncol* (2023) 24(1):77–90. doi: 10.1016/S1470-2045(22)00694-5

16. Braal CL, Jongbloed EM, Wilting SM, Mathijssen RHJ, Koolen SLW, Jager A. Inhibiting CDK4/6 in breast cancer with palbociclib, ribociclib, and abemaciclib: similarities and differences. *Drugs* (2021) 81(3):317–31. doi: 10.1007/s40265-020-01461-2

17. Hamilton E, Infante JR. Targeting CDK4/6 in patients with cancer. *Cancer Treat Rev* (2016) 45:129–38. doi: 10.1016/j.ctrv.2016.03.002

18. Goetz M, Toi M, Huober J, Sohn J. *MONARCH 3: Final overall survival results of abemaciclib plus a nonsteroidal aromatase inhibitor as first-line therapy for HR+, HER2- advanced breast cancer*. Texas (2023).

19. Tolaney SM, Sahebjam S, Le Rhun E, Bachelot T, Kabos P, Awada A, et al. A phase II study of abemaciclib in patients with brain metastases secondary to hormone receptor–positive breast cancer. *Clin Cancer Res* (2020) 26(20):5310–9. doi: 10.1158/1078-0432.CCR-20-1764

20. Schlam I, Tolaney SM. Is there a role for CDK 4/6 inhibitors in breast cancer brain metastases? *Oncotarget* (2021) 12(9):873–5. doi: 10.18632/oncotarget.27904

21. De Laurentiis M, Borstnar S, Campone M, Warner E, Bofill JS, Jacot W, et al. Full population results from the core phase of CompLEEment-1, a phase 3b study of ribociclib plus letrozole as first-line therapy for advanced breast cancer in an expanded population. *Breast Cancer Res Treat* (2021) 189(3):689–99. doi: 10.1007/s10549-021-06334-0

22. Burstein HJ, Somerfield MR, Barton DL, Dorris A, Fallowfield LJ, Jain D, et al. Endocrine treatment and targeted therapy for hormone receptor–positive, human epidermal growth factor receptor 2–negative metastatic breast cancer: ASCO guideline update. *J Clin Oncol* (2021) 39(35):3959–77. doi: 10.1200/JCO.21.01392

23. Grinshpun A, Tolaney SM, Burstein HJ, Jeselsohn R, Mayer EL. The dilemma of selecting a first line CDK4/6 inhibitor for hormone receptor-positive/HER2-negative metastatic breast cancer. *NPJ Breast Cancer*. (2023) 9(1):15. doi: 10.1038/s41523-023-00520-7

24. Teichgraeber DC, Guirguis MS, Whitman GJ. Breast cancer staging: updates in the *AJCC cancer staging manual* , 8th edition, and current challenges for radiologists, from the *AJR* special series on cancer staging. *Am J Roentgenol* (2021) 217(2):278–90. doi: 10.2214/AJR.20.25223

25. Freites-Martinez A, Santana N, Arias-Santiago S, Viera A. CTCAE versión 5.0. Evaluación de la gravedad de los eventos adversos dermatológicos de las terapias antineoplásicas. *Actas Dermo-Sifiliográficas.* (2021) 112(1):90–2. doi: 10.1016/j.ad.2019.05.009

26. Shields JA, Shields CL, Scartozzi R. Survey of 1264 patients with orbital tumors and simulating lesions. *Ophthalmology* (2004) 111(5):997–1008. doi: 10.1016/j.ophtha.2003.01.002

27. Ahmad SM, Esmaeli B. Metastatic tumors of the orbit and ocular adnexa. *Curr Opin Ophthalmol* (2007) 18(5):405–13. doi: 10.1097/ICU.0b013e3282c5077c

28. Palmisciano P, Ferini G, Ogasawara C, Wahood W, Bin Alamer O, Gupta AD, et al. Orbital metastases: A systematic review of clinical characteristics, management strategies, and treatment outcomes. *Cancers* (2021) 14(1):94. doi: 10.3390/cancers14010094

29. Valenzuela AA, Archibald CW, Fleming B, Ong L, O'Donnell B, Crompton JJ, et al. Orbital metastasis: clinical features, management and outcome. *Orbit* (2009) 28 (2–3):153–9. doi: 10.1080/01676830902897470

30. Lell M, Schulz-Wendtland R, Hafner A, Magener A, Bautz WA, Tomandl BF. Bilateral orbital tumour as the presentation of mammographically occult breast cancer. *Neuroradiology* (2004) 46(8):682–5. doi: 10.1007/s00234-003-1106-x

31. Shields JA, Shields CL, Brotman HK, Carvalho C, Perez N, Eagle RC. Cancer metastatic to the orbit. *Ophthal Plast Reconstruct Surg* (2001) 17(5):346–54. doi: 10.1097/00002341-200109000-00009

32. Goldberg RA, Rootman J, Cline RA. Tumors metastatic to the orbit: A changing picture. *Surv Ophthalmol* (1990) 35(1):1–24. doi: 10.1016/0039-6257(90)90045-W

33. Spitofsky NR, Barke MR, Shields CL. Orbital and eyelid metastases 42 years after primary breast carcinoma. *Ophthal Plast Reconstruct Surg* (2023) 39(4):e135. doi: 10.1097/IOP.0000000000002304

34. Weber AL, Romo LV, Sabates NR. PSEUDOTUMOR OF THE ORBIT. *Radiol Clinics North America* (1999) 37(1):151–68. doi: 10.1016/S0033-8389(05)70084-1

35. Ben Simon GJ, Annunziata CC, Fink J, Villablanca P, McCann JD, Goldberg RA. Rethinking orbital imaging. *Ophthalmology* (2005) 112(12):2196–207. doi: 10.1016/j.ophtha.2005.09.013

36. Rana K, Juniat V, Patel S, Selva D. Extraocular muscle enlargement. *Graefe's Arch Clin Exp Ophthalmol* (2022) 260(11):3419–35. doi: 10.1007/s00417-022-05727-1

37. Mombaerts I, Rose GE, Verity DH. Diagnosis of enlarged extraocular muscles. *Curr Opin Ophthalmol* (2017) 28(5):514–21. doi: 10.1097/ICU.0000000000000395

38. Tomizawa Y, Ocque R, Ohori NP. Orbital metastasis as the initial presentation of invasive lobular carcinoma of breast. *Internal Med* (2012) 51(12):1635–8. doi: 10.2169/internalmedicine.51.7641

39. Framarino-dei-Malatesta M, Chiarito A, Bianciardi F, Fiorelli M, Ligato A, Naso G, et al. Metastases to extraocular muscles from breast cancer: case report and up-to-date review of the literature. *BMC Cancer.* (2019) 19(1):36. doi: 10.1186/s12885-018-5253-1

40. Portschy PR, Marmor S, Nzara R, Virnig BA, Tuttle TM. Trends in incidence and management of lobular carcinoma in situ: A population-based analysis. *Ann Surg Oncol* (2013) 20(10):3240–6. doi: 10.1245/s10434-013-3121-4

41. Christgen M, Steinemann D, Kühnle E, Länger F, Gluz O, Harbeck N, et al. Lobular breast cancer: Clinical, molecular and morphological characteristics. *Pathol - Res Practice* (2016) 212(7):583–97. doi: 10.1016/j.prp.2016.05.002

42. Jakobiec FA, Stagner AM, Homer N, Yoon MK. Periocular breast carcinoma metastases: predominant origin from the lobular variant. *Ophthal Plast Reconstruct Surg* (2017) 33(5):361–6. doi: 10.1097/IOP.0000000000000793

43. Borst MJ, Ingold JA. Metastatic patterns of invasive lobular versus invasive ductal carcinoma of the breast. *Surgery* (1993) 114(4):637–41.

44. Ferlicot S, Vincent-Salomon A, Médioni J, Genin P, Rosty C, Sigal-Zafrani B, et al. Wide metastatic spreading in infiltrating lobular carcinoma of the breast. *Eur J Cancer.* (2004) 40(3):336–41. doi: 10.1016/j.ejca.2003.08.007

45. Simpson E, Rubin G, Clyne C, Robertson K, O'Donnell L, Davis S, et al. Local estrogen biosynthesis in males and females. *Endocrine-related cancer* (1999) 6:131–7. doi: 10.1677/erc.0.0060131

46. Spelsberg H, Klueppel M, Reinhard T, Glaeser M, Niederacher D, Beckmann MW, et al. Detection of Oestrogen receptors (ER) α and β in conjunctiva, lacrimal gland, and tarsal plates. *Eye* (2004) 18(7):729–33. doi: 10.1038/sj.eye.6701314

47. Raap M, Antonopoulos W, Dämmrich M, Christgen H, Steinmann D, Länger F, et al. High frequency of lobular breast cancer in distant metastases to the orbit. *Cancer Med* (2015) 4(1):104–11. doi: 10.1002/cam4.331

48. Spitzer SG, Bersani TA, Mejico LJ. Multiple bilateral extraocular muscle metastases as the initial manifestation of breast cancer. *J Neuro-Ophthalmol* (2005) 25(1):37–9. doi: 10.1097/00041327-200503000-00010

49. Dieing A, Schulz CO, Schmid P, Roever AC, Lehenbauer-Dehm S, Jehn C, et al. Orbital metastases in breast cancer: report of two cases and review of the literature. *J Cancer Res Clin Oncol* (2004) 130(12):745–8. doi: 10.1007/s00432-004-0606-3

50. Bedford PD, Daniel PM. Discrete carcinomatous metastases in the extrinsic ocular muscles* *From the department of ophthalmology, mount Sinai hospital and clinic. *Am J Ophthalmol* (1960) 49(4):723–6. doi: 10.1016/0002-9394(60)92047-X

51. Capone A. Discrete metastasis of solid tumors to extraocular muscles. *Arch Ophthalmol* (1990) 108(2):237. doi: 10.1001/archopht.1990.01070040089037

52. Glazer LC, Harris GJ, Simons KB. Orbital metastasis as the presenting sign of adenocarcinoma of the breast. *Ophthal Plast Reconstruct Surg* (1991) 7(4):252–5. doi: 10.1097/00002341-199112000-00003

53. Rhatigan MC, Ashworth JL, Shah S, Bonshek RE, Leatherbarrow B. Bilateral orbital metastases from breast carcinoma masquerading as thyroid eye disease. *Eye* (1995) 9(5):653–5. doi: 10.1038/eye.1995.161

54. Po SM. Bilateral lagophthalmos. *Arch Ophthalmol* (1996) 114(9):1139. doi: 10.1001/archopht.1996.01100140341019

55. Zambarakji HJ, Simcock PR, Kinnear PE. Bilateral orbital metastases in a woman with breast carcinoma. *J R Soc Med* (1997) 90(12):684–4. doi: 10.1177/014107689709001214

56. Garcia GH, Weinberg DA, Glasgow BJ, Hunt KE, Venegas R, Goldberg RA. Carcinoma of the male breast metastatic to both orbits. *Ophthal Plast Reconstruct Surg* (1998) 14(2):130–3. doi: 10.1097/00002341-199803000-00010

57. Toller KK, Gigantelli JW, Spalding MJ. Bilateral orbital metastases from breast carcinoma. *Ophthalmology* (1998) 105(10):1897–901. doi: 10.1016/S0161-6420(98)91037-5

58. Lacey B, Chang W, Rootman J. Nonthyroid causes of extraocular muscle disease. *Surv Ophthalmol* (1999) 44(3):187–213. doi: 10.1016/S0039-6257(99)00101-0

59. Stuntz M, Yamini D, Moss J, Klein S, Khalkhali I. Bilateral orbital metastases as the presenting finding in a male patient with breast cancer: A case report and review of the literature. *Breast J* (2000) 6(3):204–8. doi: 10.1046/j.1524-4741.2000.97090.x

60. Gonçalves AC, Moura FC, Monteiro MLR. Bilateral progressive enophthalmos as the presenting sign of metastatic breast carcinoma. *Ophthal Plast Reconstruct Surg* (2005) 21(4):311–3. doi: 10.1097/01.iop.0000167786.00697.0b

61. Peckham EL, Giblen G, Kim AK, Sirdofsky MD. Bilateral extraocular muscle metastasis from primary breast cancer. *Neurology* (2005) 65(1):74–4. doi: 10.1212/01.WNL.0000156359.93206.99

62. Kuchel JM, Bowling JC. Bilateral lower eyelid masses—Quiz case. *Arch Dermatol* (2006) 142(10). doi: 10.1001/archderm.142.10.1351-c

63. Gasperini J, Black E, Van Stavern G. Perineural metastasis of breast cancer treated with optic nerve sheath fenestration. *Ophthal Plast Reconstruct Surg* (2007) 23 (4):331–3. doi: 10.1097/IOP.0b013e318073cc6d

64. Milman T, Pliner L, Langer PD. Breast carcinoma metastatic to the orbit: an unusually late presentation. *Ophthal Plast Reconstruct Surg* (2008) 24(6):480–2. doi: 10.1097/IOP.0b013e31818b6adc

65. Kouvaris JR, Gkongkou PV, Papadimitriou CA, Papacharalampous XN, Antypas CE, Balafouta MJ, et al. Bilateral metastases to extraocular muscles from lobular breast carcinoma. *Onkologie* (2008) 31(7):387–9. doi: 10.1159/000129689

66. Jaspers H, Blaisse R, Maessen-Visch B, Mattijssen V. Bilateral swollen eyelids occurring during adjuvant treatment with tamoxifen for early breast cancer. *Netherlands J Med* (2009) 67(6):245–6.

67. Murthy R, Gupta A, Hegde S, Honavar S. Bilateral multiple extraocular muscle metastasis from breast carcinoma. *Indian J Ophthalmol* (2011) 59(5):381. doi: 10.4103/0301-4738.83616

68. Kim JH, Choi SY, Cho CK, Yang KM, Noh WC, Kim MS. Bilateral orbital metastases from breast cancer: A case report of successful palliation using stereotactic radiotherapy. *Breast J* (2011) 17(6):669–71. doi: 10.1111/j.1524-4741.2011.01165.x

69. Kim HJ, Wojno TH, Grossniklaus H. Atypical bilateral orbital metastases of lobular breast carcinoma. *Ophthal Plast Reconstruct Surg* (2012) 28(6):e142–3. doi: 10.1097/IOP.0b013e318249d5c0

70. Wiggins RE, Byrne SF. Metastatic tumor to the extraocular muscles: Report of 5 cases. *J Am Assoc Pediatr Ophthalmol Strabismus* (2012) 16(5):489–91. doi: 10.1016/j.jaapos.2012.06.009

71. Khan NA, Morlese J, Khan A. Radiological foresight: a rare case of breast cancer metastases to the extraocular muscles. *BMJ Case Rep* (2015), bcr2015211264. doi: 10.1136/bcr-2015-211264

72. Blohmer M, Zhu L, Atkinson JM, Beriwal S, Rodríguez-López JL, Rosenzweig M, et al. Patient treatment and outcome after breast cancer orbital and periorbital metastases: a comprehensive case series including analysis of lobular versus ductal tumor histology. *Breast Cancer Res* (2020) 22(1):70. doi: 10.1186/s13058-020-01309-3

73. Marotta DA, Jabaay MJ, Zadourian A, Kesserwani H. Bilateral orbital metastases masquerading as ocular myasthenia gravis: A case report and review of the literature. *Cureus* (2020) 12(7):1-5. doi: 10.7759/cureus.9105

74. Dimopoulos A, Zeng J, Shinder R. Breast carcinoma metastatic to the bilateral orbits. *Orbit* (2020) 39(2):153–3. doi: 10.1080/01676830.2019.1603314

75. Muhammad-Ikmal MK, Masnon NA, Hayati F, Wan HItam WH. Sino-orbital metastasis as the initial presentation of advanced breast cancer. *BMJ Case Rep* (2022) 15 (11):e250108. doi: 10.1136/bcr-2022-250108

76. Tsutsui S, Kawata K, Ubagai T, Okimoto S, Fujihara M, Maeda T, et al. Orbital metastasis of invasive lobular carcinoma of the breast. *J Surg Case Rep* (2022) 2022 (1):1-3. doi: 10.1093/jscr/rjab619

77. Karimaghaei S, Raviskanthan S, Mortensen PW, Malik AI, Lee AG. Metastatic breast cancer presenting as progressive ophthalmoplegia 30 years after initial cancer diagnosis. *J Neuro-Ophthalmol* (2022) 42(1):e446–7. doi: 10.1097/WNO.0000000000001385

78. El-Khazen Dupuis J, Marchand M, Javidi S, Nguyen TQT. Enophthalmos as the initial systemic finding of undiagnosed metastatic breast carcinoma. *Int Med Case Rep J* (2021) 14:25–31. doi: 10.2147/IMCRJ.S282113

79. Gennari A, André F, Barrios CH, Cortés J, de Azambuja E, DeMichele A, et al. ESMO Clinical Practice Guideline for the diagnosis, staging and treatment of patients with metastatic breast cancer. *Ann Oncol* (2021) 32(12):1475–95. doi: 10.1016/j.annonc.2021.09.019

80. Thill M, Lüftner D, Kolberg-Liedtke C, Albert US, Banys-Paluchowski M, Bauerfeind I, et al. AGO recommendations for the diagnosis and treatment of patients with locally advanced and metastatic breast cancer: update 2022. *Breast Care* (2022) 17(4):421–9. doi: 10.1159/000524789

81. Barke MR, Agrawal KU, Shields CL. Abemaciclib and fulvestrant for bilateral choroidal metastasis from breast carcinoma. *JAMA Ophthalmol* (2022) 140(10):1026. doi: 10.1001/jamaophthalmol.2022.3453

82. Goduni L, Ashkenazy N, Hansen E, Soyano-Muller A, Correa ZM, Harbour JW. Iris metastasis from breast cancer successfully treated with abemaciclib and letrozole. *Retinal cases Brief Rep* (2023) 17(2):123–5. doi: 10.1097/ICB.0000000000001176

83. Burris HA, Chan A, Bardia A, Thaddeus Beck J, Sohn J, Neven P, et al. Safety and impact of dose reductions on efficacy in the randomised MONALEESA-2, -3 and -7 trials in hormone receptor-positive, HER2-negative advanced breast cancer. *Br J Cancer.* (2021) 125(5):679–86. doi: 10.1038/s41416-021-01415-9

84. Liew DFL, Leung JLY, Liu B, Cebon J, Frauman AG, Buchanan RRC. Association of good oncological response to therapy with the development of rheumatic immune-related adverse events following PD-1 inhibitor therapy. *Int J Rheuma Dis* (2019) 22 (2):297–302. doi: 10.1111/1756-185X.13444

85. Hua C, Boussemart L, Mateus C, Routier E, Boutros C, Cazenave H, et al. Association of vitiligo with tumor response in patients with metastatic melanoma treated with pembrolizumab. *JAMA Dermatol* (2016) 152(1):45. doi: 10.1001/jamadermatol.2015.2707

86. Vitorino M, Baptista de Almeida S, Alpuim Costa D, Faria A, Calhau C, Azambuja Braga S. Human microbiota and immunotherapy in breast cancer - A review of recent developments. *Front Oncol* (2022) 11:815772. doi: 10.3389/fonc.2021.815772

87. Alpuim Costa D, Nobre JG, Batista MV, Ribeiro C, Calle C, Cortes A, et al. Human microbiota and breast cancer—Is there any relevant link?—A literature review and new horizons toward personalised medicine. *Front Microbiol* (2021) 12:584332. doi: 10.3389/fmicb.2021.584332

88. Gately S. Human microbiota and personalized cancer treatments: role of commensal microbes in treatment outcomes for cancer patients. *Precision Medicine in Cancer Therapy* (2019) 178:253–64. doi: 10.1007/978-3-030-16391-4_10

89. Panebianco C, Andriulli A, Pazienza V. Pharmacomicrobiomics: exploiting the drug-microbiota interactions in anticancer therapies. *Microbiome* (2018) 6(1):92. doi: 10.1186/s40168-018-0483-7

frontiers | Frontiers in Oncology

TYPE Case Report
PUBLISHED 01 February 2024
DOI 10.3389/fonc.2024.1189287

OPEN ACCESS

EDITED BY
Giuseppe Giaccone,
Vice President Global Development,
United States

REVIEWED BY
Byeongsang Oh,
The University of Sudney, Australia
Nicholas Adam Young,
Private Health Management Inc, United States

*CORRESPONDENCE
Tamiko R. Katsumoto
tkatsum@stanford.edu

RECEIVED 18 March 2023
ACCEPTED 15 January 2024
PUBLISHED 01 February 2024

CITATION
Wilson KL, Grewelle RE, Gupta T, Kim SH and Katsumoto TR (2024) Aromatase inhibitor-induced arthralgia ameliorated by Mediterranean diet and active lifestyle guided by continuous glucose monitoring: a case report and review of the literature.
Front. Oncol. 14:1189287.
doi: 10.3389/fonc.2024.1189287

Aromatase inhibitor-induced arthralgia ameliorated by Mediterranean diet and active lifestyle guided by continuous glucose monitoring: a case report and review of the literature

Kalin L. Wilson[1], Richard E. Grewelle[2,3], Tanya Gupta[4], Sun H. Kim[5] and Tamiko R. Katsumoto[6*]

[1]Department of Medicine, Stanford University School of Medicine, Stanford, CA, United States, [2]Department of Biology, Stanford University, Stanford, CA, United States, [3]Department of Genetics, Stanford University School of Medicine, Stanford, CA, United States, [4]Department of Medicine, Division of Oncology, Stanford Cancer Institute, Stanford University School of Medicine, Stanford, CA, United States, [5]Department of Medicine, Division of Endocrinology, Stanford University School of Medicine, Stanford, CA, United States, [6]Department of Medicine, Division of Immunology and Rheumatology, Stanford University School of Medicine, Stanford, CA, United States

Aromatase inhibitors (AIs) are a cornerstone adjuvant treatment of many hormone receptor-positive breast cancers, and nearly half of women taking aromatase inhibitors suffer from AI-induced arthralgia (AIA), also known as AI-associated musculoskeletal syndrome (AIMSS), for which there are limited evidence-based treatments. Pharmacologic management and complementary methods including supplements, exercise, physical therapy, yoga, acupuncture, and massage have all shown mixed results. Comprehensive diet and lifestyle strategies are understudied in AIA/AIMSS despite their disease-modifying effects across many chronic conditions. Here we report a case of a woman with stage 2 estrogen and progesterone receptor-positive invasive ductal carcinoma on adjuvant anastrozole whose AI-induced arthralgia was durably controlled through a Mediterranean plant-forward diet and daily physical activity guided by continuous glucose monitoring. We posit that diet and a lifestyle inclusive of daily physical activity constitute a low-cost, low-risk, and potentially high-reward strategy for controlling common AI-induced musculoskeletal symptoms and that more investigation in this arena, including well-designed randomized trials, is warranted.

KEYWORDS

hormone receptor-positive breast cancer, aromatase inhibitor-induced arthralgia, continuous glucose monitoring, Mediterranean diet, lifestyle medicine

1 Introduction

Breast cancer is the most common malignancy affecting 2.1 million women worldwide each year and second most common cause of cancer-related death among women in the United States (1, 2). Aromatase inhibitors (AIs) are central to the treatment of many estrogen and progesterone receptor-expressing breast cancers, which comprise 70-75% of all breast cancers (2, 3). However, they are associated with adverse effects, including a constellation of symptoms referred to as aromatase inhibitor-induced arthralgia (AIA) or more broadly as aromatase inhibitor-associated musculoskeletal syndrome (AIMSS), with criteria proposed by Niravath (4).

AIA/AIMSS classically presents with symmetrical joint pains affecting the hands, wrists, ankles, and/or knees; other symptoms include morning stiffness, myalgias, tenosynovitis, carpal tunnel syndrome, and trigger finger (4–6). This syndrome affects nearly 50% of women taking AIs (7) and contributes strongly to medication nonadherence and discontinuation (8). There are limited treatments for AIA/AIMSS other than drug discontinuation; pharmacologic and complementary management approaches have shown mixed results (9, 10). Furthermore, data on dietary interventions most often focus on a single diet modification or complementary diet supplement rather than on comprehensive diet change. Despite clear evidence that a healthy diet and active lifestyle can positively impact the course of many chronic conditions, there is a dearth of literature systematically investigating such interventions jointly for patients with AIA/AIMSS. Herein we present the case of a patient with AIA/AIMSS effectively controlled through comprehensive changes in diet and daily physical activity facilitated by continuous glucose monitor (CGM) use.

2 Case description

The patient, a 46-year-old female, presented with right breast mass in August 2017 and was diagnosed with stage 2, grade 3 estrogen receptor, progesterone receptor, and human epidermal growth factor receptor-expressing (ER+/PR+/HER2+) invasive ductal carcinoma (IDC) with associated ductal carcinoma *in situ* on MRI-guided biopsy. She underwent neoadjuvant therapy with 4 cycles of doxorubicin and cyclophosphamide (ddAC) and 16 cycles of paclitaxel, trastuzumab, and pertuzumab (THP), then proceeded to right partial mastectomy which revealed residual IDC, ER+/PR+/HER2+ (stage ypT1b(m)N0). Following a second resection due to proximity of IDC to the margin and a course of radiation therapy, she initiated tamoxifen in August 2018. She then transitioned to AI therapy with anastrozole in July 2020 when she was felt to be in menopause with multiple ultrasensitive estradiol levels<15 pg/mL (Figure 1).

Two months after initiating anastrozole, the patient developed ankle pain prompting medication discontinuation for two weeks. After restarting, she presented in February 2021 with bilateral hand and wrist pain and tingling, 30 minutes of morning joint stiffness, swelling, and decreased grip strength as well as right Achilles tendon pain and stiffness which she rated as an 8 out of 10 at worst. She preferred to remain on AI rather than returning to tamoxifen. Persistence of these symptoms prompted a switch from anastrozole to letrozole. However, on letrozole she experienced greater morning hand stiffness and new trigger finger such that letrozole was discontinued. Her stiffness then improved and she resumed anastrozole. She was referred to rheumatology for evaluation, where initial exam in July 2021 revealed right third and fourth PIP joint tenderness and a palpable, tender Achilles tendon nodule. Her labs were notable for normal ESR, borderline

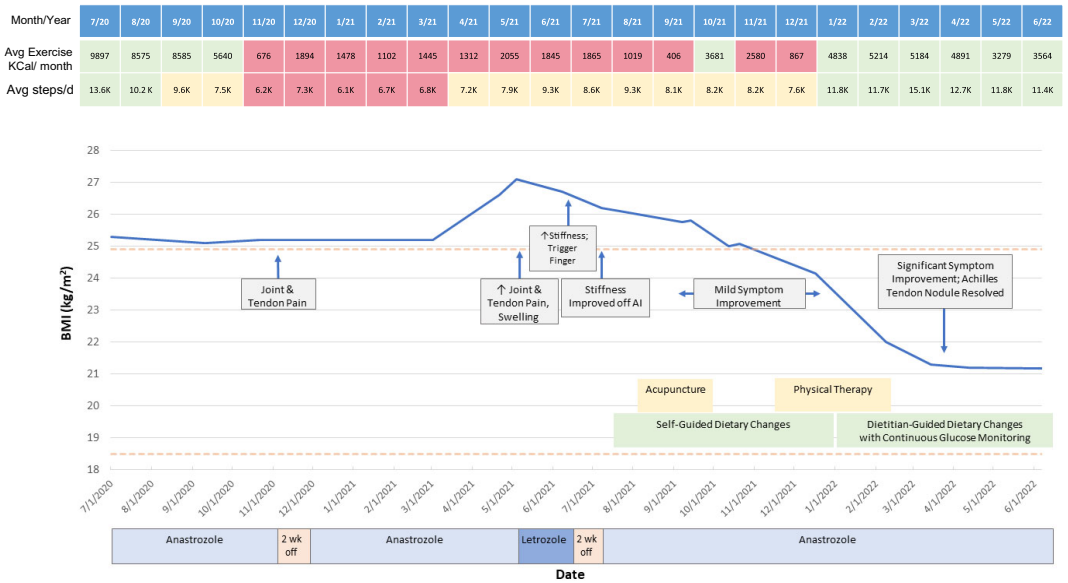

FIGURE 1
Timeline of patient symptoms, interventions, and BMI. Wk, week.

CRP, and negative ANA, RF, and CCP antibodies. She was diagnosed with AIA; alternative diagnoses considered included carpal tunnel syndrome and inflammatory arthritis including seronegative rheumatoid arthritis and the spondyloarthritides. Around this time, she was also diagnosed with prediabetes with a hemoglobin A1C (HgbA1c) of 6.3% and her pre-existing mild hepatic steatosis worsened to moderate nonalcoholic fatty liver disease based on ultrasound findings (see Supplementary Figure 2). She reported a diet with an abundance of high glycemic index foods such as bread, pasta, pizza, and several sweets (cookies, cakes). She thus opted for a trial of nonpharmacologic symptom management through modification of diet and physical activity. During this period she also briefly tried acupuncture without benefit and participated in three months of ankle physical therapy with some improvement in Achilles tendon pain but with persistence of hand stiffness and trigger finger symptoms.

On her follow up rheumatologic evaluation in March 2022, the patient had lost 17 pounds, a 12.5% loss from her peak body weight. She reported enrolling in a dietitian-supervised program most closely approximating a Mediterranean plant-forward diet with high intake of olive oil, fruits and vegetables, and less than 20% fish, poultry, or meat alternatives rather than red and/or processed meats and stated that she achieved her macronutrient goals (20% protein, 45% carbohydrates, 35% fat) over 90% of the time (Figure 2). Over the period of interest, she slowly transitioned more toward plant-based protein options. She also eliminated dairy, decreased the length of her daily food consumption window, and continued a consistent pattern of moderate aerobic exercise. She aimed to achieve approximately 40 minutes of exercise and 12,000 steps daily; however due to her significant arthralgias, her average daily step count and total number of calories burned (Peloton workout) initially declined from baseline (see Figure 1). Finally, she began using a CGM (Dexcom G6) to help lower daylong glucose and guide selection of lower glycemic index (GI) foods with less impact on postprandial glucose. The CGM also provided feedback regarding interventions to moderate rise in blood glucose of certain challenging foods. For example, she noted postprandial blood glucose elevations > 140 mg/dL after eating portions of cooked sweet potato, which led her to experiment with exercise and consumption techniques around this food item. She found that the same quantity of the same batch of cooked sweet potato would produce a less pronounced increase in blood glucose if she engaged in 20-30 minutes of moderate aerobic exercise (i.e., brisk walking or trampoline) before or after her meal or if she ate a portion of lean protein before consuming the sweet potato (Supplementary Figure 1). The patient incorporated these lessons into her daily practice, demonstrating that CGM usage can encourage exercise and diet modification. The CGM data reveal trends toward reduced glucose variability and increased time in the target range (70-140 mg/dL) (Figure 3). Consistent with these changes, her HgbA1C improved from 6.3 to 5.8% between December 2021 and August 2022. Her hepatic steatosis fully resolved by January 2023 (Supplementary Figure 2).

Subsequently, the patient's stiffness, pain, and tingling significantly improved. Her Achilles tenosynovitis fully resolved and the nodule was no longer palpable, concordant with a substantial increase in her exercise patterns (daily step counts and calories burned in her Peloton workouts, Figure 1). She continues to tolerate AI therapy with anastrozole through the time of publication.

3 Conclusions

Herein we present the case of a 46-year-old female with ER+, PR+, HER2+ breast cancer on anastrozole who developed classic features meeting Niravath's proposed criteria for AIA/AIMSS. After failing to improve with acupuncture, physical therapy, or switching AIs, she was able to durably control her symptoms non-pharmacologically through dietary changes, active lifestyle, and weight loss.

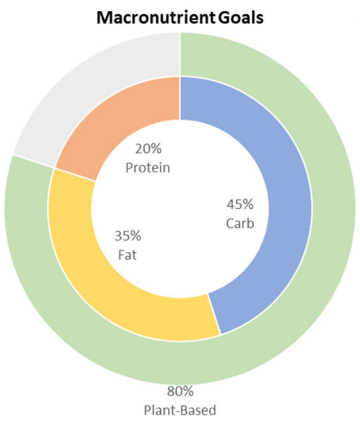

Goal Intake*	Typical Meals
1612 KCal/Day	Breakfast 2 egg white omelet with mushrooms and spinach Steel cut oats with flax or chia and blueberries Smoothie with mixed fruits and greens
80 ounces water	Lunch/Dinner 2 quinoa and black bean tacos on flour tortillas or jicama wrap with guacamole, tomatoes, cheese, and side of fruit. Leafy green salad topped with diced vegetables and pine nuts or bean sprouts Baked salmon filet with roasted vegetables Lentil soup Roasted chicken and vegetables Poke bowl with tuna, tofu, edamame, mixed vegetables, rice
	Snacks Yogurt with granola Nuts Fruit **Patient reports meeting macronutrient and caloric goals >90% of days*

FIGURE 2
Summary characteristics of the patient's dietitian-guided diet pattern with recommended macronutrient breakdown and examples of typical meals consumed by the patient.

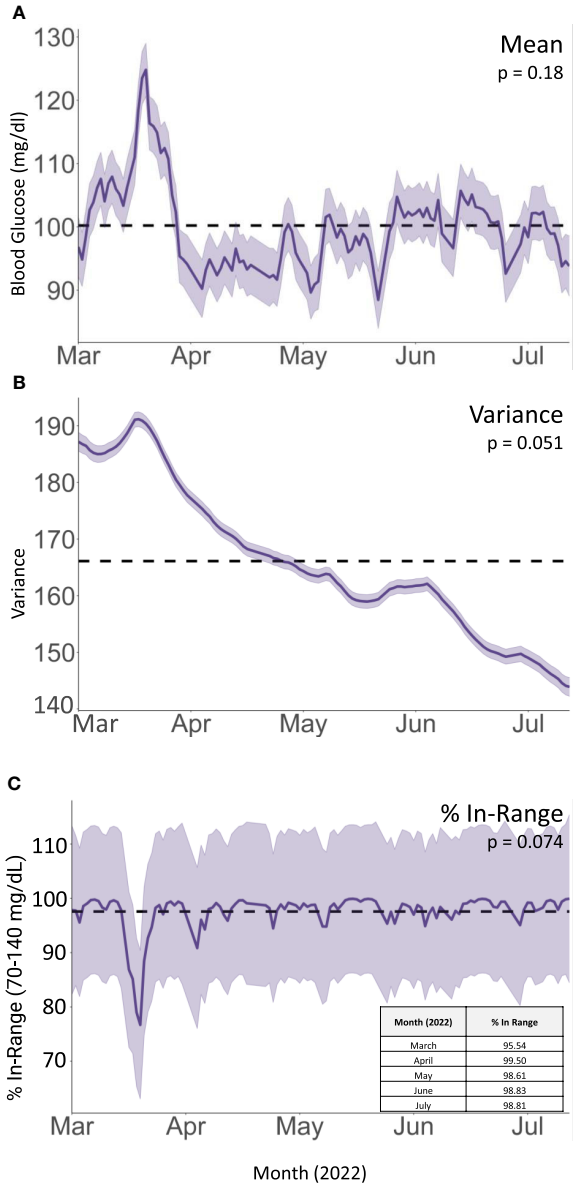

FIGURE 3
Integrated Nested Laplacian Approximation (INLA) model of **(A)** mean glucose values, **(B)** within-day variance in blood glucose values (σ^2), and **(C)** fraction of CGM readings within target glucose range. Shaded area represents 95% confidence interval. Dotted line represents overall mean for the dataset.

This patient's course was notable in that after attempting several commonly cited management options, she was able to reduce her AIA/AIMSS symptoms through a diet most closely approximating a Mediterranean plant-forward diet coupled with other healthy lifestyle practices, an intervention without any adverse effects and indeed would be expected to positively impact health in other domains (e.g., type 2 diabetes, nonalcoholic fatty liver disease). To date, there have been no high-quality randomized controlled dietary intervention studies for the treatment of AIA/AIMSS. Importantly, a recruiting phase I/II trial plans to investigate an anti-inflammatory/Mediterranean diet for breast cancer patients on AIs (11).

Although some pharmacologic approaches have demonstrated success in curbing AIMSS symptoms, associated side effects may limit their tolerability. Although a large RCT testing duloxetine showed significant reduction in mean average pain score at week 12 in those with a BMI > 30 kg/m2, adverse effects were seen in 78% (vs. 50%) of participants on duloxetine compared with placebo (primarily fatigue, dry mouth, and headache) (12, 13). One week of low-dose prednisolone similarly reduced pain in about two thirds of individuals, with one third reporting persistent benefit at one month and one quarter at two months (14); while this might constitute an adequate temporizing measure, most patients continue AI therapy for years, and glucocorticoids would not be a viable therapeutic option over this period due to adverse metabolic effects and risk of bone loss.

Potentially lower-risk interventions include complementary approaches such as nutritional or herbal supplementation, acupuncture, meditation and mindfulness, and physical activity. It is challenging to assess the overall effectiveness of these interventions given the paucity and variable quality of data available in the literature. A recent Cochrane review on RCTs for AIA/AIMSS (15) identified 17 high-quality studies (4 prevention studies, 13 treatment studies) with over 2000 randomized patients, and the results are summarized in Table 1. Overall, there was very low-certainty evidence for the evaluated systemic therapies for the prevention or management of AIA/AIMSS. Single-agent dietary supplements such as omega-3 fatty acids and Vitamin D supplementation have tended not to induce a durable reduction in pain (Table 1). Quality of the studies included in the Cochrane review was variable, with differences in endpoints, timing of measurements, study conduct, and risk of bias. Therapies evaluated in this systematic review included etoricoxib (17), testosterone (18, 19), duloxetine (12), calcitonin (20), omega-3 fatty acid supplementation (21, 22), vitamin D3 supplementation (23–26), tart cherry (27), bionic tiger bone capsules (28), Yi Shen Jian Gu granules (29), emu oil (30), and Cat's claw (31). Standardization of the measurement of outcomes in AIA/AIMSS, including patient reported outcomes (PROs), and standardization of the time points for assessment would improve research quality and reduce heterogeneity in comparing studies (15).

Another recent Cochrane review evaluated exercise as a treatment for AIA/AIMSS and included 7 studies (1 prevention study, 6 intervention studies) with 400 randomized participants (see Table 1) (32). Considerable heterogeneity was noted amongst the trials, and the meta-analysis provided no clear evidence that exercise was beneficial in AIMSS. Other meta-analyses have revealed trends toward improvement in pain scores with physical exercise and acupuncture but no significant signal for mindfulness and relaxation techniques (9, 10, 33). Briefly, diverse exercise interventions were represented, with the best signal originating from trials of mixed aerobic/resistance programs, while walking interventions and tai chi were less successful. One study by Irwin et al. (2015 JCO) showed significant improvement in worst joint pain scores in patients randomized to the exercise arm, consisting of at least 150 minutes per week of aerobic exercise and supervised strength training twice per week. Studies on yoga were too sparse and heterogeneous to allow for a systematic assessment, but

10.3389/fonc.2024.1189287

TABLE 1 Randomized controlled trials included in AIA/AIMSS Cochrane Reviews (15, 16).

	Author, year	Trial Type	N	Study details	Outcome	Caveats
MEDICATIONS						
Duloxetine	Henry 2018	Treatment	299	Significant reduction in mean average pain score (BPI-SF) at wk 12 in BMI >30 kg/m2 but not in BMI< 30 kg/m2	Positive	AEs: 78% duloxetine, 50% PBO (P<0.001), most common AEs fatigue, dry mouth, headache
Etoricoxib	Rosati 2011 (abstract only)	Treatment	182	2o EP: MSK pain significantly lower in treatment arm (50/73) than control (16/67) [RR: 2.1, 95%CI (1.29-3.43), P=0.002]	Positive	Abstract only, high dropout rate
Testosterone	Birrell 2009 (abstract only)	Treatment	90	Decreased pain VAS scores inof 43% testosterone 40 mg, 70% testosterone 80 mg vs 35% PBO, P=0.06 and P=0.04 vs PBO respectively	Positive	Abstract only, supported by Astra Zeneca
	Cathcart-Rake 2020	Treatment	227	No difference in pain or stiffness at 3 and 6 mos (BPI-AIA, item #3)	Negative	
Calcitonin	Liu 2014	Treatment	91	Pain VAS significantly decreased -3 (Calcitonin 200 IU group) vs -1 (PBO), P<0.01	Positive	Baseline difference in VAS (5.38 Calcitonin vs 4.48 Control, P=0.006), 1o EP not specified
SUPPLEMENTS						
Vitamin D3	Khan 2017	Prevention	160	Prevention of protocol defined AIMSS event 37% in high dose vitamin D 30,000 IU/week vs 51% PBO (P=0.069)	Negative	
	Niravath 2019	Prevention	93	AIMSS developed in 54% high dose vit D 50,000 IU/wk vs 57% standard dose vit D 2000 IU daily	Negative	
	Rastelli 2011	Treatment	60	FIQ pain (3.3 vs 4.6, P=0.0045), BPI worst pain (3.6 vs 5.1, P=0.04), BPI avg pain (2.7 vs 3.7, P=0.0067) better in high dose vitamin D vs PBO at 2 mos	Positive	
	Shapiro 2016	Treatment	116	No significant differences in BCPT-MS, WOMAC, AUSCAN, PROMIS, Hand grip	Negative	
Omega 3 fatty acids	Lustberg 2018	Prevention	44	2o EP: Mean BPI-SF score did not change significantly by time or treatment arm	Negative	
	Hershman 2015	Treatment	262	Mean BPI-SF score decreased by 1.74 vs 1.49 (wk 12) and 2.22 vs 1.81 (wk 24) (P=0.58)	Negative	
Tart Cherry	Shenouda 2022	Treatment	48	Mean pain (VAS) decrease by 34.7% tart cherry vs 1.4% placebo at wk 6 (P=0.034)	Positive	12 pts excluded from analysis
Yi Shen Jian Gu granules	Peng 2018	Treatment	84	Worst pain scores (BPI-SF) decreased by 3.10 pts (50.2%) YSJG vs. 1.63 pts (26.9%) PBO, P=0.001	Positive	Limited generalizability (study population all Asian), clear diagnostic criteria and specific measures for AIMSS absent
Bionic tiger bone capsules	Li 2017	Treatment	70	New or worsening joint symptoms in 22.9% tiger bone vs. 60% PBO wk 12 (P<0.001)	Positive	
Blue Citrus	Massimino 2011 (abstract only)	Treatment	37	Mean VAS score 2.98 Blue Citrus vs 3.92 PBO (P=0.0203) at 30 d but by end of study VAS scores were 2.6 vs 3.0 (180 d)	?	Abstract only, limited data available
Emu Oil	Chan 2017	Treatment	87	No statistically significant benefit in joint pain at week 8 (VAS)	Negative	
Cat's claw	Sordi 2019	Treatment	70	Uncaria tomentosa was not more effective than placebo (BPI, DASH, VAS pain)	Negative	

(Continued)

TABLE 1 Continued

	Author, year	Trial Type	N	Study details	Outcome	Caveats
EXERCISE						
Supervised mixed aerobic/resistance training, vs usual care	Irwin 2015	Treatment	121	Worst joint pain scores decreased by 1.6 pts (29%) vs 0.2 pt increases (3%) at 12 months (P<0.001)	Positive	
Unsupervised walking, vs waiting list control	Nyrop 2017	Treatment	62	Worst pain (WOMAC) not statistically significantly different between intervention and control	Negative	Improvements in WOMAC stiffness, difficulty and total score
Patient's choice of 3 exercise intensity levels, vs usual care -	Tamaki 2018	Treatment	102	Trends for pain interference at 12 months did not reach statistical significance	Negative	
Supervised followed by independent Nordic Walking, vs usual care	Fields 2016	Treatment	159	BPI-SF decreased -1.5 (intervention group) vs. -2.5 (control group)	Negative	Feasibility study
Supervised followed by unsupervised mixed aerobic/ resistance training	Lohrisch 2011 (abstract only)	Treatment	22	Only 20 evaluable subjects, mean SF36 improved in 6 (55%) and 7 (64%)	Negative	Abstract only, limited data available
Supervised mixed aerobic/resistance training, vs usual care	Sanmugarajah 2017 (abstract only)	Prevention	20	Mean pain scores (BPI) increased by 1 unit (exercise group) vs. 5 units (PBO) at 12 mos (P>0.05)	Negative	Abstract only, limited data available
Supervised exercise program vs unsupervised walking	Varadarajan 2016	Treatment	27	Significant improvement in grip strength	Positive	Abstract only, limited data available

AE, adverse events; AUSCAN, Australian/Canadian osteoarthritis hand index version 3.1; BCPT-MS, breast cancer prevention trial-musculoskeletal scale; BPI-AIA, brief pain inventory-aromatase induced arthralgia; BPI-SF, brief pain inventory-short form; DASH, disability Arm, Shoulder, and Hand; FIQ, fibromyalgia impact questionnaire; PBO, placebo; VAS, visual analog scale; WOMAC, Western Ontario and McMaster osteoarthritis index version 3.1; 1o EP, primary endpoint; 2o EP, secondary endpoint.

generally showed improvement without serious adverse effects. Acupuncture provided pain relief in several available studies, with the substantial caveat that sham acupuncture often provided a similar benefit.

Due to its observational nature, this case study has inherent limitations. A key limitation is that the mechanism for AIA improvement is unclear as multiple changes were made simultaneously. Nevertheless, the combination of changes led to our patient decreasing BMI from a peak of around 27 to 21 over the period of interest, which can have many metabolic benefits that may have mediated her improvement in AIA. However, caution is advised in the application of these results to individuals with normal BMI. BMI > 30 or weight > 80 kg was associated with increased risk of developing joint symptoms in the ATAC (Arimidex Tamoxifen Alone or in Combination) and IES (Intergroup Exemestane Study) cohorts, respectively (34, 35). However, other studies have demonstrated that BMI did not predict time to AI discontinuation due to treatment-related symptoms, suggesting perhaps that obesity predisposes to AIMSS symptoms but does not reliably predict their severity. Further complicating matters, although obesity positively correlates with onset of AIA/AIMSS, a cross-sectional survey found that overweight women (BMI 25 to 30) experienced joint symptoms less frequently than their counterparts with BMI< 25 or > 30. Estrogen signaling is known to modulate glucose and lipid metabolism and immune function; a healthy, antioxidant-rich diet may therefore counteract AI-induced changes by enhancing insulin sensitivity, decreasing body fat, and reducing inflammation with or without augmentation by weight loss. In this patient with co-existing metabolic abnormalities (prediabetes and NAFLD) suggesting insulin resistance, weight loss likely was a contributor to her symptomatic improvement. Although it is difficult to parse the individual roles diet, exercise and weight loss as mediators given their interrelatedness, future RCTs could stratify patients based on BMI to better address this issue.

In comparison to patients enrolled in the exercise RCT for AIA (Irwin et al., 2015 JCO), our patient was younger at age 46, compared with the average age of 62 in the exercise group and 60.5 in the usual care group. Her peak BMI of 27 was slightly lower than the average BMI of 30 and 28.7 (exercise and usual care groups, respectively) and her degree of weight loss was greater (-12.5% compared with -2.4% in the exercise group and 0% in the usual care group). She was considerably more active at baseline, with approximately 525 minutes of physical activity a week (assuming 6000 steps a day), which was substantially greater than 54.8 and 60.7 minutes per week in the exercise and usual care groups, respectively. Thus, in designing future RCTs, we speculate that more ambitious exercise targets could yield more dramatic results.

This patient's favorable outcome suggests that diet coupled with a pattern of daily physical activity can be a promising, cost-effective and low-risk intervention for many patients suffering from AIA/AIMSS. This is in line with existing evidence suggesting beneficial effects of Mediterranean and plant-based diets on pain control in inflammatory arthritis, including rheumatoid arthritis (36), and with their known disease-modifying activity in conditions mediated by chronic low-grade inflammatory states, including atherosclerotic cardiovascular disease and cancer (32, 37). It also highlights the power of technologies like CGM, which was instrumental in empowering this patient to make impactful changes. A potential RCT could leverage meal delivery services that adhered to a Mediterranean plant-forward dietary pattern consisting of the macronutrient proportions described in Figure 2. In addition, group classes with a dietitian could be incorporated into the intervention to ensure optimal interpretation of CGM data as well as dietary suggestions on how to minimize the glycemic impact of foods. Additional studies are required to pinpoint key beneficial diet and exercise practices for AIA/AIMSS and the mechanisms thereof.

In summary, we propose that thoughtfully designed studies testing the use of a Mediterranean plant-forward diet accompanied by regular exercise should be pursued. Performing randomized controlled trials (RCTs) to assess multimodal interventions is challenging but feasible (38), and the use of mobile technologies (e.g. CGMs, step counters, etc.) to quantitatively assess adherence to dietary and exercise interventions can improve the fidelity of multimodal lifestyle intervention RCTs. AIA/AIMSS is a condition that impairs quality of life and interrupts a potentially life-saving therapy for substantial numbers of patients with breast cancer, and there is a clear need for more effective evidence-based AIA/AIMSS treatment strategies.

Patient perspective

I developed life impacting side effects from taking an aromatase inhibitor (AI). I dropped things because of tingling hands, slept with wrist braces because of carpal tunnel-like pain, took extra time to get out of bed due to stiff joints, and had difficulty walking with a large bump on my Achilles tendon. I was in pain, couldn't easily exercise, gained weight, developed a Non-Alcoholic Fatty Liver, showed elevated cholesterol levels, and my A1C was just under the range for Type 2 Diabetes.

While waiting to start a new medication to relieve the AI side effects, I addressed my weight and other health issues. I found a team of registered dieticians who introduced me to the Mediterranean Diet, calculated my specific macronutrient goals and supervised me while I wore a continuous glucose monitor (CGM). The Mediterranean Diet told me what to eat. The CGM data helped me understand when and how much to eat, which foods (including some unexpected ones) trigger blood glucose spikes for me, and when to get up and move my body. Together, all this information helped me keep my blood glucose steady.

I lost a significant amount of weight and many of my AI side effects disappeared. Now, my hands no longer tingle. The bump on my Achilles tendon went away and I can walk hills again. I don't need wrist braces to sleep. I have maintained my weight loss. Both my A1C and cholesterol levels have dropped. My latest abdominal ultrasound presented my liver appearance as normal - my fatty liver is gone. My AI lowers my risk for breast cancer recurrence. I am thrilled I can better tolerate this medication and keep taking it for the planned amount of time. I am excited I did this by simply making dietary and lifestyle changes and without having to add a new medication.

Data availability statement

The raw data supporting the conclusions of this article will be made available by the authors, without undue reservation.

Ethics statement

Written informed consent was obtained from the individual(s) for the publication of any potentially identifiable images or data included in this article.

Author contributions

KW and TK conducted patient interviews to gather information regarding symptoms and dietary practices. KW abstracted data from the patient chart and drafted the initial manuscript. RG performed the statistical analysis of CGM data. TK, SH, and TG provided meaningful review and revision of the intellectual content of multiple drafts. All authors approved the submitted version.

Funding

The author(s) received no financial support for the research, authorship, and/or publication of this article.

Acknowledgments

The authors thank this patient for allowing us to share their story and for providing detailed continuous glucose monitoring reports and dietary data.

Conflict of interest

The authors declare that the research was conducted in the absence of any commercial or financial relationships that could be construed as a potential conflict of interest.

Publisher's note

All claims expressed in this article are solely those of the authors and do not necessarily represent those of their affiliated

organizations, or those of the publisher, the editors and the reviewers. Any product that may be evaluated in this article, or claim that may be made by its manufacturer, is not guaranteed or endorsed by the publisher.

Supplementary material

The Supplementary Material for this article can be found online at: https://www.frontiersin.org/articles/10.3389/fonc.2024.1189287/full#supplementary-material

SUPPLEMENTARY FIGURE 1
A representative example of CGM-guided changes to diet and intake and its impacts on postprandial blood glucose trends. Blue trendline (3/15/2022): Consumption of one serving of Japanese sweet potato alone without aerobic activity produced a blood glucose spike > 140 mg/dl between 1 and 2 hours after eating. Orange trendline (6/20/2022): Consumption of one serving of the same batch of frozen and reheated Japanese sweet potato topped with quinoa, black beans, avocado, and tomatoes with a side of corn, followed by a 30 minute brisk walk. Gray trendline (6/27/2022): Consumption of one serving of the same sweet potato with ground turkey, grilled and blanched vegetables followed by a 30 minute brisk walk.

SUPPLEMENTARY FIGURE 2
Overlay of serial ultrasound measurements of hepatic steatosis on timeline reveals a delayed resolution of hepatic steatosis following diet and lifestyle modifications.

References

1. Islami F, Ward EM, Sung H, Cronin KA, Tangka FKL, Sherman RL, et al. Annual report to the nation on the status of cancer, part 1: national cancer statistics. *J Natl Cancer Inst* (2021) 113(12):1648–69. doi: 10.1093/jnci/djab131

2. Boszkiewicz K, Piwowar A, Petryszyn P. Aromatase inhibitors and risk of metabolic and cardiovascular adverse effects in breast cancer patients-A systematic review and meta-analysis. *J Clin Med* (2022) 11(11):3133. doi: 10.3390/jcm11113133

3. Harbeck N, Penault-Llorca F, Cortes J, Gnant M, Houssami N, Poortmans P, et al. Breast cancer. *Nat Rev Dis Primers* (2019) 5(1):66. doi: 10.1038/s41572-019-0111-2

4. Niravath P. Aromatase inhibitor-induced arthralgia: a review. *Ann Oncol* (2013) 24(6):1443–9. doi: 10.1093/annonc/mdt037

5. Morales L, Pans S, Paridaens R, Westhovens R, Timmerman D, Verhaeghe J, et al. Debilitating musculoskeletal pain and stiffness with letrozole and exemestane: associated tenosynovial changes on magnetic resonance imaging. *Breast Cancer Res Treat* (2007) 104(1):87–91. doi: 10.1007/s10549-006-9394-6

6. Sestak I, Sapunar F, Cuzick J. Aromatase inhibitor-induced carpal tunnel syndrome: results from the ATAC trial. *J Clin Oncol* (2009) 27(30):4961–5. doi: 10.1200/JCO.2009.22.0236

7. Beckwée D, Leysen L, Meuwis K, Adriaenssens N. Prevalence of aromatase inhibitor-induced arthralgia in breast cancer: a systematic review and meta-analysis. *Support Care Cancer* (2017) 25(5):1673–86. doi: 10.1007/s00520-017-3613-z

8. Henry NL, Giles JT, Ang D, Mohan M, Dadabhoy D, Robarge J, et al. Prospective characterization of musculoskeletal symptoms in early stage breast cancer patients treated with aromatase inhibitors. *Breast Cancer Res Treat* (2008) 111(2):365–72. doi: 10.1007/s10549-007-9774-6

9. Roberts K, Rickett K, Greer R, Woodward N. Management of aromatase inhibitor induced musculoskeletal symptoms in postmenopausal early Breast cancer: A systematic review and meta-analysis. *Crit Rev Oncol Hematol* (2017) 111:66–80. doi: 10.1016/j.critrevonc.2017.01.010

10. Yang GS, Kim HJ, Griffith KA, Zhu S, Dorsey SG, Renn CL. Interventions for the treatment of aromatase inhibitor-associated arthralgia in breast cancer survivors: A systematic review and meta-analysis. *Cancer Nurs* (2017) 40(4):E26–41. doi: 10.1097/NCC.0000000000000409

11. Carpenter CL. *Dietary and Exercise Interventions in Reducing Side Effects in Patients With Stage I-IIIa Breast Cancer Receiving Aromatase Inhibitors*. ClinicalTrials.gov. Available at: https://clinicaltrials.gov/ct2/show/NCT03953157.

12. Henry NL, Unger JM, Schott AF, Fehrenbacher L, Flynn PJ, Prow DM, et al. Randomized, multicenter, placebo-controlled clinical trial of duloxetine versus placebo for aromatase inhibitor-associated arthralgias in early-stage breast cancer: SWOG S1202. *J Clin Oncol* (2018) 36(4):326–32. doi: 10.1200/JCO.2017.74.6651

13. Henry NL, Unger JM, Till C, Schott AF, Crew KD, Lew DL, et al. Association between body mass index and response to duloxetine for aromatase inhibitor-associated musculoskeletal symptoms in SWOG S1202. *Cancer* (2019) 125(12):2123–9. doi: 10.1002/cncr.32024

14. Kubo M, Onishi H, Kuroki S, Okido M, Shimada K, Yokohata K, et al. Short-term and low-dose prednisolone administration reduces aromatase inhibitor-induced arthralgia in patients with breast cancer. *Anticancer Res* (2012) 32(6):2331–6.

15. Roberts KE, Rickett K, Chatfield MD, Woodward NE. Systemic therapies for preventing or treating aromatase inhibitor-induced musculoskeletal symptoms in early breast cancer. *Cochrane Database Syst Rev* (2018) (1):CD013167. doi: 10.1002/14651858.CD013167

16. Roberts KE, Rickett K, Feng S, Vagenas D, Woodward NE. Exercise therapies for preventing or treating aromatase inhibitor-induced musculoskeletal symptoms in early breast cancer. *Cochrane Database Syst Rev* (2020) 1(1):CD012988. doi: 10.1002/14651858.CD012988.pub2

17. Rosati MS, Di Seri M, Baciarello G, Lo Russo V, Grassi P, Marchetti L, et al. Etoricoxib and anastrozole in adjuvant early breast cancer: ETAN trial (phase III). *J Clin Oncol* (2011) 29(15_suppl):533. doi: 10.1200/jco.2011.29.15_suppl.533

18. Birrell S, Tilley W. Testosterone undecanoate treatment reduces joint morbidities induced by anastrozole therapy in postmenopausal women with breast cancer: results of a double-blind, randomized phase II trial. *Cancer Res* (2009) 69 (24_Supplement):804–4. doi: 10.1158/0008-5472.SABCS-09-804

19. Cathcart-Rake E, Novotny P, Leon-Ferre R, Le-Rademacher J, Storrick EM, Adjei AA, et al. A randomized, double-blind, placebo-controlled trial of testosterone for treatment of postmenopausal women with aromatase inhibitor-induced arthralgias: Alliance study A221102. *Support Care Cancer* (2021) 29(1):387–96. doi: 10.1007/s00520-020-05473-2

20. Liu P, Yang DQ, Xie F, Zhou B, Liu M. Effect of calcitonin on anastrozole-induced bone pain during aromatase inhibitor therapy for breast cancer. *Genet Mol Res* (2014) 13(3):5285–91. doi: 10.4238/2014.July.24.7

21. Lustberg MB, Orchard TS, Reinbolt R, Andridge R, Pan X, Belury M, et al. Randomized placebo-controlled pilot trial of omega 3 fatty acids for prevention of aromatase inhibitor-induced musculoskeletal pain. *Breast Cancer Res Treat* (2018) 167 (3):709–18. doi: 10.1007/s10549-017-4559-z

22. Hershman DL, Unger JM, Crew KD, Awad D, Dakhil SR, Gralow J, et al. Randomized multicenter placebo-controlled trial of omega-3 fatty acids for the control of aromatase inhibitor-induced musculoskeletal pain: SWOG S0927. *J Clin Oncol* (2015) 33(17):1910–7. doi: 10.1200/JCO.2014.59.5595

23. Khan QJ, Kimler BF, Reddy PS, Sharma P, Klemp JR, Nydegger JL, et al. Randomized trial of vitamin D3 to prevent worsening of musculoskeletal symptoms in women with breast cancer receiving adjuvant letrozole. The VITAL trial. *Breast Cancer Res Treat* (2017) 166(2):491–500. doi: 10.1007/s10549-017-4429-8

24. Niravath P, Hilsenbeck SG, Wang T, Jiralerspong S, Nangia J, Pavlick A, et al. Randomized controlled trial of high-dose versus standard-dose vitamin D3 for prevention of aromatase inhibitor-induced arthralgia. *Breast Cancer Res Treat* (2019) 177(2):427–35. doi: 10.1007/s10549-019-05319-4

25. Rastelli AL, Taylor ME, Gao F, Armamento-Villareal R, Jamalabadi-Majidi S, Napoli N, et al. Vitamin D and aromatase inhibitor-induced musculoskeletal symptoms (AIMSS): a phase II, double-blind, placebo-controlled, randomized trial. *Breast Cancer Res Treat* (2011) 129(1):107–16. doi: 10.1007/s10549-011-1644-6

26. Shapiro AC, Adlis SA, Robien K, Kirstein MN, Liang S, Richter SA, et al. Randomized, blinded trial of vitamin D3 for treating aromatase inhibitor-associated musculoskeletal symptoms (AIMSS). *Breast Cancer Res Treat* (2016) 155(3):501–12. doi: 10.1007/s10549-016-3710-6

27. Shenouda M, Copley R, Pacioles T, Lebowicz Y, Jamil M, Akpanudo S, et al. Effect of tart cherry on aromatase inhibitor-induced arthralgia (AIA) in nonmetastatic hormone-positive breast cancer patients: A randomized double-blind placebo-controlled trial. *Clin Breast Cancer* (2022) 22(1):e30–6. doi: 10.1016/j.clbc.2021.06.007

28. Li Y, Zhang Z, Cui F, Liu J, Wang Y, Jiang J, et al. Traditional chinese medicine bionic tiger bone powder for the treatment of AI-associated musculoskeletal symptoms. *Evid Based Complement Alternat Med* (2017) 2017:2478565. doi: 10.1155/2017/2478565

29. Peng N, Yu M, Yang G, Fu Q, Xu Y, Yu J, et al. Effects of the Chinese medicine Yi Shen Jian Gu granules on aromatase inhibitor-associated musculoskeletal symptoms: A randomized, controlled clinical trial. *Breast* (2018) 37:18–27. doi: 10.1016/j.breast.2017.08.003

30. Chan A, De Boer R, Gan A, Willsher P, Martin R, Zissiadis Y, et al. Randomized phase II placebo-controlled study to evaluate the efficacy of topical pure emu oil for joint pain related to adjuvant aromatase inhibitor use in postmenopausal women with

early breast cancer: JUST (Joints Under Study). *Support Care Cancer* (2017) 25 (12):3785–91. doi: 10.1007/s00520-017-3810-9

31. Sordi R, Nastri Castro S, Thaumaturgo Lera A, Nonato Irene M, de Melo Farinazzo M, Sette C, et al. Randomized, double-blind, placebo-controlled phase II clinical trial on the use of uncaria tomentosa (Cat's claw) for aromatase inhibitor-induced arthralgia: A pilot study. *J Natural Remedies* (2019) 19(1):24–31. doi: 10.18311/jnr/2019/22867

32. Morze J, Danielewicz A, Przybyłowicz K, Zeng H, Hoffmann G, Schwingshackl L. An updated systematic review and meta-analysis on adherence to mediterranean diet and risk of cancer. *Eur J Nutr* (2021) 60(3):1561–86. doi: 10.1007/s00394-020-02346-6

33. Bae K, Lamoury G, Carroll S, Morgia M, Lim S, Baron-Hay S, et al. Comparison of the clinical effectiveness of treatments for aromatase inhibitor-induced arthralgia in breast cancer patients: A systematic review with network meta-analysis. *Crit Rev Oncol Hematol* (2023) 181:103898. doi: 10.1016/j.critrevonc.2022.103898

34. Sestak I, Cuzick J, Sapunar F, Eastell R, Forbes JF, Bianco AR, et al. Risk factors for joint symptoms in patients enrolled in the ATAC trial: a retrospective, exploratory analysis. *Lancet Oncol* (2008) 9(9):866–72. doi: 10.1016/S1470-2045(08)70182-7

35. Mieog JSD, Morden JP, Bliss JM, Coombes RC, van de Velde CJH. IES Steering Committee. Carpal tunnel syndrome and musculoskeletal symptoms in postmenopausal women with early breast cancer treated with exemestane or tamoxifen after 2-3 years of tamoxifen: a retrospective analysis of the Intergroup Exemestane Study. *Lancet Oncol* (2012) 13(4):420–32. doi: 10.1016/S1470-2045(11)70328-X

36. Schönenberger KA, Schüpfer A-C, Gloy VL, Hasler P, Stanga Z, Kaegi-Braun N, et al. Effect of anti-inflammatory diets on pain in rheumatoid arthritis: A systematic review and meta-analysis. *Nutrients* (2021) 13(12):4221. doi: 10.3390/nu13124221

37. Widmer RJ, Flammer AJ, Lerman LO, Lerman A. The Mediterranean diet, its components, and cardiovascular disease. *Am J Med* (2015) 128(3):229–38. doi: 10.1016/j.amjmed.2014.10.014

38. Younge JO, Kouwenhoven-Pasmooij TA, Freak-Poli R, Roos-Hesselink JW, Hunink MM. Randomized study designs for lifestyle interventions: a tutorial. *Int J Epidemiol* (2015) 44(6):2006–19. doi: 10.1093/ije/dyv183

Frontiers in Oncology

Advances knowledge of carcinogenesis and tumor progression for better treatment and management

The third most-cited oncology journal, which highlights research in carcinogenesis and tumor progression, bridging the gap between basic research and applications to imrpove diagnosis, therapeutics and management strategies.

Discover the latest Research Topics

See more →

Frontiers

Avenue du Tribunal-Fédéral 34
1005 Lausanne, Switzerland
frontiersin.org

Contact us

+41 (0)21 510 17 00
frontiersin.org/about/contact